TE
662
.A3
no.
FHWA
RD.
76-72

1. Report No.	2. Government Accession No.	3. Recipient's Catalog No.
FHWA-RD-76-72		

4. Title and Subtitle	5. Report Date
Evaluation of Aerial Remote Sensing Techniques for Defining Critical Geologic Features Pertinent to Tunnel Location and Design	March 1976
	6. Performing Organization Code

7. Author(s)	8. Performing Organization Report No.
O. Russell, D. Stanczuk, J. Everett, R. Coon	

9. Performing Organization Name and Address	10. Work Unit No. (TRAIS)
Earth Satellite Corporation (EarthSat) 7222 47th Street, N.W. Washington, D.C. 20015	35B2-022
	11. Contract or Grant No.
	DOT-FH-11-8598
	13. Type of Report and Period Covered

12. Sponsoring Agency Name and Address	
U.S. Department of Transportation Federal Highway Administration Washington, D.C. 20590	Final Report August 1974-March 1976
	14. Sponsoring Agency Code
	M-0318

Dept. of Transportation

JAN 9 1978

Library

15. Supplementary Notes

16. Abstract

Operational testing and evaluation of commercially available remote sensing data including space imagery, side-looking airborne radar, black-and-white, color infrared, color, and low sun angle photography. Multispectral scanner data (including thermal infrared), and airborne geophysical systems over the East River Mountain tunnel in West Virginia and the Carlin Canyon tunnel in Nevada demonstrates that, if integrated with conventionally acquired geologic data, remote sensing can reduce the cost of tunnel site selection and evaluation and in almost every instance provides unique geologic information. There is no single array of remote sensors that is optimal for all tunnel sites, but there is a suite of remotely sensed data including space imagery, black-and-white and color aerial photography, low sun angle photography, and side-looking airborne radar (if it already exists) that should be analyzed for most sites because of high information content and relatively low cost. Several other systems including side-looking airborne radar, thermal infrared scanners, and airborne geophysical systems can provide uniquely valuable geologic information under particular sets of geologic and climatic conditions, but are deemed too expensive for inclusion in all tunnel site evaluation programs.

17. Key Words	18. Distribution Statement
Remote sensing, Geology, Tunnels, Geologic modeling, Cost effectiveness, Orbital Data, Radar, Photography, Scanners, Airborne Geophysics	No restrictions. This document is available to the public through the National Technical Information Service, Springfield, Virginia 22161

19. Security Classif. (of this report)	20. Security Classif. (of this page)	21. No. of Pages	22. Price
Unclassified	Unclassified	352	

Form DOT F 1700.7 (8-72)   Reproduction of completed page authorized

TABLE OF CONTENTS

APPENDICES

LIST OF FIGURES

ix

LIST OF PLATES (In Pocket)

LIST OF TABLES

xiii

EVALUATION OF AERIAL REMOTE SENSING TECHNIQUES FOR DEFINING CRITICAL GEOLOGIC FEATURES PERTINENT TO TUNNEL LOCATION AND DESIGN

1.0 EXECUTIVE SUMMARY

The cost of tunnel construction often far exceeds original esti-
mates due to unforeseen geological conditions that create work delays
and require more costly excavation and construction procedures. The
degree to which the rock structure and engineering properties of the
different rock materials can be predicted at tunnel depth depends upon
a number of factors such as rock type, structural complexity, climate,
and degree of surface exposure. This latter factor is extremely impor-
tant because to a large extent the prediction of geological conditions
at tunnel depth is based on the mapping of the surface geology. A
certain number of core drill tests, some geophysical surveys, and in
some instances test excavation, supplement surface mapping.

Developments in airborne remote sensing instrumentation over the
last decade or two have created a new suite of sensing systems and
improvements to existing systems. These systems show promise of ac-
quiring better and more comprehensive geological information for a
tunnel site or acquiring this information more quickly or cheaply than
the conventional investigative procedures now used.

The objective of this investigation was to conduct actual field
tests using various airborne remote sensing techniques for the purpose
of evaluating their contribution to the investigation and selection of
tunnel sites by the development of improved three-dimensional geological
models.

Two tunnels in substantially different environments were selected
for investigation. The Carlin Canyon site near Elko, Nevada, receives
approximately four inches (10cm) of rainfall annually. The East River
Mountain tunnel located in southeastern West Virginia, receives an
annual rainfall of 40-60 inches (100-150cm).

To be of greatest value any airborne remote sensing technique must
be thoroughly integrated with conventional tunnel site investigation and
evaluation programs. There is no single array of remote sensors that
will be optimal for all tunnel sites. However, there is a suite of
remotely sensed data that we believe should be acquired and analyzed for
most tunnel sites because of its relatively low cost and high infor-
mation content. This data package includes LANDSAT and Skylab satellite
imagery, black-and-white and color aerial photographs, low sun angle
photography, and side-looking airborne radar (SLAR) if it exists.
Analysis of these data and existing geologic information will provide a
basis for planning additional remote sensing surveys and the conven-
tional geologic evaluation program. A decision to use other airborne
remote sensing systems must be guided by the geology and climate of the

area, the amount of detailed geologic data that already exists, and time and budgetary limits of the program.

There are several remote sensor systems that may provide valuable information under a particular set of geologic or climatic conditions, but that are deemed to be too expensive for inclusion in all tunnel site evaluation programs. Sensors in this category are SLAR (if it must be contracted for a specific site), airborne geophysical systems, and multispectral and thermal scanner systems. Because of its high cost, SLAR should be contracted for a specific site only if the site is in an area where cloud cover has precluded the acquisition of satellite imagery and photography. If the site is in a geologically complex area where the complexities are likely to be reflected by conductive or magnetic zones, airborne geophysical systems (magnetic and electromagnetic) will provide invaluable information which can help in predicting geologic conditions at tunnel level. Airborne magnetometer and electromagnetic systems were used over the East River Mountain site. Thermal infrared scanner imagery will provide unique geologic information in areas where soil moisture difference may reflect geological structure, where there is little surface vegetation, or where differences in rock type are marked by differences in silica content or thermal inertia properties.

The results in this investigation demonstrated, as anticipated, that the color and black-and-white aerial photography were the prime sources of information. However, each sensor provided some unique information. Satellite imagery gave a synoptic overview of an area and a regional view of the geological structure. This imagery revealed long subtle, linear features, that in many instances proved to be large fracture or fault zones not identifiable on larger scale imagery. Several features of this type are present in the vicinity of the project tunnel sites, particularly the Nevada site.

Radar imagery confirmed some of the previously detected linear features and added detail to the understanding of the regional geology surrounding the tunnel sites. The imagery showed that the Nevada site is structurally complex and that major faults are present in the vicinity of the tunnel.

Color infrared photography was of little value at either site. The principal value of this photography lies in the emphasis it gives vegetational patterns. The Carlin Canyon site was overflown in late October and the East River Mountain site in early April, when the vegetation was dormant in both areas.

Low-sun-angle photography emphasizes the control that geologic structure exerts on the development of the landforms in each area. This imagery revealed numerous linear features, some of which were faults identified using data from other sensors. Multispectral and thermal infrared imagery was acquired at both test sites. The analyses of these various data were conducted using both conventional photographic and

2

computer image enhancement techniques. The tape recorded scanner data was processed with a variety of algorithms by a special purpose computer. These algorithms included density slicing, density stretching, contour enhancement, and channel ratioing. Images from this processing were further analyzed with the aid of additive color devices and photographic laboratory color processing.

Visible and near-visible multispectral scanner data of the eastern site proved of little value because of the limited number of outcrops and the masking of most rock surfaces by lichens. At the western site, where the lichen cover is more sparse, ratioing of selected spectral bands emphasized the presence of iron and specific stratigraphic horizons.

In the Carlin Canyon area, analysis of each of the two spectral bands (8-10µm and 10-12µm) of the thermal imagery provides little information except for soil-outcrop boundaries. Structural features that coincide with these boundaries are emphasized. However, ratioing of the two thermal bands accentuated several outcrops of materials high in silicate content because of the emission minima of silica in the 8-10µm region of the spectrum.

Because of the heavy lichen cover on most outcrops at the East River Mountain site, ratioing of the thermal imagery emphasized silica rich formations only in areas recently disturbed by man's activities. The two thermal bands used have nearly the same sensitivity to moisture differences, thus imagery from both bands revealed a significant number of geologic features enhanced by differences in the distribution of soil moisture.

The aeromagnetic data showed several weak anomalies that correlated well with two linear features identifiable on the photography, which supports the hypothesis that these features are faults. The strongest magnetic anomalies were associated with the steel within the tunnels.

The electromagnetic data identified two anomalous areas. One area, near the north portal of the East River Mountain tunnel is interpreted as an interconnecting, canvern-sinkhole zone, saturated with water. The second area, on the south slope of the mountain, is a circular anomaly interpreted as a water saturated intersection of two fault zones. Other remote sensing data support this interpretation.

There is no single optimum time of day or season of year for all sensors. A near-optimum time period for flying an individual sensor can be selected with little difficulty, but multiple sensor missions must be planned with consideration of a number of environmental factors prevailing at the site.

The cost of conventional procedures for geologic evaluation of a specific tunnel site are not difficult to derive. The same is true for the acquisition and analysis of any of the remote sensor data. However,

for a specific site prior to tunnel construction, it is extremely diffi-
cult to assess the cost effectiveness of using a suite of remote sensors.
If no difficulty in excavation of a tunnel is encountered after the
expenditure of a sum of money for the acquisition and analysis of remote
sensing data, the benefits will be minimal and equal only to the cost
savings of using an integrated conventional and remote sensing approach
over a completely conventional approach. However, if major problems are
detected and avoided because remote sensing was included, the benefits
may be large. We believe that the remote sensing systems tested do have
the capability of detecting problems that conventional approaches alone
might miss.

2.0 INTRODUCTION

2.1 Purpose of Investigation

A critical element in the safe and successful completion of a tunnel is the accurate prediction of the geological and engineering characteristics of the rock mass to be encountered. These predictions depend on the quality and quantity of the geological, geophysical, and engineering data collected and the proper interpretation and analysis of these data prior to the start of excavation.

The geologic data essential to tunnel planning and construction are those which define the ground conditions surrounding the proposed tunnel in terms which can be directly related to the equipment, construction materials, labor, and tunneling techniques required for safe and economical construction. In other words, the geologic data must relate to the engineering parameters required for design and construction. This generally implies a three-dimensional understanding of the distribution of pertinent geological features surrounding the proposed tunnel and extending radially from the center line of the tunnel bore far enough to include the total influence on the tunnel construction.

Geologic principles are sufficiently understood that a knowledge of geologic conditions in one area will permit the extrapolation of the known geology to an adjacent area. In other words, the visible is an inexpensive guide to the invisible. The degree of success to which this can be accomplished is dependent upon the amount of information available and the complexity of the area. For this reason tunnel geologists carefully examine the surface geology prior to embarking on any program of subsurface exploration. It is also for this reason that a variety of techniques generally described as remote sensing offer a distinct promise of assisting the initial surface geologic exploration.

The acquisition of data for planning purposes largely consists of field mapping of the geology, supplemented as necessary by accoustical and resistivity surveys, drilling programs, and aerial photographic mapping. The latter technique is classified along with other imaging and non-imaging mapping techniques as remote sensing. This term is applied herein to the use of any system used to acquire data about an object or area from a remote point. It has been applied somewhat loosely to a series of sensor systems, normally airborne, which detect reflected and emitted electromagnetic energy in the ultra violet, visible, and longer wavelength portions of the spectrum. It also includes force field detectors such as the magnetometer and the gravimeter.

The purpose of this study is to evaluate, in terms of cost and quality of data, the capability of airborne remote sensing techniques to provide geologic data for tunnel site selection and evaluation.

We wanted to make the assessment as realistic as possible (only commercially available systems are considered) and the results immediately useful to the industry (methods results and special considerations are thoroughly discussed).

Aerial remote sensing techniques can provide significant information needed by engineers and geologists for tunnel planning and design. Remote sensing is not, however, a panacea that will replace conventional geologic and engineering techniques. In fact, the maximum benefit is derived from this new technology when it is used in conjunction with conventional techniques. Remote sensing techniques can be used to acquire information more rapidly than is possible by conventional ground methods, and in many instances provides information not previously available.

For those types of data that cannot be collected from the air, remote sensing can be used to plan efficient ground surveys and can be used to rapidly extend the results of such surveys to larger areas. For example, while remotely sensed data can not eliminate the need for test boring, it may be used to guide a drilling program so as to optimize the information obtained from each hole (perhaps reducing the number of holes necessary) and providing a means of projecting this information from each hole over a larger area. Experience has demonstrated that many of the largest geologic features go unobserved during ground investigation. One of the major contributions of remote sensing to tunnel construction can be the recognition and assessment early in the planning stages of a tunnel project of geologic features such as major shear zones, serpentine bodies, and etc., which may pose a hazard.

2.2 Background

Both the engineering profession and the public generally regard tunneling as an operation involving an unusual degree of risk. The nature of this risk, however, is not well understood outside the tunneling industry. There is the risk of encountering subsurface conditions that prevent completion of the project. There are a few subsurface conditions such as very high temperatures and very high and continuous groundwater inflows which may permanently stop the advance of a tunnel, but modern tunneling technology provides the tools for coping with almost any ground condition encountered at the depth of interest in tunneling. The risk of the technical impossibility of tunneling is therefore small.

Second, is the risk of encountering subsurface conditions that will either slow or temporarily stop tunneling progress. There are many examples of this type of subsurface conditions including fallouts, flowing ground, groundwater inflows, weak zones, hard zones etc. In some instances the method of excavation or support system is modified while in other instances the method of tunneling

is completely changed to cope with these conditions. In either situation, the cost of performing the work is increased and completion of the work is often delayed.

Third, there is a risk of encountering a subsurface condition which will affect the safety of the workmen in the tunnel or the safety of surface or near surface structures or the safety of the public. Flooding of the tunnel, high temperatures, and toxic gases are examples of conditions which affect the safety of the workmen.

The degree of risk from tunnel to tunnel is not uniform, but varies with the geologic conditions, the characteristics of the tunnel and the method of construction. Risk is primarily the result of uncertainty of the geologic conditions to be encountered by the tunnel and could be largely eliminated if tunnel site investigations provided a complete and accurate picture of the subsurface conditions prior to tunnel excavation. With a perfect picture of the geologic conditions, the ground behavior during excavation could be predicted accurately and the tunnel design and method of construction could be adapted to the existing conditions. In this ideal situation, construction schedules and tunnel cost estimates would be more accurate and tunneling costs would decrease.

On some tunneling projects, the preconstruction model of geologic conditions approaches the ideal proposed above because of excellent exposures of the material present at tunnel level or an unusually intensive investigation program. However, a comparison of preconstruction and construction geologic records normally reveals that the preconstruction model of geologic conditions was incomplete and lacked information about geologic features which significantly affected construction. The preconstruction model of geologic conditions may be deficient because of inadequate investigation or an incomplete evaluation of available information, but most frequently the deficiencies of the model are the result of the limitations of conventional investigation methods.

Conventional investigations include two or more of the following methods:

> review of previous geologic studies
> review of previous construction records
> interpretation of aerial photographs
> geologic mapping
> geophysical testing
> borings
> borehole logging and testing
> exploratory excavations
> field testing
> laboratory testing

In most instances, the geologic conditions at tunnel level are predicted from an incomplete record of surface and near-surface geologic features and from a relatively restricted set of sub-surface data. Predictions generated from this information are good when the available information is representative of the bulk of the rock and at the same time identifies most of the anomalies or discontinuities.

Any means of investigation that could cost effectively improve the completness of the surface or subsurface record would naturally be of value to the tunnel industry. Recent work indicates that airborne remote sensing methods can assist tunnel site selection and investigations by providing:

A. Reconnaissance studies for highway and tunnel routing.

B. Selection of a specific tunnel site along a given route.

C. Location of features to be checked by geologic mapping.

D. Identification of geologic trends which are only partially exposed and not completely identified during geologic mapping.

E. Identification of geologic features which are concealed by soil and would be completely missed in conventional geologic field mapping.

2.3 History of Project

Work commenced on the project on 23 August 1974 upon notification by the U.S. Department of Transportation (DOT) to proceed.

The Request for Proposal listed four tunnel sites for consideration, two in the western and two in the eastern United States. One site was to be selected in each geographic area. The sites considered were:

- Big Walker Mountain Tunnel in Virginia;

- East River Mountain Tunnel on the Virginia-West Virginia border;

- Straight Creek Tunnel in Colorado;

- Carlin Canyon Tunnel in Nevada.

Straight Creek and East River Mountain seemed to offer the greatest variety of geologic and climatic conditions for testing various sensor systems. The initial assessment of the sites indicated that

8

the probable optimum seasons for remote sensor data collection were summer or early fall for the western sites and early spring for the eastern sites.

To complete the study in 18 months, it was deemed necessary to acquire data on the western site in the fall of 1974.

As it was not possible to conduct the preliminary site investigations and mobilize the survey equipment before 1 October, the Straight Creek Site in Colorado, the only tunnel in igneous and metamophic rocks, was not considered. Elevations there exceed 12,000 feet and snow cover was anticipated on the site before October. Other considerations by the Federal Highway Administration (FHWA) also negated the use of this site; consequently, the Carlin Canyon site near Elko, Nevada was selected.

Mobilization to Elko was set for 17 October. The aerial surveys were made on 18, 19, and 20 October. The color and color-infrared and low-sun-angle infrared photography was flown by Olympus Aerial Surveys, Inc., on the 18th. The scanner aircraft, supplied by Aerial Surveys, Inc., made the night time thermal infrared survey overflight between 11 and 12 p.m. on the 18th. Daytime thermal imagery and multispectral imagery were flown on the 19th. Because there was a question about quality of the thermal data recorded during the night flight, this survey was rescheduled as a predawn flight on the 20th and completed just before sunrise at aircraft altitude.

The two eastern tunnel sites, Big Walker Mountain in Virginia and East River Mountain on the Virginia-West Virginia border, are only 20 miles apart and cut nearly identical stratigraphic sections. The East River Mountain site had been tentatively selected primarily because it appeared to have better rock exposures. Field investigations in the spring of 1975 confirmed that the East River Mountain tunnel site was the the better of the two sites for the study.

The time window for the survey of the eastern site was relatively narrow and had to be made between the time of complete snow melt and development of a leaf canopy; the latter would occur in late April or early May. The photographic and scanner surveys were scheduled for the first week of April.

Mobilization by Daedalus Enterprises commenced on 31 March 1975. The survey aircraft flew to Bluefield, West Virginia, on 1 April, arriving about 12:30 p.m., and the multispectral survey of the site was made before landing. The equipment was modified for thermal mapping and daytime thermal imagery was flown about 4:30 p.m. The nighttime thermal survey was made about 11 p.m. to avoid ground fog conditions which developed in that area in the early morning hours.

9

Low sun angle photography was flown on 5 and 7 April. Color and color-infrared photography was acquired on the 6th, but had to be reflown. Cloud cover and wind delayed these reflights until 27 April.

The results of the multispectral data analyses indicated that it was desirable to acquire spectroradiometric data on the different rock types at Carlin Canyon. Although such detail was beyond the scope of work, the extra effort would enhance the results of the study. A trip to the Carlin Canyon site was made on 4-6 August 1975. An Isco Spectroradiometer was used to measure the reflectance properties of the conglomerate and limestone strata.

On 19 and 20 August a field check was made at the East River Mountain site to verify imagery analysis and acquire field data.

Dr. R.J.P. Lyon of Stanford University spent the week of 7 September at the EarthSat facility in Washington analyzing the multispectral data. During this same period Daedalus Enterprises used the services of Dr. Robert Vincent of Geospectra Corporation to independently evaluate thermal and multispectral imagery of the Carlin Canyon site. These analysis required additional field effort in Nevada to confirm the results and acquire additional radiometric information. Dr. Lyon, O. Russell, and D. Stanczuk visited the site during the week of 21 October and confirmed many of Vincent's findings and acquired additional spectroradiometric measurements with two Exotech "ERTS-band" radiometers.

Dighem Limited of Toronto Canada was contracted to make air-borne conductivity and magnetometer surveys over the East River Mountain area, and, if practical, over the Big Walker Mountain tunnel site. The helicopter and ground crew arrived at Bluefield, West Virginia on 8 October and the Virginia and West Virginia State Highway Departments were contacted and advised of the survey activity. Wind seriously hampered the investigation and the crew remained on the site nearly two weeks.

A draft of the final report was submitted to the U.S. Department of Transportation of 1 March 1976.

2.4 Objectives

Numerous advances in the development of remote sensing data collection and analysis have occurred in the last two decades. However, there are very few studies of the potential of remote sensing to aid in tunnel siting investigations. Willow Run Laboratories conducted the only study of significance in 1971 and 1972 under the auspices of the Advanced Research Project Agency (ARPA). The report of this investigation contains an evaluation of the state-of-the-art of remote sensing and an empirical assessment of its application to tunnel site selection.

The main objective of this study is to critically evaluate, through actual application, the role of airborne remote sensing in the selection and geological evaluation of tunnel sites. This involves not only determining what types of geologic data airborne remote sensors can provide, but what techniques are best for extracting, recording, and evaluating these data; it further involves an assessment of acquisition and analysis requirements in terms of money, time, and manpower. The specific objectives are:

- Determine the extent to which aerial remote sensing and geophysical systems can be utilized to develop a three-dimensional geologic model to aid in tunnel location and design.

- Determine the optimum combination of aerial remote sensors for identifying various geologic features and how these data can improve the accuracy of the three-dimensional model or reduce the time or cost necessary to obtain such a model.

- Utilize applicable computer techniques for extracting, enhancing, and classifying pertinent geologic features.

- Develop realistic economic information on cost effectiveness of the application of airborne remote sensing techniques to tunnel design and construction.

2.5 Scope

Considering the possible range of topics implied in the components, remote sensing and tunnel engineering, this study has a relatively narrow focus. The major consideration of this project is where do these two components overlap, and specifically what is the potential synergistic effect of this overlap.

The study does not discuss the theories of electromagnetic radiation, the characteristic emission spectra of rocks and vegetation as defined by previous investigators, or the theory of operation of the various sensor systems.

The evaluation of remote sensing techniques includes some of the latest developments, but is restricted to those systems which are now commercially available. The advantages of this approach are that significant results can be applied immediately by the tunneling industry and the cost effectiveness analysis will place this contribution to tunneling technology in proper prospective with current economic conditions. Only commercially available computer processing and photographic services were used for the same reasons. New remote sensing systems, new computer software, or unusual photo interpretation techniques were not developed or considered.

11

A unique aspect of this study is the application of a wide complement of existing remote sensing systems and established analysis techniques to tunnel site investigations. From the engineering point of view the study does not consider the fine points of tunnel engineering and construction, but confines itself to a discussion of the geologic information, obtained by airborne remote sensing techniques, and as this information applies, tunnel site evaluation and selection.

The study analyzes the capabilities of a suite of commercially available satellite and airborne remote sensing systems to provide data applicable to tunnel engineering and design at two specific test sites and extrapolates these observations to a variety of possible situations.

2.6 Acknowledgments

3.0 APPROACH

The evaluation of airborne remote sensing systems for providing geologic information for tunnel site selection and evaluation involved acquiring a variety of remote sensing data over two tunnel sites. One test site, the East River Mountain Tunnel, is located in Virginia and West Virginia, and the other site, Carlin Canyon Tunnel, is located in Nevada. With the exception of the airborne geophysical instrumentation, the same suite of sensors was used at both sites in order to test the relative effectiveness of these systems in two distinct geologic and climatic environments. At each site all the sensors used were flown at near the same time to permit a basis of comparison among sensors that provide similar data.

Data acquisition involved only commercially available remote sensing systems under operational conditions to insure that the results are immediately useful to the tunneling industry. This also provided a realistic basis for assessing the costs of using these systems.

Comparison of the costs of acquiring geologic data by airborne methods, and the type, importance, and level of detail to the costs and quality of data that conventional means provide, formed the basis for assessing cost effectiveness.

3.1 Underlying Assumptions

In order to evaluate as objectively and realistically as possible the contribution of each remote sensor system used, we imposed several restrictions on the study by making several assumptions.

The geologic analysis of each tunnel site was to be performed without knowledge of the geologic conditions discovered during construction of each tunnel. Therefore, the first assumption is that only preconstruction data related to lithology, structure, and ground conditions were to be used.

Second, we assumed that the route and site selection process had been completed and that data was being collected to evaluate geologic conditions and anticipate hazards of construction including the competence of the rock, slope stability at portal areas, roof collapse potential (which is related to frequency of fractures), and "wet zones" due to ground water flow.

Further, we assumed that route and site selection and site specific investigations will in the future be performed for tunnels using a multistage approach which combines conventional as well as remote sensing systems. Our analysis therefore did consider synergistic effects of using remote sensing and conventional systems.

13

The report is written for the tunnel geologist or engineer who is unfamiliar with remote sensing and how it can assist him.

Since the interests of the readers may be varied, major sections of the report have been written to stand alone. For emphasis and for the benefit of an audience of diverse interests, many concepts are reiterated in varying detail throughout the report.

The analyses of the various data types are presented in a logical sequence beginning with small scale, synoptic view, satellite imagery to the large scale, detailed view, aerial photography. The significant features are annotated on each image and discussed in the text. Judgments made are based on the analysis of the particular image and other images already analyzed. These judgments are modified where necessary as new information is derived from the analysis of additional imagery. The more technical aspects of the study are contained in the Appendices.

3.2 Literature Search

The primary value of a literature survey is that the knowledge gained can be used as a foundation from which advances in the art can be made. The literature review was conducted to define the state-of-the-art in applying remote sensing techniques to geological analysis of tunnel sites during pre-construction phases. Literature pertaining to all aspects of tunneling is quite extensive and to a slightly lesser degree the same is true for literature dealing with remote sensing. There is, however, a lack of information available on the application of remote sensing techniques to tunneling. This fact, and the intuitive judgment of the potential value of remote sensing applied to tunnel site studies, are the prime justifications for this research and development project.

In this literature search bibliographies containing over 1,700 abstracts of publications were assembled. They relate to tunnel engineering, remote sensing, geology, rock mechanics, and tunneling costs. The main sources of information included four computer bibliographic data searches, an annotated bibliography on tunneling prepared by the Department of Housing and Urban Development, conference proceedings, and publications from the files of the contractor, subcontractors, and consultants.

The specific purpose of the literature review was to identify and describe systems and techniques that can be used to select a suitable tunnel location and design. The first objective of the literature was to examine the theories of operation and reported capabilities of a variety of aerial remote sensing instruments. The second objective was to identify site selection and preconstruction engineering problems that could be addressed using

aerial remote sensing techniques. The third objective was to study the previous applications of remote sensing techniques to tunneling.

To initiate the search, two standard references of the American Society for Information Science were used:

- A Survey of Commercially Available Computer Readable Bibliographic Data Bases.

- Library and Reference Facilities in the Area of the District of Columbia, Ninth Edition.

From the survey of computer readable data bases, seven organizations were contacted. These organizations were:

- National Technical Information
     Service   One search performed.
  5285 Port Royal Road
  Springfield, Virginia 22151

- Defense Document Center
  Cameron Station   Two searches performed.
  Alexandria, Virginia 22314

- Transportation Research Board
  2101 Constitution Avenue   One search performed.
  Washington, D.C. 20418

- Rock Mechanics Information
     Service   One search performed.
  Imperial College of Science &
     Technology
  Royal School of Mines
  London, England SW7

- Engineering Index, Inc.
  345 East 47th Street   Do not perform
  New York, New York 10017   searches.

- MARC Distribution Service,
     Card Division   Do not perform
  Library of Congress   searches.
  Building 159
  Washington, D.C. 20541

- Congressional Research Service
  Library of Congress   Do not perform
  Washington, D.C. 20540   searches.

Once it was determined that certain key words related to remote sensing and tunneling did appear in the vocabulary of four of the seven retrieval systems, bibliographic searches were requested. The searches contain several hundred articles related to the key words submitted; however, not all were relevant to the study. It was therefore necessary to review the abstracts that appeared in the search and select pertinent documents. All pertinent documents were than acquired in either microfiche or paper copy form, and the bibliographies of these documents were checked in turn for pertinent references.

The bibliography, titled, "Tunneling: An Annotated Bibliography with Permuted-Title and Key-Word Index" was compiled by the Oakridge National Laboratory for the Department of Housing and Urban Development. This bibliography was obtained, but, although it contained approximately 1,200 articles, most of the emphasis was placed on small diameter tunnels in urban areas. With the exception of two publications, there was almost no mention of remote sensing applications to tunneling. A second major source of reference material was obtained from the standing files of the contractor, subcontractors, and consultants. Several papers were found in the Proceedings of the 1972 North American Rapid Excavation and Tunneling Conference. All of the documents obtained were reviewed according to subject, but formal review summaries were not prepared. The titles and authors of these documents appear in Appendix A.

3.3 Cost Effectiveness Evaluation

In approaching the question of cost effectiveness, it is not meaningful to state one cost savings figure and label it "cost savings to tunnel site investigations using remote sensing techniques," because each tunnel site is unique. The geologic, environment, and engineering considerations at a particular tunnel site determine the investigation procedures. What is more meaningful is to identify unit costs of investigation techniques and unit costs of construction. The question in this context is similar to the question of should one buy insurance. You may never need it, but if you pay a small premium to get the best coverage it may be possible to avoid financial disaster. In tunneling, the purchase of an additional unit of site investigation may not be needed, but if a feature that could slow or stop the construction is found by further investigation, then the cost is more than justified.

We made several assumptions in evaluating the cost effectiveness of applying remote sensing techniques to tunnel construction:

- The information obtained from remote sensing systems will supplement, not replace, information obtained by

16

conventional ground methods.

- As the first stage in a multistage investigation, remote sensing will optimize conventional field investigation by identifying geologic and hydrologic anomalies and directing second stage field investigations. The expenditure for field investigations may be reduced.

- The additional unique information provided by remote sensing will improve the three-dimensional geologic model for the proposed tunnel. A model is critical in estimating tunnel support requirements, selecting the method of driving the tunnel, estimating the time required to complete the tunnel, allocating resources, and planning safety procedures.

Section 9.2 and 9.3 contain a discussion of the capabilities and an approximate range of costs of conventional methods of field investigation systems. However, costs are site specific and can vary greatly depending on such factors as geologic conditions, site accessibility, local topographic relief, and climate. The effectiveness of a system is based in part on a need for information and the capability of the system to fulfill that need.

4.0 TECHNICAL DISCUSSION

This section summarizes previous work in remote sensing related
to tunneling, geology, and hydrology. It describes tunneling conditions
in terms of significant geological features and it summarizes the
design capability of various remote sensing systems and the criteria
used for selecting these systems for this investigation.

4.1 Previous Work

Whenever a new technology emerges, or an existing technology
is applied to a new area, or an old one is reborn, there is
almost invariably a flurry of experiments and investigations that
are similar to previous work. The reason for this is that most
investigations begin from common ground; that is, they are founded
on established theories and proceed toward unknown or unproven
hypotheses. Almost any literature survey supports this observation.

Parker (1968) has made the prediction that "aerial reconnais-
sance someday will supplant soil augers, rock drills, surface
reconnaissance, and geophysical surveys as the engineer's prime
means of obtaining information about soils and rocks." Although
there have been significant advances in the state-of-the-art,
aerial reconnaissance techniques can't yet replace conventional
techniques. Furthermore, it is unlikely that this will occur in
the near future. Mr. Parker notes "that the future application
of remote sensing to engineering problems is more dependent upon
improvements in image analysis rather than improvements in remote
sensing equipment." This is a significant point, because even
though experts in data analysis and photointerpretation will con-
tinue to improve their techniques, the highway or tunnel engineer
must apply these techniques, and based on his experience, must
make contributions to the development and improvement of analysis
techniques. However, as the paucity of remote sensing literature
related to tunneling attests, little interest and perhaps consider-
able skepticism surrounds remote sensing application to tunneling.

Szechy (1970) in his book "The Art of Tunneling" mentions
the importance of aerial photographs for studying geologic features
including faults, folds, and rock outcrops. He also indicates
that by analysis of vegetation types it is possible to estimate
"gross chemical characteristics, and thus the origin (igneous or
sedimentary) of the underlying bedrock." Szechy quotes a list of
geologic features and tunneling conditions published by Stinni
(1950):

18

1* The orientation of rock stratification (whether horizontal, sheet like, moderately inclined, steeply sloping, or over folded).

2* The thickness of individual layers, the regularity of the sequence of rock layers or changes in mountain types.

3* Mineralogical composition (detrimental components).

4 The crystalline structure of rocks (uniform grains, porphyritic).

5 The bonds between the individual grains (strong, weak, direct, indirect).

6* A hardness of the rocks, whether they would allow for drilling or blasting.

7* The structural form of rocks (massive, stratified, or shaley).

8* The internal structure (whether solid or porous, with closed or open voids).

9* Deformation suffered during the origin process (cleavages, joints, crushed zones, faults) or other effects (such as weathering, mylonitization, or koalinization).

10 The probable bearing and tensile strength of the mountain at various tunnel sections.

11 The stability of the mountain, the character and magnitude of probable rock pressure.

12 The bulk densities and dead weights of component rocks.

13 The anticipated durability of various rock types to be penetrated, the length of entrance sections to be lined with regard to the danger of frost effects.

14 The depth and composition of cover of each point of the tunnel for each rock constituent.

15 Temperature conditions affecting the mountain.

16* Hydraulic conditions at the construction site and its environment.

17 The possibility of the occurrence of harmful gases.

18 The susceptibility of structure to earthquakes and artificial vibrations.

19* Surface formations

20 Safety against escaping air in anticipation of operations involving compressed air.

21* Hazards to structures and especially to entrance portals by forces of nature (rock slides, rock falls, avalanches, or slumping).

The work of some of the pioneers who have applied advance remote sensing systems and analysis techniques to tunneling, geology and hydrology is presented in the overview of sensors evaluated during this study. These sensor systems include:

- SLAR (Side Looking Airborne Radar)
- Photographic systems
- Scanning systems (multispectral and thermal)
- Airborne geophysical systems
- Imaging satellite (orbital) sensor systems

The first imagery of the earth from satellite platforms, acquired in the early 1960's by the first weather satellites and early manned spaceflights, presaged the value of such data for earth resources. With increasing coverage by Gemini and early Apollo flights, it became apparent that a satellite devoted solely to the acquisition of earth resources information was needed. The first such satellite, known as ERTS (Earth Resources Technology Satellite), launched in July of 1972 not only provided earth resources data, but provided repetitive coverage of each area every 18 days. Today, a second satellite (the system is renamed LANDSAT) is orbiting in addition to the first, giving nine-day repetitive coverage.

In four years since the launch of LANDSAT-1, many investigators have described capabilities that can be of importance to tunneling. Some of these include identification of: lithology and lithologic boundaries, geologic structure, fractures, landslides, alteration zones, intrusions, and various geomorphic features.

Collins et al. (1974) and Saunders (1974) noted that the boundaries of many surficial deposits can be mapped quite accurately, but that other inferred lithologic boundaries appear to parallel, but do not necessarily correspond with previously mapped boundaries. Houston (1975) and Collins et al. (1974) noted that in some instances it was possible to identify and revise the location of contacts on existing geologic maps. Miller (1975) states that boundaries between rock types can be traced from the LANDSAT images even though the nature of the lithology is not clear. He further states that in some instances it is possible to make some identification of lithology.

Sawatzky, et al. (1975) studied the relationships of linear features to joint systems and large geologic structures and discussed techniques to extract geologic information. Other investigators have also discussed techniques to analyze structural features and lithology (Podwysocki, 1975; Goetz, 1975; and Vincent, 1973a). MacDonald and Grubbs (1975) made an important contribution to highway and tunnel construction by correlating linear features

20

detected on LANDSAT imagery with landslide prone areas along major highway routes. They state:

> "The weathering properties of various rock types, which are considered in designing stable cut slopes and drainage structures, appear to be adversely influenced by the location and trend of LANDSAT identified lineaments. Geologic interpretation of LANDSAT imagery, where applicable and utilized effectively, should provide the highway engineer with a new tool for predicting and evaluating landslide prone areas."

Campbell et al. (1975) has used satellite and aerial photography to detect lineaments for planning mine openings. Campbell also describes the use of this data and core boring to develop a geologic model of roof conditions prior to the development of an underground mine or major extension of a mine. He estimates that the labor and materials required to stabilize the roof of the mine openings may be 35% of the total cost of mining. Roof support requirements are related to geologic conditions, and therefore an accurate forecast of geologic conditions before excavation of main haulageways is essential to accurate estimates of mine development costs.

In addition to LANDSAT data, high resolution black-and-white, color, and color infrared imagery and photography is available from the three manned Skylab missions which began in 1973. Skylab photography has several advantages over LANDSAT data including greater spatial resolution, stereoscopic coverage, true color and color infrared film rather than color composites. One disadvantage, however, is that there is no repetitive coverage and areal coverage is limited.

Several investigators (Bechtold, et al., 1975, and Sawatzky, et al., 1975) identified zones of alteration associated with mineralization. They have also described the geologic significance of linear features detected on Skylab photography. Amsbury et al. (1975) used Apollo, LANDSAT, and Skylab data as a reconnaissance tool for mapping geologic features including soil tones. Cassinis et al. (1975) have used Skylab multispectral scanning imagery for hydrologic analysis. By digitally enhancing the images using a ratio and product algorithm and with suitable ground truth, Cassinis was able to identify moisture differences between soil types over paleo-river beds. The significance of this capability is that it not only predicts hydrologic conditions but estimates the trafficability of certain areas.

The overall assessment of satellite acquired data is that it is extremely useful for identifying regional geologic structural

relationships (Abdel-Gawad, 1975, Liggett, 1974, Collins et al., 1974, and Wilson, 1975).

Radar imagery has several distinct advantages over satellite data when it is used as a reconnaissance tool. Radar has an all-weather, day/night capability, it has better resolution than orbital data (16 to 25 meters), and stereoscopic coverage is available. Several authors discussed the day/night and all weather capability of radar imagery (Dellwig and Burchell, 1972; Viksne et al., 1970; Crandall, 1969; Hackman, 1967a; Am. Soc. of Photogrammetry, 1975).

The first semi-operational radar survey that generated wide-spread interest was conducted in 1967 over a 17,000 square kilometer area in Darien Province, Panama. This survey reported on by MacDonald (1969); Crandall (1969); Viksne et al. (1970); Wing (1971); Dellwig and Burchell (1972); demonstrated radar capability to: obtain slope and relief data; make lithologic boundary discriminations; identify drainage patterns; and obtain data on vegetation, geologic structure, and soil moisture. Perhaps the most impressive capability of the radar system was the ability to gather this data even though the Darien Province is almost always cloud covered.

Wing (1970) discusses the advantages of the synoptic view that radar imagery gives and the suppression of detail which often complicates the analysis of aerial photography. Many regional linear features that may have geologic significance often have topographic expression that is enhanced by radar imagery. MacDonald, et al. (1969) and Reeves (1969) discussed the importance and geologic significance of lineaments not previously mapped. Geologic analysis including identification of boundaries and description of rock type is possible also on radar imagery. "Sedimentary and volcanic rocks, their metamorphic equivalent, and igneous rocks may be separated from one another on radar imagery" (Am. Soc. of Photogrammetry, 1975). Hackman (1967) reported that gypsiferous and calcareous sedimentary rocks appeared as very light tones of gray in contrast to darker shales and sandstones on radar imagery. Moore and Dellwig (1966) differentiated between lava flows and alluvial fan deposits based on the surface texture of those features. Micro-relief (surface texture) and surface drainage patterns can often be used to infer a lithologic type. Surface texture (roughness) can, however, be a function of vegetation; therefore lithologic determinations in vegetated areas may not be as reliable (Am. Soc. of Photogrammetry, 1975).

Many authors have discussed the usefulness of radar imagery for analysis of drainage patterns and subsequent geologic interpre-

tation (Dellwig et al., 1968; McCoy, 1969; Gillerman, 1970; Wing, 1970a and b, and 1971; Simonett, 1971; MacDonald, 1969).

Several authors (MacDonald et al., 1967; Clark 1971a) discussed the similarities between radar and low-sun-angle photography (LSAP). Hackman (1967a, b,) reported on both field and modeling studies with LSAP. Among other conclusions he states that optimum solar elevation is determined by the type of terrain. Hackman (1967b), MacDonald et al. (1969), and Slemmons (1969) discussed the importance of selecting the best solar elevation and azimuth for studying terrain. Terrain features of low relief require a lower sun angle for enhancement than do features in areas of higher relief. Clark (1971a, b) stated that linear features are best enhanced with solar azimuths nearly perpendicular to those linear features. Radar has an advantage in this respect in that the azimuth can be controlled. Clark (1971a) also states that radar and low-sun-angle aerial photography are not actually competing systems because they record information from different spectral bands. Lyon (1970) discusses the simulation of radar imagery using aerial photography and concludes that photography acquired at a solar elevation of approximately 27° and processed to increase the contrast of the prints is the best procedure for simulating radar. Commercially, low sun angle photography taken with black and white infrared film has been used successfully in petroleum exploration in Indonesia (Foster, 1974).

Panchromatic (black-and-white) film is the most common type of film used for photogrammetric mapping. High spatial resolution, panchromatic film is also used for geologic structural analysis, topographic analysis, lithologic identification, and stratigraphic description (Am. Soc. of Photogrammetry, 1975). Photographs with a 50%-60% overlap are used for stereoscopic viewing. Topographic contour and structural contour maps can be drawn from stereo pairs. Stereoscopic models are particularly useful in geomorphological analyses; Wolf (1974) describes the method of constructing stereoscopic models. Tator (1949) mapped the bedrock erosion surfaces based on morphological detail. Denny (1952) also used stereoscopic models in his studies of Late Quaternary geology and frost phenomenon along the Alaskan Highway.

Aerial photographs are widely used for analysis of soil type, lithology, vegetation, and field mapping. For a discussion on the interpretation of rock characteristics based on topography, identification of rock type based on drainage patterns and identification of soil type based on erosion patterns refer to Appendix C.

The human eye has a capability of distinguishing over a hundred times more color combinations than it can gray scale values (Evans, 1948). As a result, color photographs can yield

more information for lithologic and soil identification, which are largely based on color differences. Aldrich (1966) reports that photointerpreters can "detect significantly more targets on normal color imagery than on black and white photography." Soil surveys in the past were largely conducted using black and white aerial photography. However, with the improvement of color aerial photographic films, most soil surveys are now conducted using color photos. Many investigators have demonstrated the increased utility of color aerial photographs for soil analyses (Mollard, 1968; Mintzer, 1968; Rib and Miles, 1969; and Parry et al., 1969). Meyers and Stallard (1975), have reported that the combined use of thermal infrared imagery and color aerial photography provided the best results for identification, description and mapping of soil groups (Am. Soc. of Photogrammetry, 1975). Color infrared photography is particularly useful in vegetation analyses. By the use of color infrared imagery, plant species can be differenti- ated, vigor of the vegetation can be determined, and in some cases, stress conditions can be inferred (Fritz, 1967).

When conducting aerial photographic surveys, it is helpful to visit the site at least twice; once before the survey, to plan flight lines and to make a general geologic analysis, and a second time after the imagery is acquired and after an initial interpretation is made, to verify interpreted features and to investigate areas that cannot be satisfactorily interpreted on the aerial photographs. Reed (1940) suggests that final verification be accomplished using aerial photographs by marking places on the photograph where strike and dip measurements are made, and where faults and lithologic contacts are located.

Multi-band photography and multispectral scanning are in principle the same investigation technique. In practice, one is a photographic system and the other is an optical-mechanical system. Many authors have discussed the application of multi- band (multispectral) analysis to geologic mapping (Coker et al., 1969; Fischer 1960, 1962; Meier et al., 1966; Myers and Allan, 1968; Paarma et al., 1967; Paarma and Talvitie, 1968; Pestrong, 1969; Pohn et al., 1972; Tarkington and Sorem, 1963; Vincent, 1972a; Yost and Wenderoth, 1968, 1972).

Many investigators have made attempts to use expected or empirically derived spectral signatures to differentiate, and where possible, identify various rock and soil types. Two important studies have approached the task of identifying spectral responses of rocks, soils, and vegetation on a comprehensive scale. Hunt, Salisbury, and Lenhoff (1970-1974) have published a series of papers about the spectral characteristics of minerals, rocks, and soils in the visible and near-infrared portion of the electro- magnetic spectrum. Their nine papers, to date, have examined:

I.	Silicate Minerals	VI.	Additional Silicates
II.	Carbonates	VII.	Acidic igneous rocks
III.	Oxides and Hydroxides	VIII.	Intermediate Igneous Rocks
IV.	Sulphates and Sulfides	IX.	Basic and Ultrabasic Igneous Rocks
V.	Halides, Phosphates, Arenates, Vanadates, Borates		

The second study is the NASA Earth Resources Spectral Information System: "A Data Compilation," V. Leeman et al., 1971. This report and its supplements include "bi-directional and directional reflectance, transmittance, emittance, and degree of polarization curves in the optical region from 0.2 - 22.0 μm" for rocks and minerals, soil, and vegetation. The NASA Earth Resources Spectral Information System is intended to provide a data base with which remote sensing techniques can be used to identify and describe surface features. Other investigators have analyzed spectral responses on a more limited scope. The identification and description of rocks, minerals, and soils using remote sensing techniques, however, cannot be completely accurate in most instances without field verification.

Atmospheric interference is a major factor accounting for the differences between the spectral response of a specimen in the laboratory and in the field. In the "Manual of Remote Sensing" (Am. Soc. of Photogrammetry, 1975) an entire chapter is devoted to atmospheric effects on remote sensing. They state that the characteristic spectral response of many materials under one set of environmental conditions may be different from the response under another set of conditions. Reflected and radiant energy is absorbed, scattered, and otherwise attentuated by the atmosphere depending on the temperature, type and concentration of atmospheric particulates, percent cloud cover and cloud height.

Another factor that accounts for different responses of identical specimens between the laboratory and field is background or field-of-view interference (Egbert, and Ulaby 1972). In the laboratory under controlled conditions, the energy received by the sensor comes only from the specimen or specimens and a uniform background. In the field, a rock type, for example, might occur in isolated points within the field-of-view. The background in this case may not be uniform and may contribute energy that could amplify or attenuate the energy emitted by the rock. This alteration of the spectral response could be sufficient to cause a mis-identification of the rock type.

The illumination of a specimen in the field is significantly different from laboratory illumination. In the laboratory the prime source of illumination may or may not be spectrally the same as solar illumination in the field. Surfaces surrounding the target in the field and laboratory reflect light, which in

turn, is incident upon the target. The effect of additional energy reaching the speciman from other reflecting surfaces is to alter the spectral response of the speciman. Reflected energy from clouds or the sky is also received by the target and has a similar modifying effect (Piech and Walker 1971a and b).

Another difference between laboratory and field analysis of spectral response arises when the response of a fresh rock surface is used as a standard for field targets. In the field the surfaces of rocks are contaminated by weathering products, lichen, desert varnish, soil or dust, and solution deposits of various minerals. All of these can radically influence the spectral response. This source of difference is not so difficult to control as varying illumination because the contaminated surfaces can also be tested in the laboratory. The composition of rocks, minerals, and soils using remote sensing techniques cannot be entirely based on expected spectral response of a standard or standards.

Gilbertson and Longshaw (1975) conducted an extensive evaluation of multispectral aerial photography as an exploration tool. Their approach was to:

* Measure the spectral response of rocks "in situ."

* Select photographic filters that will enhance a characteristic spectral response based on the "in situ" measurements.

* Obtain "quantitative aerial photography." They use the phrase "quantitative aerial photography to mean that ground objects receiving the same solar irradiance and possessing the same spectral reflectance properties are imaged at the same density on every frame of the final separation positive stage."

* Use additive color techniques to interpret the imagery.

Their "results indicated that the multispectral photography enhanced spectral differences between object categories and displayed geologic context more distinctly than other imagery. However, both features were also well represented in either the color or false color infrared photography. On this basis it was concluded that the additional complexity and costs involved in the multispectral approach to aerial photography was not justified."

Rains and Lee (1975) concluded after statistical analysis of over 8,000 measurements of sedimentary rocks made in the field with a photometer and a series of Wratten filters, which spanned the visible and near-visible portions of the spectrum: "No practical numerical basis exists for selecting any particular spectral band as best for rock discrimination, and in most instances

26

little numerical basis exists for selecting better spectral bands." Therefore, information useful for the design of multiband photography cannot be obtained from the type of "in situ" spectral measurements considered here. Though this may be true, whatever the spectral response of a target, once this response has been associated with that target it can be used in most situations to identify the target material elsewhere on the image. This spectral response, however, may be valid only for the specific time and place of the image. The application of the response to the analysis of imagery acquired on another day or in another location may not be valid.

Lowman (1969) and Lyon (1971) have reported that geologic analysis including description of structure and differentiation of soil and rock type using multiband (multispectral) techniques are more effective when these features are associated with vegetation.

Piech and Walker (1971a,b, 1972a,b, 1974) described positive results using multiband techniques. They developed a technique called "Scene Color Standard" which removes "peripheral effects" such as "source effects, atmospheric effects, and surface reflections" (primarily skylight reflection). This technique is applied to a ratio display (Smith, Piech, Walker 1974). Briefly, the ratio analysis is performed by making color separations from true color aerial photographs. The positive and negative transparencies of these separations from different bands are superimposed under a vidicon tube. The ratio pair is then density sliced by assigning different colors to subtle gradational changes throughout the image. The resultant image is displayed on a color cathode ray tube (CRT) for study or for photographing a permanent record.

Using this technique it is possible to identify differences in soil moisture and textural patterns. This technique promises "More precise aerial survey classification of engineering properties such as drainage class, void ratios, structure and bearing strength with further study" (Piech and Walker, 1972b).

The application of the ratioing techniques of two-channel thermal infrared data (8-14μm) to soil and rock discrimination has been discussed by Vincent et al. (1973), Vincent and Thomson (1972a), and Vincent et al. (1973). Using this technique, it is possible to discriminate between different types of silicate rocks. In their work at Pisgah Crater, California, Vincent and Thomson (1972a) reported that "dacites and basalts were clearly discriminated and were identified on the basis of their thermal ratio values." Vincent et al. (1973) have also applied ratioing techniques to soil analysis. They conclude that "soil color, terrain patterns, natural drainage, and soil texture are enhanced by ratio images."

Rowan and Cannon (1970) were able to differentiate limestone, dolomite, and granite during their work in Mill Creek, Oklahoma. From stratigraphic analysis based on this discrimination capability, they noted that topography has an important influence on the thermal emissivity. The sunlit side of a landform provides better stratigraphic information.

Another capability of thermal infrared images reported on by Rowan et al. (1970) is the delineation of faults and fracture zones. They attribute the detectability of these features to zones of soil moisture. They also note that these zones are not visible on conventional aerial photography. Other investigators (Sabins, 1969; Offield et al., 1970; and Wallace and Moxham, 1967) have reported similar results in lineament and fracture mapping using thermal imagery.

Although significant results have been reported and promising areas of future research identified for thermal imagery, most investigators will agree that these techniques must be used in conjunction with aerial photographic data and field analysis.

Extensive work has been done using airborne geophysical techniques. The two most common techniques are magnetic and electromagnetic surveys. The airborne magnetometer was developed during World War II as a submarine detection system. Following the war it was modified and applied to petroleum, and somewhat later, to mineral exploration (Hansen et al., 1967). Magnetic surveys measure the earth's magnetic field and perturbations or anomalies of the earth's magnetic field caused by varying concentrations of the common mineral, magnetite. This concentration can in turn be "interpreted in terms of rock type and geologic structure," (Strangeway, 1967; Am. Soc. of Photogrammetry, 1975). Because some rocks are more magnetic than others they can be differentiated and the approximate contacts between them located (Strangeway, 1967; Isaacs, 1967). The size, shape, and general structure of the recorded anomalies can be used to infer the shape, depth, and composition of the bodies causing the anomaly (Isaacs, 1967; Smelli, 1956; and many others). The shapes may be determined by faulting, intrusives, mineralization, folds, and flows. Other larger scale structural features can also be detected such as basins and domes. Thus, airborne magnetic surveys can provide considerable information on the structural features and distribution of rock types within a given area.

Electromagnetic systems measure the conductivity of subsurface formations. A transmitter produces an electromagnetic field which extends through the rock according to the conductivity of the rock. The signal is modified by the rocks and returned to the receiver. The most influential factor in the electrical characteristics of rocks and unconsolidated earth materials in the upper or near-surface zone is the free water in the fractures and pores. This is

especially the case at the ultra low frequencies (less than 10^4Hz) normally used in geophysical techniques in order to achieve significant depth of exploration.

The subject of the influence of pore water on conductivity has been treated by several authors, both experimentally and theoretically. Representative data are found in the papers by Zablocki (1962), by Keller (1963, 1971), and particularly those by Brace (1965, 1968a, b, 1971), Parkhomenko (1960 and 1967), and by Levin (1966, 1968, and 1971). The subject is treated by Ward and Fraser in Chapter II, Part B, "Conduction of Electricity in Rocks", in Volume II of Mining Geophysics (1967). Keller (1963) graphs the resistivity of waterbearing sandstones as a function of frequency and water content at 20°C; at 1KHz the resistivities range from 10^6ohm/m for 3.5% water content to 10^3 ohm/m for 53% water. In Parkhomenko's textbook Electrical Properties of Rocks (1967), similar data are given for a variety of sedimentary, metamorphic and igneous rocks. In a coarse grained sandstone, for example, slight variations of water content from 0.18% to 0.34% causes the conductivity to increase from 10^{-8} mho/m to 10^{-6}mho/m. In another example the conductivity of dolomite ranges over 5 decades of magnitude as the moisture content varies only from 0.1% to 1.0%.

Traditionally, airborne resistivity techniques have been used in the search for metal deposits (Mining Geophysics Vol. I and II, 1967). The application of airborne resistivity techniques to detecting differences in the pore-water content of near surface rocks and fractures is a relatively new field of endeavor. Fraser (1972a and b; 1974), Hoekstra and MacNeill (1973), Hoekstra et al. (1975), Culley et al. (1975), Dyck et al. (1974), and Sinha (1973) describe some of these efforts and results. Based on these works it appears that airborne resistivity methods have considerable potential for detecting conductive zones such as shear zones, sink holes and cavernous limestones, conductive overburden etc., of interest to tunnel site investigation. Under many sets of conditions it is possible to infer the orientation of these bodies (Fraser, 1972 a and b, 1974) using the Dighem system.

4.2 Tunneling Conditions and Significant Geologic Features

Engineers involved with the planning and execution of tunnel-driving operations are primarily concerned with the excavation characteristics of the ground and the behavior of the ground during and after excavation. The method of excavation, the construction schedule and the estimate of construction costs rest on an engineering appraisal of the following operational considerations:

a. Is the most suitable method of excavation hand spading, drilling and blasting or machine boring?

b. Will the tunnel face be stable enough to excavate the full cross section of the tunnel in a single operation or will the ground require top heading and bench or multiple-drift excavation?

c. Will the tunnel walls stand without support or will it be necessary to install an initial support system comprised of rock bolts, shotcrete, steel ribs and lagging or linear plates?

d. Will the tunnel encounter dry, moist or wet material and will it be necessary to provide pumping capacity to maintain working conditions?

e. Will the ground exposed in the tunnel bore be stable or will it deteriorate because of swelling, air slaking, or stress-relief fracturing?

f. Will the rocks exposed in the tunnel bore produce toxic or explosive gasses, requiring special safety procedures?

The term "tunneling conditions" is used in this report to collectively refer to those characteristics of the ground and the tunnel which directly affect the tunnel-driving operation.

Geologic science provides the knowledge and techniques to make a major contribution to a preconstruction evaluation of tunneling conditions. Geologic studies identify natural materials; divide these materials into units which can be mapped and projected on the ground surface and the subsurface; and provides a basic understanding of the origin and history of the materials. The end product of the geologic study of a site is a picture or model of the geologic conditions developed from incomplete information.

Tunneling conditions cannot be directly assessed from even the most complete and accurate model of geologic conditions for several reasons. First, the model of geologic conditions is limited to the composition and the geometric characteristics of the ground and does not provide information about the behavior of the ground in a tunnel opening. Second, experience has shown that geologically identical materials behave differently depending upon factors such as tunnel depth, the groundwater head over the tunnel, the cross section of the tunnel, and the method of excavation. The tunnel conditions may be determined from the geologic conditions model by using experience in similar tunnels in similar geologic environments or by using soil mechanics and rock mechanics analysis techniques.

This report is concerned with the collection of geologic information for the geologic conditions model and specifically with the application of remote sensing methods in these investigations. The best test of the application of remote sensing is the capability of these methods to locate or measure those geologic features that generally affect tunnel construction.

4.2.1 Significant Geologic Features

Tunnel site investigations are principally or essentially geologic studies with the specific goal of defining the geologic conditions that may affect the construction of the tunnel. The investigation should be designed, executed and documented so as to efficiently and economically reach this goal. Almost any geologic feature may be significant under certain circumstances, but many of the geologic details that are included in scientific reports on geology are of limited value in this context and may be confusing to the non-geologic readers. For example, the fossils present in sedimentary rocks is a normal and often major part of a geologic report on an area underlain by sedimentary rocks, but the fossils present deserve little consideration in a tunnel site investigation unless the fossils help to define the bedrock structure. The same argument for limiting geologic detail can be applied to small-scale structures or the detailed petrology of sedimentary, metamorphic or igneous rocks.

The term significant geologic features refers to those features, or classes of features, which commonly affect the construction of a tunnel:

• Soil and Rock Type	• Ground Stresses
• Alteration	• Ground Temperature
• Geologic Structure	• Hazardous Gases
• Discontinuities	• Earthquakes
• Groundwater	

These features are briefly described in the following paragraphs.

4.2.2 Soil and Rock Type

Soil type, as determined from either the simple grain-size classification of gravel, sand, silt, and clay or the more specific Unified Soils Classification system, provides a useful indication of the general engineering characteristics of the soil mass and a general indication of soil behavior in a

tunnel. Soil type alone indicates a range of permeability, strength and compressibility, the relative stability of the soil in tunnel opening and whether groundwater control will be an important aspect of construction. Although these judgments need verification by other information and definition by testing, the soil type is an excellent starting point for appraising tunneling conditions.

The geologic classification of rock, based upon mineralogy and grain size, is less helpful than soil classification in assessing tunneling conditions. Some rock types such as granite suggest a reasonably limited range of hardness, stability, and groundwater conditions to be helpful but in most instances the subsurface conditions are not so specifically related to rock type. Shale is an extreme example of a rock name applied to substances with widely varying physical characteristics. Shale may be hard or soft, stable or very unstable, and highly compressible or moderately compressible. Rock type, therefore, is a worthwhile starting point in describing a rock mass but is rarely totally diagnostic of the rock mass.

4.2.3 Alteration

Although geologic materials often appear to be imperishable, most will change if removed from the temperature, pressure, and chemical environment in which they were formed. Under new conditions the mineralogy and the physical properties will change until an equilibrium has been established with the new environment. Alteration is the term which is applied to all these changes whether they occur at the ground surface or at depth in the earth's crust. Of particular interest to tunneling are those changes that occur near the ground surface where soil and rock is exposed to weathering and those changes that occur at depth due to the presence of hot aqueous solutions.

The term weathering is applied to a host of physical and chemical changes caused by air and chemically-active groundwater. The reactions include solution, oxidation, carbonation and hydration. Weathered zones are generally found in the soil and the upper portions of the bedrock but ancient weathered material is sometimes encountered deep within the bedrock. Weathered material generally has less strength and cohesion than the unweathered host material. Weathered bedrock, for instance, may retain the structure of the host rock but have the properties of a soil. The depth of weathering is quite variable depending upon the climate, rock type, and the permeability of the host material. Evidence of

32

weathering in bedrock is often found along joints tens to hundreds of feet below the top of rock and can affect the behavior of the rock mass at tunnel level.

High temperature solutions of water and gas rise from magma sources in the earth's crust along faults and fracture zones. These solutions react with the cooler host rock, locally form ore deposits and more generally change both the mineralogy and the physical properties of the host rock. In some instances the alteration seals fracture zones and improves the bearing strength of the rock mass but these changes also create rock mass conditions that are unfavorable for tunneling purposes. These zones are difficult to locate and evaluate prior to tunneling if the depth of cover is great.

4.2.4 Geologic Structure

Geologic structure is the geometric arrangement of rock units and zones of discontinuity. In geology this term is applied to features such as folds, faults, unconformities, instrusions, joints, cleavage, and schistosity on a scale ranging from hundreds of miles (mega-lineaments) to the field of view of a microscope.

For the purposes of tunnel site selection and evolution, one generally can ignore microscopic features (they are considered properties of the rock material) and the mega-lineaments unless a fracture that is part of this major feature is present at or close to the site. Curiously, mega-lineaments are so large that they are difficult to recognize on the ground or in large scale air photographs, and yet many of them can pose major problems to tunnel construction in the form of major shear zones or seismically hazardous areas. These large features must be considered when selecting the highway route and tunnel site. Features such as unconformities, joints, cleavage and schistosity are considered separately under the term discontinuities to indicate their special significance to tunneling. Faults are considered both a discontinuity to indicate their importance as a rock defect and a structural feature to account for their influence on the distribution of rock units.

The geologic structure of a site is the spatial arrangement of the rock units. This spatial arrangement is of vital interest because the rock at the surface is normally only partially exposed and the rock at tunnel level is normally poorly explored prior to tunnel excavation. The arrangement of the units disclosed by incomplete information is a fundamental part of the interpretation of the geologic conditions.

33

4.2.5 Discontinuities

Essentially all rock masses and some soil masses contain fractures or zones of weakness which affect the engineering properties of the ground and the behavior of the ground during tunneling. These features are collectively referred to as discontinuities in this report. In rock, the discontinuities range in size from major faults, zones of sheared and crushed rock many tens of feet wide and many miles long, to microscopic fractures in the intact rock material. Most numerous are fractures known as joints which are typically less than an inch thick and long enough to cross the tunnel excavation. Discontinuities usually cause the rock mass to have a strength considerably lower than the strength of the intact rock material and also cause the rock mass to have a compressibility and permeability considerably higher than that of the constituent intact rock. At many sites the discontinuities affect the properties of the rock mass to such a high degree that the properties of the intact rock materials are of limited practical significance.

The pattern of discontinuities is usually complex and varies with location in the ground. Fortunately, the pattern can often be approximated by three to five sets of parallel discontinuities with a nearly constant orientation. One of the discontinuity sets is normally along the bedding in sedimentary rocks, the banding in igneous rocks or the foliation in metamorphic rocks. The orientation of the remaining sets depends upon the stress history of the rock mass.

The behavior of ground in the tunnel is difficult to assess because the pattern of the discontinuities is only partially defined during the tunnel site investigation and the properties of individual discontinuities may vary considerably with the detailed characteristics of the feature. Some of the more important characteristics of discontinuities are: orientation of the discontinuity with respect to the tunnel opening; orientation of the discontinuity with respect to other sets; spacing; thickness, character of the filling material; geometry of the opposing surface of intact rock; properties of the intact rock; and hydrostatic pressure. Any information which improves the pre-construction knowledge of the pattern or characteristics of the discontinuities would improve pre-construction assessments of tunneling conditions.

4.2.6 Groundwater

A tunnel is a horizontal well which can drain groundwater and even surface waters. The quantity and rate of water

inflow and the duration of inflow depend upon the local hydrologic conditions including the hydrostatic head, the length of available flow paths, and the permeability of the material around and above the tunnel.

Water inflows affect the tunnel operation in several ways. First, water inflows in either soil or rock can bring soil material into the tunnel that presents a cleanup problem and more importantly tends to weaken the surrounding ground. The loss of a relatively small amount of solid material can turn otherwise stable soil or rock into unstable ground which requires heavy support. Sometimes inflows lead to a subsidence of the tunnel cover that extends to the surface. Large quantities of water inflow present a tunnel dewatering problem which sometimes forces a shutdown of the tunneling operation. Small quantities of inflow are generally only a nuisance unless the ground exposed in the tunnel walls and tunnel floor soften upon exposure to water. Inflows of water can also deplete groundwater storage to the extent that neighboring wells go dry and surface water supplies are affected. Finally, chemically active groundwater can cause damage to the tunneling equipment, steel supports and concrete within the tunnel.

The presence of water-bearing strata, the location of the groundwater table, the potential hydrostatic head at tunnel level and the general permeability of the ground can be determined during site investigations. However, the quantity of inflow and the duration of inflow are difficult to estimate.

4.2.7 Ground Stresses

Geologic studies provide evidence that the stress conditions near the ground surface are complex. This evidence includes active faulting, fold structures formed at apparently shallow depths, and joint systems which indicate the presence of high horizontal stresses near the ground surface. Rock bursts in strong, brittle rocks in quarries and shallow mines provide additional evidence that the stress conditions present in the rock do not always reflect the existing overburden weight.

Techniques developed in recent years to measure the rock stresses around underground openings and in borings have confirmed the presence of stress conditions that are anomalous with respect to existing overburden. Vertical and horizontal stresses both higher and lower than overburden weight have been noted. These measurements indicate that anomalously high

horizontal stresses are more common than would have been suggested from geologic evidence alone.

Anomalous stress conditions are an important factor to be considered in the design of final support systems, particularly in large underground openings. The stress conditions may also be important in the design of the initial support and in the selection of tunneling methods in those geologic conditions where rock bursts may affect the safety of the work.

4.2.8 Ground Temperature

The air temperature in underground openings near the ground surface seems lower than the air temperature outside, but the ground temperature is actually close to the mean annual air temperature. At greater depths the ground temperature normally increases about one degree Fahrenheit (1.8°C) per hundred feet. Fortunately, rock with an uncomfortably high temperature is well below the depth of most tunnels.

High ground temperatures at tunnel depth are, however, encountered in some areas. Hot springs, geysers and recent volcanics are obvious surface evidence of anomalous temperature conditions. High temperatures, however, are sometimes encountered in areas that lack surface evidence of anomalous temperatures but are actually underlain by hot, igneous masses.

Moderate ground temperatures may have little influence on the tunneling operation but high ground temperatures may control the method of tunneling and the progress and cost of the work. The combination of high temperature and high humidity decreases the efficiency of the workmen and this leads to excess fatigue and safety problems. Under extreme temperature conditions, cooling sprays, refrigeration, and shortened working hours may be necessary to cope with the adverse tunnel environment.

4.2.9 Hazardous Gases

Toxic and explosive gases are a frequent hazard in the mining industry because mineral and coal deposits are commonly associated with high concentrations of natural gases. Hazardous gases are less frequently encountered in tunnels driven for civil engineering purposes because these tunnels are generally shallower and less frequently associated with gaseous

36

conditions. However, significant quantities of toxic gases such as hydrogen sulfide, sulfur dioxide and carbon dioxide and explosive gases such as methane are an operational problem at some sites.

Ventilation is the primary means of controlling hazardous gases in a tunnel. Evidence of hazardous gases obtained during the tunnel site investigation provides a warning that the ventilation system should be designed for the removal or dilution of the natural gases, rather than the less stringent requirements of simply supplying filtered air for workmen and equipment. Advance warning of the presence of explosive gases may be used as a basis for specifying the use of explosion-proof electrical equipment in the tunnel. While gas monitoring is normally performed regardless of the evidence collected during the site investigation, the previously undetected presence of hazardous gas during the tunneling operation presents a safety hazard and may delay the tunneling work.

4.2.10 Earthquakes

Tunnels are more resistant to earthquakes than most other civil engineering structures, but there is still the possibility that strong earthquakes may lead to offsets along active faults, damage to or collapse of the lining, and land-slides at the portals. Evidence of recent strong earthquakes at the site may become an important element of the tunnel design and, to a lesser extent, this information may be used in construction planning. Tunnel alignments are normally selected to avoid active faults. If an active fault must be crossed, the crossing may be enlarged to accomodate future movements.

The tunnel lining and the slopes in portal cuts are designed to minimize damage during earthquakes. In some instances the sequence of construction and the method of supporting the ground prior to the installation of the final tunnel lining may be selected so as to minimize damage and construction delays caused by earthquakes.

4.3 Airborne Remote Sensors Considered and Systems Selected for Tunnel Site Investigations

The proliferation in recent years of techniques of remote sensing of the ground environment using active and passive methods would lead one to believe that state-of-the-art devices are available to determine most engineering parameters of the terrain. Even

37

if this were true, considerations such as cost/quality trade offs, availability, and time interact to restrict the number of sensors one should use on a particular project.

During the planning phase of this study, sensing devices covering the electro-magnetic spectrum from very low frequencies (VLF) to gamma radiation (Figure 1) and force fields for application to tunnel site surveys were considered.

Many sensors, including radiometers, scatterometers, active and passive scanner imaging systems, reflectivity sensing devices and force field sensors, have demonstrated capabilities in the detection of ground characteristics under various conditions. With sensors covering such a wide spectrum, differences in emissivity, absorption, scattering, penetration, and resonances can be of value in discriminating and identifying terrain and surface features. Polarization phenomena, stereoscopic techniques, and multispectral analysis methods, such as those used with imaging and reflectivity devices, can be exploited as additional means for discrimination.

Significant surface penetration of up to several feet can be achieved with sensors that operate at the longer wavelengths (3 feet; 1 meter; or greater) or with force field sensors; therefore it is possible to obtain information bearing on subsurface layering and terrain composition with appropriate instrumentation.

Radiometers operate from the long wavelength end of the microwave spectrum into the micrometer region. These devices can provide information on the thermal state of the terrain, certain physical constants, small scale surface roughness, and soil moisture data.

Coherent and noncoherent imaging radar systems generally operate in the X- and K-band regions of the microwave spectrum. Commercially available real aperture (brute force) and synthetic aperture or coherent systems have azimuth and range resolutions of better than 30 feet (10 meters), and produce relatively high quality radar maps of the terrain. Such maps are a valuable adjunct to aerial photographs for tectonic analysis (especially fracture analysis) in the study of hydrology, structural geology, and in lithologic distribution.

Thermal infrared sensor systems (i.e., infrared spectroradiometers and infrared scanner systems) sense emitted energy in the $3.5-5.5 \mu m$ and $8-14 \mu m$ spectral range. Spectroradiometer measurements of rock types show characteristic response curves for certain lithologies, particularly in the $8-14 \mu m$ region of the spectrum, and are useful for remote differentiation and identification of rock types. Thermal scanning devices produce thermograms ("thermal images") of the terrain. Because available detectors are sensitive to a small fraction of a degree, subtle differences in emitted
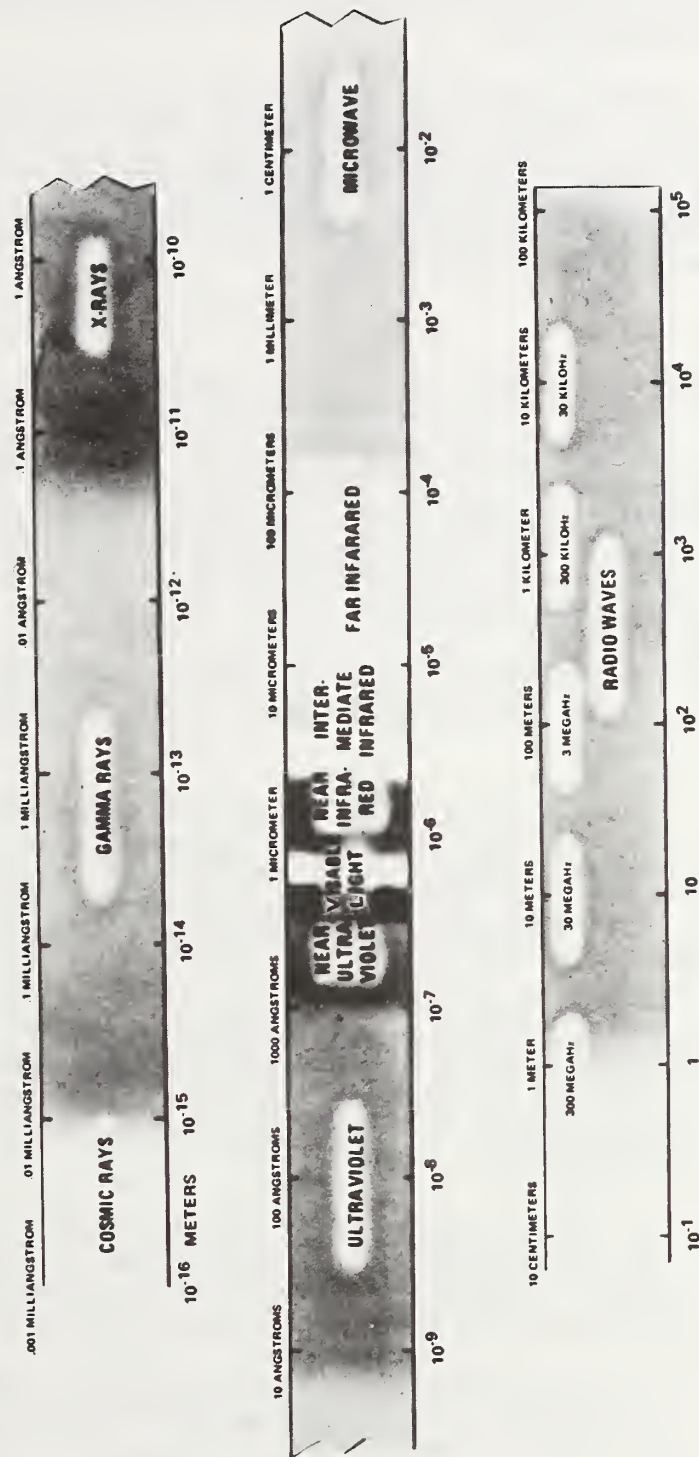
Figure I. Diagrammatic illustration of the electro-magnetic spectrum showing the relative wavelengths. The human eye is receptive to only a small portion of the spectrum lying between 0.4um and 0.7um. Commercially available remote sensors extend this range, but are largely limited to wavelengths between 10^{-7} meter and 1 meter (illustration from "Remote Sensing for Environmental Analysis", Office of Chief Engineer, Department of the Army)

energy can be mapped to provide information about rock boundaries and moisture content. Digital processing of two or more appropriate spectral bands can produce information on iron and silica content of the imaged rock.

Visible and near-visible light sensors are some of the oldest and most highly developed systems. There are numerous cameras, films, and scanner systems that can sense narrow bands in this portion of the spectrum. Appropriate analysis of data from these instruments can provide detailed information relating to a wide variety of disciplines.

4.3.1 Sensor Criteria and Airborne Sensor Selection

With the wide variety of instruments available, a major problem in the development of an airborne remote sensing system for tunnel site evaluation is the choice of the individual sensors in conjunction with the specific airborne platforms utilized and their integration into a cost effective operational system.

Criteria for evaluation of sensor systems appropriate for providing data for tunnel site selection and evaluation include:

- Significance of data to tunnel site evaluation
- Availability and reliability of instrumentation
- Compatibility with related sensors
- Avionics and installation requirements
- Amenability of data to computer analysis

The primary criterion, of course, is the sensor's ability to provide data needed for tunnel site evaluation. In selecting the airborne instrumentation package suitable for assessing the geologic and engineering properties of underlying terrain it is necessary to consider the engineering data requirements.

A second criterion is the availability and reliability of the instrumentation. Ready commercial availability and proven flight reliability of the instruments are critical for cost effectiveness and practical applicability.

In selecting an airborne system, certain compromises are required to achieve compatibility in the choice of aircraft and the desired mode of survey. It is impossible to operate all appropriate systems simultaneously in a single survey. Therefore, it is necessary to conduct multiple

40

overflights at different times and altitudes. In some instances several aircraft are necessary.

4.3.2 Airborne Remote Sensing Systems

The following discussion describes the general function of the various sensors and evaluates their potential application to tunnel site investigations.

Gamma Ray Spectrometry

A gamma ray spectrometer, which measures the gamma rays emitted by radioactive minerals, has a certain amount of application to identification of rock types. This is based on the fact that acidic igneous rocks show a higher radioactive potassium content than the more basic rock types. Characteristic uranium-thorium ratios and uranium-potassium ratios can also be identified for different rock types. Similarly, the soils derived from these rocks will exhibit the mineral composition of the underlying rocks. The gross resolution and limited discrimination of this sensor offer only marginal benefit to tunnel site evaluation, and it was not incorporated into the study.

Ultraviolet Imagery

Ultraviolet imagery can uniquely identify certain rock and soil types. Preliminary work has indicated that carbonate and phosphate rock types show characteristic spectral features in the UV range which make them easier to identify than in the visible range. Aerial photography has been obtained in two narrow bands in the UV using a camera having a quartz lens and interference filters centered in the UV, but because of the low light levels present in the UV, a long exposure time, and precise image motion compensation are necessary to obtain sharp pictures. Multispectral scanners with electronic amplification have simplified source data acquisition problems, but poor signal-to-noise ratio and low resolution due to atmospheric diffusion and attenuation limits the value of data from this portion of the spectrum for tunnel site evaluation. For these reasons no special effort was made to acquire ultraviolet imagery.   However, one band of UV data (.38μm) was acquired during the multispectral scanning survey, but did not make a significant contribution to the study.

Metric Camera

Until very recently, aerial surveys for civil engineering applications have relied largely on black-and-white

metric frame photography. The reasons include the need for geometric fidelity, the better resolution achieved with black-and-white panchromatic film compared with color film, the relative ease of black-and-white film processing, and the adaptability to photogrammetric stereoscopic plotting. Although black-and-white metric photography may continue to provide the data base against which other data can be correlated, it was necessary to evaluate conventional color and color infrared photography of various scales for site investigations.

Color aerial photography, both natural color and color infrared, should make an important contribution to tunnel site investigations. Not only can they provide quantitative topographic data, but can also contribute to the evaluation of the stratigraphy, structure, hydrology, and indirectly to the petrology of the area.

For regional evaluation of the tunnel sites, small scale color infrared photography, due to superior haze penetration properties, was considered of greatest utility. At scales larger than 1:12,000, natural color photography complements color infrared photography; therefore both film types should be used.

Low-Sun-Angle Photography

Low-sun-angle photography (LSAP) combines the high resolution and geometric fidelity of metric camera photography with the "shadow" enhancement capability of radar (SLAR) to highlight topographic features. Virtually any aerial camera can acquire LSAP by using panchromatic or black-and-white infrared film with a deep red filter. To duplicate the low angle of illumination characteristic of SLAR, imagery is acquired during the early morning or late afternoon or in the midwinter so that the sun elevation is between 10° and 30°. This produces a high contrast image with strong shadow effects that emphasize geomorphic features which may be related to geologic structure. Textural characteristics of particular rock types and linear topographic features associated with fractures are emphasized (Lyon, et al., 1970).

LSAP does not offer the complete freedom to select illumination directions that SLAR does. However, by choosing the time of year and the time of day, one can acquire LSAP photography in the northern temperate zone with illumination directions that range about 70° to 290° right azimuth. The potential of this type of imagery, plus the relatively low cost of acquisition, make this photographic technique worthy of inclusion in this investigation.

Multiband Cameras

Multiband (or multispectral) aerial photography uses several film-filter combinations to obtain a spatially coincident set of photographs in different bands of the spectrum. This technique can cover the near ultraviolet, visible, and near infrared portion of the electromagnetic spectrum. The short wavelength limit of spectral sensitivity is approximately .26μm because of ozone absorption in the atmosphere. The long wavelength limit is at .98μm imposed by the current limit of spectral sensitivity of available practical photographic emulsions.[1]

The atomic lattice structure and molecular arrangements of materials cause them to absorb, transmit, and re-radiate incident electromagnetic energy at characteristic wavelengths, intensities, and/or polarization. Surface characteristics cause diffuse or specular reflection as well as polarization changes. A difference in spectral reflectance of objects is detected as images of different density on a set of multispectral photographs. To insure that this density difference is in fact caused by the difference in spectral reflectance of the object on the ground, the camera system should be spectrophotometrically calibrated, the spectral distribution of the illumination should be known, the spectral bands covered by each photograph should be correctly chosen, and the film processing should be precisely controlled. Under such conditions it should be possible to obtain image densities which can be related accurately to the spectral reflectance of the object. Photography acquired in certain spectral intervals in the visible and near infrared, when acquired with suitable film-filter combinations, is a useful tool in the discrimination of surficial geologic character.

It is desirable to evaluate such a system in order to determine if the data derived might eliminate the need for more complex, expensive multispectral scanner data. However, because the preliminary investigations included a 10-channel multispectral scanner, this sensor, after considerable deliberation, was not selected.

_____

[1] Color infrared film has an upper spectral limit of sensitivity of 0.9μm. Black-and-white infrared films of greater spectral range are of low resolution and were deemed of little value to this study.

Multispectral Scanners

Multi-channel scanner systems detect and record energy in narrow spectral bands simultaneously over a broad range of the spectrum, extending from the near ultraviolet through the thermal infrared spectral regions. These systems convert the detected electromagnetic energy into electrical signals which are recorded on magnetic tape. These systems have several advantages over film recording devices. The spectral sensing and signal dynamic range is much greater than that of film. Low energy levels at both the upper and lower spectral limits of the visible range do not adequately expose photographic film, but this problem is less serious with scanning systems because the detected energy is electronically amplified. This amplification permits filtering to much narrower spectral bands than is possible with camera systems.

For convenience, multispectral scanners are grouped into two classes: those that detect reflected energy and must operate during daylight hours, and those that sense emitted energy and can operate day or night (thermal scanners).

The tape recorded data from multispectral scanner systems are readily adaptable to computer processing. Point by point correlations between spectral bands provides the possibility of signature analysis and image enhancement. The near infrared spectral zone, ($.7-3.0\mu m$) contains several spectral absorption bands resulting from H_2O and CO_2 concentrations in the atmosphere. For water and soil moisture discrimination a single channel of data positioned adjacent to a water absorption at $1.138\mu m$ should provide useful information concerning fractures, faults, and landslides or talus that concentrate moisture. The Fe^{+3} ferric ion has a strong reflectance minima at $0.7\mu m$ (Hunt and Salisbury, 1971) that can identify iron-rich rocks when ratioed with strong reflectance spectral bands (Hunt and Salisbury, 1971; Vincent, 1973). Because of the range of spectral coverage and flexibility in analysis multispectral scanner data was acquired for this study.

Infrared Scanners

Monochromatic and polychromatic sensing of reflected and emitted infrared energy can significantly complement visual photography and video sensors. This enables delineation of vegetation boundaries, water courses, soil moisture differences, rock discontinuities, gross lithologies, and other features of interest in site selection. In the spectral band from $.9-5.5\mu m$ the energy radiated by an object ranges from predominantly reflected solar energy at the shorter wavelengths to predominantly emitted energy at the longer

44

wavelengths. Thus, for the sensing of energy of wavelengths shorter than about 3.5μm, daylight conditions must prevail.

Of greater interest is the emitted thermal radiation from the terrain in the 8-14μm atmospheric window. Several investigators (Lyon, 1964, 1972; Watson, 1971b; Lowman, 1969) have demonstrated that soil moisture boundaries, water courses, and some lithologic boundaries can be detected by single channel analysis of day or night imagery using the differences in thermal emission between such features and surrounding terrain.

Silica exhibits emittance minima at approximately 8.1-10.1μm and 12.1-13.0μm (Vincent, 1973). Vincent (1972 b and c) reported that by ratioing appropriately selected thermal spectral bands, the presence of silica could be detected. The more acidic the rock, the greater the variation. This provides a measure of the silica content of the rock.

Based on the potential of this sensor to aid in identifying dissimilar rock types such as basic dikes in acidic rocks, sandstones from non-siliceous rocks, and subtle differences in soil moisture content, a dual-channel thermal infrared scanning system was considered to be an important sensor for testing during this study.

Infrared Spectroradiometry

Infrared spectroradiometry in the 8-14μm region can yield mineralogical and chemical composition data for dry rocks barren of vegetation by matching the incoming spectrum with standard curves in the memory of a computer.

Lyon (1964) pioneered analysis of multispectral data in the 8-14μm range and demonstrated the ability to identify gross rock types remotely by their characteristic response curves. The technique, however, is still experimental and suitable sensor systems are not commercially available.

Microwave Radiometer

A radiometer consists of a highly sensitive receiver and antenna operating in the microwave spectrum between 1 and 100 gHz; it is designed to detect apparent microwave surface temperatures. Microwave brightness depends in a complicated way on the physical, chemical, and electrical properties of the terrain observed by the radiometer. Thus, it is difficult to associate terrain composition and structure with isolated measurements of the passive emission. However, multispectral radiometric images properly corrected for atmospheric and surface roughness effects can provide lithological data. Poor

resolution and low signal levels and emission differences produced by variations in surface roughness and soil moisture make this instrument of limited value for tunnel site investigation and it, therefore, was not used.

Scatterometers

A radar designed to measure the surface scattering coefficient is called a scatterometer, and experiments conducted to define the interaction of electromagnetic waves with rough surfaces have been grouped into a field of study called scatterometry. Scattering coefficient of the terrain varies as a function of incidence angle, aspect angle, frequency, polarization, and the surface texture.

The scattering coefficient varies markedly as the angle of incidence of the transmitted wave is varied. It is determined primarily by the large scale features of the terrain at near-vertical incidence and by the small scale structure at near-grazing angle.

Because the scattering coefficient is a function of the transmitted frequency, useful information can be obtained, in principle, from a scatterometer that sweeps over a fairly narrow frequency band. Presumably a scatterometer that obtains a complete frequency response curve over several octaves of frequency would permit unique determination of most radar targets. In general, the scattering coefficient becomes independent of polarization for very rough terrain. However, for slightly rough terrain the coefficient might be greater for vertically-polarized waves than horizontally-polarized waves. Consequently, the coefficient is dependent on the frequency, angle of incidence, and the type of terrain.

The application of scatterometry to tunnel site evaluation does not appear profitable in that data analysis is complex, the results are uncertain, and other sensors and ground observations will provide better information.

Imaging Radar

Side Looking Airborne Radar (SLAR) is an all weather system which can be used day or night for imaging the earth's surface when more conventional aerial photographic means are not possible. SLAR is an active "system" because it transmits its own energy via a directable antenna and it receives that portion of the energy that is subsequently reflected by the terrain back toward the aircraft.

Radar uses electromagnetic energy of a much lower frequency and much longer wavelengths than either infrared scanners or aerial cameras, and thus achieves several advantages. These advantages include: 1) Radar wavelengths are sufficiently long such that they are not reflected or scattered by the relatively small size water particles in clouds; this makes data collection possible in areas of continuous cloud cover. 2) The longer radar wavelengths (greater than 20cm) penetrate vegetation such as scrub brush and forest canopies, and, thus, achieve more accurate depiction of terrain features. 3) The smaller scale and larger area of coverage of radar images permits regional lithologic interpretation not possible on larger scale aerial photography and not discernible on lower resolution small scale satellite imagery.

Radar frequencies range from VHF to the EHF with wavelengths ranging from 1 centimeter to over a meter. The longer wavelength radars have the greatest potential for vegetation penetration and to a more limited extent, soil penetration. Ka-band, with the shortest wavelength (1 cm), has the greatest potential for mapping vegetation and more finely "textured" terrain.

The phenomona which controls what is recorded on a radar image is called radar backscatter. Backscatter is affected by a combination of the aspect angle, surface roughness, and dialectric constant of the terrain. The greater the dialectric constant, the greater is the percent of the transmitted energy reflected. Where the energy is reflected depends upon the aspect angle and surface roughness of the terrain relative to the wavelength of the radar signal. For instance, a lake surface or a flat metal roof both have very smooth surfaces and high dialectric constants and thus will reflect a high percentage (95%) of the incident radar energy. However, because the angle of incidence is always equal to the angle of reflection, the backscattered energy reflected toward the radar aircraft from the lake will be near zero as all the energy will have been reflected away. The energy returned from the roof may be zero or larger, depending upon its aspect angle. A level plowed field and a level road have similar dialectric constants and aspect angles, but the plowed field will return much more energy because of its greater surface roughness.

Multispectral radar using two bands such as L-X Band is useful for analysis of both gross geomorphologic features and fine-textured vegetation. A given surface may appear smooth to an L-Band (30 cm) wavelength, but rough to a Ku-Band (3 cm) wavelength and discrimination between surfaces is therefore possible.

47

Polarization of the transmitted wave and acceptance polarization of the receiving equipment is another means of classifying terrain properties. Some radar systems can transmit and receive in both horizontal polarization (HH) and vertical polarization (VV), while still other systems can cross polarize (HV or VH) and do any combination of the above in two bands.

Shadowing is a normal and unavoidable phenomenon in radar mapping which occurs because the radar transmitter illuminates the terrain at a low angle. Thus, for a given altitude and ground range, if an object such as a mountain blocks the signal, no radar data will be obtained from targets behind the mountain. This "shadow" area will be imaged as black on the radar positive prints and its effect is a shadow enhancement of topographic and geologic features.

Because of its sensitivity to aspect angle and surface roughness, radar imagery provides an excellent synoptic picture for regional geological structural evaluation of an area, particularly if the area possesses moderate to low relief. The imagery is small scale, even with enlargement. However, this can be an asset because it eliminates distracting detail which might otherwise obscure useful geologic structural information. SLAR surveys require sophisticated aircraft and instrumentation, and commercial surveys are expensive. SLAR imagery flown by the U.S. Air Force was available for both test sites at a nominal cost.

Airborne Geophysical Surveys

Airborne geophysical contractors provide routine surveys that measure variations in three basic properties of rocks near the surface.

1. Variations in the magnetic field strength caused by the geometry and differences in content of magnetic minerals in the rocks.

2. Variations in the induced electromagnetic field strength caused by the geometry and primarily by differences in conductivity of near surface rocks.

3. Variations in the intensity spectra of gamma radiation caused by differences in the content of radioactive elements in the surface rocks.

The routine surveys conducted by these contractors use instrument systems that are designed with specific raw material exploration programs in mind. These systems have much higher capital costs and much higher hourly survey costs than

48

equivalent ground survey systems. The only justification for these higher costs is the much lower unit cost in large area surveys. Cost effectiveness comes generally from the mapping of relatively large areas on more of a reconnaissance basis than ground surveys. Thus, there is a great reduction in but not an elimination of the area to be covered by ground surveys.

Airborne Electromagnetic Systems

Airborne electromagnetic (AEM) systems are designed to measure variations in the conductivity of the ground beneath the aircraft. Many major fracture zones are substantially more conductive than the rocks that contain them when water, graphite, or metal sulfides are present. AEM systems operate at frequencies from about 300 Hz to 8,000 Hz. The lower frequencies explore depths down to perhaps as much as 650 feet (200m) beneath the earth's surface. The systems basically consist of two coils; a transmitter, and a receiver coil. A generator loads the transmitting coil at the frequency desired and the secondary fields at the receiver are measured and referenced as to phase. In some systems more than one receiving coil is used and in some more than one frequency is used. In general, the lower the frequency the greater the depth of penetration, but the less discrimination of conductivity and resolution of anomalies in space. Lower frequencies also require heavier power generators and larger aircraft.

There are a great many AEM systems available from many contractors, and almost all surveys are flown by the contractors because most systems are very difficult to install and operate.

The quantity measured by EM systems is the rock conductivity multiplied by some significant dimension of the conductor (for veins, fault zones and tabular bodies, it is the conductivity multiplied by the thickness of that body). The frequency range is chosen for good conductivity discrimination among the better conductors. Some of these systems are capable of determining the orientation as well as the location of conductive zones, thus making it possible to determine the strike and dip of major shear zones that contain water or for some other reason are good conductors. Such systems have the potential of providing valuable engineering data, particularly in igneous rock sites. It is also one of the few airborne sensors with a capability of sensing beneath the earth's surface. Based on these factors, it was recommended for testing on one tunnel site.

Airborne Magnetometer

Designed during World War II to detect submarines, the airborne magnetometer measures either variations in the earth's magnetic field or the total magnetic field with great precision. The variations in the earth's magnetic field are due primarily to variations in the concentration of two minerals: (1) magnetite, a very common mineral whose concentration varies systematically and predictably with rock type; and (2) pyrrhotite, a rather uncommon mineral often associated with massive copper-zinc sulfide ore bodies and sulfide-iron formations.

Aeromagnetic surveys are generally included when other airborne geophysical surveys are flown because the additional cost is small and the data are a useful aid in interpreting other sensor data. For these reasons, a magnetometer was included in the AEM survey package.

4.3.3   Satellite Remote Sensors

The LANDSAT-1 satellite can acquire multispectral imagery every 18 days, atmospheric conditions permitting, of any specific point on the earth's surface between Lat. 81°N and Lat. 81°S latitude. In January 1975, LANDSAT-2 was launched and was placed in an orbit such that it is now possible to obtain repetitive coverage every nine days, or less at higher latitudes. Four spectral bands of data ranging from .5-1.1μm are obtained simultaneously, permitting the composite reconstruction of false color images. Although the resolution of the system is approximately 250 feet (80 meters), the imagery has proven to be an excellent source of regional geologic data. This is particularly true for mapping lineaments and fractures. Analysis of LANDSAT data in conjunction with high, medium, and low altitude aerial photography has shown that many obvious lineaments on LANDSAT imagery are not identifiable on the larger scale photography. This indicates that the satellite data is a source of valuable and unique geologic information.

Imagery and photography from the Skylab satellite has better spatial resolution than that from the LANDSAT system, but only limited amounts of data were obtained because the film and tapes were hand carried back to earth.

The acquisition of LANDSAT and Skylab imagery is recommended for each site to obtain the regional geologic "picture" of the tunnel site. Selected LANDSAT imagery

obtained during the various seasons of the year should be used because experience has demonstrated that some geologic information is emphasized by certain seasonal changes.

4.3.4 Other Remote Sensors

There are several remote sensing instruments, particularly those that operate in the radio frequency range, which show some potential of providing useful data for tunnel site studies; however, they are either unavailable commercially or are in the development state. These include imaging microwave radiometers, long wavelength monocycle radar, and multifrequency SLAR systems. Still others, while available commercially, are judged to be of little value to the program, either because low value or redundancy of the data acquired, or too high a cost of data acquisition. In this category are included the scatterometer and the passive microwave radiometers. Some systems, such as the airborne gravity meter, have such gross resolution that it is of little value for tunnel site studies.

4.3.5 Sensor Complement Selected

After consideration of the potential contribution of the various remote sensors, their commercial availability and comparative cost, the following suite of remote sensors were selected for use in this investigation and evaluation:

    a. LANDSAT imagery
    b. Skylab photography
    c. Radar imagery
    d. Low-sun-angle photography (LSAP)
    e. Medium and large scale aerial photography
        1. natural color
        2. color infrared
        3. panchromatic black-and-white
    f. Multispectral scanner imagery (visible-near-visible)
    g. Dual-channel thermal infrared imagery
    h. AEM
    i. Magnetometer

51

5.0 SITES SELECTED

5.1 Carlin Canyon Tunnel Site

5.1.1 Project Area Description

The Carlin Canyon was produced by the Humboldt River where it cuts through the Adobe Pinon Range (Figure 2). This northerly trending mountain is one of a series of fault block mountain ranges characteristic of much of Nevada. The range is narrow and where intersected by the Humboldt River it is approximately four miles (6.4 km) wide.

The name, Carlin Canyon, is restricted to that portion of the river valley which forms a narrow, horseshoe-shaped bend nearly a mile (1.6 km) long and a quarter (0.4 km) wide. The canyon appears to be a superimposed stream meander, but fractures and bedrock structure have influenced the final shape of the channel.

The elevation at riverbed level is approximately 5,000 feet (1,500 m), but rises abruptly to over 5,500 feet (1,675 m) within a horizontal distance of 600 feet (180 m). More gently sloping terrain extends to an elevation of over 6,600 feet (1,830 m) at Buckskin Mountain four miles to the south.

The curvature of Carlin Canyon is too small to meet interstate highway curve specifications. It was, therefore, necessary to construct a 1,500 foot (457 m) tunnel through the 500 foot (152 m) high ridge in the canyon. This north-south trending ridge is largely covered with talus and soil on the western side. The eastern side exhibits steeper slopes, numerous bedrock exposures and scattered accumulations of thin soil.

5.1.2 Geologic Setting

The Carlin Canyon tunnel site is located in north-eastern Nevada in an area of the western United States known as the Basin and Range physiographic province. This is an area of long, narrow, fault-block mountains separated by broad closed basins that are partially filled with alluvial deposits.

The bedrock of the area is mainly marine sedimentary rocks formed in shallow and deep seas that covered the area during the middle and late Paleozoic era. These deposits were laid down in tabular units which are relatively thin but laterally extensive. Uplift and erosion interrupted deposition of these sedimentary units at least once in the Carlin

52

Figure 2. This northward looking view across Carlin Canyon shows the arid condition of the area. The angular unconformity between the Diamond Peak conglomerate and the overlying Strathearn limestone is visible in the bend of the river at the upper left corner of the picture. The same unconformity is present, but less distinct, in the lower right corner of the photograph. (Photograph courtesy of the Nevada State Department of Highways)

53

Canyon area, and destroyed the parallelism of successive units and created an angular unconformity.

Non-marine conditions have persisted in the area since the late Paleozoic era. Tectonic forces have created major faults, minor folding, and some volcanic activity. The present-day ranges are the result of movements along mainly north-south faults. The total movement along these faults appears to be on the order of 10,000 feet (3,048 m). The present maximum relief of 3,000 feet (914 m) to 4,000 feet (1,219 m) is the result of continued erosion of the uplifted ranges and partial filling of the intervening basins.

The climate of the area is arid but a more temperate climate has prevailed in the past. There is evidence that the area had a humid climate with forests and extensive lakes during the Pleistocene epoch. This more moderate climate accounts for the gently rounded upland surfaces and the presence of moderately thick soil zones at some locations.

The bedrock of the Carlin Canyon tunnel site is comprised of two formations: the Diamond Peak formation composed of conglomerates, sandstones, and some shale partings; and the Strathearn formation composed primarily of limestone. Both formations are well exposed on the spur at the tunnel and along the canyon walls upstream and downstream of the site. At the base of the canyon walls and along the river the bedrock is covered by deposits of colluvium and alluvium.

The Diamond Peak formation of Pennsylvanian-Mississippian age is the lower or older formation. It is primarily exposed on the west side of the spur and on the west end of the canyon. It is composed of 3-5 foot (1-1.5 m) beds of conglomerate and sandstone with interbeds of shale and siltstone which range in thickness from a fraction of an inch to several feet. The thick-bedded conglomerate and sandstone are well cemented by quartz, chalcedony, and iron oxide, and contain a widely-spaced pattern of joints. The thinner shale and siltstone interbeds are closely jointed in outcrop. The better cemented zones in the rock mass form conspicuous tabular units along the walls of the valley while less well cemented zones are found in narrow grooves and gullies on the outcrops.

The Strathearn formation is a Permian-Pennsylvanian age deposit of hard, medium-to-thick-bedded limestone with thin interbeds of shale. The Strathearn formation is exposed on top of the spur, on the east side of the spur, and on the walls of the eastern portion of the canyon. Most limestone outcrops display several sets of closely-spaced joints of different orientations. These joints, bedding planes, and

shale interbeds limit the average size of the intact limestone blocks to less than one foot (.3 m) in most exposures. The rock in natural exposures, however, appears relatively stable because the small rock blocks have an irregular shape and a high degree of interlock.

The bedding in the underlying Diamond Peak formation has a strike of north 10-20 degrees west and a dip of 85 degrees east. The bedding in the overlying Strathearn formation has a strike of north 15-40 degrees west and a dip of 60-80 degrees east. The contact between the two formations represents a hiatus in deposition of many millions of years. During this period the Diamond Peak formation was uplifted above sea level, eroded, and submerged. Deposition of the Strathearn formation then occurred during this submergence. This contact is termed an angular unconformity because of the angle between the bedding above and below the contact and the identifiable break in deposition between the formations.

Neither of the two major faults identified at the Carlin Canyon Tunnel area intersect the tunnel alignment. A reverse fault crosses the northeast portion of the spur coming to within 100 feet (30 m) of the east tunnel portal. The total vertical displacement on this fault is approximately 300 feet (90 m), but it is sufficient to expose the Diamond Peak rocks within the outcrop belt of the Strathearn formation. A second fault zone has been identified south of the west portal. The nature of the movement along this fault has not been defined from surface mapping but it does not intercept the tunnel. Minor faulting along the bedding has been noted in both formations.

Unconsolidated deposits of sand, gravel, and boulders are found at the west portal. These deposits include terrace remnants of the Humbolt River alluvial deposits and colluvium which has accumulated at the base of the spur.

5.1.3 Site Investigations

Most of the previous geologic investigations of the area are limited to regional bedrock studies to define general stratigraphic and structural relationships and to identify ore deposits. The reports of these investigations provide information about rock type and the geologic history of the area, but contain no specific information about the behavior of the rock in an underground excavation. Dott (1955) reported on the Carlin Canyon area and named the conglomerate series the Tonka formation, although asserting it probably correlated with the Diamond Peak formation named in 1883 at a

site 90 miles (144 km) away. Smith and Ketner (1975) believe the relationship between the two sites are adequately confirmed and have used the name Diamond Peak in the Carlin Canyon. A portion of their map is reproduced as Figure 19, Section 7.4.1.

5.1.4 Ground Conditions

The investigations indicated that the rock at the Carlin Canyon site is generally competent for the proposed tunnel excavation. Both tunnels could be excavated full face with the possibility of some difficulty in the more fractured parts of the Strathearn and at the unconformity. Fractured zones in the Strathearn near the east portal where the rock is in relatively close proximity to the reverse fault would probably represent the greatest difficulty in tunnel excavation. The angular unconformity, anticipated 800 to 1,000 feet (244 to 305 m) from the east portal, should be a feature of minor importance during tunnel excavation.

The bedrock is expected to be essentially dry throughout the length of both bores. Water inflows encountered during this work should be small and of relatively short duration because of the limited drainage area on the spur, limited rainfall in the area and pre-drainage of the ground by the adjacent railroad tunnels. There was no evidence of other geologic problems which might affect the progress of the excavation.

The investigation did indicate the presence of thick deposits of unconsolidated materials at both portals. Excavation of the portal cuts could involve the removal of a greater than anticipated volume of soil and rock in order to establish suitable foundation conditions for the portal structures and acceptable rock conditions to start the tunnel.

5.2 East River Mountain Tunnel Site

5.2.1 Project Area Description

East River Mountain Tunnel is a twin-bore tunnel for Interstate Route 77 located approximately five miles east of Bluefield, West Virginia. The tunnel provides a low-level crossing through the 1,400 foot (427 m) high East River Mountain which separates Bland County, Virginia on the south from Mercer County, West Virginia on the north. Figure 3 is an aerial oblique view of the mountain and north portal of the tunnel.

Figure 3 - South looking oblique airphoto showing the north portal of the East River Mountain tunnel in the foreground. The sharp crest of the mountain, formed by the Tuscarora sandstone, is prominent in the upper left portion of the image. The haze apparent in this picture is characteristic of the area.

5.2.2 Geologic Setting

East River Mountain is a long Appalachian Mountain ridge located on the western side of a 40-60 mile (64-97 km) wide belt of parallel ridges and valleys which extends from northern Georgia to eastern Pennsylvania. This topography is the product of long periods of erosion on folded sedimentary rocks. The ridges are underlain by rock which is resistant to erosion, while the valleys are underlain by less resistant rock. Faulting is present on both a regional and local scale. The geology is dominated by folded and faulted structure, while the topography is dominated by erosion landforms.

The bedrock is mainly Paleozoic-age sedimentary rock including sandstone, quartzite, shale, and limestone. Regional studies show that the sedimentary sequence has a total thickness of 30,000 feet (9,144 m). Individual units or formations are generally tabular in form with a thickness commonly ranging from 10-1,000 feet (3-300 m), and lateral dimensions ranging from several tens of miles to several hundred miles. These rocks were formed by deposition in a shallow sea which covered the area between the Cambrian and the Pennsylvanian periods. The formations were laid down in approximately a horizontal orientation and the contacts between adjacent units were essentially parallel. Folding arched the strata into anticlines and synclines. This folding was accompanied by uniform regional deformation which produced extensive reverse and thrust faulting. This faulting resulted in the repetition of the stratigraphic section and is expressed topographically as a series of ridges which are capped by the resistant Tuscarora sandstone (see radar imagery, Figure 10, Section 7.2.2). The ridges in the general area of East River Mountain are tilted blocks with little cross-faulting evident.

The main trend of the ridge and valley belt is east-northeast. The location of individual ridges and valleys depends upon the local bedrock structure, the relative resistance of the formations to erosion, and the depth of erosion within that area.

The master streams of the area flow across the ridge and valley belt toward the Atlantic ocean passing through the ridges in major water gaps. The secondary streams are found in the valleys parallel to the ridges. Drainage on the ridges is generally restricted to small tributaries of these secondary streams.

58

East River Mountain is topographically asymmetrical with a relatively gentle south-facing slope (approximately 20°) and a relatively steep north-facing slope (approximately 30°). The ridge is underlain by a series of strata including sandstone, shale, and limestone, which have a strike of north 65 degrees east and a dip of approximately 25-40 degrees south.

The ridge owes its existence and form to the Tuscarora sandstone cap rock which controls the topography on the upper two-thirds of the south slope. The topography of the lower part of the south slope is controlled by the less competent Rosehill shale and resistant Keefer sandstone and Rocky Gap sandstone that overlie the Tuscarora formation. The upper part of the north slope is a sheer cliff face which exposes nearly the full thickness of the Tuscarora formation. Less steep slopes are formed in the underlying Juniata shale, Martinsburg shaly-limestone, and Eggleston, Moccasin, and Gratton limestones. The limestones form a hummocky topography at the base of the slope and the floor of the adjoining valley. This area exhibits limited surface drainage and numerous sinkholes indicating the presence of extensive subsurface solution openings.

With the exception of the Tuscarora formation, there are few natural outcrops of the rocks at East River Mountain. The Tuscarora formation is well exposed in the ridge crest on both the northern and southern slopes. Outcrops of the Rosehill, Keefer, Rocky Gap, and Huntersville formations are naturally exposed in only a few places on the southern slope. The Keefer sandstone is exposed in the roadcut along State Highway 52; the Rosehill is also exposed in a road cut and slide areas along Highway 52. The Juniata, Martinsburg, and Moccasin formations do not crop out on the northern slope in the immediate area of the tunnel site because of residual soils and colluvial cover.

The soil cover on the upper part of the ridge is generally thin and discontinuous. The lower ridge, particularly on the south slope, is mantled by extensive, but thin residual soil and colluvial deposits. The deposits on the lower part of the north slope are relatively thin and composed of colluvial clay and sand, and residual clays formed on the limestones.

The St. Clair thrust fault is present approximately 2,000 feet (610 m) north of the north portal. This fault does not cut the tunnel area, although the limestones at tunnel level may be displaced on a small scale by related faults.

5.2.3 Site Investigations

Previous local and regional studies document the bedrock geology of East River Mountain. The U.S. Geological Survey mapped the area in the late 1800's and published the results of this study in the Pocahontas Folio dated 1896. Published regional studies of the Devonian age formations and the Tuscarora and Juniata formations include observations made on East River Mountain.

5.2.4 Ground Conditions

The Keefer and Tuscarora sandstones appear to be competent and, therefore, will provide good ground conditions. The Rocky Gap formation is incompetent because of clay or shale interbeds and noncemented sands. The Juniata and Martinsburg shale, shaly limestone, and siltstones, although softer than the Tuscarora and Keefer sandstones, are relatively competent. The shales and siltstones of the Rose Hill formation appear less competent because of the presence of interbedded soft shale layers. The Moccasin, Witten, and Gratton limestones are hard and relatively competent except in the vicinity of solution openings.

Artesian groundwater conditions may exist in the soil deposits and the bedrock near the south portal. The incompetance of the rock formations, the residual soil, and colluvial deposits on the south slope require excavation to the competent Keefer formation to start tunneling.

6.0 SITE INVESTIGATIONS

Field activities at each site were divided into three phases:
pre-flight, flight support, and data verification.

6.1 Pre-Flight

After tentative selection of the test sites, field parties
visited each site to make a final decision on the suitability of
the sites for the purposes of the investigation. With the
acceptance of the sites, specific plans were made for the conduct
of the remote sensor overflights and the logistic support require-
ments for these activities. In addition, during this visit to
each site, the structural and stratigraphic geology in the vicinity
of the tunnel site was inspected. Strike and dip measurements
of joints and bedding planes were recorded and rock samples were
collected for future study. Traverses were made above the tunnel
site to identify lithologic contacts, faults, discontinuities,
and other structural features, such as sink holes, which are
present at the eastern test site. Qualitative analysis of rock
properties were made, including hardness, resistance to erosion,
conformable relationships, uniformity of rock composition, presence
and density of fracturing and condition of fracture surfaces.
The results of these early field investigations are discussed in
Section 5.2.

6.2 Flight Support

A second trip to each site was made to support the flying
missions, especially for the collection of night-time thermal
imagery. Temperature measurements were made prior to the over-
flight on various target materials to determine when the effects
of the daytime solar heating had dissipated. At both test sites,
it was determined that the insolation effects were minimal by
11 p.m. and useful thermal imagery could be acquired after that
time. At the western site, pre-dawn thermal imagery was also
acquired. It was not possible to acquire pre-dawn thermal imagery
at the eastern site due to the development of ground fog during
the early morning hours.

While the thermal scanner was being flown, temperature
measurements of various target materials on the ground were again
recorded to supplement the black-body temperature reference data
from the scanner. These temperature measurements were useful

later during digital image processing when attempts were made to isolate specific targets within a narrow thermal range. To aid in data analysis, additional measurements were made including air temperature, relative humidity, wind speed, and wind direction. The flight lines for the night-time thermal survey were marked by handheld lights at predetermined locations.

At the eastern test site the survey was performed on 1 April 1975. Conditions for conducting a thermal survey were less than ideal because over two inches of rainfall had been recorded during the 72 hour period preceding the overflight. The mission could not, however, be postponed because of flight scheduling problems. Furthermore, spring emergence of leaves soon would have obscured the ground surface.

Tables 1 and 2 are summaries of pertinent data for imagery acquired for each site.

6.3 Data Analysis Verification

The third phase of the field activities involved return trips to each test site to verify the interpretations derived from the imagery and to test the hypothesis of the three dimensional geologic model. Various features of geological interest had been located and isolated on aerial photography, thermal and multispectral imagery and tentative identifications of different lithogolies had been made on the multispectral imagery. These features were investigated on the ground and the results of the investigation supported most interpretations. There were some discrepancies, however, on the multispectral ratio images between the expected response and the actual response of the sensor. A detailed discussion of these anomalies appears in Section 7.8.

At the Carlin Canyon Site, both ratioed multispectral and thermal data failed to reliably discriminate the Diamond Peak conglomerate and the Strathearn limestone. To better understand this problem, a portable spectroradiometer (ISCO Model SR) was taken to the site to make comparative measurements. The results of these measurements, given in Appendix E, indicated a maximum difference of less than 3% in relative reflectance between the weathered surfaces of the two formations in any portion of the spectrum measured.

Supplemental field examination is needed in most remote sensing surveys to verify the analysis of the data. Once the spectral characteristics of specific rock types in an area are known, the rock type can then be generally identified throughout the area. However, the effects of the local environment must be

62

Table I Summary of Pertinent Data for Imagery Acquired of the East River Mountain Virginia - West Virginia Tunnel Site

TYPE IMAGERY	IMAGE ID	DATE	TIME	ALT(AMT)	SCALE	IMAGE FORMAT
LANDSAT-1	1280-15320	73-4-29	9:30 am EST	496 n.mi.	1:3,369,000	70mm pos & neg transp.
				(920 km)	1:1,000,000	7" x 7" b&w prints
					1:1,000,000	Color composite print
LANDSAT-1	1209-15374	73-2-17	9:30 am EST	496 n.mi. (920 km)	1:3,369,000	Color composite
SKYLAB S-190A&B	RL 46-FRM22	73-9-16 73-9-16	3:50 pm EST 3:50 pm EST	235 n.mi. (435 km)	1:2,850,000 1:950,000	b&w 70mm neg. Color composite transp.
SIDE LOOKING RADAR(SLAR)	NG665-079 PN01	62-3-16			1:600,000	b&w print and pos. transp.
LOW SUN ANGLE PHOTO- GRAPHY (LSAP)		74-4-5 74-4-7	6:37 pm EST 7:35 am EST	20,000' AMT 20,000' AMT	1:40,000 1:40,000	9" x 9" b&w prints
COLOR PHOTOGRAPHY	1236-46 1219-34	75-4-27	1:20 pm EST 12:45 pm EST	18,000' 6,000'	1:36,000 1:12,000	9" x 9" color prints
PANCHRO- MATRIC PHOTOGRAPHY	555-95-57 555-114-116			6,000'	1:12,000	9" x 9" b&w prints
COLOR IR PHOTOGRAPHY		75-4-6 75-4-27	12:30 pm EST 1:20 pm EST	15,000' 3,000'	1:30,000 1:16,000	9" x 9" pos. trans.
THERMAL INFRARED & MULTI- SPECTRAL SCANNER	See Appendix F	75-4-1	4:30 pm EST 11:00 pm EST 1:45 pm EST	6,000' 2,500' 6,000' 2,500'	1:24,000 1:10,000 1:24,000 1:10,000	1/2m, 7-track mag. tape, 70mm neg. b&w prints
MAGNE- TOMETER AIRBORNE EM		75-10-8 to 75-10-22		180' 130'		line charts line charts

63

Table 2   Summary of Pertinent Data for Imagery acquired of the Carlin Canyon Nevada Tunnel Site

TYPE IMAGERY	IMAGE ID	DATE	TIME	ALT(AMT)	SCALE	IMAGE FORMAT
LANDSAT-1	1396-17590	73-8-23	10:00 am MST	496 n.mi. (920 km)	1:3,369,000	70mm neg. & pos. trans. color print
SKYLAB S-190A	85-003	73-8-12	7:44 am MST	235 n.mi. (435 km)	1:2,850,000	70mm negs.
SIDE LOOKING AIRBORNE RADAR (SLAR)	FN3123-J PN 15	73-5-3			1:400,000	
	FN 1155-G PN 01	71-6-4			1:200,000	b&w print film neg.
LOW SUN ANGLE PHOTO- GRAPHY (LSAP)	04 – 06	74-10-18	8:15 am MST	18,000'	1:38,600	b&w print
	06-08	74-10-18	5:00 pm MST	18,000'	1:38,600	b&w print
PANCHROMATIC PHOTOGRAPHY	4 – 6	74-7-25	10:20 am MST	18,000'	1:39,000	9" x 9" b&w print
	1 – 6	74-5-9	10:50 am MST	3,000'	1:6,000	9" x 9" b&w print
COLOR	23 – 25	74-10-18	11:05 am MST	15,000	1:30,000	9" x 9" color print
	16 – 22	74-10-18		3,000	1:6,000	9" x 9" color print
COLOR IR	Not num- bered	74-10-18	12:00 pm MST	15,000'	1:30,000	9" x 9" pos. transp.
	10-15		12:15 pm MST	3,000'	1:6,000	9" x 9" pos. transp.
THERMAL INFRARED AND MULTI- SPECTRAL SCANNER	See Appendix F	74-10-17 74-10-19 74-10-18	11:30 pm MST 6:40 am MST 10:45 am MST	6,000' 3,500'	1:24,000 1:14,000	1/2 inch, 7-track mag. tape, 70mm neg. b&w print

understood as they can produce anomalous results. At East River
mountain, for example, ratioed multispectral and thermal data
showed only few characteristic iron responses from the iron-rich
Rose Hill formation and a silica response was absent from the
areas where the Tuscarora Sandstone formation is located. A
field check revealed that a near 100% lichen cover on all naturally
occurring rock outcrops was the reason for the failure of the data
processing to identify and differentiate between the Tuscarora
and Rose Hill formations. This illustrates that, for proper
mission planning, a knowledge not only of the sensor capability,
but of the environmental conditions at a test site, are essential.

7.0 DATA ANALYSIS

The data from the various remote sensors were analyzed with two levels of application in mind; (a) to evaluate the regional geology and identify a potential site for tunnel construction; and (b) to acquire as much information as possible about a specific site once the location of the tunnel was established.

A regional analysis of the geology is more rapidly and often more effectively made with the use of small scale imagery, however, much of the same imagery also should be applied to the study of specific sites. In any investigation, it is most logical to proceed from the small scale imagery for establishing a regional geological setting to the large scale data for detailed site specific information. This approach also conforms to practical constraints in that the majority of investigations start with the examination of existing data, which in most instances will be small scale published geologic maps or satellite and radar imagery.

The following discussion of the interpretation and analysis of the various types of imagery is presented with the assumption that the reader has some knowledge of geological principles, but is not necessarily familiar with remote sensing. Observations are made as to what is seen on the imagery and the conclusions made. Conclusions are drawn from the independent analysis of each type of imagery; however, as in an operational situation, some conclusions are tentative and subject to later modification when higher resolution imagery is examined or data from other sources are included. To give the reader a better appreciation of what information is present in the imagery, an annotated image is included with an unannotated image where it was deemed appropriate.

7.1 Satellite Imagery

Numerous geological investigations conducted since 1972 have demonstrated that the analysis of small-scale satellite imagery may produce significant new geological information. This information is not necessarily better than other information, but it is unique. This imagery has revealed that much of the earth's surface is marked by major linear features (lineaments). Subsequent ground investigations have demonstrated with high probability that many of these features are large fracture or fault zones (Woodruff et al., 1974, Kowalik and Gold, 1975).

Imagery from LANDSAT (formerly ERTS) and Skylab satellites was examined for both test sites to establish the regional tectonic setting and to determine if major faulting in the immediate areas of the sites could be identified (a description of the LANDSAT and Skylab systems appears in Appendix I).

66

7.1.1 Carlin Canyon

A 1:500,000 scale, color composite LANDSAT image of the Carlin Canyon area was obtained from EROS Data Center (see Appendix I) for evaluation. An examination of the full LANDSAT image, which covers over 10,000 sq. miles (25,900 sq. km.), reveals evidence of major tectonic activity throughout the region with some basin and range faults extending completely across the image for a distance of over 100 miles (160 km.). Figure 4 is a portion of this image. The Carlin Canyon site (Figure 4B, Point E) appears to be situated at a flexure point or zone of change in the structural trend. To the south of the Carlin Canyon about 10-20 miles (16-32 km.), in the vicinity of Point A, the structural trend is predominantly N 10°-15° W. Immediately north of the Humboldt River, Point B, the trend is about N 20°-30° E. Such a flexure associated with basin and range type faulting can only add complexity to the structure in the Carlin Canyon area. The trend of the Humboldt River in the general area of the site, Points C and D, is southwest. However, where the river crosses the mountain range of the Carlin Canyon site, Point E, the trend changes to a northwesterly direction. The alignment of the river channel on both sides of the horseshoe-shaped Carlin Canyon suggests structural control. To the immediate south of Carlin Canyon, at points F and G, two major linear features are visible on the LANDSAT imagery. These features are quite prominent and seem to terminate at the Humboldt River on each side of the tunnel site. This is further evidence that considerable faulting has occurred in the Carlin Canyon area.

S-190A black-and-white and color Skylab photography were available for the Carlin Canyon area. Portions of these 70mm images were enlarged to a scale of 1:250,000 for analysis. The color image exhibited less resolution than the black-and-white panchromatic film, and the monotone color of the area did not contribute to the analysis. Consequently, this photography was not used for final analysis.

The black-and-white S-190A photography of the red portion of the spectrum, Figures 5A and B, shows greater detail of the area than does the LANDSAT image. This photograph confirms the structural complexity of the area and shows more clearly the two major northeasterly trending lineaments (Points A and B) bracketing the Carlin Canyon area (Point C). This further suggests that they are of structural significance. The Skylab photograph does not provide evidence that the northwesterly trend of the Humboldt River is structurally controlled, but does add detail to the change in the structural trend in the area. Numerous anomalous drainage patterns in
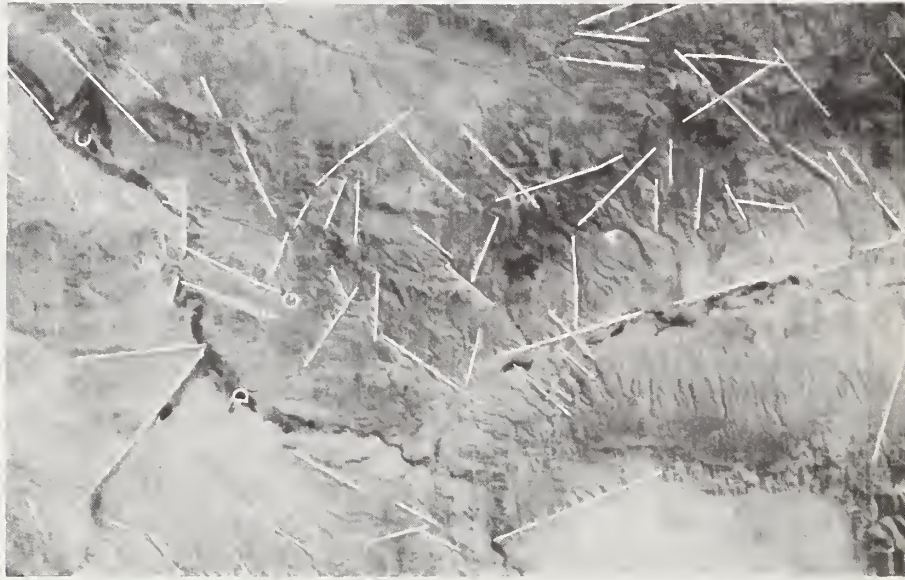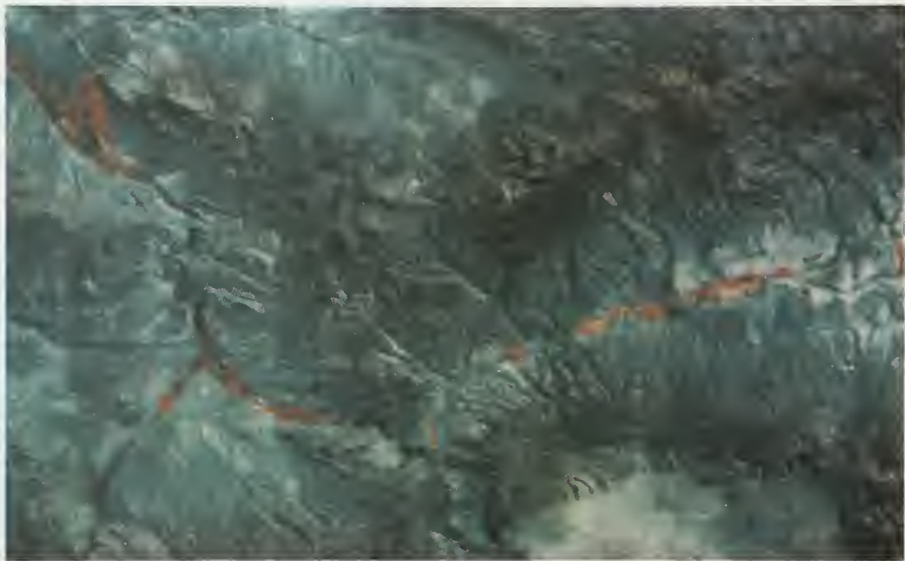
Figure 4 - Image A is a 1:500,000 scale, color composite LANDSAT image (no. 1396-17590). Image B is a black-and-white print of the red spectral band, one of the three spectral bands used to produce Figure A. Carlin Canyon lies immediately below Point A. Numerous lineaments seen on this image are significant to the understanding of the structural geology of the area. The false color rendition of the color composite image displays green vegetation in red.

68

B

A

Figure 5 - Red spectral band of S-190A Skylab image (no. 29-188) enlarged to 1 inch = 4 miles (1:250,000). Substantially more structural information is available from this photograph than from the LANDSAT image. Several lineaments are identifiable that could have significance at the tunnel site, Point C.

69

the immediate area of the tunnel site indicate control by faulting, fracturing, or bedding planes.

In summary, the LANDSAT and Skylab imagery indicates considerable structural complexity in the Carlin Canyon area. The test site appears bracketed by two major faults, and a cross-fault controlling the northwesterly trend of the Humboldt River may exist. Other lineaments in proximity to the tunnel site may represent faults or fracture zones.

7.1.2 East River Mountain

For geological analysis, LANDSAT imagery acquired in the winter months, when the solar elevation is low, provides a shadow enhancement of the terrain features not attainable at other seasons. Another advantage of winter imagery is that a thin snow cover can also enhance terrain features (Wobber, et al., 1973). A third advantage is that maximum visibility of the ground in the heavily forested, eastern test site area occurs in mid-to-late winter when the trees have lost their leaves and the leaf blanket has compacted. LANDSAT imagery of the Bluefield, West Virginia area has both a low solar elevation and a thin layer of snow.

The color composite LANDSAT image of the area, Figure 6A, clearly shows the highly dissected Cumberland Plateau at the upper edge of the image and the folded and faulted Appalachian valley-and-ridge structure in the lower two-thirds of the image. This image and Figure 6B were enlarged to a scale of approximately 1:200,000 for direct comparison with the radar image shown in Figure 10. Figure 6B is a black-and-white print of the red spectral band (.6-.7μm) used in the preparation of the color composite image. The resolution on this image is somewhat greater than for the composite image and contains considerable information on the regional geology. The color composite, perhaps because of the excessive snow cover, provides only limited information beyond that of the black-and-white print. On these images both the East River Mountain and the Big Walker Tunnel Sites are visible at A and B, respectively. These two ridges and the intervening ridges appear identical on the imagery, and it seems reasonable to assume that folding and faulting has caused numerous repetitions of the stratigraphic section. Although deformation has tilted the ridges so that the beds dip moderately to the south, the ridges appear to be reasonably continuous with little or no cross-faulting parallel to the tunnels. Consequently, at this scale, there appears to be no major fractures to complicate the construction of tunnels in these two areas.

70
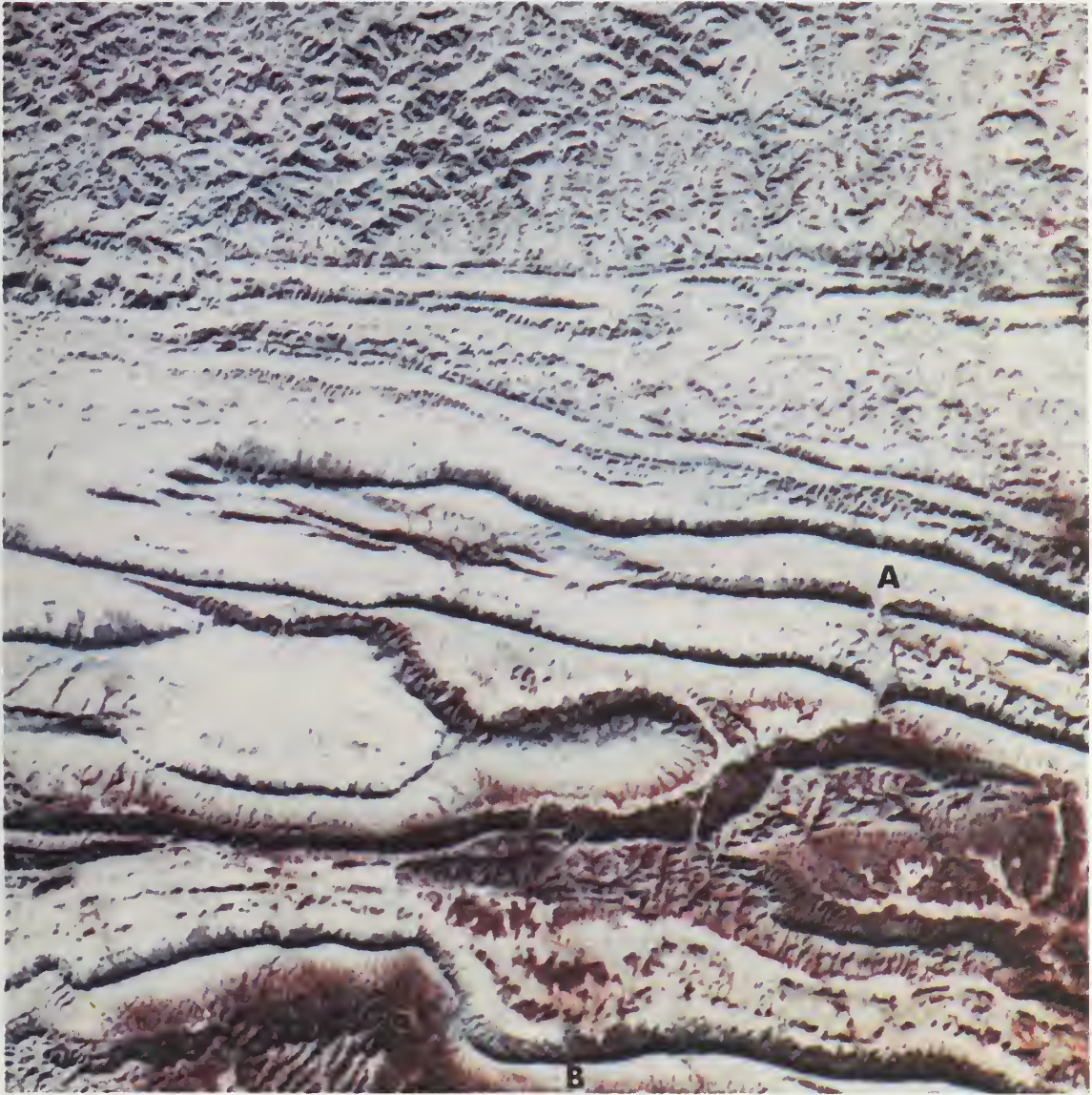
Figure 6A - This 1:200,000 scale color composite of LANDSAT image (no. 1209-15374) was acquired on February 17, 1973, when the solar elevation was about 33°. This low illumination angle emphasized the topography which reflects the geological structure of the area. This was further enhanced by a thin snow cover. See Figure 6B for the geological interpretation.

Figure 6B - This red spectral band LANDSAT image used in creating Figure 6A shows excellent detail of the geological structure. The East River Mountain tunnel is at the right center of the image at Point A. Big Walker Mountain tunnel is at bottom center at Point B.

Figures 7 and 8 respectively are 1:200,000 scale enlargements of S-190A and color S-190B Skylab photographs of the area. These photos, acquired on 16 September 1973 before the autumn die-back of the vegetation, clearly show the Interstate 77 right-of-way and the two tunnel sites. Although these photographs have a higher resolution than the LANDSAT imagery shown in Figures A and B, interpretability for geological information is not as good because of the higher solar elevation and the dense vegetation over much of the area. However, the images do show the major structural features and tends to confirm the LANDSAT imagery analysis that the ridges at the two tunnel sites are continuous and that there appears to be no complications due to major geologic structural anomalies parallel to the tunnels.

7.2 Radar Imagery

NASA (see Appendix I) and the U.S. Air Force have acquired radar imagery of large portions of the United States over a period of several years. Large quantities of the Air Force acquired imagery are available to qualified users through the Goodyear Aerospace Corporation (see Appendix H).

7.2.1 Carlin Canyon Site

Two scales of the Air Force radar imagery were obtained of the Carlin Canyon area. Small scale imagery, with a swath width of 20 nm (37 km) was acquired with a military SC-01 system on 3 May 1973. Larger scale coverage with a swath width of 10 nm (18.5 km) was taken with the same system on 4 June 1971. Figure 9 shows the latter image enlarged to an approximate scale of 1:100,000. The major northeastern trending lineaments, points A and B identified on the satellite imagery, are further documented on the radar image at Points A and B. At this higher resolution, additional parallel lineaments are visible at Point C; this supports the hypothesis that the major lineaments are fracture or fault zones. The straight character of the embankment on the south side of the Humboldt River, Point D, and the parallelism of this embankment with the trend of the river at Points E and F supports the interpretation that this embankment is structurally conways at Points G, H, and I also support the interpretation that a major fracture system of this orientation exists in the area. An east-west trending lineament immediately south of the proposed tunnel site at Point J, if it proves to be a fault, could influence the geologic structure in the tunnel area.

In summary, the evaluation of the radar imagery supports the interpretations made from the satellite imagery.
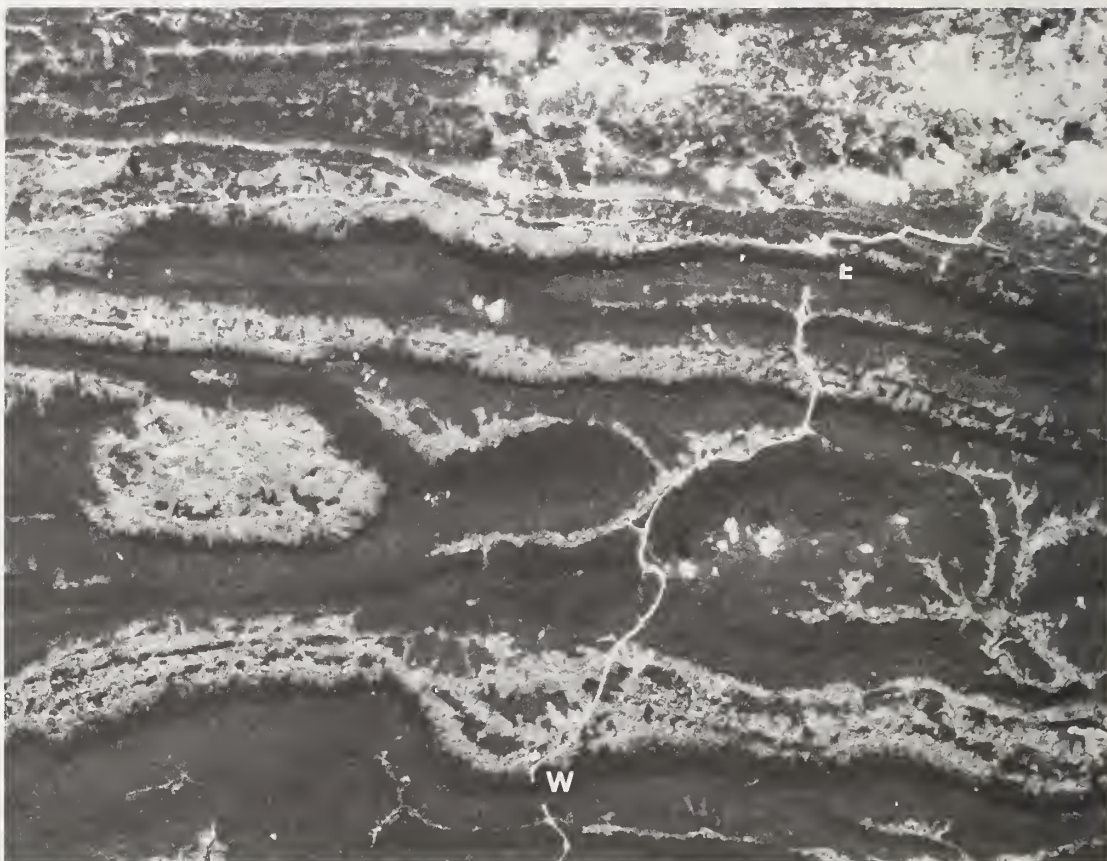
Figure 7 - The major road network is imaged in sharp detail on this red spectral band S-190A Skylab image (no. 46-022). This photograph was acquired at an original scale of 1:2,850,000, a small portion of which is shown here at a scale of 1:200,000. The geology is not as distinct on this photograph as on the lower resolution LANDSAT imagery shown in Figures 6A and 6B. The East River Mountain tunnel is at Point E and Big Walker Mountain tunnel at Point W.

Figure 8 - This scene (no. 88-056) of S-190B Skylab color photography (original scale of 1:950,000) has been enlarged to 1:200,000 for purposes of comparison with Figures 6A, 6B, 7A, 10A and 10B. This photograph was acquired on September 16, 1973 at about 11 a.m. when the sun elevation was about 51°. This high solar altitude combined with the dense vegetation cover which was still vigorous minimized the amount of geological detail observable. As in Figure 7, the East River Mountain and Big Walker Mountain tunnels are at Points E and W, respectively.

75
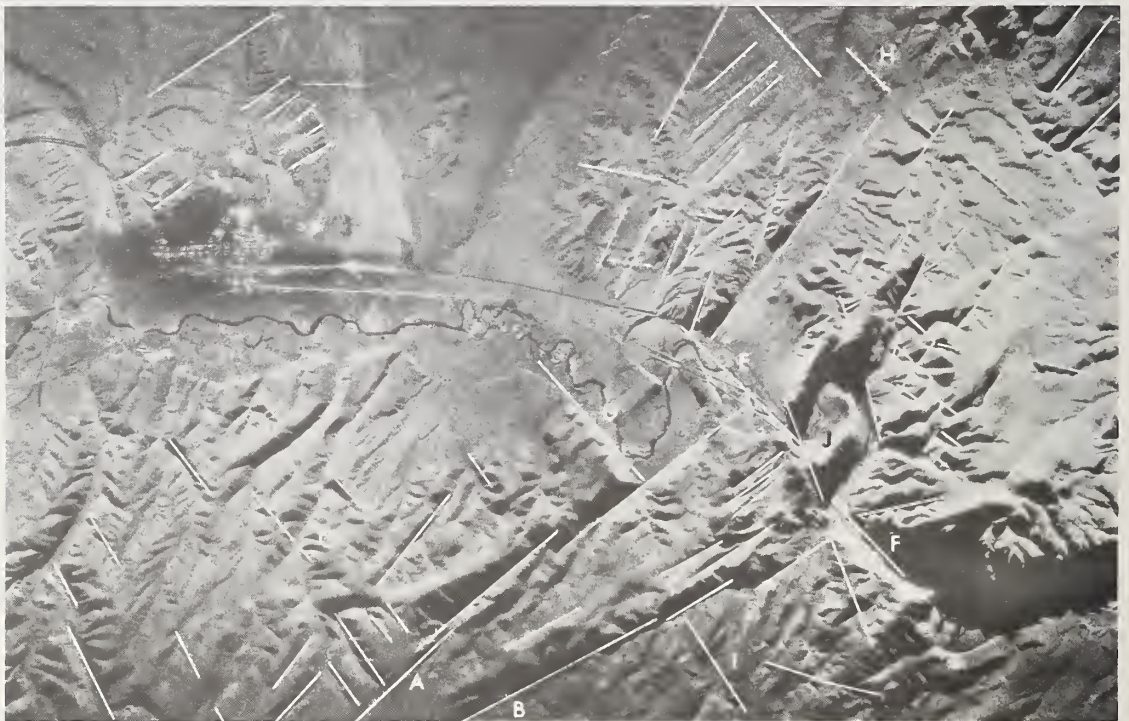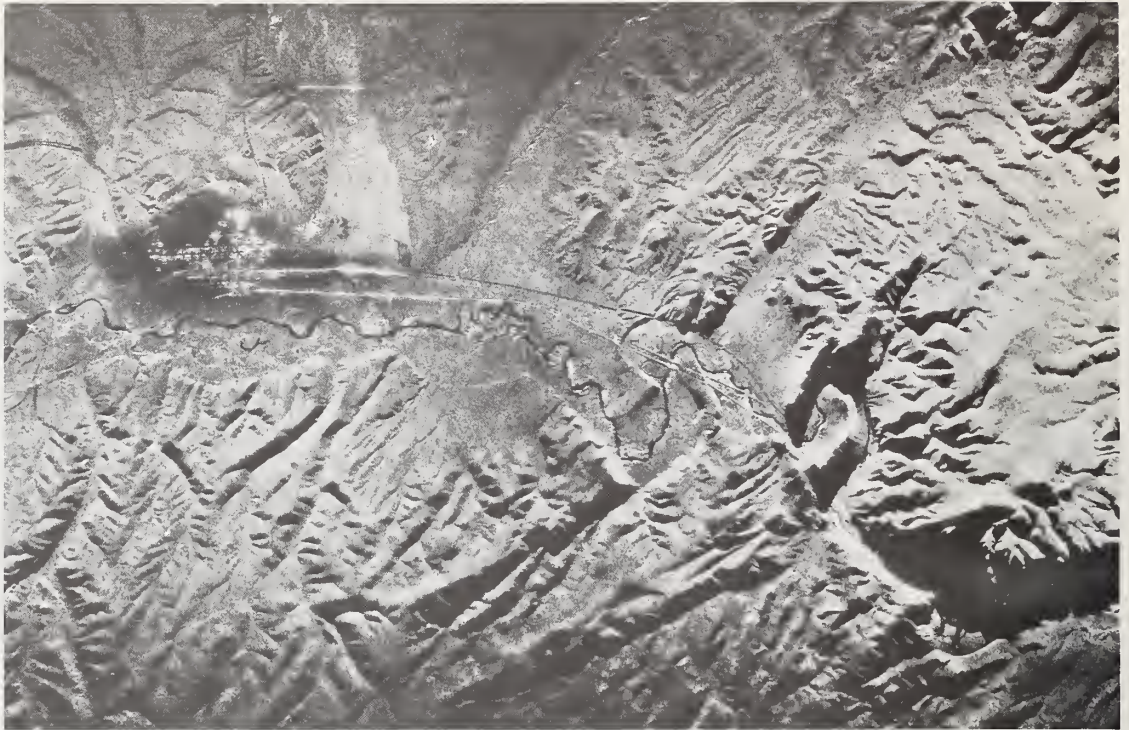
Figure 9A and B - On this radar image the town of Carlin, Nevada appears on the left and the Carlin Canyon tunnel area on the right. This image, acquired at an original scale of 1:200,000 and enlarged to 1:80,000, reveals a conjugate joint set trending at nearly right angles to each other. One joint trend, the upper left, influenced the position of the channel of the Humboldt River at Points D, E, and F. Two major lineaments, A and B, differ somewhat from the established joint trend. These features appear to bracket the tunnel site and may represent faults. Compare this image with Figure 2 for the precise tunnel location.

The higher spatial resolution of this imagery adds structural detail and gives a further indication of the overall geological complexity of the tunnel site area.

7.2.2 East River Mountain Site

The radar image, Figures 10A and 10B, of the East River Mountain site, acquired with a 73 x H3 radar system on 16 March 1962, is similar in appearance to the low sun angle LANDSAT imagery shown in Figure 6B. A more detailed geologic interpretation is possible using radar imagery because the spatial resolution and image contrast is substantially greater than for the LANDSAT image. This radar image covers both the East River Mountain and the Big Walker Mountain tunnel sites identified at Points R and S, respectively. The greater detail on the radar imagery makes it possible to identify sets of lineaments smaller than those visible on the LANDSAT image. These lineaments identified in the finely dissected, non-resistant rocks and soil aid in the regional interpretation of the fault patterns present. A comparison of the LANDSAT (Figures 6A and 6B) and radar images (Figures 10A and 10B) indicates that the structural character of the ridge penetrated by the tunnels is perhaps more easily assessed on the LANDSAT imagery. This is partly due to the lower contrast of the ridges on the satellite image and partly because the dip slope is illuminated on the LANDSAT imagery whereas it is a solid black shadow on the radar image.

In summary, although a similar general assessment of the area can be made with either the radar or the LANDSAT and Skylab imagery, the overall geological structure in the area is better determined from the radar imagery. However, judgments as to the regional structural detail and continuity of the ridges penetrated by the tunnels are more readily made on the LANDSAT imagery. It should be noted, however, that the radar imagery used was of relatively low resolution and that modern unclassified systems are capable of producing much higher resolution imagery than that used in this evaluation.

7.3 Low Sun-Angle Photography (LSAP)

For many years geologists have recognized the value of shadow enhancement of topography for geologic structural analysis. However, photography used by photogeologists is almost always acquired for reasons other than geologic interpretation; usually photogrammetric purposes. Consequently, aerial photography is normally taken when shadow effects are minimal. It is only in the last few years that serious consideration has been given the use of LSAP.

Figure 10A - This radar image of the East River Mountain area was made with a military system in 1962 at an original scale of 1:600,000. Later systems have higher resolution capabilities. See Figure 10B for an interpretation of the geology. The monochromatic nature of radar imagery, the low angle of illumination, and sensitivity of the system to terrain aspects all tend to accentuate geomorphic features.

78

Figure 10B - The detail of geological information derived from this image is substantially greater than shown on this generalized interpretation. This interpretation, however, shows the major structural features in the area that consist of folding and repeated thrust faulting of the sandstone, limestone, and shale comprising the sedimentary sequence. The East River Mountain and Big Walker Mountain tunnel sites are at Points E and W, respectively.

79

The objective of the LSAP investigation was not to simulate SLAR, but to shadow enhance the minor topography of the tunnel site for structural interpretation.

The appropriate times of day for imagery acquisition for the first site studied, Carlin Canyon, were determined empirically by the field team during the first visit to the test site. Observation of shadow length and topography suggested a solar elevation of 10°-15° above the horizon as being appropriate.

The acquisition of LSAP requires somewhat more detailed planning than does conventional photography, and details for proper planning of a mission are given in Appendix D. The solar position or elevation changes at a rate of up to one degree every four minutes,[1] thus, timing is a critical factor.

Although Clark (1971a) and Wise (1969) recommend a solar azimuth at right angles to the major structural features, this is not always possible to achieve. For instance, at the Carlin Canyon site which is at 40° N latitude, the annual extremes of solar azimuth extend over a range of only 70° for either morning or evening occurrences for an assumed solar elevation of 14°. The morning azimuths range from 70° on June 22 to 139° on December 22 and the evening azimuths range from 290° on June 22 to 220° on December 22. Although this appears to limit the usefulness of LSAP, it should be noted that jointing nearly always occurs in conjugate sets which normally are at an angle to the regional structure. This fact implies that at least one joint trend will be reasonably well illuminated regardless of solar azimuth. Even if it is not possible to determine an optimum azimuth or the scheduling of LSAP missions is inflexible, useful geologic structural information can still be acquired. Also, the geological information desired is not limited solely to structural data. Shadowing also enhances the drainage patterns[2] which aids in the interpretation of the type of surficial material present (see Appendix C).

7.3.1 Carlin Canyon Site

In the Carlin area, morning (Figures 11A and 12B) and evening (Figures 12A and 12B) LSAP photography was acquired

[1] The apparent rate of change of solar elevation of 1° every four minutes only occurs for those points on earth where and when the sun passes through the zenith. This is the maximum rate of change and can only occur for points between the Tropic of Cancer and Tropic of Capricorn, and then only twice a year. At all other places the apparent rate of change of solar altitude will be somewhat slower.

[2] Excessively low sun angles, as illustrated in Figure 12, obscure drainage detail. What constitutes "excessively low" however, is determined by the local topographic relief.

B

A
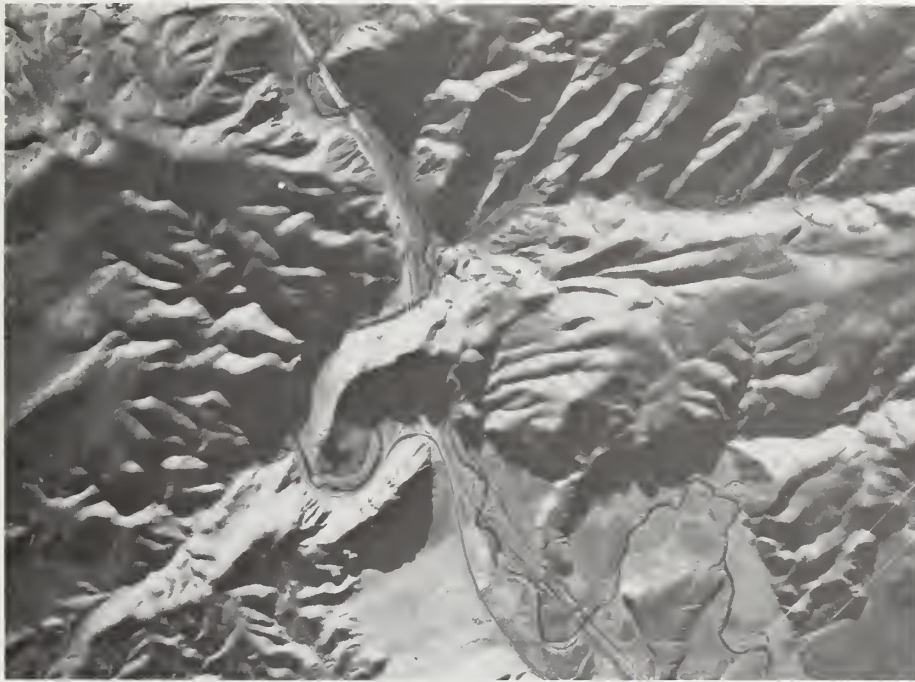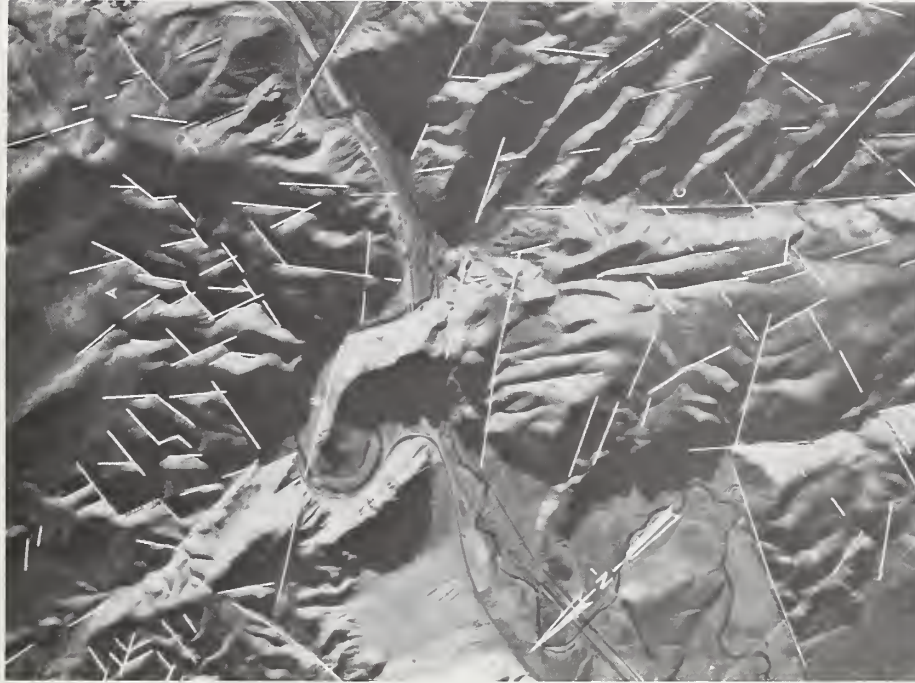
Figure 11 - LSAP Photography acquired at low sun elevations or low sun angles is a valuable geological tool. The shadowing produced enhances the interpretation of the structural influence from the topography. This LSAP was acquired at a morning sun angle of about 13° on October 18 and emphasizes the straight parallel character of a conjugate set of drainage systems. The tunnel site between linears B and C is essentially bracketed by fractures and/or faults that suggest considerable structural complexity in the area.
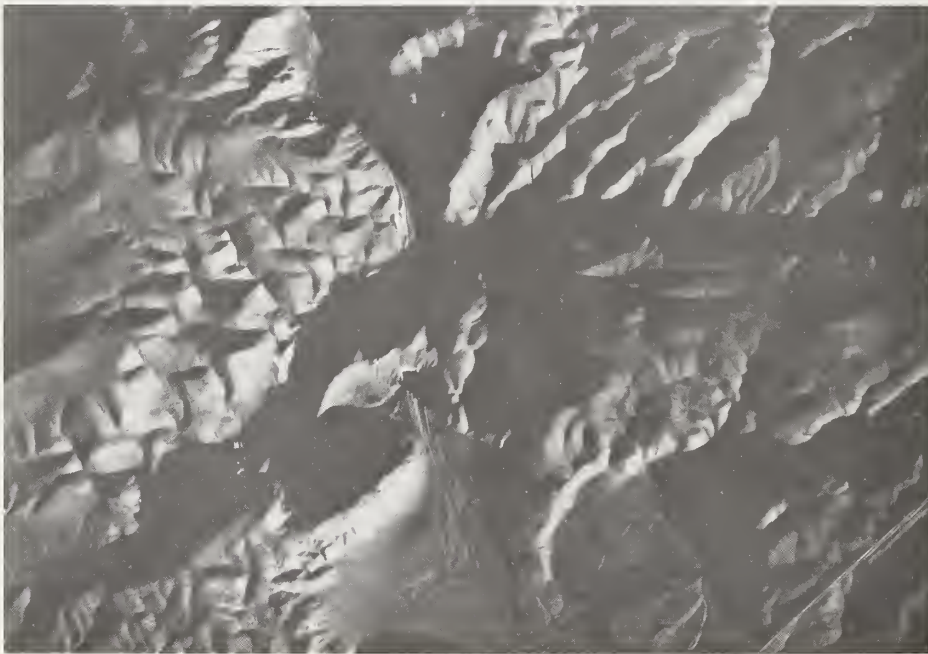
A
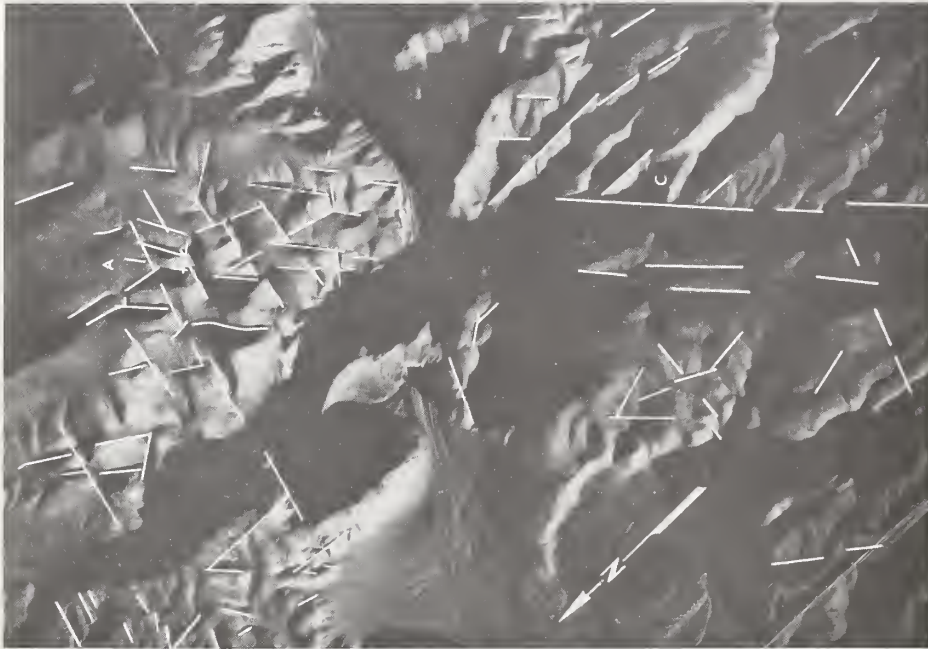
B

Figure 12 - This low sun angle photography was acquired at a sun elevation of 6°; too low for optimum structural enhancement. The area below Point A on image B, however, shows good enhancement. This hillside slopes toward the point of illumination at about 5°, which gives an effective sun elevation of 11°. The optimum solar elevation for structural enhancement is largely dependent upon the ruggedness of the topography; more subdued relief requires lower sun angles.

82

on October 18, 1974. An attempt was made to acquire the photography when the solar elevation was between 10° and 15° above the horizon. The solar elevation was 11° for the morning flight; however, a delay of 20 minutes in the evening flight produced photography at a solar elevation of only 6°. As a consequence, many important topographic features were hidden in shadow (Figure 12). On this image, the area north of the Humboldt River shows a substantially better shadow-nonshadow ratio and more structural detail than other portions of the photograph because the regional slope in that area is 5° to the west, which in effect produces a solar illumination angle of 11°. In this same general area near Point A on both Figures 11 and 12, many of the same lineaments are visible regardless of the change in solar azimuth. This increases the level of confidence one has in the features mapped. The lineament mapped on the LANDSAT image as Point G and on the radar image as Point B is evident on both morning and evening LSAP at Point C. On these photographs there is a suggestion that the feature may extend north of the Humboldt River. The lineament identified on the radar imagery at point J, Figure 9B, is also visible on LSAP photography, at point D, and it appears that it could have geologic significance. No other fracture or fault through the tunnel site can be identified on this imagery.

At the scale of the imagery, approximately 1:30,000, one can see the vertical bedding of the Diamond Peak conglomerate on the western-most sunlit side of Carlin Canyon. The angular unconformity at the north bend of the Humboldt River is also visible. With information concerning the strike of the strata and the fracturing present in the area, it is apparent that the shape of Carlin Canyon is in part controlled by differential erosion parallel to bedding (Figure 11, Point B).

The morning and evening LSAP, emphasize different sets of fracture trends, and both contribute to the understanding of the geology of the area.

7.3.2 East River Mountain Site

Low sun angle photography of East River Mountain was acquired in the evening of April 5, 1974 and the morning of April 7, with a solar elevation of approximately 12°. The parallel nature of the sides of the flatirons on the dip slope is strongly emphasized, suggesting that they are controlled by fracturing and/or faulting. Other linear features are identifiable extending across the flatirons. One of these linear features (Figure 13, Point A), which is traceable through the south portal building site, was later

A

B

Figure 13 - Morning low sun angle photography of the East River Mountain tunnel site acquired on 7 April at a sun elevation of 11° shows considerable topographic detail of possible structural significance. Only the suspect linear features which could represent joints or faults have been mapped. Linear A was later determined to be a fault. The en echelon linears in the lower left portion of the photograph are related to the St. Clair thrust fault.

84

identified as a fault (see Plate II in pocket). Another
lineament on the north slope of the East River Mountain lies
to the west of the tunnel bore (Figure 14, Point B) and it
too may represent a fault, but inadequate information is
available from LSAP to establish this fact. It does, however,
identify an area for further investigation by other remote
sensors, ground geophysical methods, or drilling.

The value of LSAP for revealing subtle land forms is
apparent in Figure 15. Shallow sinkhole depressions are
strongly enhanced and the linear orientation of many of the
depressions is obvious, reflecting bedding and jointing.

In summary, low sun-angle photography closely resembles
radar imagery. When acquired with conventional metric
camera systems, the LSAP imagery is at a substantially
larger scale and of greater spatial resolution than radar
imagery, and therefore complements, rather than replaces the
radar. Valuable geological data can be acquired with LSAP
in areas where the topography reflects the underlying geology.
The results of this investigation, and others, suggests that
this may occur in more instances than generally recognized
from the use of conventional photography.

7.4 Analysis Of Aerial Photography

The investigation of the Carlin Canyon and East River Mountain
test sites included three types of "conventionally" acquired
aerial photography (black-and-white panchromatic, color, and
"false" color infrared).

7.4.1 Carlin Canyon, Test Site

For the Carlin Canyon site the Nevada Highway Department
provided black-and-white panchromatic photography at two
different scales. One set of photography was acquired on
July 25, 1974 at an approximate scale of 1:30,000. This
photography complemented the satellite and radar imagery by
providing a regional geologic setting of the tunnel site and
a cognitive bridge between small-scale space imagery and
large-scale aerial photography. The larger scale, 1:6,000,
photography taken on May 9, 1974 was of utility for detailed
site analysis. This photography was acquired when the vegetation
was still in a vigorous growth stage and when the patterns
of differential plant growth accentuated many geologic
features, such as bedding and fractures. The time of acqui-
sition, combined with the high resolution of black-and-white
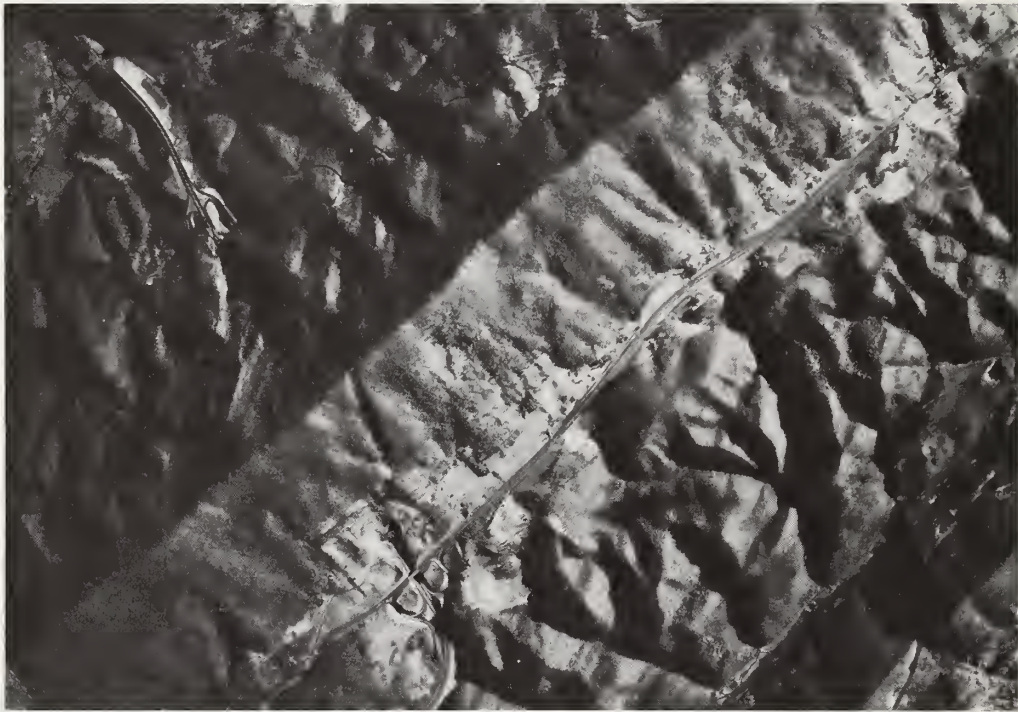
A

B

Figure 14 - Evening low sun angle photography of the East River Mountain site acquired at a sun elevation of about 11° on April 3. The scarp slope of the mountain is better illuminated at this time of day than in Figure 13, and shows a linear at Point B that could indicate a zone of fracturing in the tunnel.

86

Figure 15 - Low sun angles of illumination enhance subtle topographic features such as these small sinkholes located in the suburb of Bluefield, West Virginia. The alignment of sinkholes in this scene indicates control by both bedding and joint planes.

photography made it very useful for identifying bedrock exposures and making geologic interpretations (see Figure 16). Color and color infrared photography was acquired on 18 October, 1975 at scales of 1:30,000 and 1:6,000. At this time of the year, the vegetation in the area was largely dormant. Consequently, the strong infrared response characteristic of high vigor vegetation was not present, and the differences in vegetation vigor and growth patterns that might have provided clues to geologic structure were at a minimum (Figure 17). The natural color photography, particularly the large scale imagery (Figure 18), was of substantial value in delineating significant lithologic differences that were expressed by color. For the Carlin Canyon site, stereoscopic analysis of the large-scale black-and-white panchromatic and large scale color photography proved to be very useful for geologic interpretation.

At the beginning of the study the only geologic information available for the Carlin Canyon test site was a "sketch" map of the tunnel area provided by the Nevada Highway Department. This map indicated an unconformable contact between the older conglomeratic Diamond Peak formation and the overlying Strathearn limestone formation. The map also identified the large fault (designated F_3, in Figure 16; and in Plate I; see pocket) just north of the east portal of the highway tunnel. In late 1975 the U.S. Geological Survey published a 1:125,000 scale geological map in Professional Paper 867-E. An enlarged portion of this map is shown in Figure 19.

Faulting appears on both the black-and-white panchromatic and color aerial photography as faint linear traces, as vegetational alignments, and as obvious stratigraphic offsets. On the panchromatic photography bedding of the formations is indicated by differences in tone. On the color photography the color emphasizes the lithologic differences and adds to the utility for analysis even where color differences are subtle (compare Figures 16 and 18).

On the photography there are two sets of faults which may or may not have been contemporaneous. The major fault in the area, F_3, trends northwest, subparallel to the strike of the formations. The plane of this fault appears nearly vertical where it is visible a few feet north of the east portal (see arrow on Figure 20). Several northeast trending faults cross the bedding at nearly right angles. At least one fault, F_1, appears to displace the F_3 fault in a right lateral sense. Most of the faults of this northeasterly trend do not appear to have appreciable offset, although one of these faults, F_2, does show stratigraphic displacement on the order of 100 feet (30 m.).

88

Figure 16 - Compilation of the analyses of all the remote sensing data acquired
over the Carlin Canyon tunnel. This panchromatic photograph shows the
combined results of the sensors used on this site. The dotted lines represent
the unconformable contact between the Diamond Peak formation (MIPd) and
the Strathearn limestone (IPPs). F_3 is a major fault with as much as 400 feet
(120m) of displacement at the east portal of the tunnel. Numerous other
faults, marked by "F's," are mappable on photography. F_{11} is inferred
from the analyses of both the small and large scale imagery. It is supported
in places by field observations.

89

Figure 17 - Color infrared photography acquired on October 18 in the arid climate at the Carlin Canyon site contributed little information beyond that available from the natural color and black and white panchromatic photography. Compare this photograph with Figures 16 and 18. A lack of soil moisture and absence of growing vegetation (no precipitation for six months) minimized the value of color infrared photography in this area.

Figure 18 - This natural color stereo triplet of the Carlin tunnel area illustrates the difficulty of distinguishing the conglomeratic Diamond Peak formation, and the Strathearn limestone, and the resulting problems of interpreting the structure. Stereoscopic viewing of aerial photography not only adds the third dimension to the image but contributes immeasurably to the geologist's ability to interpret the stratigraphic and structural relationships. These photographs contributed a great deal to the interpretation presented in Figure 16.

EXPLANATION

Mesozoic and younger rocks

Permian and Upper Pennsylvanian rocks
PPu, *undivided*
Puc, *carbonate rocks, siltstone and much chert*
PPs, *Strathearn Formation*

PERMIAN

UNCONFORMITY

PENNSYLVANIAN

Pt, Ptm, Pm, Pcs

Tomera and Moleen Formations
Pt, *Tomera Formation*
Pm, *Moleen Formation*
Ptm, *undivided*
Pcs, *nearly all siliceous clast conglomerate and sandstone*

Diamond Peak and
Chainman Formations
PMd, *Diamond Peak Formation*
Mc, *Chainman Shale*
Mdc, *undivided*

Webb
Formation

MISSISSIPPIAN

UNCONFORMITY

Vinini Formation

ORDOVICIAN

0   1
1 MILE

From U. S. G. S. Professional Paper 8 6 7 - A

Figure 19. Geological map of the Carlin Canyon, Nevada tunnel area.

Figure 20 - This westward view to the immediate north side of the east portal of the Carlin Canyon tunnel shows the proximity (see arrow) of the major fault, F_3. The limestone to the left of the fault is highly fractured and considerably altered.

The limestone in the vicinity of the east portal is highly fractured and some faults, F_5 and F_7, of the undetermined displacement are visible. Figure 21 shows the striated fault plane surface of fault, F_5, exposed during clean-off above the east portal. This local area also shows deep weathering and alteration of the limestone. Consequently, competency of this rock material at the east portal does not appear to be as great as elsewhere and considerable problems could have been anticipated in construction as well as in maintaining the slope above the portal after construction.

Two factors complicate the analysis of the geological structure in this area: 1) the high percentage of area mantled by a varied thickness of soil and talus, and 2) the lack of knowledge as to the precise nature of the unconformable relationship between the Diamond Peak formation and the overlying Strathearn limestone. Studies of this unconformity reported in the U.S. Geological Survey Professional Paper 867-A indicate that the relationship varies from place to place; i.e., the strike of the two beds or formations are in places similar and in other places substantially different. For instance, at the north bend of the Humboldt River in Carlin Canyon, measurements above the road cut indicate that the strike of the two formations are identical, but the Diamond Peak formation is dipping 17° more steeply than the overlying Strathearn limestone.

On the hillside to the south of the east portal of the highway tunnel, the Strathearn limestone is deposited over an irregular surface of the Diamond Peak conglomerate (Figure 22). The basal limestone unit, i.e., the first limestone strata deposited over the old topography, appears to be draped over the old land surface. Younger strata, however, appear to have been deposited horizontally pinching out against the higher portions of the ocean floor.

It is difficult to determine the validity of this interpretation. However, any other explanation of the relationships observed on the aerial photography would require an extremely complex history of strike-slip faulting. Although the simpler explanation appears more desirable, the latter interpretation should not be completely rejected. The major fault, F_3, in the area appears to have had strike-slip movement. Possible fault, F_{11}, south of the east portal, also may have strike-slip displacements. Because of the extensive faulting, the projection of the unconformity to tunnel level can only be approximated.

94

Figure 21 - This fault plane in the Strathearn limestone shows slippage striations (slickensides) exposed during the "clean-off" above the east portal of the Carlin tunnel. This fault, labeled F on Figure 16, is one of several faults of apparently small but undetermined displacement in this local area.

Figure 22 - This view of the east side of the ridge or meander spur formed by the Humboldt River shows the steeply dipping strata and unconformity between the Diamond Peak conglomerate (left) and the Strathearn limestone (right). East Portal of the Carlin Canyon tunnel is visible on the right.

A recumbent fold on the north side of the river valley,
a mile east of the tunnel site, graphically demonstrates that
structure in the Carlin Canyon area is complex. Also, 400
yards (366m) to the south of the west portal, a major, high-
angle, reverse, F_{12}, is identified on the geological map
(Figure 19) and on the black and white panchromatic aerial
photography of the test area. This fault has displaced the
older Mississippian age siltstones and mudstones of the Webb
formation over the younger Diamond Peak conglomerates.

7.4.2 East River Mountain Tunnel Site

    The East River mountain site, which receives 40-60
inches (100-200 cm) of annual rainfall, is densely wooded.
Consequently, it was necessary to acquire both photography and
scanner imagery of the site while there was no leaf canopy to
obscure the ground surface in the tunnel area.

    The West Virginia Department of Highways provided
panchromatic photography of the area, at a scale of 1:12,000.
The dates of the overflights for this imagery are not known
but they were made during early construction phases of the
tunnel and at a time when the vegetation obscured much of the
surface detail essential for accurate geological mapping.

    Color and color infrared photography taken on 5 and 6
April 1975, had to be reflown because of technical deficiencies.
Due to winds and cloudy weather, reflying was not accomplished
until 27 April. Portions of the color infrared photography
from the earlier date (Figure 23A) were usable. Comparison of
this photography with the color infrared photographs from the
April 27 flight (Figure 23B) shows the rapid development of
the deciduous vegetation in the spring. In the photograph of
the later date, the leaf cover, although only partially
developed, appears to have obscured much of the ground. The
color infrared photograph from the 6 April overflight shows
only minor amounts of green vegetation (red coloration) in
some of the lower meadows and fields, thus, any geologic
structure, such as faults, that may be enhanced by differ-
ential vegetational growth rates are not evident. Three weeks
later, (27 April) the leaf cover is nearly universally pre-
sent, except near the upper part of the mountain, and again no
emphasis of jointing or fracturing is apparent. The absence
of such indications is probably due to the abundant rainfall
which occurred throughout the late winter and early spring.
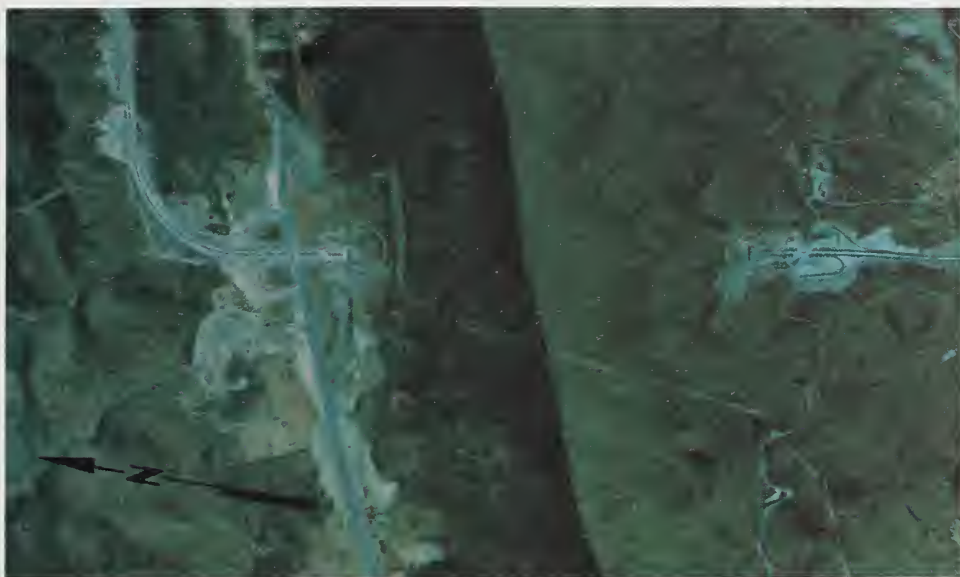
Figure 23 - Color infrared images of the East River Mountain site taken three weeks apart. Scene A was taken on 6 April before vegetation development. Scene B was acquired on 27 April. In this short interval the trees "leafed out" to the extent that the entire area shows high infrared reflectance. This illustrates the critical timing required for some remote sensor missions to obtain optimum data.

Two scales of color and color infrared photography were flown. The photography shown in Figures 23A and 23B is at a scale of 1:30,000 which is excellent for a synoptic view of the area, but somewhat small for detailed geologic analysis. Large scale photography was flown at an altitude of 3,500 feet (1066 m) AMT (above mean terrain). The detail provided by this photography is good for geologic analysis, however, the topographic relief of the mountain produces a parallax in this larger scale imagery that is too extreme for comfortable stereoscopic viewing. East River Mountain is approximately 1,000 feet (306 m.) high which is over 28% of the aircraft altitude used, consequently the scale of the photography ranges from 1:7,000 for the valleys to 1:5,000 for the mountain top. A flight altitude of 6,000 feet (1,835 m) would have been a better choice as a compromise between image scale and resolution of surface detail. In spite of the difficulty of viewing, the stereographic photography provided excellent detail for analysis of the stratigraphy and structure, particularly on the dip slope of the mountain.

Few rock outcrops exist in the area, except for the resistant Tuscarora sandstone which forms the caprock of the mountain (Figure 24). Here the thick sandstone unit forms a vertical cliff along most of the mountain crest. Although the rock has no soil cover, it is nearly 100% lichen covered. Figure 25 illustrates what may be considered a typical exposure. In many places a leathery species of lichen produces an even thicker cover on the rock.

A natural color photograph, (Figure 26), taken at the same time as the color infrared photograph in Figure 23B, does not show the pronounced effects of leaf canopy development and the deciduous trees appear essentially bare. This photography, both the large and small scale, was used for most of the photo interpretation of the tunnel site. The large scale imagery was a valuable tool for mapping the various stratigraphic horizons and structure. It was possible to locate accurately the different stratigraphic horizons and faults of small displacement. Two faults were positively identified in the vicinity of the tunnel. Several other lineaments may be faults or joints with no displacement.

Fault, F_1, shown on Plates II and V (see pocket) was tentatively identified on LSAP photography. Its presence was further substantiated in the photo interpretation phase of the analysis. This fault should have little or no effect on the tunnel construction, but the south portal building appears to be on the fault trace.

Figure 24 - The highly resistant Tuscarora sandstone is shown in this view along the crest of East River Mountain. This sandstone is the major ridge forming strata in the region. Note the vertical cliff which is in places nearly 50 feet (15m) high.

Figure 25 - Lichens are ubiquitous on rock outcrops and seriously interfere with lithological discrimination by remote sensing methods in southern Virginia-West Virginia. Here an outcrop of Tuscarora sandstone is completely covered with lichens. This is typical of over 95% of the rock exposures not disturbed by man's activities.

Figure 26 - Natural color stereogram of the East River Mountain site. It was taken simultaneously with Figure 23B, indicating that although the leaf canopy had started to develop, much of the ground surface was still exposed. Stereoscopic viewing of this stereogram (and larger scale photography) permitted the detailed delineation of the stratigraphy and structure in the area.

Fault, F_2, which lies mostly outside the area of interest has an undetermined displacement. It has an estimated ten foot (3m) displacement on the ridge crest. Displacement, however, appears to increase to the south and several tens of feet of stratigraphic offset appears probable where it extends into the map shown on Plate II.

Linear feature, F_3, if a fault, does not extend to the crest of the ridge, but displacement appears possible where it crosses younger strata outside the map area. This feature does not appear to extend to the tunnel alignment. Linear, F_4 is another probable joint. It parallels the dominant joint pattern in the area and seems to be an extension of a fracture identified on the dip slope outside the mapped area.

The upper two-thirds of the north slope (scarp slope) of the mountain is composed of relatively non-resistant siltstones, shale and shalely limestones of the Juniata and Martinsburg formations. The contact between these two formations is not identifiable on the photography and the boundary shown on the cross-sections (Plate II) is based on the tunnel contractor's preconstruction site report.   On the photography, there is an identifiable topographic break, some distance below the supposed basal contact of the Juniata. This topographic break, apparently created by a more competent horizon within the Juniata, is the only distinguishable stratigraphic feature on the scarp slope.

The dense limestone present at the north portal is easily eroded in the present moist environment and, conse-quently, is a valley forming unit. It contains numerous sinkholes which are easily identified by stereoscopic exam-ination of the photographs (see the stereogram in Figure 26).

From the aerial photography it is possible to judge that the soil cover on the south slope (dip slope) of the mountain is relatively thin, probably less than 3 feet (1 m.) thick. Soil thickness on the north slope is more dif-ficult to judge. The lower portion of the slope, consisting of limestones, has a thin soil cover of only a foot or two (.3-.6 m) in most places. The upper slope, below the sand-stone escarpment, appears to be covered with soil and weathered shale with an estimated thickness of as much as 10 to 20 feet (3-6 m).

The sinkholes near the north portal indicate subterranean drainage and solution cavities. The presence of such features could indicate a need to fill the voids for structural strength and to prevent the inflow of water.

On the south side (dip slope) of the mountain the prominant jointing in the Tuscarora, Rose Hill and Keefer formations could be avenues for water percolation to depth. This could cause a water problem for approximately the first 1,200 feet (366 m) of tunnel construction from the south portal.

The Rocky Gap formation, which crops out at the south portal is, in most places, a resistant sandstone unit. Locally, however, the cementing material has been leached away leaving a soft friable sand.

7.5   Multi-Band Photography

Multi-band photography is a technique of simultaneously obtaining black-and-white photographs of a target using filters for several bands of the visible or near-visible portions of the spectrum. The theory of multiband sensing is that objects reflect energy of varying intensity in different portions of the spectrum, unless the object is pure white or pure black. Once the spectral "signature" of an object has been determined, it should be possible to acquire appropriately filtered imagery that will differentiate the object from the background and, thus, enable objects to be identified and described. Each photograph can be studied individually or in combination on a color additive viewer to provide a natural color or a range of false-color composites which may improve the interpretability of the image. Several investigators have evaluated the use of multi-band photography for discriminating rock types (Marrs, 1973; Longshaw and Gilbertson, 1975 and others). Most of the results attained with multiband photography show only moderate success in discriminating lithologies or the results were not sufficiently better than those derived from conventional photography to justify the additional cost of multiband photography. Such conclusions, plus economic considerations, eliminated airborne multi-band photography from the current investigation. Also, we felt that the multispectral scanner would provide an adequate assessment of the utility of the multispectral imagery for rock identification even though the resolution of the MSS imagery is inferior to photography. However, during the actual imagery analysis there was difficulty in discriminating the Diamond Peak conglomerate and Strathearn limestone using color aerial photography and multispectral imagery of Carlin Canyon. The difference in color of the two rock types is not pronounced; one being light yellow brown and the other gray. Both rocks have appreciable lichen cover, some of which has turned bright orange, thus, both rock types appear similar in color when viewed from a distance. The weathered surfaces, plus a partial coating of lichen growth,

tends to mask the true spectral response of the rocks. Figures 27 and 28 are, respectively, ground photographs of typical exposures of the Diamond Peak conglomerate and the Strathearn limestone. This prompted field spectroradiometric measurements of the reflectances of the two lithologic units. At this point it was also decided to include multiband photography taken from ground stations as part of this expanded study effort.

Multiband photography of three selected target areas was acquired on October 23, although rapidly moving cloud shadows interfered somewhat. The different spectral band exposures were made sequentially using a 4" x 5" press camera. Only a few minutes separated the exposures and it is felt that this slight time lapse had little effect on the documentation of the spectral response of the rocks. However, cloud movement between exposures produced bizarre colors in cloud and shadow areas on the color composite images.

Kodak Tri-X Pan Professional film No. 4164 was used with Wratten filters Nos. 26 (red), 48 (blue) and 58 (green). High Speed Infrared film No. 4143 was exposed with Wratten filters Nos. 29 and 55 combined. Figure 29 shows the relative spectral transmittance of the filters and the film response. The visible band imagery was properly exposed but the infrared film was overexposed to the extent that a reliable evaluation of the utility of that spectral band could not be made. Positive transparencies of the multiband imagery were studied with the aid of an additive color viewer.

Various combinations of color coding and color intensity were tested in an attempt to increase the interpretability of the conglomerate and limestone units. The final judgment was that the natural color display presented the best lithologic discrimination. Although a one-to-one comparison cannot be made between the ground multiband photography and the color aerial photography, the multiband color composite, Figure 30, shows substantially better color saturation than does the large scale color aerial photography (Figure 18) taken at an altitude of 3,000 feet (914 m). Based on this series of comparisons, lithologic differentiation can be made more confidently on the multiband color composite photograph than on the color aerial photograph.

To further test the information content of multiband photography, photo ratioing techniques, similar to those developed by Piech and Walker (1971a, 1972a, b and c) were used. A series of black and white, high, medium, and low contrast positive and negative transparencies were made of the red, green, and blue spectral band photographs. These were sandwiched in various combinations to mask out a single rock type and thus accentuate the imaging of the other rock type.
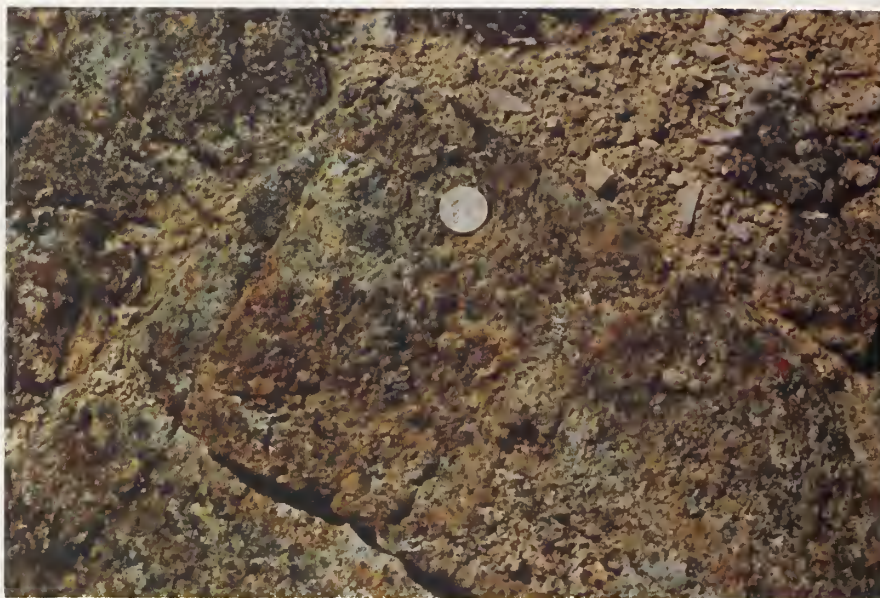
Figure 27 - The weathered surface of the Diamond Peak conglomerate is shown on this photograph (silver dollar gives scale). The rock surface, which consists largely of chert pebbles is partially coated with a lichen growth and discolored with a thin coating of desert varnish.

Figure 28 - This photograph of the Strathearn limestone, typical of outcrops near the top of the ridge, shows the limestone weathers to a light gray (silver dollar scale). Lichens coat the surface in varied amounts and the bright orange color of the lichen, when viewed at a distance, contributes to an appearance similar to the conglomerate surface. This photograph, however, is deceiving in that much of the light colored surface is actually covered with lichens which bleach white when they die.

104
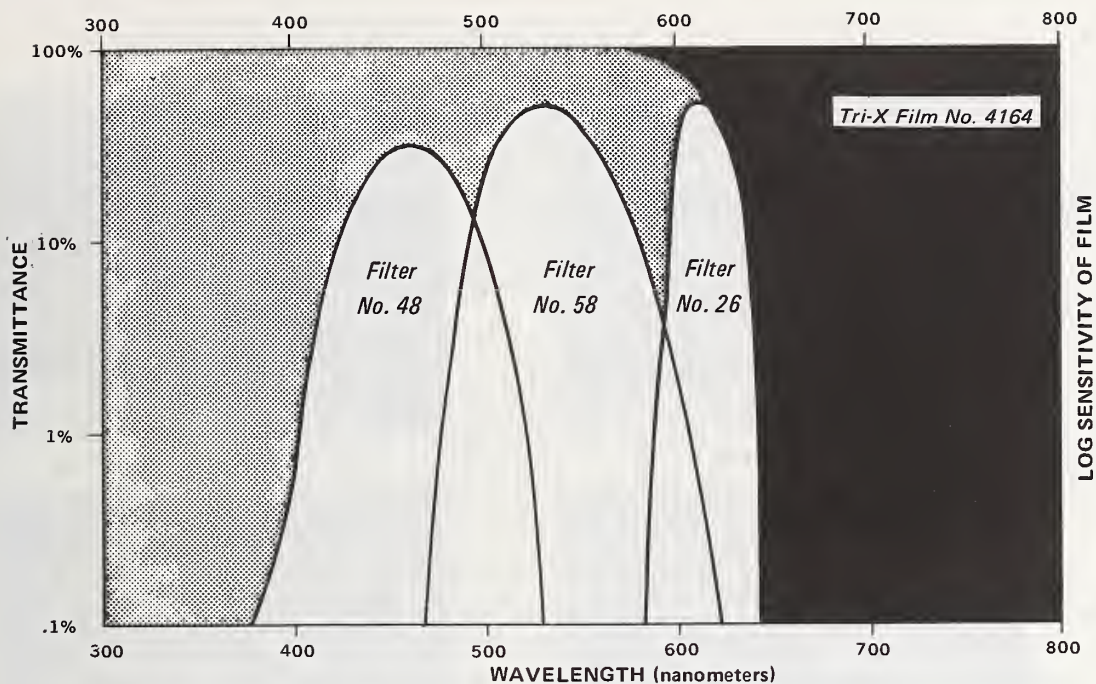
Figure 29A illustrates the relationship of the spectral sensitivity of Kodak Tri X Pan Professional Film, which is relatively flat from 380 to 640 nanometers, to the spectral transmission of the three Wratten color separation filters used. The blue filter, W. 48, has a peak transmission of 33% at 460 nm., with half-peak transmissions at 430 and 490 nm. These values for the green filter, W.58 are, peak of 54% at 530 nm., and half-peak at 505 and 560 nm. The red filter, W. 26, half-peak occurs at about 605 nm; 78% is reached at 620 nm. and 86% at 640 nm. Beyond this point the film sensitivity is essentially zero.
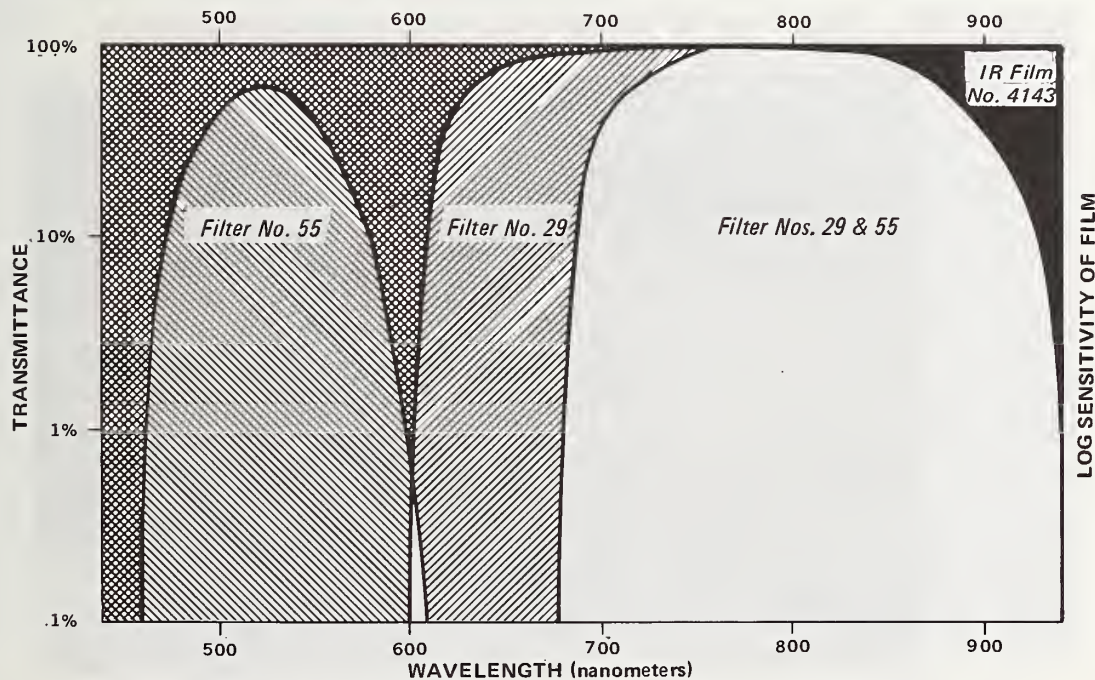
Figure 29B illustrates the relationship between the spectral sensitivity of Kodak High Speed Infrared Film 4143, and combined characteristics of Wratten filters 29 and 55. These filters, when combined, begin to transmit at about 695 nm., with 25% transmission at 700 nm. and a maximum of 90% at 800 nm. The film sensitivity peaks at about 800 nm.; the half-peak points of the film/filter combination are are approximately 710 and 900 nm.

105

Blue image (Wratten filter No. 48)

Green image (Wratten filter No. 58)

Red image (Wratten filter No. 26)

Infrared image (Wratten filters Nos. 29 + 55)

Figure 30. This color composite image was produced by combining the black and white images above with the appropriate color filters. This type of photographic processing permits the adjustment of the saturation of each color to produce the best discrimination of rock types.

106

Figure 31 represents the best results of the wide variety of
combinations tested. This image is a product of sandwiching a
high-contrast, red band positive; a low-contrast, green band
positive; and a low-contrast, blue band negative. Similar results
were obtained with a low-contrast, red band positive and a high-
contrast, blue band negative, but better differentiation is
possible with the multiband color composite image shown in Figure
30.

This test is considered only an indication of the full
potential of multiband photography because the acquisition of the
photography was not adequately controlled, the filters used were
not necessarily the best choices, and the imagery was not analyzed
exhaustively. The results do justify further investigations.

Large scale, multiband aerial photography of tunnel sites
acquired using the new Kodak Multispectral Infrared Aerial film,
SO 289 would permit the reconstruction of both natural color and
standard color infrared (false-color) images as well as a variety
of other false color presentations. With this approach only one
camera would be required to produce the results of all the dif-
ferent film products normally used. The results obtained with
such imagery, properly filtered, can be expected to be as good,
and possibly better, than with conventional color and color-
infrared films of comparable scale.

Figure 31 - Photo "masking" techniques were tested with the multi-band images shown in
Figure 30. This consisted of making positive and negative transparencies of various densities
of each spectral image. These were sandwiched in various combinations in an attempt to
mask out the Diamond Peak formation and enhance the Strathearn limestone outcrops.
These tests were not successful.

7.6 Multispectral Scanner (MSS) Imagery

For many years physicists have known that different objects
have unique reflectance and emittance characteristics. If these
differences in energy levels are sensed in enough narrow spectral
increments, theoretically, a unique "signature" for each object
could be identified. The imaging of a scene in a series of dis-
crete narrow spectral bands is possible with electro-mechanical
systems. Recording of such data on magnetic tape provides a flexi-
bility in analysis and interpretation difficult or impossible to
obtain with photographic systems. If a diagnostic "signature" for
a particular target exists within the spectral limits of the system,
computer processing can be used to differentiate the target and the
background. For instance, ferric iron bearing rocks normally
appear reddish because rocks absorb the blue and green portions of
the spectrum and reflect the red. Imagery filtered to sense only
the red portion of the spectrum should show the iron bearing rocks
as brighter targets than the non-iron bearing formations. The
contrast can be further enhanced by producing a computer ratioed
red/blue image (Vincent and Thompson, 1972b).

Goetz (1975), Vincent et al., (1973) and other investigators
have obtained impressive results applying similiar computer pro-
cessing techniques to LANDSAT imagery which is separated into
green, red, and two near-infrared bands. Goetz et al., (1975) were
able to enhance subtle differences in rock types and recognize
zones of weathering and alteration, particularly in igneous rocks.

7.6.1 Carlin Canyon Test Site

The ground surface at the Carlin Canyon test site
consists principally of limestone and chert pebble conglo-
merate and the resulting soil products of both formations.
Minor amounts of siltstone shale and coarse sandstones are
interbedded with the conglomerate. Minor beds within the
conglomerate contain hematite (Fe_2O_3) and are colored various
shades of red. Locally, the cementing material in the con-
glomerate also contains considerable limonite ($HFeO_2$), and
where this occurs, the rocks and soil appear yellowish. The
more intensively colored areas are identifiable on the color
aerial photography. With few exceptions, the two rock types
are similiar in appearance from a distance. An almost com-
plete covering of living and dead lichen increases the similar-
ity in appearance.

Multispectral imagery of the site was acquired on
October 18, 1974, (see Appendix F for system description).
Imagery in ten spectral bands was acquired simultaneously
over a spectral range extending from the near ultra-violet
into the near-infrared. Table 3 lists the tape channel and
spectral bandwidths recorded.

Table 3   Multispectral Channels and Bandwidths used in this Investigation

Channel	Bandwidth (μm)
1	.38-.42
2	.42-.45
3	.45-.50
4	.50-.55
5	.55-.60
6	.60-.65
7	.65-.69
8	.70-.79
9	.80-.89
10	.92-1.1

Densitometry of Multispectral Images

Images from the individual spectral bands look similar
with only minor exceptions as shown in Figure 32. These
images are spot samples in the spectral range of blue (.45-
.50μm), orange (.6-.65μm), red (.65-.69μm) and near infrared
(.80-.89μm). This lack of difference in spectral brightness
tends to confirm photometric field studies made by Rains and
Lee (1975) on a variety of rock types.

In order to determine the relative brightness of several
sets of targets, a series of points known to represent dif-
ferences in lithology were selected within the imaged area.
Paper positive strip prints of single channel, channel
ratios, channel combinations, and combination ratio images
were used for analysis. Using a Macbeth, densitometer,
Model TD 504, an extensive series of photographic density
measurements were made and evaluated in an attempt to:

1.   Determine the relative brightness of critical
      outcrop areas in each channel of spectral data
      (Table 4).
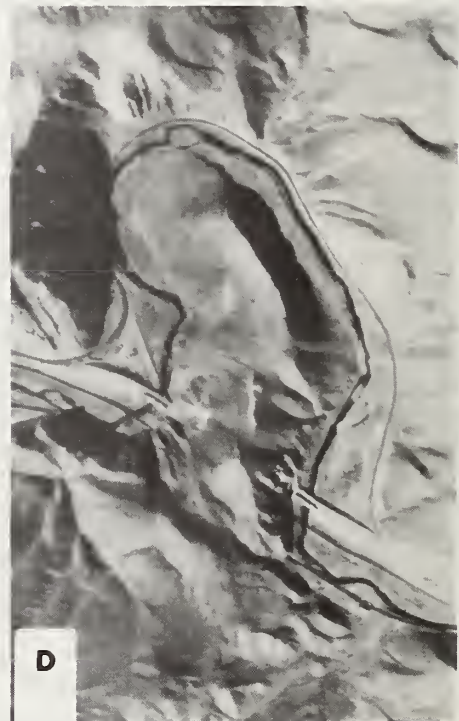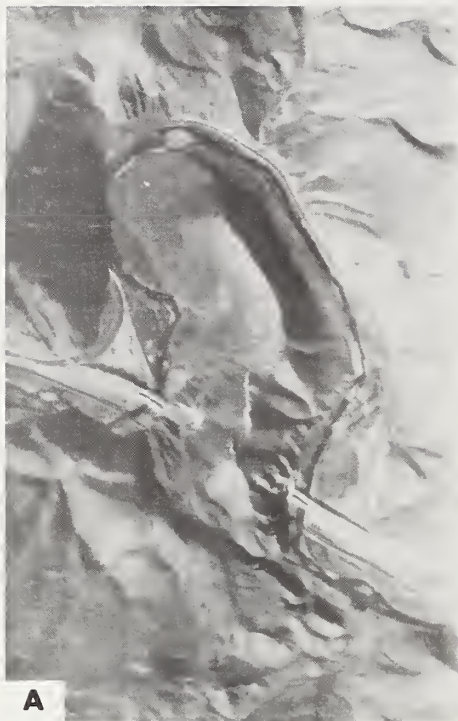
Figure 32. The soil and rocks of the Carlin Canyon area shown in these multispectral scanner images, display similar reflective characteristics over a wide spectral range. Figure A was acquired in the spectral range of .45 - .50 um, B in .60 - .65 um, C in .65 - .69 um and D in .80 - .89 um. Compare images A and B with Figure 34 which is a ratioed image of B/A.

Table 4   Densiometric Measurements of Multispectral Analog Prints   (Partial Tabulation)

CH NO.		Calibration		Blackest Image		Whitest								
		Black Edge	White Back	Shadow A	Shadow B	Ls. Talus	Ls. (6N)	Sandbar	Ls. (4E)	Cong. (4W)	Ls. (A2S)	Cong. (A2N)	Ls. (BE)	Cong. (BW)
10	Density	1.43	.11	1.17	1.12	.18	137	192	183	186	193	1.10	.83	.75
	Reflectance			7	8	66	43	12	15	14	12	8	15	18
	Normalized to 100%			0%	2%	100%	61	8	14	12	8	12	14	19
8	Density	1.40	.11	1.12	1.08	.10	.21	.69	.66	.67	.80	1.03	.61	.56
	Reflectance			8	8	79	62	20	22	22	16	9	25	28
	Normalized to 100%			0%	2%	100%	76	17	20	20	11	1	24	28
6	Density	1.40	.11	1.17	1.08	.13	.35	.79	.81	.84	.90	1.08	.80	.73
	Reflectance			7	8	74	45	16	15	14	13	8	16	19
	Normalized to 100%			0%	1%	100%	57	13	12	10	9	1	13	18
4	Density	1.42	.11	1.14	1.04	.17	.43	.91	.84	.92	.93	1.05	.84	.86
	Reflectance			7	9	68	37	13	14	12	12	9	14	14
	Normalized to 100%			0%	3%	100%	49	10	11	8	8	3	11	11
2	Density	1.41	.11	.89	.78	.18	.35	.61	.61	.69	.73	.82	.62	.63
	Reflectance			13	17	66	45	24	25	20	19	15	24	23
	Normalized to 100%			0%	8%	100%	60	21	23	13	11	4	21	19

Ls. = limestone   Cong. = conglomerate

111

2. Establish that the resultant relative brightness of combinations of channels are logical developments from their "raw" image data.

3. Select a set of channel combinations of the original taped data to produce images that would optimize the relative brightness differences.

Additive Color Enhancement

A series of images from channel combinations selected to simulate LANDSAT spectral bandwidths were combined to simulate (a) normal color, (b) color infrared, and (c) very "false-color" to maximize the spectral differences.

As one can see in the aerial color photograph of the Carlin Canyon test site, Figure 18, there is little variation in the uniform light yellow brown to white color over the area. The reconstruction of natural color imagery, (Figure 33) produced from the proper combination and color coding of the appropriate spectral bands, did not produce significantly different information. The image does, however, demonstrate some of the versatility of multiband imagery. A color infra-red multiband composite, also did not provide additional useful information for structural analysis or discrimination of rock types. The latter result, however, is judged to be largely due to the season in which the data was acquired. Consequently, these examples should not be interpreted as condemning the use of additive color processing of multi-spectral imagery. Because additive color viewers permit the selection of color filters and the intensity of light to be used in viewing each spectral band image, features of interest can usually be exhibited in greater contrast than they appear on natural color photography.

Spectral Band Ratioing

A number of computer ratioed images were made in an attempt to enhance geologic features in the area. These efforts concentrated on enhancing faults and fractures and on lithological discrimination. Most of this type of processing was restricted to the Carlin Canyon site because rock outcrops were more extensive and visible at this site than in the East River Mountain area. The most significant result was the enhancement of the ferric iron bearing zones. Ratios of the .60-.69μm band or .60-.65μm band to the .45-.50μm band appear to provide the best discrimination of ferric iron. The latter ratio provides somewhat better image contrast or enhancement and is shown in Figure 34. Areas of concentration of ferric iron are imaged as above average in brightness;

Figure 33 - Color composite image from the multispectral scanner
imagery produced by printing spectral bands .42-.50um in blue,
.50-.60um in green and .60-.69um in red. Because the spectral
"cutoff" characteristics of the grating in the multispectral scanner
is much sharper than that of the color film, the color of this image
only approximates that of Figure 18. This does, however, illustrate
some of the versatility of multispectral scanner imagery.

113

Figure 34 - Ratio image produced from spectral bands .60-.65um/.45-.50um. The resulting image emphasizes in lighter tone the ferric iron zones in the Diamond Peak conglomerate. Compare this image to Figures 32A and B from which it was produced. Points d, e, f, and g can be seen in Figure 18.

the lighter the image tone, the greater the iron concentration. The more obvious areas are at Points A, B, C, D, E, F, and G. All of these bright areas are restricted to the Diamond Peak conglomerate outcrops with the exception of Point C which is freshly exposed alluvial terrace gravels of probable Pleistocene age. These terrace deposits are reddish toned and contrast with the overlying light gray limestone talus (see Figure 18).

Several combinations of the ratioed images were examined with an additive color viewer. The combination which provided the most contrast between the limestone and the conglomerate was used to produce the image shown in Figure 35. The letter designations shown on Figure 34 will be used in the following discussion concerning this color composite image.

In Figure 35, the distribution of the yellowish-orange areas should be compared with the geologic map over print in Figure 16. It is evident that Figure 35 is predominately blue on the right and reddish on the left which roughly is the distribution of the Strathearn limestone and the Diamond Peak conglomerate. However, the contact as shown in Figure 16 does not coincide with the distribution of the two colors in Figure 35. Examination of Figure 16 and the color stereogram, Figure 18, shows that Points D, E and F are separated by talus material eroded from the overlying limestone, which appears as blue. Much of the west slope of the spur is also mantled with talus from the limestone ridge. Points A and B are exposures of the conglomerate beds in which the iron appears predominantly limonitic and yellowish in color. Points D, E and F are hematitic and all are reddish, particularly Point F. Point C is the exposed iron bearing terrace materials overlain with limestone talus.

The faint yellowish streaks to the east of the Humboldt River at Points H and I occur on limestone talus slopes. Field examination of these points indicated that numerous limestone cobbles and pebbles were stained with a thin ferric iron coating. This indicates the high degree of sensitivity of this system for the detection of ferric iron. Another point of passing interest is that the Pinon pines present on the hillsides to the north of the river are imaged as white.

In summary, the densitometric studies and the ratioing and additive color processing of the multispectral imagery made in this study established that there was little if any spectral difference between the limestone and the conglomerate formations in the area except where localized reddening of the conglomerate could be easily found as bright hazy spots
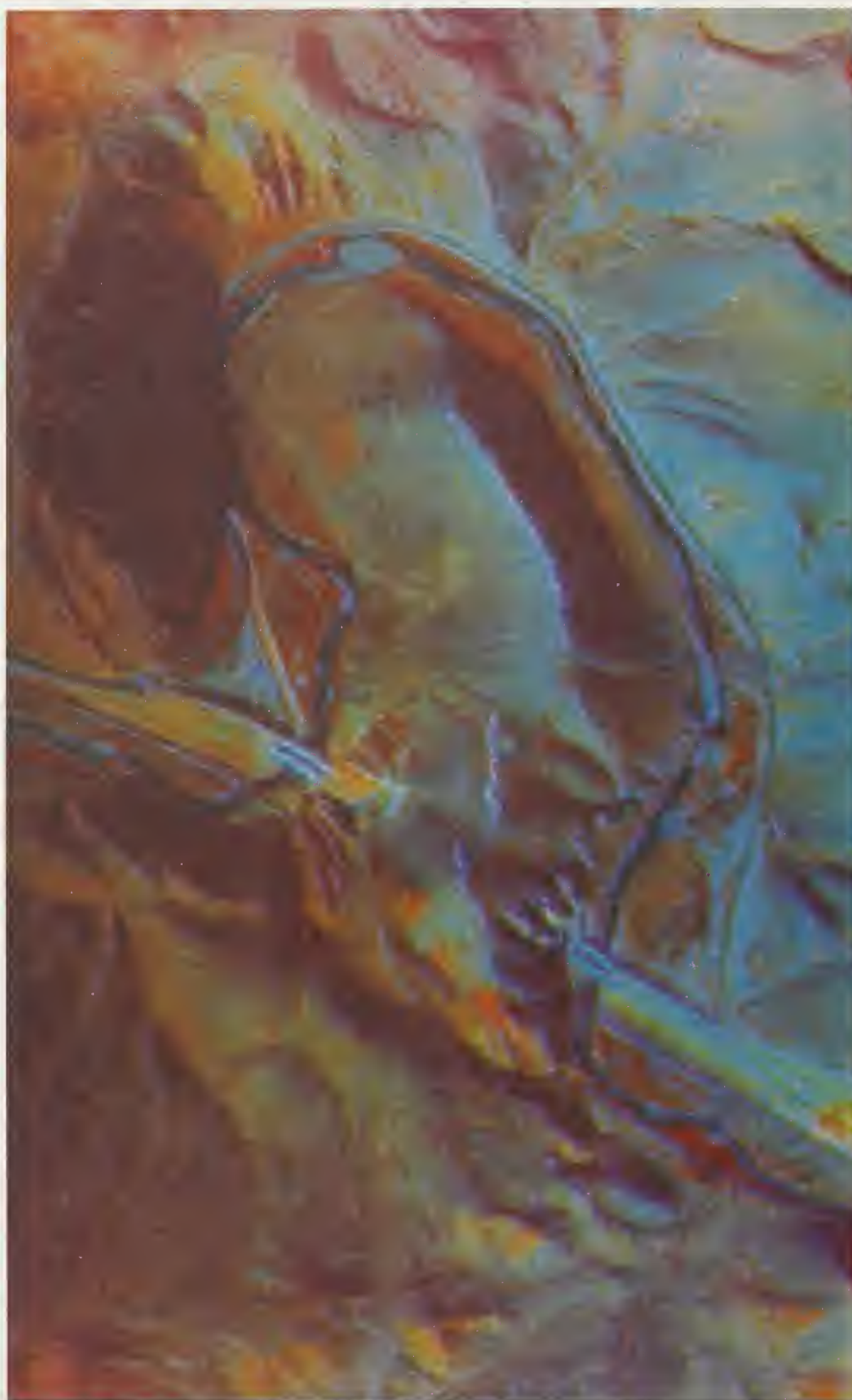
Figure 35 - This color composite image was constructed from three ratioed images as follows: blue from .45-.55um/.65-.79um, green from .60-.69um/.70-.79um and red from .45-.55um/.65-.79um. Here, the presence of ferric iron is emphasized by varied shades of yellow and orange.

in areas on a .55-.60μm/.50-.55μm or a .60-.65μm/.45-.50μm
ratioed image. With the color-coded, ratioed images, the
lithologic discrimination of the materials is more pronounced
than on any other type of imagery.

Spectroradiometric Investigations

To further calibrate the airborne data two series of
reflectance measurements were made in August 1975 with an
ISCO scanning spectroradiometer and in October 1975 with two
Exotech four-band radiometers filtered to correspond in
bandwidth to the spectral range of the four LANDSAT multispectral
scanner channels. The details of these investigations are
presented in Appendix E.

7.6.2 East River Mountain

Visible and near-visible multispectral scanner imagery
of the East River Mountain was acquired near noon on 1
April, 1975. Single channels of data provided no significant
information that was not available from the aerial photography.
Also, ratioing of various spectral bands did not appreciably
increase the geologic information that could be extracted.

Of only casual interest to tunnel site studies, a
ratio of bands .60-.69 μm/.80-.89 μm greatly increased the
discrimination between evergreen trees from the dormant
deciduous vegetation cover. Pine trees are scattered over
much of the south slope of the mountain and only locally do
they occur in groves. The high reflectance of the evergreens
as measured in the infrared band, when ratioed with the low
reflective response in the red band, markedly enhanced the
image contrast of these trees.

7.7 Thermal Infrared Imagery

Imagery acquired in the 8-14 μm spectral band can provide
unique geologic information. The type of information derived
depends in part on the system used. Thermal scanners are available
with single detectors which sense energy emitted throughout the
8-14 μm atmospheric window or filters can be used to restrict or
divide the bandwidth sensed. Some systems have the capability of
simultaneously sensing in 2 or 3 bandwidths that are narrower
than the full 8-14 μm window. Such systems permit manipulation
of the data by computer processing to extract geologic information
not evident on a single channel of data.

A two-channel thermal scanner system was used for this investigation. The spectral bandwidths sensed were 8-10 μm and 10-12 μm (see Appendix F for more detailed information on the system).

Thermal scanner imagery was acquired of the eastern and western test sites within 24 hours of the overflight for the multispectral scanner data. The same scanning system was used to acquire both types of imagery, but equipped with appropriate detectors and filters for the different missions. Overflights for thermal imagery were made during the day and at night. Daytime thermal imagery is generally considered not to be as good as night time imagery for most purposes. However, for detecting soil moisture by the effects it has upon the apparent temperature of the ground surface, daytime imagery has proven to be useful. Thus, daytime overflights may be valuable for the detection of water concentrations in fracture zones and faults. Further, daytime differential solar heating of the irregular ground surface produces pseudo-shadow patterns which appear similar to low-sun-angle photography.

7.7.1 Carlin Canyon Test Site

Thermal imagery of the Carlin Canyon site was acquired on October 17, 18, and 19, 1974. Daytime temperatures ranged from 70° to 75° F. (21° to 24° C) and night time temperatures dropped to 32° F. (0° C) by 10:30 in the evening. Night time overflights were made on October 17 at about 11:30 p.m. There was a question as to the quality of the recorded data from this flight, and the flight was repeated before dawn (6:30 a.m.) on October 19. Daytime thermal imagery was acquired at about 10:45 p.m. on October 18. During each of the missions, overflights were made at two different altitudes. A single overpass made at an altitude of approximately 6,000 feet (1828 m.) provided a synoptic view of the area. Multiple overflights made at an altitude of approximately 3,000 feet (914 m.) obtained the desired detail concerning the geology of the test site. At this site the larger scale imagery flown in overlapping flight lines allowed the imagery to be viewed stereoscopically. Stereoscopic viewing of thermal imagery can be useful in analysis although it is not an essential requirement if, as it should be, the thermal imagery is analyzed in conjunction with aerial photography.

The majority of the analyses conducted on the Carlin Canyon imagery was with Flight Line D from the mission flown just before midnight on October 17. A number of different

processing techniques were used on the data (see Table 16 in Appendix F).

Little difference between the two spectral bands could be detected by visual examination on the imagery. Neither spectral band showed any lithologic discrimination between the limestone and the conglomerate, although the thermal inertia properties of the solid rock outcrops caused them to be imaged as warmer than the adjacent soil cover. Figure 36 is an example of the 8-10 μm band image. Because of the outcrop and soil patterns the angular unconformity between the Diamond Peak conglomerate and the Strathearn limestone is prominent and easily recognized in the bend of the river. For the same reason some of the minor faults and fractures can be seen to the north of the east portal of the tunnel.

A ratioed image (8-10 μm/10-12 μm) from the midnight overflight was rather disappointing. As previously discussed silica (SiO_2) exhibits an emission minima in the 8-10 μm range, therefore, diagnostic information relating to the silicia content of the Diamond Peak formation should be derivable from this ratioed image. The discrimination of siliceous rocks by thermal image ratioing does not rely on thermal contrast between rock types, but upon emission minima produced by silica in the 8-10 μm band. When the signal levels of the two channels are essentially equal, which is true for most materials, the value of the ratioed signal will be near unity and all such features will appear as a uniform gray tone on the image. Those features that produced different voltage levels on the individual taped channels will appear either lighter or darker in the ratioed image.

As mentioned in Section 7.5 and illustrated in Figures 27 and 28, both rock types have appreciable lichen cover. The weathered surfaces, plus the partial coating of lichen growth, tend to mask the true spectral response of the rocks and minimize the emission differences anticipated between the silica rich conglomerate and the limestone.

The image shown in Figure 37 was made from the predawn thermal data. This ratioed product reveals substantially more significant geologic detail than that from the midnight data in spite of the light and dark tone banding across the image produced by "bounce" in one of the detectors ("bounce" occurs when one of the detectors does not maintain a constant base level of response).

Figure 36 - The high thermal contrast between the rock outcrops and the adjacent soil on this 8-10um thermal infrared image is due to the high thermal inertia properties of the dense rock material. No discrimination between the two dissimilar rock lithologies is possible on this image. Some anomalous linear features can be identified because of the rock-soil thermal contrast.

120
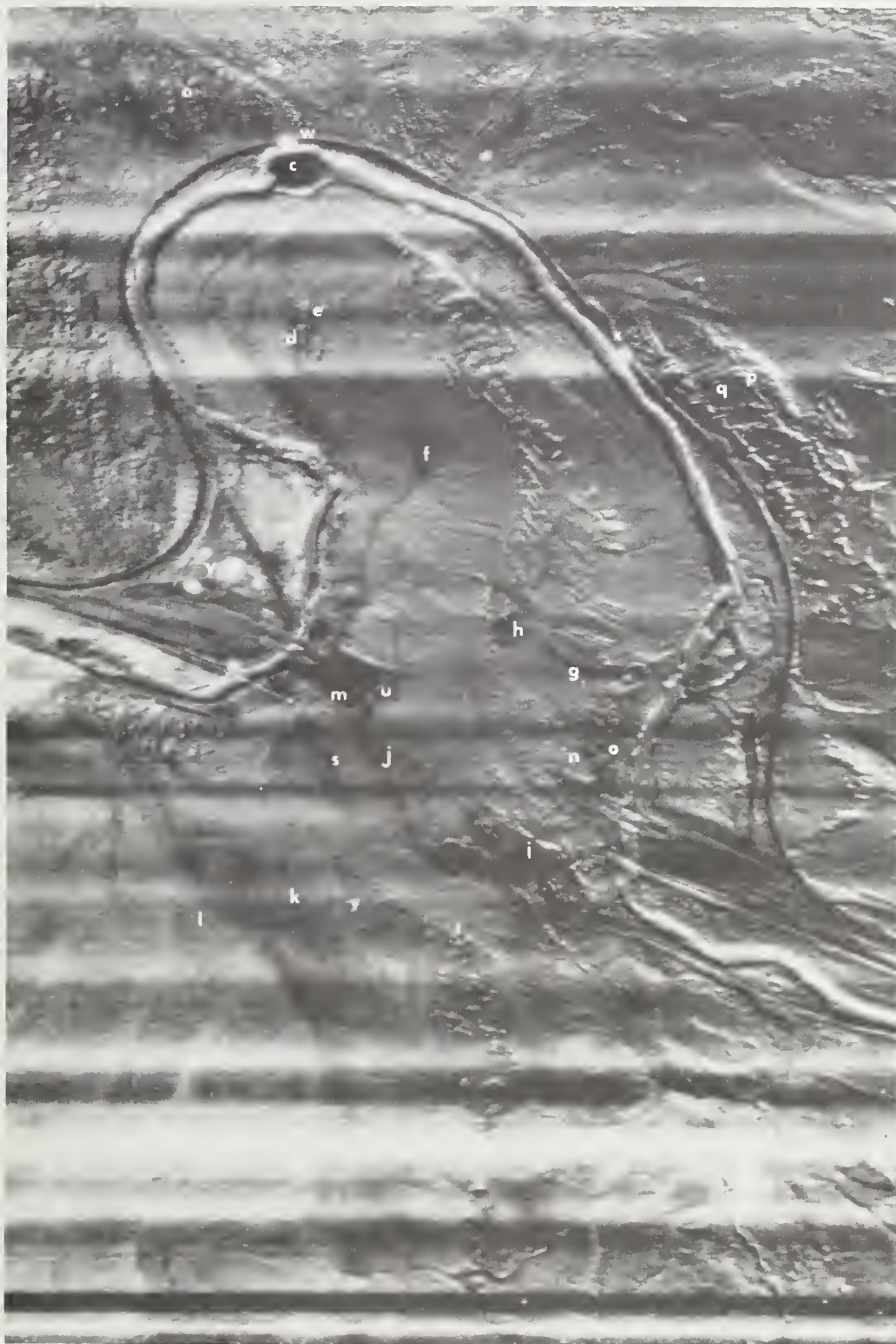
Figure 37 - Silica bearing rocks exhibit an emission minima in the 8-10um range and should appear dark on this 8-10um/10-12um spectral band ratioed image. This was partially accomplished on this image. See the text for details concerning the annotation.

Points a and b on this image represent the Diamond Peak conglomerate and the Strathearn limestone, respectively. Although differences are not pronounced, the more siliceous conglomerate appears somewhat darker on this image. Point c is an island in the Humboldt River, barren of vegetation, which consists predominantly of silica sand, consequently, it appears dark on the image. Points d and c lie on the contact between the two formations. The dark streak at Point d is a chert conglomerate bed. Point f is an area that was disturbed by a bulldozer. This area was excavated to considerable depth and refilled, and no doubt, the soil exposed in this area contains a higher percentage of silica than the surrounding limestones talus. Point h is on the trace of the large fault that separates the Strathearn limestone from the Diamond Peak formation (F_3 on the map in Plate I and Figure 16). The area designated by h is anomalous and could not be resolved with the remote sensor imagery. A field check indicated that it is an area of concentration of chert pebbles and sand material weathered from the Diamond Peak formation. It is topographically slightly higher than the surrounding area, thus, the material has not been contaminated with limestone debris. The darktoned arcuate area designated Point g is also anomalous and probably cannot be explained without detailed soils analysis. The dark zone coincides with a minor drainage channel on the hillside. Field examination disclosed that there are small outcrops of the Diamond Peak conglomerate in this channel, however, the rock exposures are not continuous and soil material forms the bed of the remainder of the gully. It is surmised that this soil, although similar in appearance to the surrounding area, contains a higher percentage of siliceous sand. There is also less vegetation present.

The difference in tone between Points n and o (Figure 37) mark the large fault F_3 shown on Figure 16. The fault trace here is somewhat more clear than on the aerial photography. Point m marks the river terrace material and Point u, the limestone talus exposed when the west portal was excavated. The underlying terrace deposit contains substantially more quartz sand than the overlaying talus, consequently, Point m is imaged much darker than the remainder of the area. Points s and j are slightly darker bands which are outcrops of conglomerate beds.

Points l and k lie in an area of the highly siliceous Webb formation. The line between these two areas is a gully, the sides of which are quite steep. Field examination of this area indicates that area l has more soil cover then does area k. Consequently more siliceous rock fragments are exposed on the surface in area k accounting for the darker tone. Point t marks the fault F_{11} shown on Figure 16. The dissimilar

appearance of the areas along this line is in part due to rock texture or size of the material exposed at the surface, and in part due to a greater development of soil cover to the north of Point t. Point v marks the fault, F_{12} shown on Figure 16 and the trace here can be identified for the same reasons. In neither case can the full extent of the fault be drawn on the basis of this image. The white spots on the road are vehicles.

In summary, the pre-dawn data produced substantially better results than that produced from the data acquired at midnight. The ratioed image from the pre-dawn overflight contains substantially more geological information than does either single channel image. Some of the information is as well or better expressed on this image than on any other remote sensor data product.

7.7.2 East River Mountain Test Site

Thermal imagery of this site was acquired on 1 April, 1975 at approximately 4:30 in the afternoon and at 11:30 at night. Some rain had fallen within the 24-hour period prior to the overflights and approximately six inches of rain had fallen within the three weeks prior to the mission, thus, the soil was very wet. In spite of this, the imagery contained considerable useful geologic information. The afternoon, thermal imagery Figure 38, looks similar to aerial photography acquired at a low sun angle. Those areas not in direct sunlight are cooler and consequently image in darker tones. Density slicing of the image into eight gray scale levels emphasizes the contrast between targets of slightly different temperatures. With the system used, this density slicing is keyed to the black body reference temperatures, established at the time of data acquisition. Consequently, each gray level on the image represents a known range of radiant temperature.

Figure 39, daytime thermal imagery processed with the contour algorithm (see Appendix F for further detail), emphasizes the linear nature of several features. The linear labeled W in the upper left corner of Figure 39 is pronounced on this image, but it is difficult to see on the eight-level processed image and is extremely subtle on the continuous tone (analog) print. Detailed examination of the large scale color photography lends some support to the presence of a fracture, but without the emphasis provided by contouring the analyst overlooked the feature. Linear X, prominant on this image as on other types of remote sensor data, is interpreted as a fault. Linear Y is an extremely straight side of a flatiron

Figure 38 - Thermal infrared imagery acquired during daylight hours has an appearance similar to low-sun angle photography. This 10-12um image of the East River Mountain site, acquired in the afternoon on April 1, shows a pseudo-shadow effect. The dark areas are not shadows, but there is a direct correlation with the true shadows of the visible spectrum. The shaded areas and those areas not exposed to direct sunlight, are cooler and emit less heat, and thus, are imaged as darker tones. Compare this image with Figures 13 and 14.
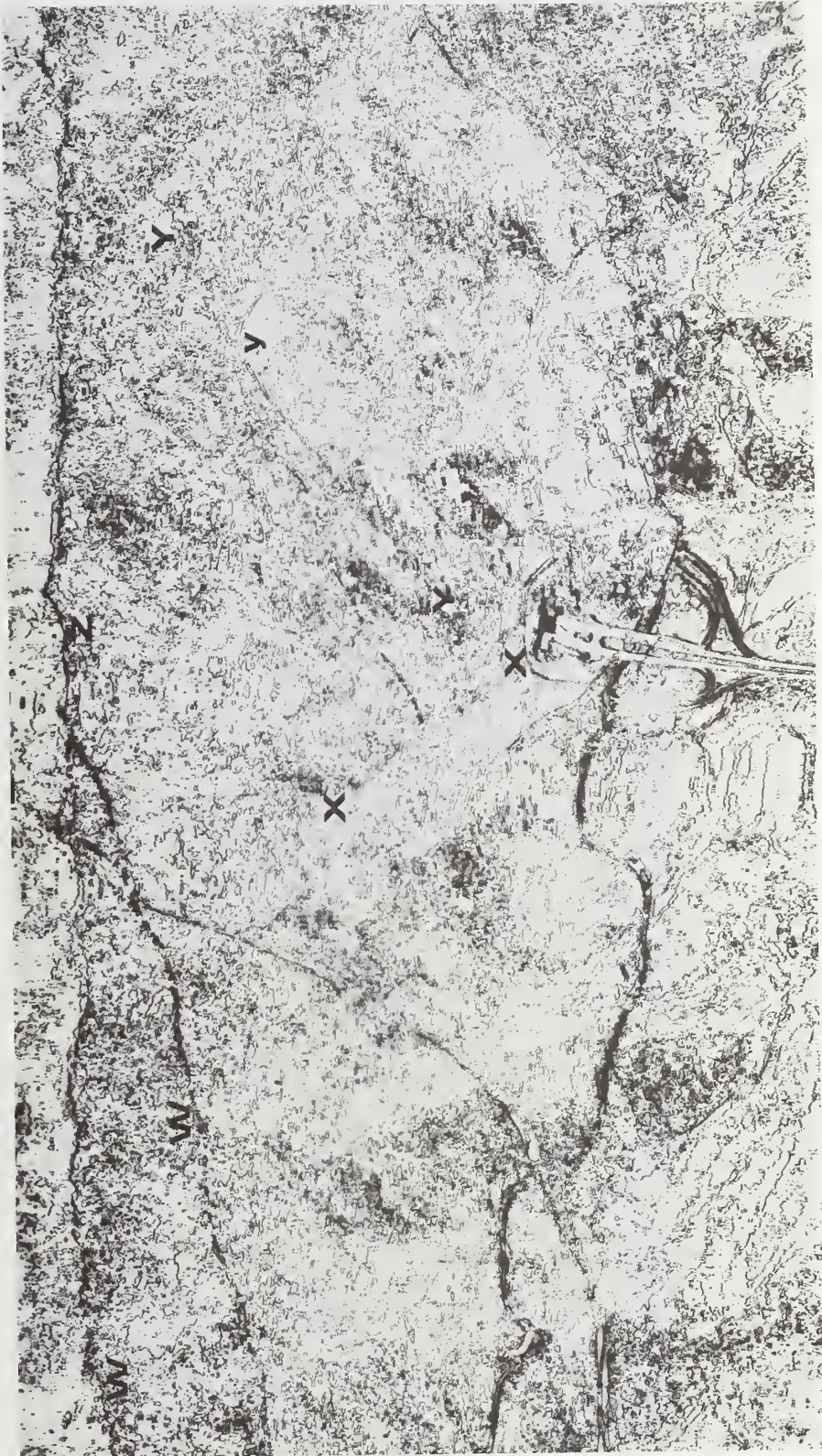
Figure 39 - This figure illustrates the "contour" technique of image processing. The day time thermal image of the south slope of the East River Mountain shows several linear features of possible structural significance not identified by other processing techniques. The production of such imagery is described in Appendix F.

125

of Keefer sandstone, and, consequently, is suspect of being a
fault. The tip of the flatiron is near Point y, but the
linear appears to extend beyond the crest of the ridge which
further supports the hypothesis that it is a fault. Inter-
pretation of the aerial photography, however, does not indi-
cate any appreciable displacement across this feature. It
could represent a prominent fracture and, from an engineering
point of view, be of concern in tunnel boring. Linear Z is
less obvious on this image, but is of such length that it
could intersect the tunnel near the north portal. Numerous
other linear features visible on this image may be of struc-
tural significance. It is emphasized, however, that thermal
imagery should be analyzed in conjunction with aerial photo-
graphy. This is particularly important with imagery such as
Figure 39 which has lost most of its "photographic" character.

The two bands of the thermal imagery, Figures 40A and
B, acquired during the 11:30 p.m. overflight, look essentially
identical. The only large rock exposures in the area are of
the Tuscarora sandstone along the crest of the mountain. Here,
Point K, Figure 40B, it consists of two massive resistant
sandstone beds (light toned) separated by a softer shaly sand-
stone unit (dark toned). The two resistant units appear warmer
on the imagery because of the high thermal inertia of the sand-
stone. The Juniata shale and sandstone sequence underlies the
Tuscarora sandstone, Point L. The upper portion of this unit
appears darker or cooler than the underlying strata on the scarp
slope. This may be because the area immediately below the
Tuscarora escarpment is shaded for a major portion of the day
and is more sheltered from insolation than other parts of the
mountain. The scarp slope consists of relatively non-resistant
rock and the entire slope is covered with a soil mantle of
varied thickness. The only place the Juniata formation outcrops
is near the top of the slope where the soil is thinner. The
difference in the emissivity characteristics of the Juniata
bedrock exposures and the thin soil cover also may contribute
to the differences in apparent temperature.

The dip slope of the East River Mountain is moderately
dissected with small drainage systems between the flatirons.
Many of these drainage channels, particularly on the upper
portion of the mountain, Points M, Figure 40B, are substantially
lighter in tone, appearing much like the bare rock exposures
of the Tuscarora sandstone at the crest of the mountain.
Field examination of several of these drainage systems
revealed that there are boulder trains composed of large
blocks of Tuscarora sandstone concentrated in the gulleys.
Several dark tone features of linear nature can be seen on
the imagery. Linear, X, in Figure 40B, is identical to "X"

Figure 40A - This image and the one in Figure 40B are, respectively, thermal images acquired simultaneously in the 8-10um and 10-12um spectral ranges. The two images appear nearly identical; compare on both images Point T which is an operating sand quarry. Also, note the tonal character of the areas U and V in front and behind the south portal. Compare the tonal character of these points with Figure 41.

127

Figure 40B - Thermal infrared imagery acquired in the 10-12um range contains numerous anomalous temperature patterns indicating features of geological interest. The dark toned (cooler) area, Z, approximately coincides with the outcrop pattern of the Rose Hill formation, a ferruginous sandstone-shale sequence. Linear, X, is a fault trace (see the text for further discussion).

on Figure 39 and is the fault identified as F_1 on Plate II and V (in pocket). On this imagery, it is seen as a faint dark line extending from the ridge crest to the south portal of the tunnel. Another dark toned linear feature identified as Y in both Figures 39 and 40B and as F_4 on Plate II and V, extends from the tunnel course in a northeasterly direction.

In this heavily vegetated area, the ground is nearly totally covered with a blanket of dead leaves. The area around Point P, Figure 40B, has been partially cleared and heavily used as a livestock holding area. Considerably more bare ground is exposed here than in the adjacent areas. The wet ground has been cooled by evaporation, thus, appears as dark-toned. The dark zone labeled N is a power line right-of-way that has had the vegetation removed and bare ground exposed.

Figure 41, the ratioed image of the two thermal channels, shows close similarity in the response of the two spectral bands except for two distinct areas. Theoretically, areas of high silica content should appear dark on this image. The sand quarry at Point T is dark just as theory predicts.

The area, V, a short distance above the south portal building appears equally dark on both channels of thermal imagery, Figure 40 A and B. These dark tone areas proved to be of comparable apparent temperatures and, thus, essentially cancelled out on the ratio image. In contrast, the area U in front of the south portal appears dark, indicating considerable silica (quartz sand) within this area. Examination of the aerial photography and field observations indicates that the area was freshly tilled and probably seeded, but not overgrown with grass. The area behind the portal building was approximately 50% covered with lespedeza[3] which was apparently adequate to mask the silica response on the 8-10 μm band imagery.

Sink holes known to be present in the vicinity of the north portal are not easily seen on the thermal imagery. This is not surprising, as at least one of two factors would need to be present for them to stand out on the imagery. First, there would need to be a substantial difference in soil moisture content in the depressions and the surrounding area to create a thermal contrast. The excessive rainfalls that occurred in this area immediately before the overflights

---

[3] A shrubby leguminous plant widely used in eastern United States to improve soil and to impede erosion.

Figure 41 - The ratioing of two channels of nearly identical information will produce a near constant level output as shown in this ratio of 8-10um/10-12um thermal infrared data (the same channels of data used to produce Figures 40A and 40B). The sand quarry at Point P appears dark in this ratioed image because of the 8-10um emission minima of silica. Compare the thermal response of Point T on this image with that on Figures 40A and 40B. The area U on this image is dark, also indicating a high silica content, whereas area V which was dark on both thermal band images appears a uniform gray, indicating equal thermal response from both spectral bands.

precluded this difference being present. Second, sink holes
connected to an open underground cavern system may exhale
warmer air at night which would then warm the soil around the
opening in the sink hole. The cavern system in the area north
of the ridge was probably filled with water because no such
warm spots are identifiable. One or two of the sink holes
which contain standing water appear on the thermal imagery as
warmer areas. These, however, could only be identified after
correlation with aerial photography.

In summary, the thermal imagery of both the Carlin
Canyon and the East River Mountain test sites produced new
information as well as corroborated information from other
sources. The identification of features on the thermal
imagery that were originally mapped by other techniques prove
that these features are real and may be of structural sig-
nificance and important to engineering decisions.

All of the stratigraphic units on the dip slope of the
East River Mountain contain a substantial quantity of silica.
However, the only place that the ratioed image indicated a
concentration of silica was in a small borrow pit where fresh
exposures exist. None of the natural exposures of bedrock
appear to conform to the theory that silica-rich rocks show
an emission minima in the 8-10 μm spectral range. Figures 25
and 42 are ground photographs of the Tuscarora and the Rose
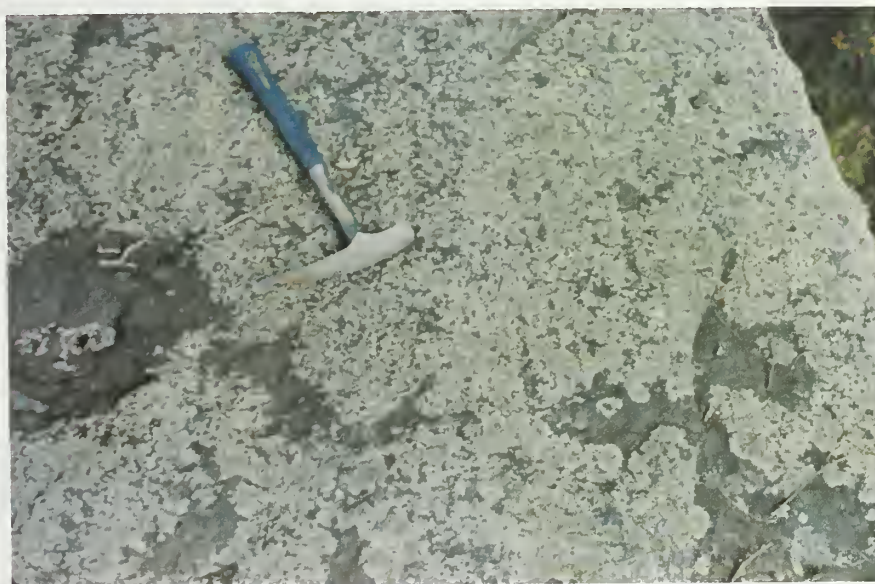
Figure 42 - This outcrop of ferruginous Rose Hill sandstone shows the typical lichen
coating prevalent in this area.

131

Hill formations and are typical examples of the nature of the rock outcrops in this area. In all instances the surface of the natural rock exposures are almost completely covered by lichens. Because the depth of sensing of thermal imagery is only a few micrometers, the lichen cover effectively masks the true nature of the rock.

Based upon the results of the thermal survey at this site dual-channel thermal imagery and ratio analyses provides little additional information of geological significance in a humid environment. Single channel imagery, on the other hand, contains substantial information of geological significance.

7.7.3 Additional Examples of Thermal Imagery

One might argue that the tunnel sites used in this investigation were poor for demonstrating the full capabilities of thermal remote sensing. However, the sites were selected arbitrarily, without bias, except for climatic conditions, and the sites are typical of most tunnels located in similar climatic zones.

The Carlin Canyon site is a well drained meander spur in an area of low rainfall, four inches (10 cm) per year. The imagery was acquired after an extended dry period (six-seven months). If the faulting would ever have been detectable with thermal imagery as a result of differential moisture concentration along fault traces it would have been shortly after the rainy season, i.e., April or May.

The East River mountain site receives 40-60 inches (100-150 cm) of rainfall per year. The test area was overflown as late in the winter season as practical (1 April); further delays ran the risk of having a leaf canopy mask the ground. This necessitated acquiring the thermal imagery after heavy rains (six inches, 15 cm., in the previous three weeks). The ground was saturated and differential moisture concentrations along fault zones were minimal.

Thermal scanning systems are generally considered to provide consistently better results for geological analysis in arid environments because of better rock exposures and the marked effects small moisture differences can have on the radiometric temperatures of rocks and soils. It is this latter property that can produce unique results with thermal scanning not obtainable with shorter wavelength sensing systems.

It is felt that the full potential of thermal infrared imagery was not adequately demonstrated in the results of the investigation. Thus, additional examples of 8-14 μm imagery are included. However, in all honesty, these examples represent exceptionally good results and should be judged in that context.

Figures 43 and 44 are examples of thermal imagery and black and white panchromatic photography of an area in southwestern United States. The value of the thermal imagery as a complement to conventional photography is obvious. Although the thermal image, Figure 43, has not been corrected for scan angle distortion, correlation between the two images is not difficult. The stratification of the alternating sequence of limestone (light tone) and carbonaceous shale (dark tone) on the thermal imagery, Points a, b, c, and d are more distinct on the thermal image. Faults F_1 and F_2 are evident on both the photography and the thermal imagery, however, fault F_3 is much less distinct on the photography. The higher tonal contrast between the different lithologies as shown on the thermal image permits greater reliability in correlation of stratigraphy across the fault.

The value of thermal imagery for locating hidden faults under certain conditions is illustrated in Figures 45A and 45B. The upper image is a black and white panchromatic photograph of a dry desert wash. The lower figure is an 8-14 μm thermal image of the same area (the arrows on each image will help to correlate the scenes). In the aerial photograph there is no visible evidence of faulting. However, in the thermal image the dark tone area appears bounded by two faults (see arrows) that are upthrown on the lower left and the lower right. These faults have formed a barrier to groundwater movement and the evaporative cooling effects produced by the higher concentration of soil moisture behind these barriers have created a temperature differential sufficient to be detected by the thermal sensor.

Small scale thermal imagery can be useful where there is inadequate information on the regional geology of an area of interest. Figure 46 is an example of imagery acquired at an altitude of about 25,000 feet (7260 meters) AMT. It shows numerous lineaments that can only be explained as faults or fractures.

Thermal imagery, as emphasized above, is sensitive to temperature differences produced by small variations in the moisture content of soils. Differences in thermal inertia of materials can also be a significant indicator of geology.

133
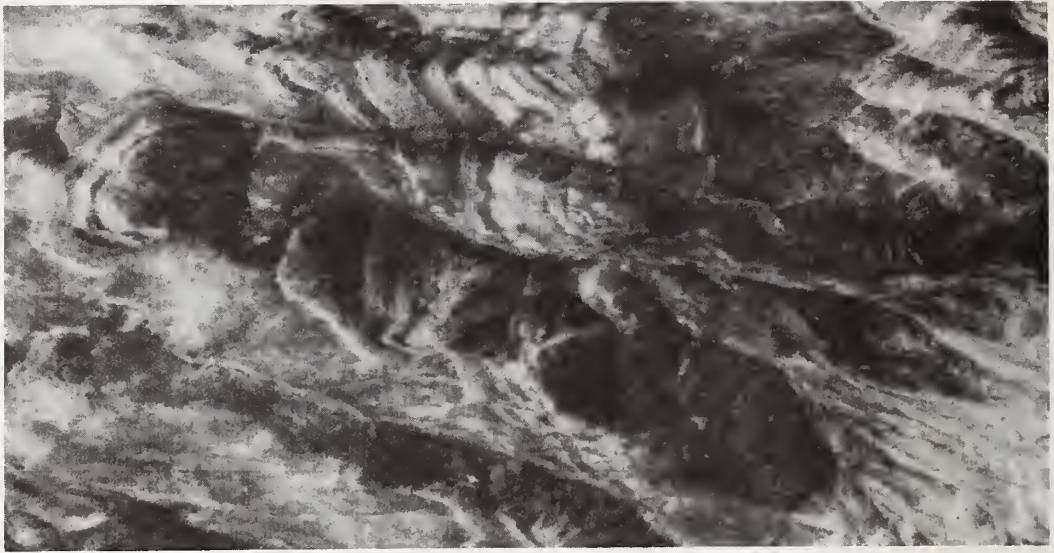
A
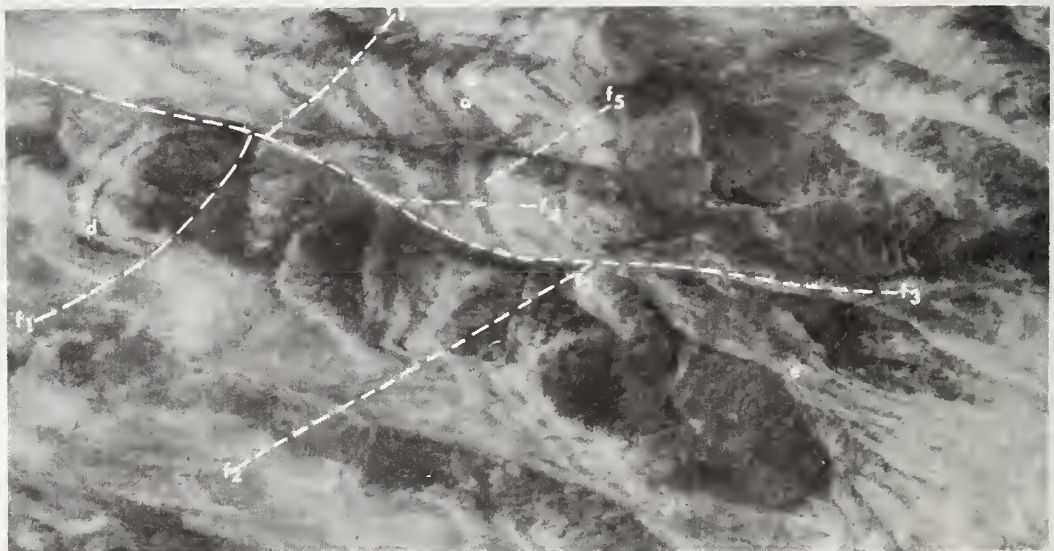
B

Figure 43 - The light and dark toned banding on this 8-14um thermal image shows a marked difference in thermal response of the limestone (light toned) and the black, carbonaceous, blocky shale. This sharp display of the stratigraphy is an aid in mapping faults and fractures as shown in image B. Compare this image with Figure 44 which is a panchromatic aerial photograph of the same area.

Figure 44 - Lithological discrimination on this panchromatic aerial photograph is typical of such photography in arid regions. A resistant strata, probably limestone or sandstone, is underlain by strata which appear faintly on this photograph as alternating bands of light gray. Anomalous topography and vegetation alignments show several faults or fractures present in the area. Compare this image with Figure 43.
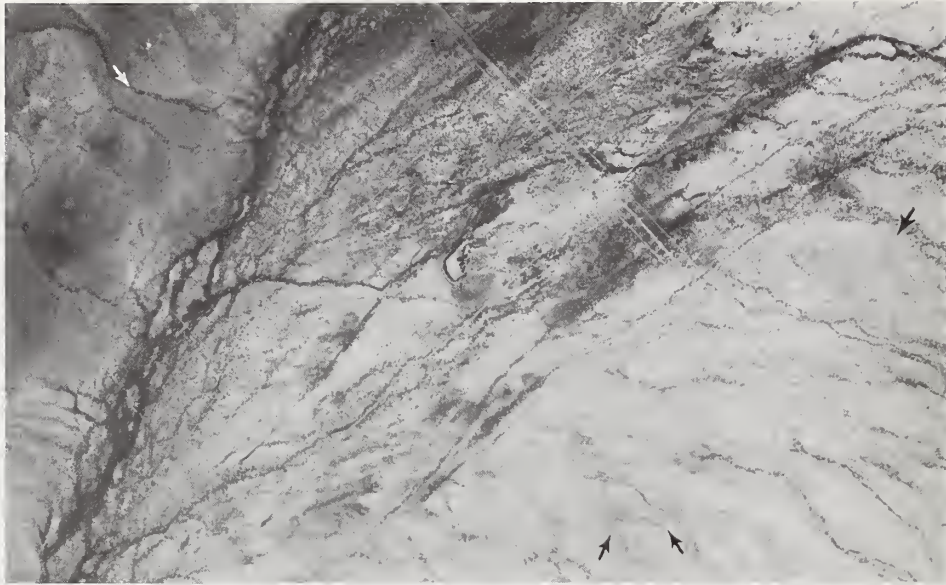
A

B

Figure 45 - Much of the arid desert area of the Western United States is covered with extensive sheets of alluvial and colluvial waste material which disguises much of the structural geology. In this matching pair of images of panchromatic photography (image A) and 8-14um thermal infrared imagery (image B), the utility of thermal imagery for revealing some of the hidden structure is illustrated. The obstruction of the movement of groundwater by faulting is shown by the cooler dark toned area.

Briefly, less compact materials generally have a lower thermal inertia than more dense materials. This property combined with the effects of soil moisture differences makes the thermal scanner an effective tool in evaluating an area for potential landslides. Figure 47 A is an 8-14 μm thermal infrared image of an area near Newport Beach, California. This imagery was acquired near midnight in November after an extended dry season. Figure 47 B is an aerial photograph of the same area showing old landslides identified by Vedder (1957). The main areas of interest in this photograph are the sides of the large elongate hill traversed by the dirt road. The letter symbols identify the same areas on both images. The majority of the dark tones occur within identified bounds of landslides and are interpreted as areas of looser soil compaction and higher concentrations of soil moisture. This is indicative of the slide areas that have not completely stabilized. Any construction that cuts into these areas would probably reactivate movement. Note that some dark toned areas lie outside the slide areas suggesting that movement has been more extensive than mapped.
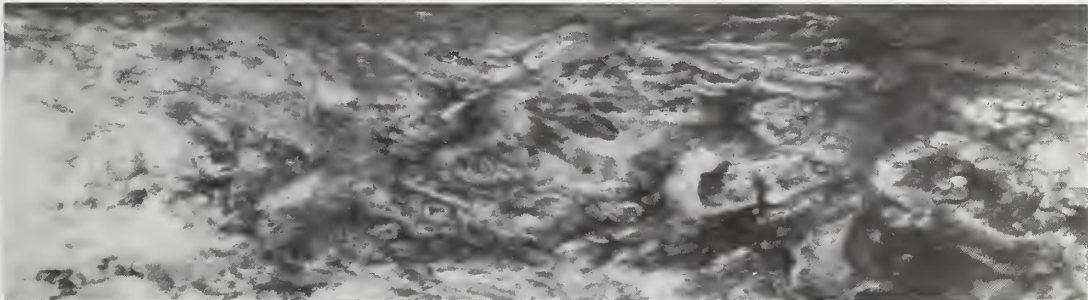
Figure 46 - Small scale thermal infrared imagery can have utility in geological mapping as is illustrated in this image from the Western United States. This image was acquired at an altitude of about 25,000 feet (7,600m) and covers a distance of approximately 9 miles (14.5km). It shows several linear features of obvious structural significance that do not appear on the state geological map.
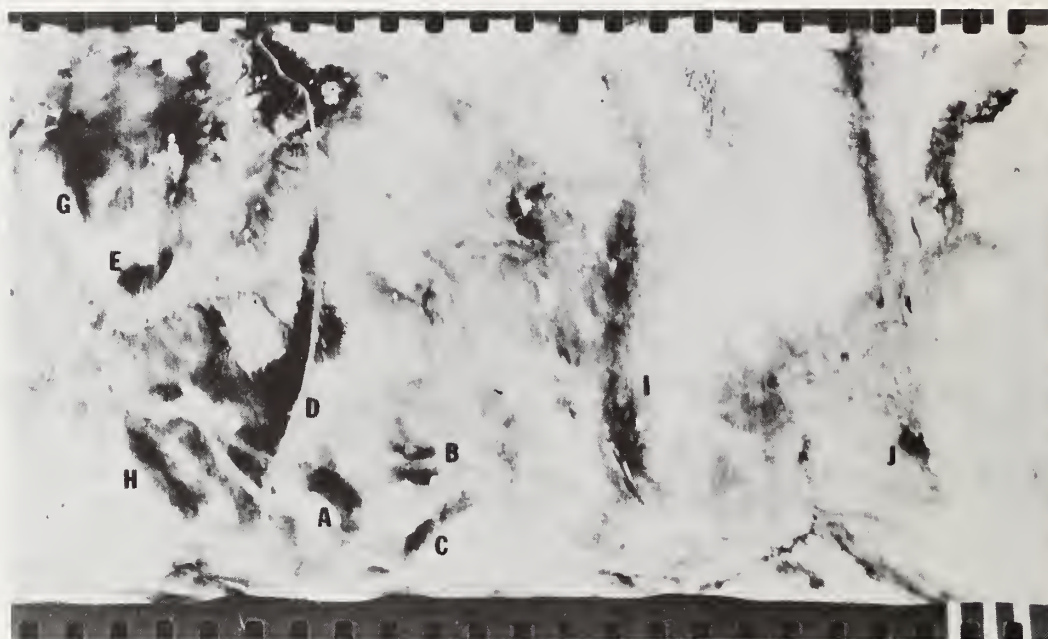
A

B

Figure 47. On the 8-14um thermal infrared image (upper image) of an area near Newport Beach, California, acquired after an extended dry period, the dark toned zones are interpreted as cooler because of higher concentrations of soil moisture. These areas show a high coincidence with areas mapped as landslides by the U. S. Geological Survey. The mapped landslide areas are annotated on the aerial photograph in heavy black lines with arrows showing direction of movement. The moist areas identified from the thermal imagery are outlined on the photograph by dotted lines and are letter coded for correlation on the two images. The heavy dashed lines show the area of coverage from the thermal scanner mission.

One can infer from the correlation shown that the soils and bedrock in this area are prone to slumping and that, although the slides are presently stabilized, portions could be reactivated by disturbance of the toe of the slide or by unusually heavy rainfall.

138

7.8 Magnetometer Survey, East River Mountain

A review of the map in Plate III, the contoured aeromagnetic data, shows a magnetic response only to the reinforcing steel in the concrete of the East River Mountain tunnel. This map shows a linear anomaly along the tunnel path with peaks over each portal as expected. The contour interval on this map is 25 gammas, which is approximately the minimum allowed by the line spacing and the noise level of the data ($\pm$ 5 gamma). The outcrop line of the Rose Hill formation (a ferruginous Clinton iron formation equivalent) may be indicated by a faint eastward bulging of the contours on the south slope of East River Mountain; however, this could not be interpreted from contour maps as delivered by the geophysical survey subcontractor.

Because of the possible importance of the Rose Hill Formation as a magnetic stratigraphic marker[4] in the structural interpretation, the original data strips were examined for evidence of small anomalies. The geophysical interpretation plate indicates the location of minor magnetic peaks that might be correlated with a very weak magnetic horizon in the sediments on the south slope of East River Mountain. These series of peaks form two northeast trending lines, f_5 and f_6, Figure 48, just west of the south portal. f_6 when extended across the fault, f_1, (see Plate V) coincides with the straight side of a Keefer sandstone flatiron. This is interpreted as indicating a possible fault in the section. This reinforces the photogeologic interpretation of the physiography and suggests that one effect of the fault movement is to move the Rose Hill formation up on the southeast relative to the northwest side of the fault. The effect of this movement at tunnel level would be to effectively thicken the Rose Hill formation over the expected thickness derived from careful measurement of a stratigraphic section.

Because of the direction of movement on these northeast trending faults which causes a repetition of section across them, they are readily defined by the magnetics. The fault shown in a north-northwest direction is much more difficult to define magnetically, perhaps because of the direction of movement, but also perhaps because of the direction of the flight lines.

A magnetic survey of this sort is generally flown with noise levels below one gamma. This allows contouring of the data to about five gammas. However, the electromagnetic system and the magnetic system cross-feed slightly, and to obtain the best possible EM signal a slight degradation of the magnetic signal was allowed. A five-gamma contour interval would have better defined the Rose Hill formation on the contoured aeromagnetic map.

---

[4] Magnetic susceptibility tests conducted on Rose Hill samples show very weak responses. Measured on cored samples with a bridge circuit, the average response was .05 x 10-3cgs/cc.
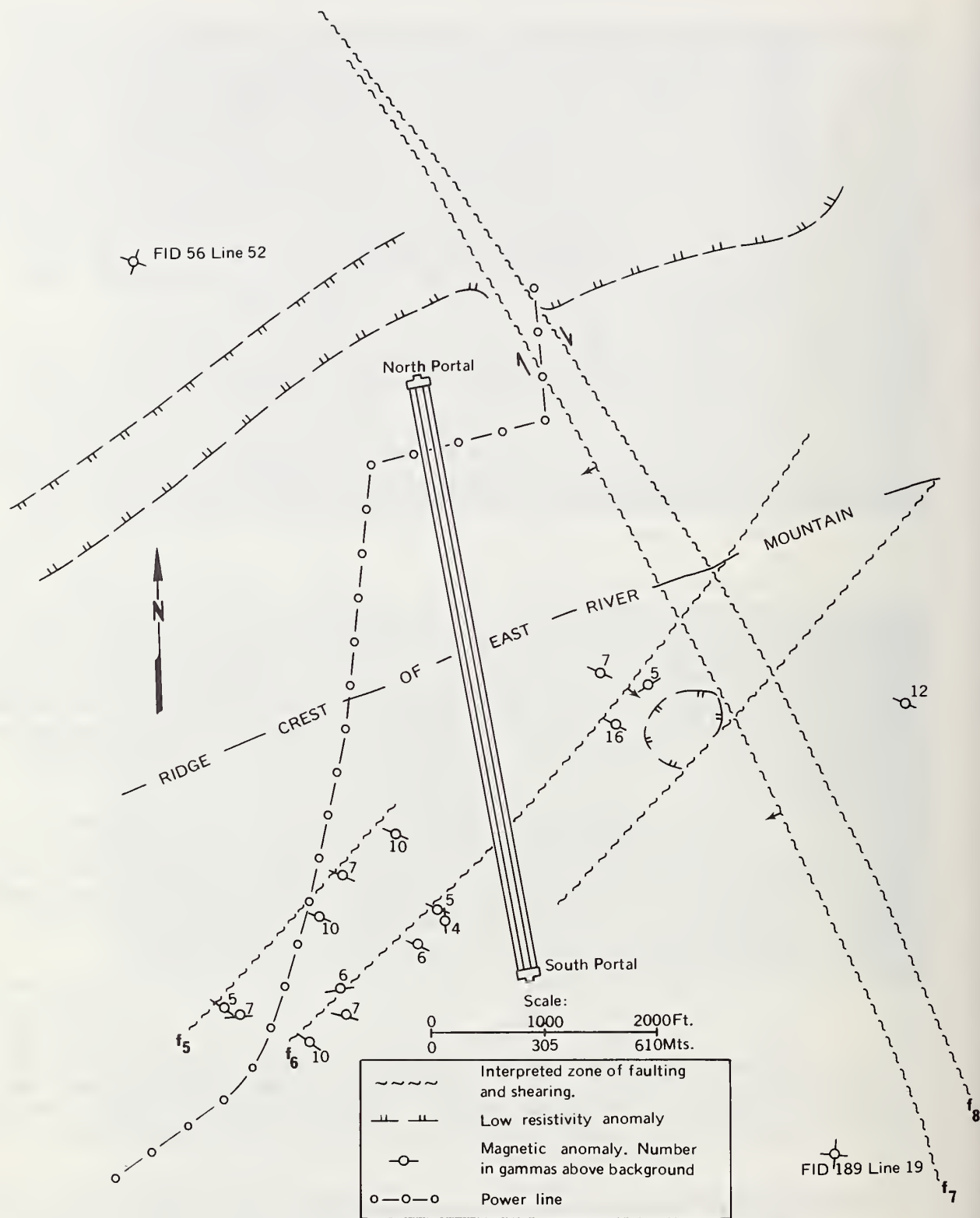
Figure 48. Geological structure map prepared from the detailed evaluation of airborne magnetic and resistivity chart records in conjunction with the analysis of aerial photography.

140

An important conclusion from this phase of the project is that, in order to obtain maximum benefit from an aeromagnetic survey, the data, must be interpreted in conjunction with all available geologic data.

7.9 Airborne Electromagnetic Surveys (AEM) East River Mountain

The Dighem AEM system provided the data for the contoured resistivity map. This map is an apparent resistivity map in the sense that the earth was modeled as a uniform conducting half space and the resistivities were calculated from the whale tail (see Appendix G for a description of the system) coil response based upon that assumption. At the frequency of about 900 Hz, the system is sensitive to resistivities in a range from 1 to 1,000 ohm-meters The resistivity map shows apparent resistivity contours in this range. which may be interpreted as the average resistivity from the top of the first conducting zone to a depth of about 150 feet (45m).

The contoured apparent resistivity map shows essentially four kinds of "anomalous" response, two from cultural features and two from near surface geologic features. The first culturally derived anomaly is the sharp linear power line anomaly that trends sub-parallel to the tunnel (north-northeast) across the survey area. This is a major powerline, well balanced and grounded so that the reponse is a purely conductive one from the amount of conductive metal in the line. There is no response on the 60 Hz monitor or the flight line record, but the sharpness of the response on each flight line and the linearity of the plan pattern would leave little doubt as to its cause even if the powerline structures were not visible on the photography. The other culturally derived anomaly is manifested over the two portals of the tunnel. These anomalies would be suspected upon examination of the photo-mosaic because of the surface disturbance shown. They are due to both a conductive response and a magnetic response from the maximum con-centrations of near surface iron as shown in the magnetic contour map. This is apparent in the electromagnetic data strips as a negative response in the quadrature (out of phase) output of the minimum coupled receiver coil.

The two responses from geologic sources are both of interest in tunnel site investigation. The broad linear northeast trending anomaly to the immediate north of the north portal is interpreted as an anomalous response from the outcrop band of the Moccasin and Eggleston limestones. This limestone sequence has many small sink holes along the outcrop. From the conductive response we may conclude that these sinkholes and underlying channels are saturated with ionized groundwater and that the interconnective "plumbing" of

141

the groundwater system is very good. In other words, an advancing tunnel face may encounter water filles cavaties which may affect tunneling progress and stability of the opening.

The second geologic anomaly is located east of the tunnel high on the south slope of the East River Mountain. The anomaly is nearly circular in plan and is calculated to be 200 feet (61m) deep. This anomaly is interpreted as a water saturated fault intersection. One of the faults in the northwest trending zone, f_7, Figure 48, extends just to the northeast of the north portal and is interpreted as having a steep westward dip. The other fault zone is interpreted from the aeromagnetic data. It is difficult to determine which zone offsets which at the point of intersection. They may mutually offset each other and such a mechanism may have produced an unusually porous, permeable, nearly vertical plunging zone that might cause great difficulty in tunneling. It is probable that the zone is both unusually broken for the area and that it is saturated with ground water. Such a zone would be difficult to detect in this area except by the most detailed ground resistivity survey.

A similar condition may have also existed at the present tunnel site. The same sets of faults appear to intersect in the same way just above the south portal on East River Mountain, but it is not possible to detect it now because, if actually present, the zone would have been drained by the tunnel. The ability to detect the zone with conductivity measuring devices is dependent upon the conductivity of the rock aided by interconnected water zones. It should be also noted that this is a local condition of small areal extent and avoidable with only very minor realignment of the tunnel. The small area covered by most ground resistivity surveys might not indicate how localized this condition is and how avoidable it is.

The unique contributions of the airborne magnetic and electro-magnetic data are that they measure directly the response from a volume of rock and the inferences involved in the interpretations are inferences concerning volume of rock, not simply the surface manifestation of subsurface conditions. When interpreted in conjunction with all available geologic data, airborne geophysical data provide uniquely powerful information about subsurface conditions.

8.0 THREE-DIMENSIONAL MODELING

The ultimate goal of a tunnel site investigation is to provide the engineer with an understanding of the geologic and engineering conditions at tunnel level. This is done by extrapolating geologic conditions observed at the surface into the subsurface. These extrapolations are supported by basic geologic principles, data from borings, exploratory excavations, geophysics and any other subsurface data as available. However, there are many limitations and inaccuracies associated with both conventional and remote sensing site investigation techniques when they are used to predict subsurface conditions. In order to minimize the possibility of incorrect conclusions one strives for a convergence of evidence provided by using several techniques. Each additional unit of information supports and serves as a check on other information. With subsurface data acquired using airborne geophysical techniques and surface data acquired using airborne remote sensing and field mapping, it is possible to construct a three-dimensional geologic model of the site. This preliminary mode provides a framework for guiding the collection and evaluating the results of subsurface and ground geophysical studies.

A three-dimensional geologic model of a tunnel site is an abstraction that embodies the arrangement of geological features. In its most complete form it would include not only the distribution, geometry, attitude, and composition of all of the lithologic entities and features that act as discontinuities, but the hydrologic and engineering properties of all materials present as well. It would be prohibitively expensive and physically impossible to acquire all of the data necessary to create this ideal model. In addition, short of using an immense amount of computer storage space it would be impossible to represent the model in any useful way. However, in practical terms it is possible to present the data acquired by remote sensing and conventional methods in a variety of ways; one of the most useful is a series of parallel and intersecting cross-sections. As the site investigation progresses, additional data can be added to the originally chosen cross-sections or new cross-sections constructed.

Beginning with remotely sensed data such a model is constructed from a series of cross-sections drawn from topographic maps. The sections are selected so that they will intersect significant geologic features identified during the data analysis phase. Important features for three dimensional modeling are lithological boundaries, stratigraphic continuity, faults, joints, and other structure. With photogrammetrically determined (or field measured) strikes and dips, apparent dips along the section can be calculated and a bedding plane or contact can be projected from the surface to tunnel level. Similarly, fault planes, offsets along these planes, and associated fractures can also be projected to tunnel level.

By constructing a cross-section along the alignment of the proposed tunnel the approximate location in the tunnel of specific geologic features can be determined. For example, the horizontal extent of a certain rock unit in the tunnel can be estimated, the point at which fractured rock might be encountered and other features such as subterranean solution cavities and water can be estimated. This simple physical model not only portrays the data in an easily understandable form, but can act as a check on the validity of inferences and indicate areas or features where further investigations should be concentrated.

8.1 Carlin Canyon Model

The geologic analyses of Carlin Canyon made using data collected by different remote sensing systems were compiled on black-and-white panchromatic photography. A GMB stereoscopic plotter was used to produce a topographic map and to transfer the geologic interpretations from the photographs to the map. Strike and dip measurements were made photogrammetrically, where possible, to supplement the field data. These measurements were used to calculate the apparent dip along the cross-sections drawn for the Carlin Canyon site (see Plate II in pocket).

Where observed, the fault planes were nearly vertical and this premise was used throughout model construction. The displacement on some of the faults would have been very difficult to determine without constructing the model. By studying the contact between the Strathearn limestone and the Diamond Peak conglomerate at cross-sections D-D' and F-F', the displacement of the fault F_1 on cross-section D-D' was determined to be approximately 65 feet (20 meters). The displacement of the other faults could not be determined due to the lack of specific evidence such as stratigraphic correlation on opposite sides of the fault.

From the first version of the model it was apparent that the position of a portion of the Diamond Peak - Strathearn contact, where it had been inferred, by considering soil and talus cover, had to be repositioned.

Using the model it was possible to estimate the location of the faults and the horizontal extent of each rock type in the tunnel. The three-dimensional model was important in evaluating the validity of the geologic interpretation of this site.

8.2 East River Mountain Three-Dimensional Model

Like Carlin Canyon, the geologic analysis at East River Mountain was based on data from several different remote sensing systems.

144

The analyses from all sensors were compiled on a topographic map that was prepared with a photogrammetric plotter. Natural color photographs were used to make the stereo plates. Some difficulty was encountered when the contact between formations, as mapped photogeologically, were incorporated into the three-dimensional model. The error in plotting the contacts resulted in inconsistent thicknesses of a formation without evidence of faulting. Construction of the three-dimensional model not only made the error apparent, but it indicated along which cross-section a re-interpretation had to be made.

Fault F_1 on Plate I offsets the contact between the Keefer and the Rocky Gap formations. The amount of displacement is difficult to estimate on the aerial photograph; but using the model the displacement could be estimated to be at least 50 feet (15m.).

Because there are no outcrops of the Juniata and Martinsburg formations at or near the tunnel site it was difficult to locate the contact between them. The contact of the Juniata and Martinsburg was drawn based on the thickness of the Juniata estimated in a preliminary report by Smith (1968). There is, however, evidence of a change in lithology considerably below this approximated contact. The evidence is a bench which is most prominent on section C-C' on the north slope. A dashed line on the profile indicates this stratigraphic break. Photogrammetric plotting of other lithologic contacts produced formation thicknesses that correspond reasonably well with the thicknesses reported by the tunnel contractor with the exception of the Rocky Gap formation (Table 5) which appears substantially thicker than reported.

Table 5 Comparison of Formation Thickness at East River Mountain

| | PREVIOUS WORK | | | | MODEL ANALYSIS | | | |
FORMATION	THICKNESS FEET	METERS	TUNNEL LENGTH		THICKNESS FEET	METERS	TUNNEL LENGTH	
ROCKY GAP	25	8	50	15	210	64	250	76
KEEFER	40	12	88	27	55	17	160	49
ROSE HILL	185	56	393	120	180	55	430	131
TUSCARORA	155	47	367	112	165	50	390	119
JUNIATA	320	97	690	210	320 (650)	97 (198)	740 (1400)	225 (427)
MARTINSBURG	1500+	457	2705	824	1600 (1300)	488 (396)	3150 (2480)	960 (756)
MOCCASIN	380	116	615	187	-	-	410	125

8.3 Limitations of the Three-Dimensional Model

The description of surface features using remote sensing systems and three-dimensional modeling of these features at tunnel depth is a useful combination of techniques for predicting conditions to be encountered during tunneling. However, this combination cannot totally eliminate the need for actual subsurface measurement, seismic surveys, boring or excavation. Remote sensing and modeling can greatly reduce the quantity of subsurface measurements required by indicating where the information is needed.

To summarize, three-dimensional modeling of the geologic conditions at a proposed tunnel site is a valuable tool for the design and construction engineer. Surface data, acquired by remote sensing methods, combined with subsurface data, the acquisition of which is directed by prior surface data analysis, can be used to produce an accurate assessment of many conditions along the tunnel route. Three-dimensional models not only present geologic data in an easily understood form, they can point out errors of interpretation, indicate areas that require further investigation, and guide the collection of subsequent data.

9.0 ECONOMIC ANALYSIS OF REMOTE SENSING AND CONVENTIONAL SITE INVESTIGATION TECHNIQUES

9.1 Introduction

A tunnel site investigation is planned and executed on the basis of incomplete information about the site geology and fragmentary information about the eventual tunnel design, method of construction and construction cost. The investigator is, therefore, at a disadvantage when he makes his decisions with respect to the quality, quantity, and the methods for most efficiently obtaining the geologic information required for the project.

The problem of planning a tunnel site investigation could be routinely handled if the relationship between investigation cost and construction cost savings were fixed or could be defined through economic analysis. The cost effectiveness of each increment of the investigation, however, is difficult to define in practice because the cost of both the investigation and the construction are affected by site conditions and the characteristics of the tunnel project. The quantity and quality of geologic information obtained by a specific method, for instance, varies with environmental conditions and the site geology. The value of the geologic information in turn varies with the tunnel design, the method of construction, the character of the construction plans and specifications, and the efficiency of the contractor's operations. The investigator can normally expect to have only a crude basis for evaluating the cost effectiveness of alternative investigation methods.

Fortunately, most investigation methods involve a relatively small investment when contrasted with the cost of tunnel construction. On most projects the cost of the entire site investigation is less than 1% of the cost of construction. The cost of difficulties resulting from incomplete geologic information, on the other hand, may be many times greater than the cost of the investigation. The investigator, therefore, can normally assume that a method which offers some possibility of providing additional geologic information will be cost effective.

The goal of the investigation plan is to locate and measure the geologic features which will affect tunnel design and construction. Whether conventional or remote sensing techniques, the methods selected for the work and the extent to which each method is used depends on the investigator's appraisal of the capabilities of alternative investigative methods available, the level of accuracy required for the proposed construction, and the limitations imposed by the investigation budget. Some geologic features may be satisfactorily investigated by a single method because of either the high capability of the method or low accuracy requirements, or both. In other instances, two or more methods are required to investigate a single class of geologic features.

147

It is obvious that unit investigation costs and environment-dependent capabilities of a sensor cannot be definitively stated. In addition to these problems, there is no specific remote sensing experience base in tunnel activities from which to derive empirical cost data. In this analysis the data assumptions, cost estimates, and results are made as explicit as possible, but it is important that both analysts and decision makers who will use these results recognize the potential error that they may introduce without careful consideration of the variables for each specific project.

This section is addressed to the investigator who is faced with a problem of designing a tunnel site investigation program comprising both conventional and remote sensing methods. From the material presented, he will become familiar with the capabilities of various conventional and remote sensing systems. The range of costs presented are averages based on the experience of the authors. With this information the investigator will be able to design a multi-stage route and site investigation program while considering the variables and conditions of his specific project.

9.2 Conventional Means of Data Collection

The following is a brief description of the methods currently used in tunnel site investigations and a discussion of the advantages, limitations, and costs associated with each method. Table 6 summarizes the major points presented in the chapter.

9.2.1 Information Search

A tunnel site investigation normally starts with a file and library search to obtain pertinent geologic and construction information. Publications of federal and state geological surveys and other government organizations such as the U.S. Bureau of Reclamation, Corps of Engineers, or Soil Conservation Service often contain information about the soil, bedrock and groundwater conditions of the site. This information may be supplemented by geology thesis studies on file in local college libraries, consulting engineering files, logs of local well drillers and other records of building, pipeline, highway and tunnel construction.

Most of this information is available free of charge or for a nominal fee. The greatest investment is generally the time to collect and review a wide range of reports and records. It is very unusual to find sufficient information from these sources to completely define the subsurface conditions of a tunnel site because the information is usually collected for

148

Table 6 Conventional Investigation Techniques for Tunneling.

Investigation Methods	Information Collected	Application	Limitations	Costs
Information Search	Geologic, Hydrologic, Topo-graphic maps, published reports on rock properties stratigraphy, structure	-Synopsis of geo-environmental conditions at the proposed site -Direction for next stage of investigation	Provides mostly general and little specific information	$1,000-10,000
Aerial Photographic Interpretation	-Topographic relief -Rock outcrop and rock type distribution -Soil type distribution -Structure	Direction for next stage of investigation	-Field verification required	$2,000-10,000
Surface Mapping	-Orientation of strata -Identification of fault zones -Soil moisture -Rock type	-Geologic information projected to tunnel level -Length of rock in tunnel -Hazards and bad ground -Rock stability and character-istics	Surface exposures are limited and may not be representative of conditions at tunnel level	$100-$400 per sq. mi.
Surf. Geophys. Testing	-Homogeneity of rock in subsurface -Orientation of strata -Location and extent of faults -Soil moisture and ground water conditions	-Subsurface orientation, sequence and type of rock -Hydrologic conditions at depth -Hazards	Pertinent physical conditions are inferred from measurements, analysis required simplifying assumptions about the geometry of geologic units	$500-10,000 per mi. of traverse
Soil and Rock Borings	-Subsurface samples -Ground water flow	-Stability of unconsolidated subsurface material -Engineering characteristics of rock at tunnel level -Hydrologic conditions -Location of faults and contacts	Important features may be located by chance, lost samples are more important than recovered samples orientation of features is uncertain	3-inch soil boring: $10-20/ft. up to 100 ft. w/samples every 5 ft. 3-inch rock core: $15-30 per ft. up to 500 ft. w/continuous rock core

Table 6 Conventional Investigation Techniques for Tunneling—Contd.

Investigation Methods	Information Collected	Application	Limitations	Costs
Borehole Logging	-Rock types and physical characteristics -Photography -Electrical characteristics of rocks resistivity and initial potential	-Stability of unconsolidated subsurface material -Engineering characteristics of rock at tunnel level -Hydrological conditions -Locations of faults and contacts	Limitations of geophysical testing. Caving and blockages of hole. Borehole fluids may affect geophysical test and obscure rock conditions	$400-$800 per 500-ft. hole. 2 types of logs in each hole. Several holes must be logged
Exploratory Excavation	-Hydrology -Orientation of physical features -Physical parameters of rock -In situ rock and soil tests	-Equipment and design requirements -Drainage requirements -Length of rock in tunnel -Support requirements -Boring conditions -Hazards	Very expensive. Difficult to extrapolate behavior in small tunnel to that in a large tunnel. Only practical for a large tunnel	$400-500 per lineal ft. depending on ground conditions and size of tunnel
Laboratory Testing	-Soil parameters -Water composition -Rock physical parameters	-Structural support requirements -Safety considerations -Drainage and ventillation requirements -Boring conditions -Equipment and design requirements	Does not measure effect of in situ conditions and rock defects	$10-100 per test

150

an entirely different purpose and the geologic observations are generally limited to the ground surface. Although most of the information is of limited value to a tunnel investigation, a careful information search usually reveals enough pertinent information to make the search of value on most projects. In some instances the information search reveals conditions which might have been overlooked in field studies or discovered only by the use of expensive field investigation methods.

The cost of the information search depends upon the character, volume and availability of pertinent records. Normally the information search will cost from $1,000 to $10,000.

9.2.2 Aerial Photograph Interpretation

Aerial photographs are commonly used during the early stage of a tunnel site investigation to identify exposures of bedrock, to delineate major bedrock structures, and to identify pertinent geologic features and the presence or absence of ground water and surface water. The results of aerial photograph interpretation are generally considered tentative until checked by surface and subsurface investigation.

Aerial photographs of most sites are available from governmental agencies and industrial sources at a nominal cost. The site may be photographed for the tunnel investigation to obtain more complete or updated coverage. The expense of this work is usually moderate compared with other investigation methods and the new photographs are normally required for both geologic and topographic phases of the investigation. The cost of interpretation of the aerial photographs is nominal.

9.2.3 Surface Mapping

Surface mapping is the classical method of obtaining information about subsurface conditions. Surface mapping involves the inspection and recording of soil, bedrock, and water conditions exposed in cliffs and stream beds and in man-made excavations for buildings and highways. Supplemental bedrock exposures may be obtained by use of hand or portable powered equipment. Surface mapping provides a two dimensional view of the geology. This information is projected to the depth of the proposed tunnel to obtain a three-dimensional picture of the site conditions.

The reliability of surface mapping to identify the significant geologic features depends on both the geologic conditions and the nature of proposed project. The reliability of the geologic projections depends upon the extent of surface exposures, the nature of the geologic units, the complexity of the geologic structure and the continuity of the surface and subsurface features. The degree to which tunnel construction will be effected by variations in the geologic conditions depends upon the depth of the tunnel, the tunnel bore diameter, and the method of excavation and support of the ground to be used during tunnel construction.

Reliable projections of ground conditions can be expected for a tunnel alignment at moderate depth in massive, well-exposed granitic rock. The reliability of surface projections is less in terrains underlain by bedrock with a complex geologic structure. The reliability may also be low in terrain underlain by alternating competent and incompetent sedimentary rocks because the incompetent rock may be poorly exposed or completely obscured by soil deposits. For shallow tunnels in glaciated terrain, ground condition predictions based solely on surface mapping can be dangerous because the depth to bedrock and the condition of the bedrock along the tunnel alignment may not be evident in surface exposures.

Despite these limitations, surface mapping is a normal and useful part of a tunnel site investigation. Surface mapping is normally performed because it provides direct evidence of the character of the ground and usually provides a basis for planning the more expensive subsurface investigations. The cost of surface mapping varies with the extent of surface exposures and the difficulty of access to various parts of the site but should be on the order of $100 to $400 per square mile.

9.2.4 Surface Geophysical Surveys

Surface geophysical surveys have been used on tunnel sites to locate groundwater levels, determine depth-to-bedrock, to estimate excavation characteristics of soil and rock and to locate weak or incompetent zones within the bedrock. Seismic and electrical resistivity surveys are the geophysical methods most commonly used in tunnel investigations but gravity and magnetic surveys have application in certain terrains. Most surface geophysical testing is performed in the vicinity of proposed portal sites.

152

Seismic surveys are based upon the principle that shock waves, created by mechanical vibrations or blasting, travel through different rock materials at different velocities and are reflected and refracted in accordance with the basic laws of optics. Under these conditions, the travel time between the energy source of the shock wave and the seismometer or geophone detectors can be used to calculate both the propogation velocity through subsurface materials and the depth to the interface between materials with contrasting velocities. A general knowledge of the subsurface materials provides a basis for converting the resulting velocity profile into a generalized geologic profile.

Electrical resistivity surveys are based on the principle that the conductivity of earth materials varies with the nature of the material and the nature of the contained fluids. Resistivity surveys are made by either measuring the natural ground currents or by measuring artificially induced currents between two or more electrodes at a known spacing. The scale of the test and the depth of the investigation can be varied by changing the distance between the electrodes. A series of measurements can provide a resistivity profile which in turn can be converted into a generalized geologic profile.

The assignment of material type and material properties to the velocity or resistance measurements is the most critical step of the survey. If the analyst has a good knowledge of the local geologic conditions, and rock material properties, and if these conditions are relatively simple, the resulting geologic profile will be reliable. However, if the subsurface conditions are complex, the geologic profile could be less accurate. Because of these limitations, surface geophysical surveys are used to define the general trend of subsurface conditions and the survey results are normally verified by borings or other excavations.

The cost of a surface geophysical survey varies with the accessibility of the test site and the required density of measurements. A cost of $500 to $10,000 per mile of traverse is normal for this work.

9.2.5 Soil and Rock Borings

Borings ranging from 1 inch (2.5 cm) to more than 1 foot (30.5 cm) in diameter provide samples of subsurface materials at depths ranging from a few tens of feet to more than 1000 feet (305 meters). Most soil borings are three to five inches (7.5 to 12.7 cm) in diameter and are advanced by alternately drilling and sampling. Core borings in bedrock are generally

153

two to three inches (5 to 7.5 cm) in diameter and are sampled continuously. The samples and a log of observations made during the drilling operation provide a valuable indication of the nature of subsurface soil, rock and groundwater conditions. This record may be supplemented by borehole logging techniques described in the following section.

Although borings are generally considered the most important technique now available for subsurface exploration, they have many limitations. Some of these limitations are:

1. The samples are small with respect to the size of the tunnel. In soil this may not be an important limitation as a small sample can be representative of the soil mass. In rock, the core sample is generally not representative of the rock mass because the rock mass behavior is controlled by a system of fractures which are imperfectly represented in the core sample.

2. Borings are relatively expensive particularly if access to the drilling site is difficult, the drilling conditions are difficult, and the depth to tunnel level is great.

3. Rock and soil samples provide essentially a one-dimensional view of the subsurface soil or rock mass. Features immediately outside the limits of the boring are unknown. In some situations it is considerably more difficult to visualize the three-dimensional environment of the tunnel from core samples than to visualize the same environment from two-dimensional outcrop observations.

4. Core samples are generally not oriented. If core recovery is relatively good it is possible to measure the dip of geologic features such as bedding, joints and faults but the strike of these features is unknown unless special oriented drilling techniques are employed.

5. The softer and less competent materials are commonly lost during the drilling and sampling. While the character of these materials is often critical to the evaluation of subsurface conditions, the samples merely indicate that the material lost in the sampling operation were less competent than the recovered material.

The cost of soil and rock borings varies with the size
and depth of the boring and the surface and subsurface condi-
tions at the drilling site. A soil boring less than 100 feet
(30 meters) deep can be expected to cost from $10 to $20 per
linear foot while a rock boring less than 500 feet (150 meters)
deep can be expected to cost from $15 to $30 per linear foot.

9.2.6 Borehole Logging

In recent years downhole logging techniques, originally
developed for logging oil wells, have been adapted for use in
soil and rock borings on engineering projects. The techniques
include electrical resistivity, sonic velocity, radioactivity,
gravity, temperature and caliper logs. In the same period,
devices have been developed for taking photographs or tele-
vision pictures of small-diameter borings.

Geophysical well logging has been successfully used in
the petroleum industry because oil wells are sampled by cut-
tings and limited cored intervals and the reservoir character-
istics of oil-bearing strata can be assessed by geophysical
measurements. The application of geophysical logging to
tunnel site investigations is less certain because the investi-
gator is more interested in the stability of the rock mass
than the permeability of the rock mass. Application of these
logging techniques should be viewed as experimental at this
time but these logging devices may be useful in logging deep,
partially cored borings.

Photographic logging of borings has been more widely
accepted because borehole photographs directly supplement
borehole records and samples. Borehole photographs can be
used, for instance, to orient each feature noted in the core
samples and might be used in place of coring to document the
rock conditions in a boring. Under favorable conditions,
borehole photography can be used to identify materials in
zones of core loss.

Both geophysical and photographic logging are limited
by borehole conditions. Caving and blockages in the completed
boring may prevent a complete logging of the hole and, in some
instances, may result in the loss of an expensive borehole
probe. Although geophysical logging methods provide informa-
tion about the rock around the boring, the depth of penetra-
tion is usually on the order of a few inches or a few feet.
Even with geophysical measurements, the borehole is still
essentially a one-dimensional probe of subsurface conditions.

Geophysical and photographic logging are generally performed by well logging service companies. The cost of this service is presently dominated by the charge for mobilizing and demobilizing the equipment and crews. While the time on site may be just a few hours, the cost of making two logs in a 500 foot deep boring can be $400 to $800. The unit cost of the service decreases with an increase in the footage logged but the cost increases with the number of logs performed in each borehole.

9.2.7 Exploratory Excavations

Adits and shafts are occasionally used to explore ground conditions in portal areas and in fault zones and permeable zones along the tunnel alignment. These excavations normally have the smallest cross section which can be conveniently excavated by hand and small power equipment. In most instances these excavations extend a few tens to several hundred feet from the ground surface. These openings provide an opportunity to observe and test the ground conditions which is generally not available until construction of the full-size tunnel. These openings are carefully mapped in all instances and may be used for large scale pumping tests and tests which measure the compressibility or strength of the ground.

Exploratory excavations are relatively expensive, ranging from $400 to $700 per linear foot. The excavation and support of these openings usually cost nearly as much as the excavating and lining of the full-size tunnel because mobilization costs are distributed over a relatively short length of excavation and the work is less mechanized than the work in a full-size tunnel. Cost is probably the main reason why these excavations are used only in areas where known or suspected ground conditions may have a major influence on the design of the project and the cost of construction.

9.2.8 Laboratory Testing

Laboratory testing is performed on soil and rock specimens to measure the engineering properties of earth materials and to measure other properties which may be correlated with the engineering properties. The soil tests include water content, unit weight, Atterberg limits, unconfined compressive strength, and triaxial testing. The tests on rock include unit weight, water content, abrasion resistance, hardness, tensile strength, unconfined compressive strength and triaxial testing.

156

The basic engineering properties of soil and rock are strength, compressibility and permeability. Tests on representative soil specimens can provide the essential information to analyze the behavior of soil masses in a tunnel. Tests on representative specimens of intact rock, on the other hand, do not directly measure the engineering properties of the rock mass because rock mass behavior is largely controlled by discontinuities. The behavior of a rock mass is assessed by comparing the laboratory test results and the field exploration information with theoretical models of rock behavior or previous tunnel observations in similar materials.

9.3 Effectiveness and Cost of Remote Sensing Systems

A discussion of the capabilities of an information gathering system must precede any estimate of the effectiveness of that system. The optimum capability of each airborne sensor depends on several factors which include: cloud cover, season (with respect to solar elevation and azimuth, snow and ice conditions, and phenological changes of vegetation), soil moisture, depth to bedrock, altitude of imaging platform, vegetation cover, cultural interference and quality of data processing.

The capabilities of sensors often overlap, but even though two different sensors can identify the same feature, the level of detail may be quite different. Overlapping capabilities and duplicate data can be limited, but it is often helpful to have duplication and verification of information.

The costs for data acquisition using different sensors are difficult to estimate. Costs for acquiring the same data can vary widely from site to site, and therefore, it is not common practice for flying survey companies to quote unit prices. In addition it is most efficient to use a single aircraft to acquire several types of data making it difficult to partition the cost of the aircraft among the several sensors flown. Table 7 lists factors and special requirements that control the cost of acquiring certain types of data. Table 8 is a summary of remote sensing investigation techniques, their applications, limitations, and costs.

Five basic types of remote sensing data evaluated during this investigation were data from;

- Satellite imagery
- SLAR (Side Looking Airborne Radar)
- Camera systems (various film types)
- Scanner systems (multispectral, thermal)
- Airborne geophysical systems

157

Table 7   Factors Controlling Cost of Remote Sensing Data Acquisition

Factors	Elements
Data acquisition	Labor
Film and processing or recording medium	Type of film, special processing requirements
Data processing	Computer enhancement, special photo lab processing, stereoscopic plotting
Field crew	Number, level of training
Equipment rental	Type of equipment, amount of time needed, operator
Special equipment purchase	
Mobilization and demobilization	Accessibility of the site, travel cost to and from site and per diem
Stand-by (non-surveying time on site)	Size of contract, season, geographic location of site
Repeat flying	Equipment malfunction, weather, errors (pilot, operator), data unacceptable to client
Special requirements	Specific time of day, weather, special reports

Table 8   Remote Sensing Site Investigation Techniques for Tunneling

Investigation Method	Information Collected	Application	Limitations	Cost
LANDSAT	Regional lineaments Regional folds Regional topography Regional drainage pattern Regional vegetation pattern Regional lithology Regional stratification Regional soil type	Geologic trends and structure hazards can guide the choice of route for the highway and to selection of a site for tunnel construction. Can identify some major geologic hazards.	These data do not provide specific information required for the engineering design of the tunnel.	Approx. $75.00 (color and black-and-white at a scale of 1:250,000)
Skylab	Similar to LANDSAT but high resolution	Same as LANDSAT	Same as LANDSAT	Approx. $20.00 for black-and-white at a scale of 1:250,000
Side-Looking Airborne Radar (SLAR)	Same as LANDSAT	Regional to local topography, regional to local geologic trends. Both can be used for highway route and tunnel site selection.	Resolution on some systems is very low. Ten foot (3 meter) resolution now permissible.	Expensive to contract. Existing data may be purchased for approx. $100 to as much as $20,000 per site.
Multiband Photography	Same as panchromatic black-and-white photography	Same as color aerial photography. Improved spatial resolution - more accurate identification of rock and soil type based on specific signatures.	Geological identification required for field verification.	$4,000 to $7,000 (scale 1:5,000 to 1:20,000 stereo coverage)

159

Table 8 Remote Sensing Site Investigation Techniques for Tunneling—Contd.

Investigation Method	Information Collected	Application	Limitations	Cost
Low Sun Angle Photography (LSAP)	Good topographic enhancement and identification of local geological structures. Identification of major fractures.	Local drainage patterns - orientation of rock fractures - site accessibility based on topography.	Precise timing of over-flights is critical to obtaining useful data.	$2,000 to $3,000
Black-and-white Panchromatic Photography	Rock fractures Folds Topography Drainage patterns Vegetation type and pattern Lithology Stratification Soil type Cultural features Water bodies	Precise stereoscopically plotted maps - location and extent of faults - projected extent of rock units at tunnel level. Stereo coverage permits evaluation of site accessibility based on topography. Orientation of rock strata and thickness - estimates of depth of unconsolidated overburden.	Soil type and lithology is difficult	$2,000 (scale 1:5,000 to 1:20,000 stereo coverage)
Color Aerial Photography	Same as panchromatic black-and-white	Location extent and type of faults - orientation sequence and thickness of strata - site accessibility based on topography. Good rock and soil identification and delimination of rock units.	Slightly lower spatial resolution capability than panchromatic black-and-white photography.	$2,000 to $4,000 (scale 1:5,000 to stereo coverage)
Color Infrared Photography	Same as panchromatic black-and-white	Identification of vegetation type and vigor; useful as indicator of soil moisture, i.e., location of moisture along faults - estimates on slide and slump potential at portals.	False color rendition of soil and rock type makes identification difficult. Field verification required.	$2,000 to $4,000 (scale 1:5,000 to 1:20,000 stereo coverage)

160

Table 8 Remote Sensing Site Investigation Techniques for Tunneling—Contd.

Investigation Method	Information Collected	Application	Limitations	Cost
Multispectral Scanner	Same as color photography	Same as color photography. Improved discrimination of rock types in certain areas based on spectral signatures.	Lichen or desert varnish on rocks prohibits specific characteristic response. Field verification required.	$6,000 to $10,000
Thermal Infrared	Same as color infrared Improved detection of soil moisture and wet fractures and landslides	Identification of soil moisture - location of thermal anomalies - slide and slump potential at portals - location of rock outcrops.	To be most effective requires same amount of soil moisture, but less effective with extremely high soil moisture.	$6,000 to $10,000
Airborne Electro-Surveys (AEM)	Orientation strata Location and extent of faults Hydrologic conditions at depth Geologic hazards Identification of bad ground (serpentine, altered rock material, sinkholes, etc.).	Provides direction for additional surface geophysical testing and boring.	Geological information inferred at depth. Surface geophysical testing required for verification. Must be interpreted in light of other geological data.	$15,000 to $25,000
Airborne Magnetic Surveys	Fracture zones, large magnetic bodies (dikes, sills, serpentines) limited rock composition based on magnetic content	Location of major fractures and potential hazards, such as dikes and serpentines. Guides to further ground geophysics and boring valuable low cost adjunct to AEM.	Same as AEM	$1,000 to $5,000

From the users standpoint, most of the cost factors listed in Table 5 do not apply to the cost of data acquired from orbital platforms. Standard data are available for a single unit price regardless of the geographic location of the site or season of acquisition. Likewise if data from other remote sensing systems exist, it is possible that it also may be available for purchase at some nominal unit cost. The cost information in this section is based on costs actually incurred during the study at the two specific test sites.

9.3.1 Satellite Data

The two types of data acquired from orbital satellites used in this study were LANDSAT and SKYLAB imagery. LANDSAT (formerly known as ERTS) is a sun synchronous satellite with a four channel multispectral scanning system whose bandwidth ranges from .5-1.1μm. An S-190A multispectral camera and an S-190B high resolution camera acquired the SKYLAB data. Color and black-and-white images are available or can be reconstructed from both systems.

The spatial resolution of LANDSAT imagery is approximately 80 meters, however identification of linear features less than one tenth that width is sometimes possible if image contrasts are extreme. Scales best suited for geologic interpretation are 1:500,000, and 1:250,000. Band 7 (.8-1.1μm) on LANDSAT imagery gives the best information on geologic structure and topographic landforms. This is not to say that other bands should be ignored. Bands 5 and 6 imagery are capable of providing good terrain detail. Band 4 imagery, however, is often hazy, depending on atmospheric conditions.

The most outstanding advantage of LANDSAT imagery is provided by the broad synoptic view. This is important to tunnel site investigation in that regional geologic trends can be related to a specific site. Many tunnel sites are selected without considering regional geologic trends because there are other factors that bear a more immediate impact on the site selected. Some of the factors that control site selection include:

- The orientation of existing highways or railroads
- Economic factors (labor, materials cost)
- Site restrictions due to population concentrations
- Facilities which cannot be relocated
- Local geologic parameters.

These factors, more often than not, claim a higher priority in site selection than regional geology even though some elements of the regional geology may directly and significantly affect the cost and safety of a tunnel.

In addition to the synoptic coverage of LANDSAT, there are several other areas of utility which are of great importance to tunneling. They include: the identification of linear features often indicative of the fracturing (faults and joints) of the rock, identification of drainage patterns, information regarding soil types, and rock types and their resistance to erosion.

The cost per frame of LANDSAT is nominal. Black and white and color imagery costs approximately $75 at a scale of 1:250,000. The EROS Data Center price list of LANDSAT and SKYLAB data appears in Appendix I.

The utility of SKYLAB imagery are similar to that of ERTS imagery. The SKYLAB camera system has a greater spatial resolution (approximately 20 meters) and therefore permits more detailed mapping of the regional geology at a scale of 1:250,000-1:125,000 and even 1:50,000.

9.3.2 Side Looking Airborne Radar (SLAR)

An important capability of SLAR is that it provides synoptic, relatively high resolution, high contrast images, that are useful for interpreting geomorphology and structural geology. SLAR is an active system (emits its own energy) that can operate day or night regardless of most weather.

Radar emits pulses of microwave energy directed toward the ground and records the energy the ground reflects back to the antenna. Areas shielded by topography from incident radar energy of course do not reflect and therefore appear black on the image. Acquisition of SLAR imagery does not depend on solar illumination and the energy penetrates most clouds; therefore it is not dependent upon time of day or weather conditions. Because the system is independent of solar illumination, any side of a topographic landform can be "illuminated" or shadowed by radar impulses if different flight lines are used. The angle of illumination on most SLAR units can be adjusted to enhance low and high topographic features.

The cost of conducting a SLAR survey for tunnel site investigations is high. The cost could range from $30,000 to $100,000. Alternatively, one could purchase SLAR imagery from previous missions, either commercial or military. The U.S. Air

Force has acquired SLAR imagery over approximately 70% of the United States; the existing imagery is available for $20-$100 per image. Some parts of the United States have been flown commercially and high quality imagery is available (see Appendix H).

9.3.3 Airborne Camera Systems

The cost of airphoto surveys depends on the type of film and camera system used. Color film costs are three to four times more than black-and-white film, and the processing of color film is about three times the amount of black-and-white film. However, this is not to say that the acquisition of color photography is three times more expensive than acquisition of black-and-white photographs. Several other factors common to the use of both film types contribute to the cost. These include aircraft rental, salaries of pilot and cameraman, and reflight and standby factor costs. Color photos can be obtained for approximately $2,000-6,000, depending on the location of the area, whereas, black-and-white photography can be obtained for approximately $2,000-4,000.

Low sun angle photography (LSAP) sometimes referred to as simulated radar, can provide geological information on a local and regional scale. The versatility of LSAP is somewhat limited by the relatively small range of shadow aspects provided by the morning and evening sun through the seasons. Different shadow aspects occur at different times of the year and the angle of illumination depends on the time of day that the imagery is acquired. The advantage of varying the illumination angle is that shadow length can be adjusted according to local topography. The lower the local topographic relief of the area, the lower the sun angle needed to highlight topographic features. An area of high topographic relief will require a higher solar elevation.

Black-and-white panchromatic photography provides better spatial resolution than can be obtained with color film, and the processing of such film also is more economical. Panchromatic photography can provide detailed information relating to the geologic structure of the area, topography, hydrology, vegetation and in some instances, soil types. The spatial resolution and geometric fidelity of panchromatic photography makes it well suited for stereo-plotting of geologic information using photogrammetric instrumentation.

Although the spatial resolution of color photography is somewhat less than that of black-and-white photography, the human eye can separate more than 100 times more color combinations (hues, values, chromas) than gray values (Evans,

1948). The identification of many rock, soil, and vegetation types depends on subtle color discriminations, thus, color aerial photographs are valuable for tunnel site investigations.

Color infrared photography is excellent for identifying vegetation type, vigor, and stage of phenological development. Vegetation analysis can be important to tunnel site investigations where rock outcrops do not exist, especially if geobotanical indicators exist that can indirectly help to identify soil type and soil moisture differences. Color infrared photography also can be useful for locating moist fracture zones as well as standing and flowing water bodies.

Generally speaking, color infrared film has a higher contrast than standard color film and making proper exposures is more critical. It may be necessary to re-fly the imagery if the exposure is not correct; particularly if overexposed. In most areas color infrared photography is not as useful as natural color for geologic analysis. The false color imparted to surface features increases the chances for mistaken soil or lithologic identification. In general, conditions necessary to obtain the optimum performance of color infrared film are a certain degree of soil moisture, vegetation in the non-dormant state, and as little cloud cover as possible.

Multiband photos are used to discriminate between soil and rock types based on their spectral differences. Multiband photos are obtained using panchromatic film, and a series of spectrally calibrated filters. By assigning primary colors to photo transparencies in the appropriate spectral range, and superimposing the photos, a wide variety of false colors and near true-color photos can be created. By accenting and subduing colors, the spectral differences between rocks and soils can be enhanced.

9.3.4 Scanning Systems (Multispectral, Thermal)

Multispectral scanners record energy emitted in ranges within the visible and near-visible portion of the electro-magnetic spectrum. With varied limits all materials have characteristic spectral signatures which can be used to discriminate one object from another. In some areas it is possible to identify the different rock and soil types based on their relative reflectivity in different bands of the spectrum.

Optimum performance of a multispectral scanning system for geological analysis depends on certain factors:

- Rock and soil surfaces must be partially free of vegetation (trees, shrubs, lichen)

- Unequal illumination (due to clouds or shadows) of the subject should be avoided.

Multispectral scanners are commercially available with as many as 11 separate channels, ranging from .38-1.1μm. The data are recorded on magnetic tape which provides the flexibility of generating either a direct image or a computer-enhanced image in hard copy format. Computer processing the data can greatly expand the interpretability of the scanner imagery. Many geologic and hydrologic features which are obscured by the detail of the original image may be selectively enhanced by proper data processing.

If the geology of the area is complex enough to warrant the expenditure, and the proper environmental conditions exist, multispectral scanning data can be valuable. If near optimum conditions do not exist, cost versus effectiveness is greatly reduced. Acquisition of multispectral scanner data, computer processing and interpretation of the imagery should range from $10,000 to $20,000 per site (cost factors in Table 7 included).

While conducting a multispectral scanner survey over a site, it is usual practice to acquire thermal infrared data using the same scanner system. Because thermal emissivity is related in part to the composition of an object, thermal mapping can be used to identify differences in lithology and soil. Thermal scanners are also useful for mapping fault zones by detecting the differences in soil moisture between the fault zone and the surrounding area. Thermal scanner data can be computer processed using the same algorithms as used for multispectral scanner data.

Thermal imagery is very sensitive to differences in soil moisture, and, consequently, is an excellent tool for detecting and locating springs and seeps, potential landslides, and hydrologic hazards in general. Thermal surveys cannot be fully effective if they are conducted when the ground is extremely wet. The soil moisture tends to reduce or mask emissivity differences between objects and this produces a low-contrast image. The addition of a thermal survey to a multispectral survey would represent an increase in cost of approximately 20% (or $2,000 to $4,000).

166

9.3.5 Airborne Geophysical Systems

Airborne geophysical systems offer the only airborne method of directly detecting geological conditions significantly below the ground surface.

Airborne electromagnetic (AEM) systems detect differences in resistivity in near surface (0-200 feet; 61 m) rock and soils. Thus, these data can indicate the presence of water saturated alluvial and colluvial deposits, mineralized or saturated shear zones, basalt dikes and water filled cavernous limestone. The Dighem dipole-dipole system used during this study can indicate the subsurface orientation of planar features, such as fault zones and serpentine bodies, making it unique among the sensors tested.

Aeromagnetic data are a valuable complement to AEM data. Airborne magnetometers sense differences in the magnetic susceptibility of subsurface soil and rocks, thus, allowing for the discrimination of magnetite bearing rocks and for the recognition of major discontinuities. This makes it possible in some situations to infer the displacement of lithologic units across faults. The rather gross resolution of aeromagnetic data and the cost suggest that over most tunnel sites an aeromagnetometer should not be flown alone. However, the additional cost of aeromagnetic data acquisition is small if they are acquired at the same time as AEM data.

The cost of acquiring airborne geophysical data is relatively large - $20,000 to $35,000 per site for AEM. Aeromagnetic data acquired at the same time might add $1,000 to the survey costs. However, in many geologic situations these data are invaluable, particularly if faulting and water problems are anticipated.

9.4 Appraisal of Combined Conventional and Remote Sensing Investigation Systems

The goal of a tunnel site investigation is to collect an adequate body of geologic information to form the basis for an accurate assessment of pre-construction tunneling conditions. This goal may be easy or difficult to attain depending upon the surface and subsurface conditions, the characteristics of the proposed tunnel, and the time or funding limitations of the investigation. The many tunnels constructed without major difficulty indicate that current investigations, using two or more conventional methods to provide geologic information, are at least partially successful. Many of the tunneling problems that do arise are the result of encountering an unforeseen geologic "weak link" such as a fault

zone, an altered zone or areas of high groundwater inflows. The failure of the conventional investigation system to identify a critical geologic feature may be the result of limitations of the methods of investigation or interpretation used, the investigation system, or time and funding available for the investigation.

In current practice, a tunnel site investigation will almost always include an interpretation of aerial photographs, surface geological mapping, and borings. Surface geophysical testing is sometimes used in critical areas such as portals and low-cover reaches of a proposed tunnel. The variety of logging methods available are seldom employed in the boreholes produced. With the exception of small scale permeability tests in the exploratory borings, field testing is rarely used unless there is a possibility that the information from the tests will affect design decisions and result in major construction cost savings. Some laboratory testing of boring samples and outcrop samples is a normal part of the investigation.

The confidence placed in the boring samples may range from high to very low depending upon the uniformity of the geological conditions, the skill with which the borings are sited, and the recovery of cores and cuttings.

The end product of a typical tunnel site investigation using conventional methods is normally an incomplete picture of the surface conditions and inferences about the subsurface supported by a few spot checks. Surficial geology may be well exposed in a rocky, desert environment permitting accurate and comprehensive geologic mapping and photo interpretation, but in a temperate environment the ground surface is generally poorly exposed because of soil and vegetation cover.

There are many instances where an analysis of remote sensing imagery can make an important contribution to the tunnel site investigation. Some examples observed during previous work in remote sensing and during this investigation are;

I. Identification or differentiation of lithologic units

    a. Identification of rock units over large areas prior to surface mapping

    b. Rock unit identification on remote outcrops

    c. Rock unit identification determined from residual soil

168

II. Alteration and weathering

    a.   Indications of hydrothermal alteration

    b.   Depth of weathering, depth of alluvial or colluvial deposits, depth to bedrock

III. Discontinuities

(Discontinuities are one of the most common problems in rock tunnels.)

    a.   Trace major fault zones under overburden

    b.   Define major joint and bedding trends which are difficult to identify because of deep weathering or limited exposure

IV. Structure

    a.   Regional mapping to define regional structural pattern

    b.   Locate and delineate concealed structures

    c.   Help to define partially exposed complex structures

    d.   Measure the attitude of planar entities (beds, fractures, etc.)

V. Groundwater

    a.   Identify seasonal changes in hydrology

    b.   Identify springs and high water table

VI. Temperature

    a.   Identify high ground temperature areas

VII. Earthquakes

    a.   Topographic evidence of recent earthquakes

    b.   Thermally active areas

Examples of conditions for which remote sensing can be expected to be less satisfactory than conventional methods are:

I.   Rock Type Identification

   a.   Identification of rock type in areas where exposures are
        abundant and previous field mapping provide at least
        general geologic information

   b.   Identification of rock composition in absence of field
        data

II. Alteration

   a.   Areas with deep residual weathering

   b.   Areas with deep hydrothermal alteration

III. Discontinuities

   a.   Subsurface location of non-planar major discontinuities

   b.   Location and orientation of small-scale discontinuities

IV. Groundwater

   a.   Location of deep water tables

   b.   Distinguishing between artesian and non-artesian con-
        ditions where the piezometric surface is below the ground
        surface

V.   Stresses

   a.   Location of high horizontal zones

VI. Natural Gas

   a.   Location of gas saturated zones

Table 9 presents an assessment of the capability of the
conventional and remote sensing methods to identify, locate, and
measure significant geologic features under optimum conditions.
The significant geologic features, which are described in Section
4.2, are those features which most affect tunnel design and con-
struction. The capability ratings range from "0", indicating no
useful information to "5", indicating a high capability to precisely
locate and measure the geologic feature.

170

Table 9   Capability Ratings of Conventional and Remote Sensing Methods Under Optimum Conditions

Investigation Methods Conventional Methods:	Soil & Rock Type	Alteration	Discontinuities Maj.	Min.	Structure	Groundwater	Stresses	Temp.	Nat. Gas	EarthQuakes
1. Information Search										
$1,000-$10,000 Geologic records	2	2	3	2	3	2	1	1	2	3
Construction records	3	3	3	2	3	3	2	1	1	2
2. Black-and-White Aerial Photographs $1,000/15 sq. mi.	3	1	3	2	3	1	1	1	1	2
3. Surface Geologic Mapping $100-$400/sq. mi.	4	4	4	3	4	2	2	1	1	2
4. Surface Geophysical Testing* $500-$10,000/mi.	2	2	4	2	3	3	0	0	0	3
5. Soil and Rock Borings* $10-$30/ft.	4	3	4	3	3	4	2	2	3	0
6. Borehole Logging* $400-$800/50 ft.	3	3	3	3	3	4	2	4	4	0
7. Exploratory Excavation* $400-$700/lin. ft.	4	4	4	4	5	5	3	5	5	0
8. Field Testing—Stress, deformation, pumping $1,000-$20,000/test*	5	5	5	5	0	5	5	0	0	0
9. Laboratory Testing* $10-$100/test	5	5	4	4	0	1	1	1	0	0
Remote Sensing:										
10. LANDSAT $75	1	0	2	0	1	0	0	1	0	1
11. Skylab $30	1	0	2	0	1	0	0	1	0	1
12. SLAR existing $100-$20,000 contract $40,000-$100,000	1	0	2	1	2	0	1	0	0	1
13. Simulated Radar (LSAP) $2,000-$3,000	1	0	3	2	2	0	1	0	0	1
14. Panchromatic photography $2,000-$6,000	3	1	3	2	3	1	1	1	0	2
15. Multispectral Scanner $6,000-$10,000	3	1	3	2	2	1	1	1	0	1
16. Thermal Imagery $6,000-$10,000	3	1	3	2	3	3	0	3	1	2
17. Magnetometer* $20,000-$35,000	2	1	2	1	2	0	0	0	0	0
18. EM* $20,000-$35,000	2	1	2	1	2	2	0	0	0	0

*Provide information on subsurface conditions.

0 = method provides no useful information about the feature.

1 = method provides an indication that the feature may be present (detection).

2 = method provides a reliable indication that the feature is present.

3 = method provides information to precisely locate the feature at one or more locations and provides general information about the extent of the feature (identification).

4 = method provides information to precisely locate the feature and generally assess the properties of the feature (analysis).

5 = method provides information to precisely locate the feature and provides a quantitative measure of the properties of the feature (mensuration).

The capability ratings in Table 9 assume near optimum conditions because all methods will yield inferior information if used under adverse environmental conditions or improperly located with respect to the feature. For example, an aerial photograph taken on a cloudy day would be inferior to one taken under good visibility conditions. A boring sited to intercept a fault might yield valuable information if the fault is crossed and less important information if the fault is missed. The capability rating represents the highest quality information that the technique can provide.

The capability rating of most of the methods is "3" or less even under optimum conditions, which indicates that most methods have the capability to identify and partially locate, but not to measure, the significant geologic features. In general, ground surface methods and remote sensing methods have low to intermediate ratings, borings have intermediate ratings, and exploratory excavations and field tests performed primarily in exploratory excavations have the highest ratings.

Remote sensing and surface mapping methods are given lower ratings because the exposed material is normally altered by surface weathering and is under lower stress conditions than the material in the subsurface. Almost invariably projection of surface geologic features to tunnel level involves uncertainty as to location and characteristics in the subsurface that cannot be resolved until the material is exposed in the tunnel. Surface and airborne geophysical methods are given a low rating because they provide only an indirect measure of subsurface conditions (it is important to note that these are measurements, even though indirect, rather than inferences). Borings are given an intermediate rating because they

172

provide essentially a one-dimensional sampling of the subsurface materials and are generally limited to some extent by sample losses and sample disturbance. Exploratory excavations are given high ratings because these man-size openings provide access for observing the three-dimensional layout of subsurface features and the behavior of the material in a tunnel. Field tests are also highly rated because these tests provide a quantitative measure the response of a medium to large scale section of the rock mass to compressional loads, shear loads, or percolation.

Table 9 also indicates that the investigation methods with the higher capability ratings costs more. Exploratory excavations and some field testing methods are the most expensive with progressively lower costs for borings, geologic mapping and aerial photograph interpretation. Logically, most tunnel site investigations will involve the maximum use of the lower unit cost methods and minimum use of the higher unit cost methods.

Using the terminology developed for conventional methods, it is evident in Table 9 that the remote sensing methods have a low to intermediate unit cost and have low to intermediate capability ratings. These observations suggest the following conclusions with respect to the application of remote sensing methods to tunnel site investigations.

a. Remote sensing methods have the same general limitations as other surface investigation methods.

b. Remote sensing methods can supply some information more completely, cheaply, and quickly than surface methods.

c. Some remote sensing methods, such as SLAR, have high unit costs with respect to other surface methods.

d. Remote sensing methods do not have a sufficiently high capability rating to replace borings or exploratory excavations.

e. Certain remote sensing techniques, when used in conjunction with conventional tunnel investigative methods, increases the reliability of the three-dimensional model of the tunnel site.

9.5 Cost Effectiveness of Combined Conventional and Remote Sensing Systems

Cost is a major consideration during the planning and execution of a tunnel site investigation. While the budget for a tunnel site

173

investigation is generally large in contrast to budgets for foundation investigations or investigations for shallow surface excavations such as highway cuts, the funding does sometimes limit the type and extent of the site investigation. The budget for the investigation work is normally established in the planning stage based upon a preliminary assessment of the geologic conditions, the investigation goals, and the type and extent of investigative work to be performed. As the work progresses, an improved understanding of geologic conditions at the site often leads to a revision of the investigation plan and some strain on the funds available.

An investigator using conventional and remote sensing methods must give consideration to the following questions in planning and performing a tunnel site investigation:

1.   What proportion of available funding should be used for remote sensing?

2.   Will remote sensing provide an adequate geologic information base to guide or decrease the conventional investigation work?

3.   Will the remote sensing information have a tangible influence on the cost of tunnel construction?

There are no universally valid answers to these questions but the following paragraphs may be of some assistance.

The response to the first of these questions is the amount of funding will be dependent upon the potential value of the results. It should be recognized that remote sensing methods will generally be most useful to the investigation if they are used during the early part of the program. The relatively inexpensive, small-scale satellite imagery and available black-and-white photography should be obtained and analyzed during the planning stage of the project. This imagery should be used regardless of the level of detail of existing information available for the site. In almost all instances the imagery will provide a perspective that is not provided by existing information.

In all areas where there is little information from previous conventional investigations, the imagery will provide insight into the geologic and regional setting and will serve as an initial basis of planning for subsequent investigations. In all but a very few instances it will be desirable to plan for the acquisition of additional remote sensing data prior to surface investigations.

After the initial regional surface mapping, the investigator should evaluate the contribution of the less expensive forms of special remote sensing data. If SLAR imagery is available for the site (see Appendix H) it should be ordered. If SLAR does not

exist, acquisition of LSAP imagery should be planned as part of the initial program of photographic data acquisition. The initial acquisition program should also include either color or color infrared imagery at medium and large scales. The value of the information contained in these data far outweighs their moderate cost in almost all environments. If hydrologic problems are known to exist or are suspected, thermal infrared scanner imagery should be included in the initial remote sensing data acquisition. If the area is known to contain major fracture zones, serpentine bodies or basalt dikes, AEM may also be incorporated.

The response to the second question depends on the site being investigated. Assuming that remote sensing techniques are used, preliminary interpretation of the initial data set will enable the planning and direction of the surface geologic investigation, thereby making optimum use of time and resources. This optimization is possible because the geologist has become intimately familiar with the area during the photo interpretation phase of the investigation; he has placed the site geology into a regional setting, and has identified and located specific hazards or problem areas that require special attention. The result is that the entire field operation becomes more efficient and productive. The amount of field time that is usually spent in trying to locate fracture zones, contacts, and thick alluvial or colluvial deposits is greatly reduced.

Following the surface investigation and prior to the beginning of the subsurface investigation, field and remote sensing data should be integrated to produce a three-dimensional model of subsurface conditions. This integrated interpretation should be used to plan and guide the subsurface investigation and to determine the need to use the more expensive forms of remote sensing such as AEM, EM, MSS, and TIR. At this stage, the investigator will have a sufficiently detailed concept of the site conditions to realistically appraise the contribution of these additional remote sensing methods.

Table 10 summarizes the response to the third question. The table compares the units of exploratory work and the units of construction work which could be purchased for $10,000 in 1975. The sum of $10,000 was selected as being a normal increment of cost for remote sensing data acquisition and analysis.

The unit prices shown in Table 10 do not refer to a specific site or a specific set of geological conditions, but rather they are presented as representative of typical investigation and construction costs. The sum of $10,000 will provide one of the following conventional investigations; a field geologist's time to map most tunnel sites; seismic testing along a major portion of a tunnel alignment; one or two deep borings; or the excavation of a short section of exploratory adit. Ten-thousand dollars of remote sensing imagery and interpretation is sufficient to provide an analysis of

175

Table 10   Comparison of Investigation and Construction Cost
(Reference amount is $10,000 at 1975 prices)

Investigation

Units	Unit Cost ($)	Description
50 man days	$ 200/day	Field geologist for mapping
5,000 linear ft.	2/ft.	Refraction seismic testing
400 linear ft.	25/ft.	Nx core drilling and sampling
20 linear ft.	500/ft.	Exploratory adit
20,000 sq. mi.	0.50/sq. mi.	Satellite imagery and interpretation
25 sq. mi.	400/sq. mi.	Acquisition and interpretation of LANDSAT, Skylab, SLAR (SAC), high altitude B&W, low and medium altitude color and black-and-white photography and LSAP photography.*

Construction

900 man hours	$ 11/hr.	Miner for tunnel excavation
24 crew hours	415/hr.	38 man crew for tunnel excavation
10 linear ft.	1,000/ft.	Excavate and install basic lining for a 35 ft. highway tunnel in poor ground conditions
8 steel ribs	1,250/rib	8 inch wide flange steel rib weighing 67 lbs. per foot with fittings and connectors for 35 ft. tunnel
12 days	830/day	Operation of fans to provide normal ventilation capacity in a 35 ft. tunnel

* TIR over the same site (acquisition and interpretation) would cost about $14,000 and AEM about $30,000.

the regional and local geology based on satellite photography, black-and-white, color and low-sun-angle photography flown specifically for the site and SLAR imagery if it previously existed. The same $10,000 in construction will purchase a few feet of a single bore highway tunnel with the initial support system without lining, pay the salaries of a tunneling crew for about 24 hours, purchase a few steel ribs, or ventilate a tunnel for about two weeks.

This comparison between conventional and remote sensing investigation costs and construction costs has little meaning until one compares tunneling costs with the influence of adverse geologic conditions. Tunneling experience indicates that previously unknown geologic features such as faults or weathered zones that extend a few feet to a few tens of feet along a tunnel alignment can result in the installation of additional steel ribs and may create tunneling delays which range from a few hours to a few days. A previously unknown zone of adverse geological conditions ranging in length from tens of feet to hundreds of feet can create extra support costs and delays which can range from $10,000 to easily over a million dollars. While knowledge of adverse geologic features will not change the character of the work required, this knowledge can prevent the adoption of tunnel designs which are not appropriate for the geologic conditions and can prevent construction delays. If, therefore, previous investigations indicate the possibility of adverse geological conditions, but do not completely document their location or characteristics, an additional investment in the site investigation of $10,000 to $30,000 could result in construction cost savings much greater than the investment in the investigation.

To summarize, once the engineer is familiar with the capability of remote sensing techniques, it will become apparent to him that these techniques can be used to provide new information, augment the data commonly acquired using conventional site investigation techniques, and to guide conventional site investigation programs. The synoptic characteristic of airborne data will be helpful in directing surface investigations from general surface mapping to ground geophysical surveys and rock borings. The information obtained by integrating the two techniques will be more valuable and effective than the information obtained separately by either technique. The incremental cost of site investigation should be weighed against the incremental cost of delay that can result from insufficient data. The additional increment of investigation cost using an integrated investigation approach may save many increments of construction costs.

The final assessment, therefore, is remote sensing techniques can be combined with conventional investigation techniques to produce the best and most cost effective description of tunneling conditions.

10.0 CONCLUSIONS

The following are the principal conclusions arising from this investigation:

- Inclusion of remote sensing techniques into the process of selecting and geologically evaluating a tunnel site will be most effective when thoroughly integrated with conventional techniques.

- Aerial remote sensing techniques can provide a substantial amount of information for developing a three-dimensional geologic model and aid in tunnel location and design.

- Analysis of the capability of a variety of airborne and satellite systems, demonstrates that certain geologic features are more readily detectable with one system than another. However, because the capabilities often overlap there can be flexibility in selecting an array of sensors for gathering the required information. Therefore, selection of an optimum remote sensing system for site investigations will depend on the specific conditions at a site.

- Computer analysis of geologic data acquired during this study indicates that this approach can be extremely useful in certain areas. However, we conclude that the full potential of computer analysis of geologic data cannot be demonstrated using data from the two test sites selected for this study.

- The effectiveness of a remote sensing system is related to the capability of that system and the need for the information supplied by that system. The cost of a system is more practically considered in terms of percentage of total project cost, or compared to increments of construction cost. If an additional increment of site investigation cost has the potential of avoiding 10 increments of construction costs, (for example, slower drive rate, additional roof support), or avoiding delays that cost many times more than the investigation increment, then the additional increment of investigation should be spent.

The above conclusions require some qualification. Satellite and aerial remote sensing techniques can provide only a partial description of the advantages and disadvantages of a certain route and a partial description of the tunneling conditions at a specific site. Realistically, remote sensing techniques cannot replace conventional investigation techniques, but when the two are thoroughly integrated the results are more reliable and valuable than those that could be achieved by either method separately.

Another premise that was established early in this study was that there is no optimum combination of sensors that can be recommended and applied to all proposed tunnel sites. It is possible, however, to make a conditional recommendation of sensors to be used at various stages of a tunnel site investigation.

Because the costs of conducting remote sensing surveys and analyzing the data vary considerably, the most realistic approach to an economic analysis would deal with the costs of investigation relative to the costs of construction. The cost-effectiveness conclusions are based on semi-quantitative estimates of costs for acquiring and analyzing data from several types of remote sensing systems. These remote sensing costs are low compared to the cost of constructing the tunnel. A single unit of investigation cost may save many units of construction costs that are due to unpredicted hazards.

The remainder of this discussion will be an expansion of the points above, and specific conclusions on the utility and contribution of various remote sensing techniques when used separately or in combination.

Satellite data, both LANDSAT and Skylab, are useful for tunnel route selection and regional geologic analysis. Regional geologic features that are interpreted on satellite data invariably have smaller scaled features associated with them, and these smaller features can have direct impact on the tunneling conditions at a specific site. Satellite data allow gross regional estimates of lithology and hydrology, but satellite data are most effective when used in conjunction with larger scale aerial photography and imagery. Because the cost of satellite data is low, the information is extremely cost-effective and should invariably be acquired for route and site investigations.

The all weather capability of side-looking airborne radar (SLAR) is valuable in areas where there is a high percentage of cloud cover throughout the year. With the higher resolution and synoptic view of the terrain provided by SLAR imagery it is possible to make regional geologic analyses of greater detail than those attainable from satellite imagery. SLAR data is particularly useful for identifying topographic expressions of structural features. As with satellite data, however, SLAR imagery is more effective when it is used with larger scale photography and imagery. Acquisition of new SLAR data is normally too expensive for a specific site unless the area is cloud covered to the extent that other imagery cannot be obtained. Therefore SLAR, although it can be very useful for tunnel route and site selection, is recommended only if it is already available. Only then will it be cost effective.

The appearance of low-sun-angle photography (LSAP) is similar to that of SLAR imagery. The spatial resolution of LSAP is higher than SLAR imagery as it is normally acquired at a larger scale. It thus provides shadow enhancement to small structures of interest to tunnel site investigations. LSAP is most useful when it is used in combination with

179

other photographic data. It is relatively inexpensive to acquire and can be effectively substituted for SLAR data.

Black-and-white panchromatic photography obtained with a metric camera provides the best spatial resolution and geometric fidelity of all the sensors employed in this study. This photography is useful for stereoscopic plotting of topographic maps and for transfer of photointerpreted geologic and hydrologic information to the topographic base maps. Spatial resolution of large scale, black-and-white, panchromatic photography permits the detailed mapping of the stratigraphy and structure when it is visible at the surface. The cost of acquisition and processing of such photography is the most economical of all of the photography and imagery acquired during this study.

Color aerial photography is an essential data type for site investigations. Its prime utility is in the identification of lithologies, structural features, soil types, and vegetation. When used in combination with other systems such as LSAP and black-and-white panchromatic photography the structural and stratigraphic map produced will be as comprehensive and complete as is practical to be obtained with the more standard remote sensing methods. This information will contribute to an understanding of the relationships between subtle tone differences in rock types or soil types. The cost of color film and processing is greater than that for black-and-white, but the added expense is more than offset by the gain in information.

Color infrared photography is the most useful type of photography for the identification of vegetation type, vigor, and phenological stage of development. Vegetation patterns are largely controlled by the type of soil and availability of soil moisture and these patterns may mark fracture zones in some instances. The presence of certain vegetative types may indirectly indicate the chemical composition of the soil. The concentration and type of vegetation can provide information about the surface hydrology, soil moisture patterns, and possibly the landslide potential of the slopes in the area of planned tunnel portals. Due to the limited color range of rock and soil as rendered on the false color image of color infrared photography, some misinterpretation of these features may occur if the analysis is based on this type of imagery alone. The cost of acquisition and processing of color infrared photography is similar to that for color aerial photography.

Although acquisition of multiband photography was not originally part of this investigation, it seemed desirable to acquire multiband photography as a demonstration of an alternative to multispectral scanning systems. Consequently, we acquired limited multiband ground photography. This photography demonstrates that multiband photography can produce a color composite image that is very nearly the true color of the scene, yet maintain a high spatial resolution similar to that of black-and-white panchromatic photography. The flexibility in producing the near true color format and the additional capability of generating color infrared and a variety of composites suggests that it is possible to

180

satisfactorily substitute multiband photography for black-and-white panchromatic photography, color aerial photography, and color infrared aerial photography with actual improvement of interpretability if comparable scaled imagery is obtained. The cost of acquiring and processing multiband photography is higher than it is for the acquisition and processing of color aerial photography. Limited availability of camera systems accounts for most of the cost increase. The analysis must also be performed with specialized color additive viewers and production of hardcopy requires the services of a specialized photolab. If these facilities are available, the use of multiband photography in lieu of black-and-white panchromatic, color, and color infrared can perhaps be the most cost effective approach to airborne remote sensing.

Multispectral scanner imagery is most useful in areas where rock outcrops exist and where those outcrops are not obscured by vegetation, lichen, desert varnish or other surface contamination. Lithologic analysis and rock type discrimination are largely restricted to outcrops that are relatively fresh, but this phenomenom is uncommon in the field. The utility of multispectral scanning imagery is increased by the fact that the images are recorded on magnetic tapes, which permits computer enhancement of the images. However, the resolution remains relatively low. Enhancement of the imagery may include ratioing between spectral bands to highlight differences in the spectral signatures of various targets. Because multispectral scanner data is relatively expensive to acquire and analyze, its use in tunnel site investigations, in most situations, cannot be justified.

Thermal infrared scanning systems which operate in the 8-14 μm spectral range sense emitted rather than reflected infrared radiation. This capability can be used effectively in tunnel site investigations for the identification of soil moisture differences which are characteristic of fracture zones in the rock and which may be detectable through a thin soil cover. The identification of areas of high soil moisture may also indicate zones of potential slides and slump. As used in this investigation, thermal imagery provided unique information concerning the chemical composition of rocks within the area of interest. The practical value of this capability is limited in most tunnel site investigations because a visit to the site, which must be made, will answer questions of rock composition.

Data from a thermal scanner system, like the multispectral scanning system, is relatively expensive to acquire and process. Generally, thermal infrared scanning data would not be acquired unless, based on preliminary geologic analysis of the site, hydrologic problems are anticipated.

Airborne geophysical systems (electromagnetic and magnetic) were the only systems used in this investigation that provided direct information about the subsurface. These systems are particularly good for detecting certain classes of features such as wet fault or fracture zones, conductive strata such as graphite bearing rocks, or other lithologies

181

possessing magnetic properties that indicate zones which may pose major construction problems and increased costs. Electromagnetic systems detect differences in resistivity in near-surface rock and in soils, and are, therefore, potentially valuable tools for tunnel site investigations. Airborne magnetometers systems record remnant magnetization and differences in the magnetic susceptibility of subsurface soil and rocks. This is an important capability for tunneling applications in that it makes it possible in some situations to infer the displacement of lithologic units across faults. It also allows some discrimination of rock types and recognition of major discontinuities. Both airborne geophysical systems should be flown together. The cost addition of aeromagnetics when added to the airborne EM system is negligible. Airborne geophysical data will be most effective when used in conjunction with data from other airborne sensor systems.

11.0 RECOMMENDATIONS

11.1 Recommended Sensor Compliment

Selection of sensor types is largely dependent on the geological, hydrological, and climatological conditions at a specific site. The utility of a sensor may vary as the environmental conditions vary. It is, therefore, difficult to recommend an optimum compliment of sensors for all sites; however, some conditional recommendations of sensors can be made. These recommendations are based on the cost of aquisition, cost of processing and interpretation, and the effectiveness of the sensors. There are three recommended categories of remote sensing data:

Category 1. Data from these systems should be acquired for all sites if continuous cloud cover, haze or fog does not occur.

Category 2. These systems should be used only if severe hydrologic problems are anticipated or if the surface geologic structure is sufficiently complex that only subsurface data will make the three-dimensional geologic model more reliable.

Category 3. This system should be flown at a specific site only if clouds, fog, or haze prevent or hamper the acquisition of data by other sensors, and if conventional ground techniques are deemed inadequate.

Category 1 remote sensing systems include;

LANDSAT	Color Infrared Photography
Skylab	LSAP
Black-and-white Panchromatic Photography	Multiband Photography
Color Photography	Existing SLAR

All of these systems are photographic except LANDSAT multispectral scanner imagery and SLAR data. LANDSAT imagery and Skylab photography should be obtained because of the low cost and the valuable route selection and regional geologic information that these systems provide. Metric black-and-white panchromatic photography should be obtained for stereoscopic plotting, and for its high spatial resolution and geometric image fidelity. Color should be acquired for best lithologic and soil discrimination. Color infrared photography can provide valuable data on vegetative vigor and geologic structure; the selection of the appropriate season for acquisition of data is more critical than for other photography. Multiband photography

183

should be obtained instead of black-and-white panchromatic, color, CIR, if the facilities for interpretation are available. Many of the capabilities of these airborne photographic systems can be duplicated by multiband photography with proper color additive viewing and photolab processing techniques.

Low sun angle photography probably should be acquired at all sites. The solar azimuth, which is dependent on the time of the year, is important for proper enhancement of structural and topographic features. The time of acquisition will vary from site to site.

Existing SLAR imagery from government sources is inexpensive and should be acquired if available. LSAP and SLAR systems provide similar information; although, SLAR has poorer spatial resolution, it provides a shadow-enhanced, synoptic view of the regional geologic structure and topography.

Category 2 remote sensing systems include:

-   Two channel thermal infrared scanner (8-10μm/10-12μm)

-   Multispectral scanner

-   Airborne geophysical (electromagnetic, magnetic)

Two-channel thermal infrared scanning data is an order of magnitude more expensive to acquire, process and interpret than color photography, but if hydrologic problems are suspected or anticipated, the detection of potentially "wet" fractures and anomalously high concentrations of soil moisture may help to avoid delays during construction. Multispectral scanning surveys are comparable in cost to thermal surveys, but much more data is normally acquired, consequently, the processing and analysis of the data can be substantially more expensive. Although interesting geological information can be derived from these data, e.g., the accentuation of the iron-oxide concentrations in certain strata at the Carlin Canyon site, the utility of this information to tunnel siting studies is negligable. Other features of surface geology are more readily and accurately mapped on high resolution aerial photography. This system is not recommended for tunnel site investigations because it does not contribute cost effective data or improve the three-dimensional geologic model.

Airborne geophysical (AEM) surveys should be conducted in geologically complex areas, e.g., if it appears that groundwater flow may be a problem or if graphitic or other conductive zones are present that could represent areas of structural weakness. Airborne magnetometer data should be acquired in conjunction with AEM surveys to support and improve the three-dimensional geologic interpretation. Airborne geophysical systems are expensive, ranging from 10 to 20

184

times more than a color photographic survey, but they may contribute to a cost savings by optimizing the surface geophysical and rock boring program analysis.

The third category sensor is side-looking airborne radar. Since much of the equipment is bulky and normally requires sophisticated aircraft, the acquisition of SLAR is very expensive. Survey costs range from 15 to 30 times more than for color photography, but if imagery does not exist for a given site, it should be acquired only if cloud conditions make acquisition of other airborne data impractical. Perhaps the only other unique capability that might make acquisition of SLAR worthwhile is that the variation in look angle for SLAR is not dependent on solar azimuth as is LSAP.

Actual application and experience in the use of remote sensing systems to tunneling investigations will improve future recommendations of sensor complements. The final evaluation of the cost effectiveness of the systems will occur only after tunnel construction. If geological conditions are simple and few delays and hazards occur, then the Category 1 remote sensing systems are most cost effective and should be used. If geological and hydrological conditions are complex, Category 2 systems will reduce the probability of encountering unexpected hazards and delays and they become cost effective. The use of Category 3 systems is based almost entirely on climatological conditions at the site. If satellite or airborne data cannot be collected then the expensive SLAR systems may become cost effective.

11.2 Considerations of Seasonal and Diurnal Effects

Seasonal and diurnal effects related to climate vary with geographic location. This statement is of course obvious, but it is the basis of the observation that a single recommendation of optimum time of year or day to acquire remote sensing data is meaningless unless it is related to a specific site. The conditions that vary with the season and time of day can affect visibility, alter emitted, reflected and transmitted energy, and affect the stability of the aircraft carrying the sensor.

Rather than attempting to consider all possible combinations of seasonal and diurnal variables in making a recommendation, the variables themselves and their influence on the sensors will be presented. With this information, and climatological and meteorological data for a specific site the geologist or tunnel engineer will be able to select the proper time to acquire remote sensor data.

185

The seasonal and diurnal conditions to be considered when planning a remote sensing mission include:

- Surface moisture
- Snow cover
- Surface temperature
- Air temperature
- Wind
- Sferics
- Humidity

- Clouds
- Haze/fog
- Phenological stage of vegetation
- Solar elevation and azimuth

Surface moisture differences will change the tonal character of most targets in the visible and near-visible range of the spectrum. Therefore, imaging and photographic systems that operate in that range may produce different images of the same target under different surface moisture conditions. In most instances there is no distinct advantage to imaging an overall wet or dry surface, but it is important to be consistent when obtaining data from different sensors at different times. Surface moisture increases the radar reflectivity of the target thereby masking detail of the image. It is recommended, therefore, that when possible, radar imagery should be acquired during a period when surface moisture is low. Surface moisture affects the information that can be obtained using thermal infrared scanners by either highlighting or supressing structural geologic features. Such scanners are most effective when minor or moderate amounts of soil moisture are present. If soil moisture is excessive the thermal gradient between emitting surfaces will be considerably reduced, minimizing the contrast between target materials. Surface moisture also affects airborne geophysical surveys, specifically, resistivity surveys. It can increase the conductivity of the surface materials, giving spurious surface information as well as obscuring the detail of subsurface information. If there is insufficient or excessive surface moisture, fractures and sinkholes may go undetected.

Snow cover has the effect of either increasing the interpretability of imaging and photographic system data or it can obscure important geologic information. A certain amount of snow cover, e.g., less than two inches, will enhance topographic and geologic features on satellite imagery, aerial photography, and multispectral scanner data. If the snow is too deep it will obscure significant geological features on imagery from these types of sensors. With radar imagery some penetration of the snow cover can be expected. However, if the snow is extremely wet there may be some increased reflection from wet surfaces. Snow cover affects airborne geophysics in that wet snow may increase the conductivity of the surface and near-surface materials. Snow enhancement of geologic features is difficult to plan for because the amount of snow cover for proper enhancement can rarely be predicted in time to organize a photographic mission.

186

Surface temperature has little effect on radar, satellite imagery, aerial photography, or airborne geophysical data; however, it does affect the information obtained by thermal infrared scanning. Surface temperatures are generally a direct result of solar heating. Differential insolation effects on the ground surface due to topographic shadowing can generate a thermal image similar to that acquired by low-sun-angle aerial photography. This is, in effect, a thermal shadow enhancement of geologic and topographic features. Differential cooling of the surface, notably in fracture zones which generally appear cooler due to moisture concentrations, produce surface temperature anomalies important in geological mapping.

Actual air temperature has little effect on the sensors used during this investigation except for the thermal scanners. Therefore, it is a relatively insignificant consideration in planning most remote sensing missions. The air, although transparent and undetectable in the 8-14μm spectral range, can transfer heat to or from a target material and influence the detected temperature. This is particularly so if there is an appreciable difference between the air and ground temperatures or if there is substantial air movement. A knowledge of those conditions that prevailed at time of data collection is essential to effective data analysis.

Wind has no effect on orbital platforms, but does have considerable effect on radar, photographic, scanner, and airborne geophysical systems. Obtaining good quality information (geometric image fidelity and proper orientation of imagery) is dependent upon a stable platform; therefore, surveys should not be conducted during excessively high winds. In some geographic locations, certain times of the year are characterized by high winds, those periods should be avoided when possible.

Sferics are the natural fluctuations of the electromagnetic field of the earth; they are caused by lightning discharges on a global scale. Sferics affect only the airborne electromagnetic system that was used during this investigation. For this reason the airborne geophysical surveys should not be conducted during times when excessive electrical activity exists. An auxilliary sferics monitor should be used.

Humidity affects thermal scanning systems; however, the humidity has to be extremely high (85-100%) before thermal radiation in the 8-14μm range is attenuated significantly.

Clouds obscure the ground from orbital and airborne platforms. They do not, however, affect radar imagery unless condensed water vapor is present in the clouds in appreciable quantities. Clouds do not directly affect airborne geophysical sensing, but such surveys are conducted at low altitudes where good visibility is essential. Partial cloud cover can be tolerated on some photographic missions, but the illumination of the target area may be affected and, consequently, the color balance. Cloud shadows within the target area

187

can degrade daytime thermal infrared imagery and may result in misinterpretation. This statement applies to LSAP also, particularly if thin cirrus clouds cast linear shadows which could be interpreted as ground features.

Haze and fog can severely attenuate reflected and emitted energy. Satellite and airborne photographic and scanner data will have less resolution and clarity and detail if acquired during haze and fog conditions. Haze and fog, however, do not affect airborne geophysical or radar systems.

Stages of phenological development of the vegetation are important to all systems used during this investigation except airborne geophysics. Vegetation can either obscure or enhance structural and topographic detail. For geological analysis (lithology, structure, stratigraphy) it is recommended that in areas where leaf canopy can be a problem the aerial photography be acquired during the late winter or early spring. This is the period of maximum leaf compaction on the ground and before spring leaf development. For hydrologic investigations, color infrared imagery should be obtained in the spring as the leaf canopy begins to develop. In arid regions vegetation may reflect subtle changes in soil composition and moisture content. This, in turn may emphasize lithologic differences and structural features. Consequently, the best time to acquire this type of photography in areas of low precipitation is during the wetter season. Geobotanical indicators are often used to identify varying amounts of soil moisture and chemical properties of the soil. These above factors apply to satellite and airborne photographic and scanner data. On radar imagery vegetation has the effect of altering the texture of the image. Geophysical systems are not affected by vegetation.

For passive imagery systems solar elevation and solar azimuth have the effect of enhancing topographic and geologic features provided that the solar elevation is low enough (10° to 25°) to cast a substantial shadow. Radar and geophysical systems, however, do not depend on solar energy for operation.

The influence of seasonal and diurnal conditions on the quality of remote sensor data will vary with the severity of the condition and the system used. In many instances these conditions can be tolerated if they are unavoidable, but it is necessary to be aware of the influence that the particular condition will have on the quality of the data. Based on this brief summary of seasonal, diurnal, and climatic effects on various remote-sensing systems and the recommended procedures for acquiring data, the engineer or geologist can select sensor types for almost any proposed tunnel site.

11.3 Recommendations For Future Work

In a report such as this it is difficult to be totally comprehensive in evaluating all of the capabilities of commercially available airborne remote sensing systems. Furthermore, it is even more difficult within the scope of this report to describe the details of selecting sensors under all environmental conditions, contracting for services, interpretation of data, and application of results to tunnel site investigations. Therefore, we believe that the work begun during this contract should be continued and expanded. Our recommendations for future work are:

- Selected remote sensing techniques should be applied to additional tunnel sites to verify their utility in different geologic environments;

- A remote sensing handbook for tunneling should be prepared for agencies who may be preparing bids and contracts and contracting for the construction of tunnels and for organizations involved in the construction of tunnels.

The additional site should be in a more complex nonsedimentary geologic environment. The handbook would describe in laymen's terms how various remote sensing techniques can be applied during the feasibility and final design investigations for tunnels, and include information on relative cost and utility of the sensors examined, given a variety of geologic environments.

Remote sensing techniques were applied in this study to two tunnel sites, one in the Eastern and one in the Western United States. These sites were selected for a variety of reasons including the fact that remote sensing data could be collected for each site during optimal seasons and within the performance period on the contract. Unfortunately, both sites are in relatively similar geologic environments and both involve relatively simple geologic structure. The fact that positive results on the application of remote sensing in these two instances were obtained, lead us to believe that these techniques should be tested in other more complex geological environments. By the addition of such sites the reliability and utility of the sensors tested could be further substantiated and extended. The present sites were not adequate to fully test the capabilities of some of the sensors examined (notably airborne electromagnetic and thermal infrared) and their potential contributions to tunneling. Airborne multiband photography was not used at either site because of its expected duplication of multispectral scanner data. Based on our use of ground multiband photography at Carlin Canyon, we believe that airborne multiband photography may provide an inexpensive but effective substitute for multispectral imagery. Additional sites would provide the opportunity to compare the two sensor systems.

189

The additional sites should include at least one in a crystal-
line terrain - that is, in igneous, metamorphic or volcanic rock.
Such sites should adequately test and demonstrate capabilities of
the recommended sensors beyond those capabilities demonstrated in
sedimentary rock. The sites can be an existing or proposed tunnel
but it need not be a highway tunnel. It could be for water or rail.
Several candidate sites include:

- The Straight Creek tunnel, which was among those considered
  originally,

- The Caldecott highway tunnel, in California

- The Berkeley Hills BART tunnel, California area,

- A water tunnel in California

Potential users of the results of this investigation will
require some assistance in applying the results to specific siting
and engineering problems. Although this final report documents the
capabilities of the various sensors tested as well as recommends
situations in which those sensors may be most usefully employed, we
believe that a shorter and more general handbook (one that could be
used by tunneling engineers and understood by managers with a variety
of technical backgrounds) is required if these techniques are to be
applied in operational programs. Such a handbook would contain
easily understood text, tables and charts which would assist the
user in planning remote sensing missions designed to increase know-
ledge of a particular site or sites.

It is clear from these investigations that there is no single
optimum combination on airborne sensors which might be applied to
any potential tunnel site. The sensor complement and capabilities
of selected sensors will vary from area to area depending primarily
on the geology, climatic environment and vegetation cover of the
area. Geologists and engineers having less than a full understanding
of the techniques employed will, with the handbook, be able to
select a combination of sensors and design a remote sensing program
which will provide the information they require for engineering and
construction purposes.

The information in the handbook should be presented in such a
way that engineers involved in site selection might derive the
maximum benefit from remote sensing. This would require a descrip-
tion of the capabilities and limitations of each of the sensors as
well as a discussion of their relative cost and a listing of firms
which provide those services. In addition, some discussion of the
variety of geologic conditions likely to be encountered in tunnel
site selection and engineering and the utility of each of the

190

sensors for those given conditions should also be included. Specific examples of each sensor and the information extracted as well as a discussion of problems associated with data acquisition for each sensor should be included. Specifically, data acquisition constraints such as time of day, season, and weather conditions would be indicated.

Because purchasing services from remote sensing companies will be an uncommon experience for most firms involved in tunnel construction, some advice regarding the technical aspects and contract specifications should be provided. This discussion should provide general guidance to the engineering or tunneling firm on mission planning, contractor selection, flightline layout, incorporation of corollary data and ground support. While it is recognized that in most instances the actual analysis of the data may have to be done by specialists familiar with tunnel engineering problems, geology, and remote sensing, it is necessary for those contracting for remote sensing services and employing remotely sensed data in solving engineering problems to understand the techniques employed and the conclusions drawn. It is also necessary for the user to specify that the data and analysis requirements be met with a report, models or maps which satisfy his specific needs.

To summarize, an outline of the remote sensing handbook for tunneling should include the following:

- Application of Techniques
- Capabilities, Limitations, Problems in Acquisition
- Geologic Environments
- Selection of Sensors
- Examples of Sensor Data
- Presentation of Remote Sensing Analysis Data
- Mission Planning - Flight Lines, Contractor Selection
- List of Flying Companies and their services (abridged)
- Relative Costs
- Relative Utility (Effectiveness)

12.0 FIELD VERIFICATION PLAN

It is clear from the results presented in Section 7 of this report that many of the features and anomalies identified in the remotely sensed data require further investigation in the field. This section presents a plan for verifying the interpretation and inferences made from remote sensing data. The goal of this plan is not simply to verify features interpreted from the surface, but to extrapolate them into the subsurface as accurately as possible. The features to be extrapolated are primarily structural and geohydrologic, and include faults, joints, linears, lineaments, sinkholes, and karst topography. Other conditions to be considered in designing the field verification plan are seepage through permeable rocks or along faults. The most accurate way to verify these features is with the aid of an integrated program of surface geologic investigation, geophysical surveying and drilling.

Once a model of the subsurface geology has been postulated on the basis of remote sensing data and geological observation, the results of the geophysical surveys can then be used to refine the model and optimize the selection of the location of core borings and drill holes. It is important that they be placed where they have the best chance of intersecting possible problem areas which the subsurface model suggests may exist. It is equally important that the holes be logged geophysically, as well as geologically, in order to obtain the greatest return per foot of hole drilled. The following field verification plan is designed presuming that the tunnels at each test site have not yet been constructed. We assumed that this work is being done while the tunnels are being designed and that the geophysical and drilling programs are yet to begin.

12.1 Carlin Canyon Site

12.1.1 Geology

The geology of the site has been fully described earlier in Section 5.1. The remote sensing data aquired over it has been analyzed in Section 7.0. They will be briefly summarized here. The two geologic formations present at the tunnel site are the Diamond Peak (Upper Mississippian in age) on the western end of the tunnel striking N15°W and dipping 85°W; and the Strathearn formation (Upper Pennsylvanian) cropping out on the east end of the tunnel, striking approximately N25°W and dipping 70°NE. An angular unconformity exists between the two formations. The Diamond Peak formation consists predominantly of conglomerates and quartzites, which range in thickness from three to five feet and are well cemented by chert, quartz, and iron oxide. They contain a widely-spaced pattern of joints. The thinner interbeds of shale and siltstone are also well cemented, and are more closely jointed than the sandstone and conglomerate.

The Stratheam formation is a hard, medium-to-thick-bedded limestone with thin inner beds of shale. It is exposed on top of the meander spur, on the eastern side of the spur and on the eastern canyon wall. Most outcrops of limestone display several sets of closley-spaced joints. These joints, bedding planes, and shale inner beds all combine to limit the average size of the limestone blocks to less than one foot (.3m) in most exposures. The rock and natural exposures, however, appear relatively stable because the small blocks have an irregular shape and high degree of interlock.

Unconsolidated deposits of sand, gravel, and boulders are found at the west portal. These deposits include remnants of terraces deposited by the Humbolt River and colluvium which has accumulated at the base of the spur.

More than 11 faults, linears, and lineaments have been identified on the imagery. Neither of the two major faults identified intersect the tunnel alignment selected. A major northwest trending reverse fault crosses the northeastern portion of the spur. The fault trace is identified within 100 ft. (30m) of the proposed eastern portal. The total vertical displacement of this fault is approximately 300 ft. (90m). A second major fault zone has been identified south of the western portal. Neither the displacement along this fault nor its dip have been determined from surface mapping, but it is not likely to intercept the tunnel.

Faulting, both cross and parallel to the bedding planes, was observed in both formations. The dips of the fault planes are unknown, but these noted near the east portal were nearly vertical. The displacement along these faulting appears minor but the number of faults may be extensive given the proximity of the major fault. Such faults do not form to the exclusion of others, but instead, as the product of the opening of myriad microscopic cracks throughout the rock which are so ordered that they propagate in various amounts, some enough to finally coalesce to form a through-going fault zone in the midst of less through-going fractures (Johnson, 1970).

12.1.2 Features to be Verified

The faults mapped from the remote sensing data and observed in the field pose the most obvious problem for tunnel-ing. The minor faults associated with the major reverse fault north of the east portal could lead to blockcaving during excavation if there has not been some degree of recementing since their formation. Groundwater circulating down the major

193

or minor faults or along the unconformity could cause caving or flooding during tunneling. However, because of the arid climate in this region and the general structure of the ridge as a whole, there is probably little chance of encountering groundwater at the depths of the tunnel.

12.1.3 Verification Plan

Table 11 is a list of geophysical methods, their applicability to the problems associated with tunneling, and their relative costs. The technique that shows the greatest promise for detecting groundwater at this site is EM, and for detecting dry fault zones and changes in gross bulk modulae, seismic reflection.

The most likely configuration for an EM survey for this application would be an active AFMAG system that has a vertical transmitting loop with producing frequencies of 130 Hz and 475 Hz. The portable receiver is tuned to a narrow dynamic range centered on each frequency and will show magnetic field strength as a vector function of azimuth and dip. Parallel traverses of the receiver at right angles to the proposed tunnel direction could be run with the transmitting source set up at a location near the east portal. The strongest conductors are assumed to be water filled fractures, since massive sulfides and other conductive rock types are not present in either formation.

If a serious groundwater problem is suggested by the EM survey, it will most likely be localized in a fault zone at this site. The fault zone carrying it can best be further resolved by a seismic reflection survey. Delineating the fault at tunnel depth would require a high-energy, truck-mounted source. Portable seismic equipment cannot provide readings beyond approximately 200 ft. (see Table 11). The maximum thickness of the rock above the tunnel is approximately 500 ft. The reflection method is better than the refraction method, because of the steeply dipping beds at the Carlin site, and is recommended. Possible problems with the reflection surveys are that access roads are necessary for operational positioning of the seismic trucks, and could be nearly as expensive as the survey itself. Offsetting these costs are the value of additional data obtained by the survey which bear on the bulk material properties of the rock. The data will help resolve the fracture density in the rock along and near the route of the tunnel. Additionally, it would resolve the question of the subsurface location and dip of the major faults and the angular unconformity.

Table 11 Ground Geophysical Methods for Surveying Tunnel Sites

Technique	Rock Soil Interface	Identifying Rock Types	Groundwater Detection	Structure Attitude of Beds	Faults	Effective Depth, Penetration And Accuracy	Best Tunnel Application & Limitations	Cost Per Survey
Seismic								
(1) Micro-seismic, both re-fraction and re-flection	Excellent for shallow depths of soil allu-vium	Fair--depends on known velocities for differing rock types in refraction mode	Poor	Good	Good	0-75 feet for hammer and possible to 300' with blasting caps, good accuracy on depth cal-culations	For determining alluvium cover at portal sites, if shallow port-able and easy to survey in areas of steep topo-graphy	Low
(2) Deep Seismic (Vibra-tor truck)	Excellent	Good	Fair	Good to Excellent	Good	$\pm$500 feet to unlimited with good accuracy on depth esti-mates	Measure depths to various rock layers, contin-uity of layers, and locate dis-continuity, such as faults; also provides data on stratigraphic conditions. Need vertical velocity calibration for depth determina-tions. Roads are needed for truck access.	High/per point cost reduces with in-crease in area. Not economic for small jobs (see text for more details)

195

Table 11 Ground Geophysical Methods for Surveying Tunnel Sites—Contd.

Electrical and Electromagnetic

Method								
(1) Resistivity (2) EM, & (3) AFMAG w/active transmitter	Fair depending on moisture content	Poor except for gravel deposits or massive ore	Excellent	Poor	Good for shallow water-bearing faults	Depending on coupling, max. voltage and array configuration up to 400-500'. Depth determination and location fair to poor	Best for detecting groundwater and faults that contain groundwater	Low to intermediate, depending on desired exploration depth

Magnetics

| Magnetometer Gradiometer | Poor | Fair | Not Possible | Poor | Fair | Can locate both shallow & deep anamalous sources, accuracy of depth estimates +20% on average higher for gradiometer configuration | Best for mapping rock types with large susceptibility contrasts, i.e., greenstones and contacts with sedimentary rocks or locations of ultrabasic intrusions, also buried iron pipelines, etc. | Low for ground survey & intermediate on airborne depending upon mobilization distances & total areas to be covered |

| Gravity | Good for near surface depending upon density contrast | Poor | Not Possible | Poor | Fair | Can locate both shallow & deep anomalous sources depending upon density contrasts accuracy ~ $\pm$ 20% | Best for measuring lateral changes of rock types, locations of caverns. Limited results in steep topography | Intermediate depending upon vertical control required |

196

If the results of the EM survey do not produce any large anomalous conductors, the tunneling would most likely not be troubled with problems associated with groundwater seepage, and there would be no further need to pursue that question. Only the question of dry faults and closely jointed shale, siltstone and limestone would remain. These questions could best be addressed by running a seismic reflection survey using portable seismic equipment from above and south of the east portal to the reverse fault 100 feet (30m) to the north. This would economically provide information on the bulk modulus of the Strathearn formation from the surface into the subsurface and from the tunnel to the reverse fault, and would indicate any change in the density of jointing. This, when interpreted in the context of data from three holes drilled to slightly below tunnel level, one on the center line of the tunnel and cored and two between there and the fault, one beginning in shale and one beginning in limestone, each of which should be logged with a borehole acoustic log as well as spontaneous potential and resistivity, would provide adequate resolution of the question of the mechanical properties of the Strathearn.

Another problem apparent from the remote sensing and surface investigations is the Humbolt River terrace materials at the west portal. Because of the steep topography of each portal and the shallow depth to the target, seismic refraction should be used to determine the depth to the soil-bedrock interface, and that several shallow boreholes be drilled to below tunnel depth and logged with the above mentioned suite of logs. This information would be useful in ascertaining if rock collapse will occur during and after portal construction. It would also be useful in determining the horizontal distances over which the tunnel will need support before competent rock is encountered.

12.2 East River Mountain Site

12.2.1 Geology

Geology of the East River Mountain tunnel area has been discussed in detail in Section 5.2 of this report, and will be mentioned only briefly in this section. East River Mountain is a ridge capped by Tuscarora sandstone and underlain and overlain by sandstones, shales, and limestones, which strike N65°E and dip approximately N25-40° SE. The topography of the lower part of the slope is controlled by the overlying and less competent Rose Hill shale, the resistant Keefer and Rocky Gap sandstones. The upper part of the north slope is a cliff which exposes the Tuscarora sandstones. Less steep slopes below it are formed by the underlying Juniata shale, Martinsburg shaly

limestone, and Eggleston, Moccasin, and Gratton limestones.
The limestones that form a hummocky topography at the base of
the slope and across the floor of the adjoining valley, and
have a landscape with limited surface drainage and numerous
sinkholes, including a line of sinkholes parallel to the
Cumberland Road and a few hundred feet north of the north
portal. All of these features indicate the presence of ex-
tensive solution and groundwater flow between the surface and
subsurface. The Juniata, Martinsburg, and Moccasin formations
do not crop out on the northern slope in the immediate area of
the tunnel because they are covered by residual soils and
colluvium.

12.2.2 Features to be Verified

There are two general problems to be clarified: 1)
distribution of groundwater in the rocks of the tunnel area,
and 2) ground conditions in the area, especially in the vicin-
ity of interpreted fractures.

The engineering properties of sandstones and limestones
are generally good except for those containing interbeds of
shale. The Juniata and Martinsburg shale, which also contain
shaly limestone and siltstones, although softer than the
Tuscarora and Keefer sandstones, are relatively competent for
tunnel excavation and support. However, the shales and silt-
stones of the Rose Hill formations and the poorly indurated
sandstones of the Rocky Gap formations are far less competent.
The limestones are hard and relatively competent except for the
vicinity of solution openings.

Artesian groundwater conditions may exist near the south
portal. Groundwater can be an important element in the overall
cost of tunneling and its occurrence should be carefully
noted. Extensive jointing, shear zones, and faulting, coupled
with formations that are good aquifers, can create difficult
tunneling conditions, especially if they are not well mapped in
advance of the actual tunnel excavation.

The St. Clair thrust fault is exposed approximately
2,000 ft. north of the north portal. Although this fault zone
dips SE and so does not cut the tunnel area itself, the lime-
stones, sandstones, shales, and siltstones at tunnel level are
undoubtedly fractured and displaced somewhat by related faults.
These fractures are seen as joints in the outcrops of Tuscarora
where they are spaced about 10 feet apart. This is fairly
dense joining for a thick-bedded quartzite such as the Tuscarora
and indicates that even denser jointing can be expected in the

198

less competent and thinner-bedded rock types. If the relation-
ship established by Harris et al. (1960) holds here, the joint
density in limestone and sandstone may be expected to range
from 4 to 8 feet, with the primary effect probably being an
increase in permeability both laterally and vertically through-
out the section. It also creates blocks of a size which may be
a hazard during tunneling if not expected.

12.2.3 Verification Plan

Groundwater poses the most important question at the
East River Mountain tunnel site. A ground electrical resis-
tivity survey along the proposed tunnel route would help in
delineating areas of groundwater accumulation and indicate
locations where boreholes would be most valuable. A dipole-
dipole survey is least effected by steep topography and would
be suitable here. It uses a time-domain transmitter and re-
ceivers coupled with a large power generator (approximately
40Kw), and would give the best results. For this amount of
power an excellent signal-to-noise ratio can be maintained and
deeper exploration depths obtained than are possible with the
typical mining resistivity and induced polarization equipment.
Boreholes located to further resolve the problems of ground-
water distribution along the tunnel route as delineated by the
resistivity survey should be logged with spontaneous potential
and resistivity borehole logs. The data from these sources,
when integrated with the remote sensing data, would produce the
best possible estimates for drypack, grouting, padding, and
other necessary design features. This would greatly aid in
anticipating other groundwater problems which may be encoun-
tered during tunneling.

If severe groundwater and associated caving problems are
determined to exist by the above model as refined by the
resistivity survey and accompanying boreholes and geophysical
logs, it is recommended that a horizontal diamond wire line
core hole be drilled rather than further vertical drilling.
This would both provide additional design information prior to
tunneling and serve as a drain.

The problem of bad ground at the portals occasioned by
the incompetent residual soils and colluvium as well as the
incompetent rock formations indicates that the south slope may
require excavation down to the competent Keefer formations
prior to tunneling. The electrical resistivity survey would
not offer as fine a resolution for the determination of this
interface as would a refraction seismic survey done only at the

portals with portable equipment. Such a survey would determine
the attitude of the contact with the Keefer much more accuratly
than is possible using the resistivity survey alone. Three
boreholes logged with spontaneous potential and resistivity
logs would yield adequate correlation points between the
Keefer and the overlying material.

APPENDIX A:

REFERENCES CITED AND BIBLIOGRAPHY

References cited in the text are indicated by an asterisk.

*Abdel-Gawad, Monem, 1975, Identification and interpretation of tectonic features from ERTS-A imagery: NASA Goddard Space Flight Center, Greenbelt, Maryland. (Available through the National Technical Information Service, Springfield, Va.)

Abdel-Gawad and Silverstein, 1972, The fault pattern of southern California - A model for its development: (abs.) Geol. Soc. America, p. 23.

Adams, John B. and Felice, Alan L., 1967, Spectral reflectance 0.4 to 2.0 microns of silicate rock powders: J. Geophys. Res., v. 72, no. 22, p. 5705-5715.

*Aldrich, R.C., 1966, Forestry applications of 70mm color: Photogrammetric Engineering, v. 32, p. 802-810.

*Allum, J.A.E., 1966, Photo geology in regional mapping: Pergamon Press, New York, 107 p.

American Geological Institute, 1972, Glossary of geology: Washington, D.C.

American Society of Photogrammetry, 1960, Manual of photographic interpretation: Washington, D.C., 868 p.

*American Society of Photogrammetry, 1968, Manual of color aerial photography: Falls Church, Virginia, 550 p.

*American Society of Photogrammetry, 1975, Manual of remote sensing, v. 1 and 2: Falls Church, Virginia, 2144 p.

*Amsbury, D.L. et al., 1975, Small scale imagery: A useful tool for mapping geological features in the Texas gulf coastal plain: NASA Earth Resources Sur. Symp., Houston, Texas, Proc., v. 1B, p. 833-849.

Barr, David J. and Miles, Robert D., 1970, SLAR imagery and site selection: Photogrammetric Engineering, v. 36, no. 11, p. 1155-1170.

*Bechtold, I.C. et al., 1975, Application of Skylab imagery to resource exploration in the Death Valley region: NASA Earth Resources Sur. Symp., Houston, Texas, Proc., v. 1B, p. 665-672.

Bocker, A., 1969, Simulation of time-domain airborne electromagnetic system response: Geophysics, v. 34, p. 739-752.

*Brace, W.F. and Orange, A.S., 1968a, Electrical resistivity changes in saturated rocks during fracture and frictional sliding: J. Geophys. Res., v. 73, no. 4, p. 1433-1445.

_____., 1968b, Further studies of the effect of pressure on electrical resistivity of rocks: J. Geophys. Res., v. 73, no. 16, p. 5407-4420.

*Brace, W.F. et al., 1965, The effect of pressure on the electrical resistivity of water-saturated crystalline rocks: J. Geophy. Res., v. 20, no. 22, p. 5669-5678.

Brekke, T.L. and Howard, T.R., 1972, Stability problems caused by seams and faults: First North American Rapid Excavation and Tunneling Conf., Chicago, Illinois, Proc., v. 1, Ch. 6.

Brennan, B. and Bandeen, W.R., 1970, Anistrophic reflectance character- istics of natural earth surfaces: Applied Optics, v. 9, no. 2, p. 405.

Busch, Richard A. et al., 1974, Physical property data on coal waste embankment materials: U.S. Bur. of Mines, RI 7964, 149p. (NTIS No. PB-240-022).

*Campbell, J.A.L., et al., 1975, How to predict coal mine roof condi- tions before mining: Mining Engineering, v. 27, no. 10, Oct. 1975, p. 37-40.

Campbell, M.R., 1896, Pocahontas folio. Virginia-West Virginia: Geo- logic Atlas of the United States, No. 26, U.S. Geol. Sur., 5 p. 5PL, 4 maps.

Canada Centre for Remote Sensing, 1974. Towards a Canadian policy on remote sensing from space: A special report to the Canadian Advisory Committee on Remote Sensing. 18 p. (NTIS No. PB-238-846).

Carter, Ralph P. et al., 1974, Surface mined land in the Midwest: A regional perspective for reclamation planning: U.S. Bur. Mines report OFR 59 74, S01-33127, 675 p. (NTIS No. PB-237-830).

Cassinis, 1974, Contribution of space platforms to a ground and airborne remote sensing program over active Italian volcanoes: NASA Goddard Space Flight Center, Greenbelt, Maryland. (Available through the National Technical Information Service, Springfield, Va.)

*Cassinis, R. et al., 1975, Application of Skylab imagery to some geo- logical environmental problems in Italy: NASA Earth Resources Sur. Symp., Houston, Texas, Proc., v. 1B, p. 851-867.

*Clark, M.M., 1971a, Comparison of SLAR images in small scale low sun aerial photographs: Geol. Soc. America, bull. v. 82, p. 1735-1742.

*_____., 1971b, Solar position diagrams - Solar altitude, azimuth, and time at different latitudes. U.S. Geol. Sur. Prof. Paper 750D, p. D145-D148.

*Coker, W.E. et al., 1969, Application of computer processed multi-spectral data to the discrimination of land collapse (sinkhole) prone areas in Florida: Proc., Sixth Symp. Remote Sensing of the Environment, Univ. of Michigan, Ann Arbor, p. 65-77.

*Collins, Robert et al., 1974, An evaluation of the suitability of ERTS data for the purposes of petroleum exploration: NASA Goddard Space Flight Center, Greenbelt, Maryland. (Available through the National Technical Information Service, Springfield, Va.)

Cook, John C., 1972, Seeing through rock with radar: First North American Rapid Excavation and Tunneling Conf., Proc., v. 1, ch. 9.

Condit, H.R., 1972, Application of characteristic vector analysis to the spectral energy distribution of daylight and the spectral reflectance of American soils: Applied Optics, v. 11, no. 1, p. 74-86.

Condit, H.R., 1970, The spectral reflectance of American soils: Photogrammetric Engineering, v. 36, p. 955-966.

Cooper, J.R., 1966, Geologic evaluation: Radar imagery of Twin Buttes area, Arizona Test Site 15: U.S. Geol. Sur. report NASA-CR-76004, p. 15 (NTIS no. N70-40311).

Coulson, Kinsell L., 1966, Effects of reflection properties of natural surface in aerial reconnaissance: Applied Optics, v. 5, no. 6, p. 905-917.

*Crandall, C.J., 1969, Radar mapping in Panama: Photogrammetric Engineering, 1969, v. 35, p. 641-646.

*Culley, R.W. et al., 1975, E-phase system for detection of buried granular deposits: Symp., Modern Innovations in Subsurface Exploration, 54th Ann. Meeting, Transp. Res. Board, Washington, D.C.

Dedman, Emory V. and Culver, John L., 1972, Airborne microwave radiometer survey to detect subsurface voids: Highway Research Record no. 421, p. 66.

Deere, D.U. et al., 1970, Design for tunnel support systems: Highway Research Record no. 339, p. 26.

*Dellwig, L.F. and Burchell, C., 1972, Sidelooking radar - Its uses and limitations as a reconnaissance tool: Highway Research Board, no. 421, p. 1-9.

*Dellwig, L.F. et al., 1968, The potential of radar and geological exploration: Proc., Fifth Symp. Remote Sensing of Environment, Univ. of Michigan, Ann Arbor, p. 757-764.

*Dennis, John G., ed., 1967, International tectonic dictionary: English terminology: Am. Assoc. Petroleum Geologists. Mem. 7. 196 p.

*Denny, C.S., 1952, Lake Quaternary geology and frost phenomenon along Alaska highway, northern British Columbia and southeastern Yukon: Geol. Soc. America, bull. v. 63, p. 883-992.

*Dott, R.H., Jr., 1955, Pennsylvanian stratigraphy of Elko and northern Diamond ranges, northeastern Nevada: Am. Assoc. Petroleum Geologists bull. v. 39, no. 11, p. 2211-2305.

Drake, Ben et al., 1971, Tunnel-site selection by remote sensing techniques: Univ. of Michigan, Ann Arbor, Inst. of Science and Technology 10018-7-p. (NTIS no. AD-734-028).

*Dunbar, Carl O., and Rogers, John, 1957, Principles of stratigraphy: John Wiley, New York, 356 p.

*Dyck, A.V., Becker, A., and Collett, L.S., 1974, Surficial conductivity mapping with the airborne INPUT system: Can. Inst. Mining, bull., v. 67, p. 104-109.

Edgerton, Alvin et al., 1971, Microwave radiometric investigations of mine subsidence in Rock Springs, Wyoming: Aerojet General Corporation, El Monte, Calif., Microwave Div. AGC 1721-2. U.S. Geol. Sur. Interagency 217, HO 110156, 97 p.

*Egbert, Dwight D. and Ulaby, Fawwaz T., 1972, Effect of angles on reflectivity: Photogrammetric Engineering, v. 38, no. 6 p. 556-564.

Estes, J.E., and Senger, L.W., eds, 1974, Remote sensing: Techniques for environmental analyses: Hamilton Press, Santa Barbara, California.

*Evans, R.M., 1948, An Introduction to Color, John Wiley, New York, p. 370.

*Fischer, W.A., 1962, Color aerial photography in geologic investigations - Some results of recent studies: Photogrammetric Engineering, v. 28, p. 133-139.

*Fischer, W.A., 1960, Reflectance measurements as a basis for film filter selection for photographic differentiation of rock units: U.S. Geol. Sur. Prof. Paper 400B, p. B36-B138.

*Foster, Norman H., 1974, Geomorphic expression of pinnacle reefs in Salawati Basin, Irian Jaya, Indonesia: Proc., v. 1, Am. Assoc. Petroleum Geologists and Society Econ. Paleontologists and Mineralogists, Annual Meeting Abstracts, San Antonio, Texas.

*Fraser, D.C., 1974, Survey experience with the Dighem AEM system: Can. Inst. Mining, bull. v. 67, p. 97-103.

_____., 1973, Magnetite ore tonnage estimates from an aerial electromagnetic survey: Geoexploration, v. 11, p. 97-105.

*_____., 1972a, A new multicoil aerial electromagnetic prospecting system: Geophysics, v. 37, p. 518-537.

*_____., 1972b, The Dighem aerial electromagnetic system: 24th International Geol. Congress, Section 9, p. 51-63.

Frischknecht, F.C., 1967, Fields about an oscillating magnetic dipole over a two-layer earth, and application to ground and airborne electromagnetic surveys: Colorado Sch. Mines Quart., v. 62, no. 1.

*Fritz, N.L., 1967, Optimum methods for using infrared sensitive color film: Photogrammetric Engineering, v. 33, p. 1128-1138.

Gates, David M., et al., 1965, Spectral properties of plants: Applied Optics, v. 4, p. 11-20.

Gawarecki, Stephen J., 1973, Asian seminar and workshop on remote sensing, held at University of Philippines: Diliman, Quezon City, Republic of the Phillipines, May 7-8, 1973: U.S. Geol. Sur., Report no. IR DC 28, 41 p. (NTIS no. PB-237-155).

Gier, J.T. and Dunkle, R.V., 1954, Spectral reflectivity of certain minerals and similar inorganic materials: Unpublished Paper.

*Gilbertson, B. and Longshaw, T.G., 1975, Multispectral aerial photography as an exploration tool - Part I - Concepts, techniques, and instrumentation: Remote Sensing of the Environment, v. 4, p. 129-146.

*Gillerman, E., 1970, Rosselle lineament of Southern Missouri: Geol. Soc. America bull., v. 81, p. 975-982.

*Goetz, A.F.H., 1975, Application of ERTS and EREP images to geological investigation of basin and range Colorado plateau boundary in Arizona: NASA Goddard Space Flight Center, Greenbelt, Maryland.

Grant, F.S. and West, G.F., 1975, <u>Interpretation theory in applied geophysics</u>: McGraw-Hill, New York.

Griffiths, D.H. and King, R.F., 1965, <u>Applied geophysics for engineers and geologists</u>: Pergamon Press, Oxford, England.

Gupta, R.R. et al., 1972, Seismic determination of geological discontinuities of rapid excavation: First North American Rapid Excavation and Tunneling Conf., Chicago, Illinois, Proc., v. 1, ch. 17.

*Hackman, Robert J., 1967a, The geologic evaluation of radar imagery in Southern Utah: U.S. Geol. Sur. Prof. Paper 575-D, p. D135-D142.

*Hackman, Robert J., 1967b, Time, shadows, terrain and photointerpretation: U.S. Geol. Sur. Prof. Paper 575-B, p. B155-B160.

Hansen, D.A. (ed.) et al., 1966, <u>Mining Geophysics</u>, v. 1, Case Histories: Soc. Exploration Geophysicists, 492 p.

*Hansen, D.A. (ed.) et al., 1967, <u>Mining Geophysics</u>, v. 2, Theory: Soc. Exploration Geophysicists, 708 p.

Harris, J.F., et al., 1960, Relation of deformational fractures in sedimentary rocks to regional and local structure: Am. Assoc. Petroleum Geologists bull., v. 44 p. 1853-1873.

*Hoekstra, P. and McNeill, D., 1973, Electromagnetic probing of permafrost: The North American Contribution to the Second International Conf. Nat. Acad. Sci., Washington, D.C.

*Hoekstra, P., Sellman, P.V., and Delaney, A., 1975, Ground and airborne resistivity surveys of permafrost near Fairbanks, Alaska: Geophysics, v. 40, p. 641-656.

Holl, Herbert B., 1967, Specular reflection and characteristics of reflected light: Optical Soc. America, v. 57, no. 5, p. 683-690.

*Hood, Peter, 1974, Mineral exploration: Trends and developments: Can. Mining J., v. 95, no. 2.

*Houston, Robert S., 1975, The analysis of ERTS imagery and application to the evaluation of Wyoming natural resources: NASA Goddard Space Flight Center, Greenbelt, Maryland. (Available through the National Technical Information Service, Springfield, Va. NTIS no. N75-26468.)

Hovis, W.A., Jr., 1966a, Infrared spectral reflectance of some common minerals: Applied Optics, v. 5, no. 2, p. 245-246.

_____., 1966b, Optimum wavelength intervals for surface temperature radiometry: Applied Optics, v. 5, no. 5, p. 815-818.

_____., 1966c, Infrared reflectance spectra of igneous rocks, tuffs, and red sandstone from 0.5-22μm: J. Optical Soc. of America v. 56, no. 5, p. 639-643.

*Hunt, Graham R., Salisbury, John W., Lenhoff, Charles J., 1974, Visible and near-infrared spectra of minerals and rocks: IX Basic and ultrabasic igneous rocks: Modern Geology, v. 5, p. 15-22.

*_____., 1973a, Visible and near-infrared spectra of minerals and rocks: VI Additional silicates. Modern Geology, v. 4, p. 85-106.

*_____., 1973b, Visible and near-infrared spectra of minerals and rocks: VII Acidic igneous rocks: Modern Geology, v. 4, p. 217-224.

*_____., 1973c, Visible and near-infrared spectra of minerals and rocks: VIII Intermediate igneous rocks: Modern Geology, v. 4, p. 237-244.

*_____., 1972, Visible and near-infrared spectra of minerals and rocks: V Halides, Phosphates, Arenites, Vanadates, Borates: Modern Geology, v. 3 p. 121-132.

*_____., 1971a, Visible and near-infrared spectra of minerals and rocks: III Oxides and Hydroxides: Modern Geology, v. 2, p. 195-205.

*_____., 1971b, Visible and near-infrared spectra of minerals and rocks: IV Sulphides and Sulphates: Modern Geology, v. 3, p. 1-14.

*Hunt, Graham R. and Salisbury, John W., 1970, Visible and near-infrared spectra of minerals and rocks: I Silicate Minerals: Modern Geology, v. 1, p. 283-300.

_____., 1971, Visible and near-infrared spectra of minerals and rocks: II Carbonates: Modern Geology, v. 2, p. 23-30.

Irwin, William H. et al., 1970, Tunnel site investigations and geologic factors affecting mechanical excavation methods: Highway Research Record No. 339, p. 34.

*Isaacs, K.N., 1967, Geophysical case history of the Rosebell - Bonnidoro group, Surinam, South America: in Soc. of Exploration Geophysics, Mining and Geophyics, v. I, Case Histories, p. 28-35.

*Johnson, Arvid, 1970, Physical processes in geology: Freeman-Cooper, San Francisco, California, 379 p.

Kaiser, P.K., 1971, Luminance and brightness: Applied Optics, v. 10, no. 12, p. 2768.

Katz, I. and Spetner, L.M., 1960, Polarization and depression-angle dependence of radar terrain return: Part B. Radio Propagation, J. Res. Natl. Bur. Standards, v. 64D, no. 5, p. 483.

*Keller, George V., 1971, Electrical studies of the crust and upper mantle: Am. Geophysical Union, Geophys. Monograph 14, p. 107-121.

*_____., 1963, Electrical properties in the deep crust: Proc. Inst. Electronics and Electrical Engineers, v. AP-11, no. 3, p. 344-357.

Keller, George V., et al., 1970, Evaluation of airborne electromagnetic surveying for mapping variations in rock strength: A.F. Cold Regions Lab.-70-0701, 66 p. (NTIS no. AD-718-438).

Kiefer, Ralph W., 1972, Sequential aerial photography and imagery for soil studies: Highway Research Record no. 421, p. 85.

*Kowalik, W.S., and Gold, 1975, Application of satellite photographic and MSS data to selected geologic and natural resource problems in Pennsylvania: Proc. NASA Earth Resources Sur. Symp., Houston, Texas, v. IB., p. 933-950.

Leeman, V., 1972, The NASA earth resources spectral information system: A data compilation: First supplement (NTIS no. N72-30345), Willow Run Laboratories Inst. Science and Technology, Univ. of Michigan, Ann Arbor.

Leeman, V. et al., 1971, NASA earth resources spectral information system: A data compilation: Report no. 31650-24-T, Willow Run Laboratories Inst. Science and Technology, Univ. of Michigan, Ann Arbor.

Levi. Leo, 1974, Blackbody temperature for threshold visibility: Applied Optics, v. 13, no. 2, p. 221.

*Levin, S.B., 1971, Radio propagation through the crust: Retrospect and prospect: Am. Geophysical Union Geophys. Monograph 14, p. 333-336.

*_____., 1966, Lithospheric radio propagation. Advisory Gp. Aerospace Res. and Development Conf. Proc., no. 20, Subsurface Communications, p. 149-178.

*_____., et al., 1968, A model for electromagnetic propagation in the lithosphere: Proc. Inst. Electronics and Electrical Engineers, v. 56, no. 5, p. 779-804.

Liggott, 1974, A reconnaissance space sensing investigation of crustal structure for a strip from the eastern Sierra Nevada to the Colorado plateau: NASA Goddard Space Flight Center, Greenbelt, Maryland. (Available through the National Technical Information Service, Springfield, Va.)

Longshaw, T.G. and Gilbertson, B., 1975, Multispectral aerial photography as an exploration tool - II: An application in the Bushveld igneous complex, South Africa: Remote Sensing of the Environment, v. 4, p. 147-163.

Lowe, D.S. and Wilson, C.L., 1972, Multispectral scanning systems: Their features and limitations: Highway Research Record no. 421, p. 22.

Lowman, P.D., Jr., 1969, Apollo 9, multispectral photography: Geologic analysis: Report no. X-664-69-423 NASA Goddard Space Flight Center, Greenbelt, Maryland, 53 p.

_____., 1968, Geological orbital photography: Experience from the Gemini program: Report no. E-444-68-228 Goddard Space Flight Center, Greenbelt, Maryland, 34 p.

_____., 1965, Space photography - A review: Photogrammetric Engineering, v. 31, p. 76-86.

*Lyon, R.J.P., 1972, Infrared spectral emittance in geological mapping: Airborne spectrometer data from Pisgah Crater, California: Science, v. 175, no. 4025, p. 983-986.

*_____., 1971, Comparison of airborne infrared spectral emittance and radar and scatterometer data from Pisgah Crater lava flows: Proc. Seventh International Symp. Remote Sensing of the Environment, Univ. of Michigan, Ann Arbor.

*_____., 1970, The multiband approach to geological mapping from orbiting satellites. Is it redundant or vital?: Remote Sensing of Environment, v. 1, p. 237-244.

*_____., et al., 1970, Pseudo-Radar: Photogrammetric Engineering, v. 36, p. 1257.

_____., 1968, Field analysis of terrain. Final report: NASA-CR-100368 (NTIS no. N69-20189), 128 p.

*_____., 1964, Evaluation of infrared spectrophotometry for compositional analysis of lunar and planetary soils: Rough and powdered surfaces: Final report, Pt. 2, NASA Contract NAS-49(04), Stanford Research Inst., Menlo Park, California.

*MacDonald, Harold C. and Grubbs, Robert S., 1975, LANDSAT imagery analysis an aid for predicting landslide prone areas for highway construction: NASA Earth Resources Sur. Symp., Houston, Texas, Proc., v. 1B, p. 769-778.

*MacDonald, Harold C., 1969, Geologic evaluation of radar imagery from Eastern Panama and Northwestern Columbia: Modern Geology, v. 1, p. 1-63.

* _____., et al., 1969, The influence of radar look direction and the detection of selected geological features: Proc. Sixth Symp. Remote Sensing of the Environment, Univ. of Michigan, Ann Arbor, p. 637-650.

* _____., et al., 1967, Geologic evaluation of radar of NASA sedimentary test site: Inst. Electronics and Electrical Engineers, Transcripts Geoscience Electronics, GE-5, p. 72-78.

Marine Coastal Studies, Center for, 1974, Proceedings of a Conference on Coastal Management held in Beaufort, N.C., May 16-17, 1974. Report no. 746., NOAA 75011602. 189 p. (NTIS no. COM-75-10191).

*Marrs, R.W., 1973, Application of remote sensing techniques to the geology of the Bonanza Volcanic Center: Bonanza Remote Sensing Project Report 73-1, Colo. Sch. of Mines, 281 p.

Matich, M.A.J. and Brownridge, F.C., 1964, Soils investigation for the Rainy Lake causeway: Highway Research Record no. 57, p. 1.

Maxwell, E.L. and Morgan R.R., 1966, A 10-khz effective conductivity map of North America: Advisory Gp. Aerospace Res. and Development Conf., Proc. no. 20, Subsurface Communications, p. 239-264.

*McCoy, R.M. 1969, Drainage network analysis with X-Band radar imagery: Geographic Review, v. 59, p. 493-512.

McLellan, A.G. and Bryand, C.R., 1975, The methodology of inventory: A practical technique for assessing provincial aggregate resources: Can. Inst. Mining, bull., v. 68, no. 762, p. 102-108.

McMurtry, George J., 1975, Interdisciplinary applications and interpretations of ERTS data within the Susquehanna River basin: Preliminary Report, NASA Goddard Space Flight Center, Greenbelt, Maryland. (Available through the National Technical Information Service, Springfield, Va.)

*Meier, M.F. et al., 1966, Multispectral sensing tests at South Cascade Glacier, Washington. Proc., Fourth Symp. Remote Sensing of the Environment, Univ. of Michigan, Ann Arbor, p. 145-159.

Merritt, Andrew, 1972, Geologic predictions for underground excavations: First North America Rapid Excavation and Tunneling Conf., Chicago, Illinois, Proc., v. 1, ch. 11.

*Meyers, L.D. and Stallard, A.H., 1975, Soil identification by remote sensing techniques in Kansas, Part II: State Highway Commission of Kansas in cooperation with Federal Highway Administration.

*Miller, John B., 1975, LANDSAT image studies as applied to petroleum exploration in Kenya: NASA Earth Resources Survey Symposium, Houston, Texas, Proc., v. 1B, p. 605-624.

*Mintzer, O.W., 1968, Soils, Section 10.22, Manual of color aerial photography: Am. Soc. of Photogrammetry, p. 425-430.

Moffatt, David L. and Peters, Leon Jr., 1972, An electromagnetic pulse hazard detector system: First North American Rapid Excavation and Tunneling Conf., Chicago, Illinois, Proc., v. 1, ch. 18.

*Mollard, J.D., 1968, Landform analysis, Section 10.13. Manual of color aerial photography: Am. Soc. of Photogrammetry, p. 406-407.

*_____., 1957, Supplementary lecture notes on air photo-interpretation, Harvard University. (unpublished)

Moore, Richard K. and Simonett, David S., 1967, Radar remote sensing in biology: BioScience, p. 384.

*Moore, Richard K. and Dellwig, L.F., 1966, Terrain discrimination by radar image polarization comparison: Inst. Electronics and Electrical Engineers Proc., v. 54, no. 9, p. 1213-1214.

Mossman, R.W. and Heim, George E., 1972, Seismic exploration applied to underground excavation problems: North American Rapid Excavation and Tunneling Conf., Chicago, Illinois, Proc., v. 1, ch. 14.

Muray, J.J. et al., 1971, Proposed supplement to the SL nomenclature for radiometry and photometry: Applied Optics, v. 10, no. 6, p. 1465.

Murphy, Vincent J., 1972, Seismic velocity measurements for moduli determinations in tunnels: First North American Rapid Excavation and Tunneling Conf., Chicago, Illinois, Proc., v. 1, ch. 16.

*Myers, D.I. and Allen, W.A., 1968, Electro-optical remote sensing methods as non-destructive testing and measuring techniques in agriculture: Applied Optics, v. 7, no. 9, p. 1819-1838.

Nevins, J.L., 1973, Research workshop on sensors for automation: Lexington, Mass., Proc., NSF GK 37898, 154 p. (NTIS no. PB-231-180).

Noble, D.F., 1972, Utilization of remote sensing in the preliminary aerial survey: Highway planning stage in Virginia. Highway Research Record no. 421, p. 41.

Obukhov, A.I. and Orlov, D.S., 1964, Spectral reflectivity of the major soil groups and of using diffuse reflection in soil investigations: Lomonosov State Univ., Moscow, USSR.

Offield, T.W., 1975, Thermal infrared images as a basis for structure mapping, front range and adjacent plains in Colorado: Geol. Soc. America bull., v. 86, 7 figs., p. 495-502.

*Offield, T.W. et al., 1970, Linear geologic structure and mafic rock discrimination as determined from infrared data: NASA earth resources program review, Houston, Texas, Proc., v. 3, 18 p.

Orlov, D.S. et al., 1966, Analysis of the distribution of iron oxide compounds and humus in the soil profile from spectral brightness curves: Translated from Nauchnyye Doklady Vysshey Shkoly, Biologicheskiye Nauki, no. 1:217-222, p. 1482.

Orlov, D.S., 1966, Quantitative patterns of light reflection by soils influence on particle (aggregate) size: Translated from Nauchnyye Doklady Vysshey Shkoly, Biologicheskiye Nauki, no. 4:206-210.

Overbey, W.K., Jr. et al., 1973, Predicting probable roof fall areas in advance of mining by geological analysis: U.S. Bur. Mines, TPR 70. 21 p. (NTIS no. PB-221-626).

*Paarma, H. and Talvitie, J., 1968, On high altitude false color interpretation in prospecting: Manual of Color Aerial Photography. Am. Soc. of Photogrammetry, p. 431-438.

Palacky, G.J. and Jagodits, F.L., 1975, Computer data processing and quantitative intepretation of airborne resistivity surveys: Geophysics, v. 40, p. 818-830.

*Parker, Dana C., 1968, Developments in remote sensing applicable to airborne engineering surveys of soils and rocks: Materials Research and Standards, v. 8, no. 2, p. 22-30.

*Parkhomenko, E.I., 1967, Electrical properties of rocks: Plenum Press, New York, 308 p.

*Parkhomenko, E.I. and Bondarenko, A.T., 1960, Effect of uniaxial pressure of electric resistivity of rocks: bull. (Izv.) Acad. Sci. USSR, Geolphys. Ser., no. 2, 326 p.

*Parry, et al., 1969, Soils study using color photos: Photogrammetric Engineering, v. 35, p. 34-57.

*Pestrong, R., 1969, Multiband photos for a tidal marsh. Photogram-
     metric Engineering, v. 35, p. 453-470.

*Piech, K.R., 1972, Photometric mensuration of site soil character-
     istics: 38th Ann. Meeting of the Am. Soc. Photogrammetry, p. 95.

*Piech, K.R. and Walker, J.E., 1972a, Outfall inventory using airphoto
     interpretation: Photogrammetric Engineering, v. 38, p. 907.

*_____., 1972b, Thematic mapping of flooded
     acreage: Photogrammetric Engineering, v. 38, no. 11, p. 1081.

*_____., 1971a, Aerial color analysis of water
     quality: J. Surveying and Mapping Div., Natl. Soc. Civil Engineers.

*_____., 1971b, Photographic analysis of water
     resource color and quality: Proc. 37th Ann. Meeting of the Am.
     Soc. Photogrammetry.

*Pirsson, Lewis V., 1915, Physical Geology: John Wiley, New York, 404
     p.

*Podwysocki, M.H., 1975, Quantification of geologic lineaments by manual
     and machine processing techniques: NASA Earth Resources Survey
     Symp., Proc., v. 1B, p. 885-903.

*Pohn, H.A. et al., 1972, Geologic material discrimination from Nimbus
     satellite data. NASA Fourth Annual Earth Resource Program Review,
     Houston, Texas, Proc., v. 3, p. 15.

Pohn, H.A. et al., 1970, Linear geologic structure and mafic rock dis-
     crimination as determined from infrared data. NASA Third Annual
     Earth Resources Program Review, Houston, Texas, Proc., v. 3, 18 p.

Poole, D.H., 1971, The development of criteria for recognizing and
     identifying slope failure forms as depicted by remote sensor re-
     turns: East Tenn. State Univ., Johnson City, Tenn. (NTIS no. AD-
     750-732).

*Raines, G.L. and Lee, K., 1975, In-situ rock reflectance: Photogram-
     metric Engineering and Remote Sensing, v. 41, no. 2, p. 189-198.

Raines, G.L., 1974a, Evaluation of multiband photography for rock dis-
     crimination. Colo. Sch. Mines (NASA-CR-138226) 119 p. (NTIS no.
     N74-23047).

_____, 1974b, Rock discrimination by multiband photography:
     Colo. Sch. Mines. (NTIS no. AD-782-190)

*Reed, J.C., 1940, The use of airplane photographs in the geologic study of the Chicago mining district - Alaska: Photogrammetric Engineering, v. 6, p. 35-44.

Reeds, R.G., 1969, Structural geological interpretation from radar imagery: Geol. Soc. America bull., v. 80, p. 2159-2164.

*Reeves, R.G., 1969, Structural geological interpretations from radar imagery: Geol. Soc. America bull., v. 80, p. 2159-2164.

Resources Technology Corp., 1972, Detection and definition of subsurface void spaces by ground-based microwave radiometers: Report No. FHWA-RD-73-52, prepared for Federal Highway Administration, Washington, D.C.

Rib, Harold T., 1972, Partnership in research: A cooperative remote sensing research program: Highway Research Record no. 421, p. 33.

*Rib, Harold T. and Miles, R.D., 1969, Multi-sensor analysis for soils mapping: Highway Research Board Special report 102, p. 22-37.

Robinove, C.J. and Skibitzke, H.E., 1967, An airborne multispectral television system: U.S. Geol. Sur. Prof. Paper 575-D, p. D143-D146.

Robinson, Charles, S., 1972, Prediction of geology for tunnel design and construction: First North American Rapid Excavation and Tunneling Conf. Chicago, Illinois, Proc., v. 1, ch. 10.

Robinson, Charles S. and Lee, F.T., 1964, Geologic research at the Straight Creek tunnel site, Colorado: Highway Research Record no. 57, p. 18.

Robinson, Charles S. and Lee, F.T., 1967, Results of geologic research at the Straight Creek tunnel pilot bore, Colorado: Highway Research Record no. 185, p. 9.

Ross, Howard P. et al., 1969, A statistical analysis of the reflectance of igneous rocks from 0.2-2.65 microns: ICARUS 11, p. 46-54.

Rowan, L.C., 1972, Near-infrared iron absorption bands: Applicatons to geologic mapping and mineral exploration: NASA Fourth Ann. Earth Resources Program Review, Houston, Texas, Proc., v. 3, p. 18.

Rowan, L.C. and Watson, K., 1970, Multispectral analysis of limestone, dolomite, and granite, Mill Creek, Oklahoma. NASA Third Annual Earth Resources Program Review, Houston, Texas.

Rowan, L.C. and Cannon, P.J., 1970, Remote sensing investigations near Mill Creek, Oklahoma: Reprinted from Oklahoma Geology Notes, v. 30, no. 6, p. 127.

*Smellie, D.W., 1956, Elementary approximation in aeromagnetic inter-
    pretation: Geophysics, v. 21, p. 1021-1040.

*Smith, Fred J. Jr., and Ketner, Keith B., 1975, Stratigraphy of Pleis-
    tocene rocks in the Carlin Pinon Range area, Nevada. U.S. Geol.
    Sur. Prof. Paper 867-A.

*Smith, James D., 1968, Geology, its relation to the design of the River
    Mountain Tunnels: Proc., 19th Annual Highway Geol. Symp., W. Va.
    Geol. and Econ. Surv. Circulation Series, no. 10.

*Smith, P., Piech, K.R., and Walker, J.E., 1974, Special color analysis
    techniques: Photogrammetric Engineering, v. 40, no. 11, p. 1315-
    1322.

Smith, Traves W., 1964, Ground water control for highways: Highway
    Research Record no. 57, p. 35.

*Smithsonian Meteorological Tables 6th revised edition. Smithsonian
    Miscellaneous Collections, v. 114, p. 495-505.

Stallard, Alvis H., 1972, Use of remote sensors in highway engineering
    in Kansas: Highway Research Record no. 421, p. 50.

Stingelin, Ronald W., 1972, Airborne infrared imagery and its limi-
    tations in civil engineering practice: Highway Research Record no.
    421, p. 14.

*Stinni, J., 1950, Tunnelbaugeologie: Springer, Vienna.

Stoeckeler, E.G. et al., 1975, Multidisciplinary analysis of Skylab
    photography for highway engineering purposes: (NASA-CR-141942)
    Maine Dept. of Transportation, Augusta. 125 p.

*Strangeway, D.W., 1966, Rock magnetism in geologic correlation: Mining
    Geophysics, Society of Exploration Geophysics, v. 1, p. 54-66.

Suits, Gwynn H., 1972, The calculation of the directional reflectance of
    a vegetative canopy: Remote Sensing of Environment, v. 2, p. 117-
    125.

*Szechy, K., 1970, The Art of Tunneling: Akademiai Kiado, Budapest,
    885 p.

*Tarkington, R.G. and Sorem, L.A., 1963, Color and false color films for
    aerial photography: Photogrammetric Engineering, v. 29, p. 88-95.

*Tator, B.A., 1949, Valley widening processes in the Colorado Rockies:
    Geol. Soc. America bull., v. 60, p. 1771-1783.

Tipper, D.B., et al., 1971, Laverton-Edjudina airborne magnetic and
    radiometric survey, Western Australia 1969. Bur. Mineral Resources,

Geology and Geophysics (Australia), bull. 118, 112 p. (NTIS no. N72-28365).

Trytten, Grover and Flowers, Wayne, 1966, Optical characteristics of a proposed reflectance standard: Applied Optics, v. 5, no. 12, p. 1895.

*Vedder, J.G. et al., 1957, Oil and gas investigations: U.S. Geol. Survey, Map OM 193.

*Viksne, A. et al., 1970, SLR reconnaissance of Panama: Photogrammetric Engineering, v. 36, p. 253.

Vincent, R.K., 1974, Mapping exposed silicate rock types and exposed ferric and ferous compounds from a space platform: Quart. report 8 Sept. - 8 Dec., 1973. Environmental Res. Inst. Michigan, 5 April 1974, 2 p. (NTIS no. N74-19953)

*_____ et al., 1973, Geologic reconnaissance and lithologic identification by remote sensing: Final report no. AD-771-278, prepared for Advance Research Projects Agency, U.S. Bur. of Mines.

*_____., 1973a, The NASA Earth Resources Spectral Information System: A data compilation, second supplement. (NASA-CR-134267) Environmental Res. Inst. Michigan, 140 p. (NTIS no. N74-22051).

_____., 1973b, A thermal infrared ratio imaging method from mapping compositional variations among silica rock types: Un-published Ph.D. dissertation, Univ. Michigan.

*_____., 1972, An ERTS multispectral scanner experiment for mapping iron compounds. (abs) Eighth International Symp. Remote Sensing of the Environment, Univ. Michigan, Ann Arbor, p. 123.

Vincent, R.K. and Thomson, F.J., 1972a, Rock type discrimination from ratioed infrared scanner images of Pisgah Crater, California: Science, v. 175, p. 186-188.

_____, 1972b, Spectral compositional imaging of silicate rocks: J. Geophys. Res., v. 77, p. 2473-2477.

_____, 1971, Discrimination of basic silicate rocks by recog-nition maps processed from aerial infrared data: Seventh Inter-national Symp. Remote Sensing of the Environment, Univ. of Michigan, Ann Arbor.

*Wagner, T.W., 1972, Multispectral remote sensing of soil areas: A Kansas study: Highway Research Record no. 421, p. 71.

*Wagner, T. et al., 1972, Tunnel site selection by remote sensing techniques: Univ. Michigan Inst. Science and Technology. (NTIS no. AD-748-663).

*Wallace, R.E. and Moxham, R.M., 1967, Use of infrared imagery in study of the San Andreas fault system, California: U.S. Geol. Sur. Prof. Paper 575-D, p. D147-D156.

*Ward, S.H., and Fraser, D.C., 1966, A conducting permeable sphere and cylinder in an elliptically polarized alternating magnetic field: J. Geomag. and Geoelectricity, v. 18, p. 23-40.

Watson, R.D. and Rowan, L.C., 1971, Automated geologic mapping using rock reflectances: Seventh International Symp. Remote Sensing of the Environment, Univ. of Michigan, Ann Arbor. Proc., v. III, p. 2043-2052.

Watson, R.D., 1971, Spectral and bidirectional reflectance of pressed vs. unpressed Fiberflax: Applied Optics, v. 10, no. 7, p. 1685-1686.

*Watson, R.D., 1972, Spectral reflectance and photometric properties of selected rocks: Remote Sensing of Environment, v. 2, p. 95-100.

West, Terry W., 1972, Engineering soil mapping from multispectral imagery using automatic classification techniques: Highway Research Record no. 421, p. 58.

Wickham, G.E. and Tiedemann, H.R., 1974, Ground support prediction model: U.S. Bur. Mines (H022 0075) (NTIS no. AD-773-018).

Wilson, John C., 1975, A proposal to participate in ERTS-A flight investigations: NASA Goddard Space Flight Center, Greenbelt, Maryland. (Available through the National Technical Information Service, Springfield, Va.)

*Wing, R.S., 1970a, Structural analysis from radar imagery, eastern Panamanian isthmus: U.S. Army Topographic Command Corp of Engineers. Engineer Topographic Lab, Fort Belvoir, Tech. Report no. 133-15, CRES, The Univ. Kansas, Lawrence. 156 p.

*Wing, R.S., 1970b, Bholame Area - San Andreas fault zone, California: A study in SLAR: Modern Geology, v. 1, no. 3, p. 173-186.

Wing, R.S., 1971, Structural analysis from radar imagery of the eastern Panamanian isthmus, Part 1: Modern Geology, v. 2, p. 1-21; Part 2, p. 75-127.

*Wise, D.U., 1969, Pseudo radar topographic shadowing for detection of subcontinental sized fractured systems: Proc. Sixth International Sym. Remote Sensing of the Environment, Univ. Michigan, p. 603-615.

*Wobber, F.J., et al., 1973, Exploitation of ERTS-1 imaging utilizing snow enhancement techniques: Proc. Symp. on Significant Results from the Earth Resources Tech. Satellite, NASA Goddard Space Flight Center, Greenbelt, Maryland, March 1973.

*Wolf, P.R., 1974, Elements of Photogrammetry. McGraw-Hill, New York.

Woodruff, K.D. et al., 1974, Selection of sites for high yielding wells in the Delaware piedmont: (abs) N.E. Section, Geol. Soc. America, Baltimore, Md.

*Yost, E.F. and Wenderoth, Sondra, 1968, Precision multispectral photography for earth resources applicatons, Long Island University. Science Engineering Research Group, Brookville, New York, 153 p.

*Yost, E.F. and Wenderoth, Sondra, 1972, Multispectral Photography for Earth Resources. West Hills Printing Co., Huntington, New York, 289 p.

*Zablocki, C.J., 1962, Electrical and magnetic properties of a replacement type magnetic deposit in San Bernardino County, California: U.S. Geol. Sur. Prof. Paper 450-D, p. 150.

GLOSSARY

The following definition of terms are drawn largely from the Manual of Remote Sensing (Am. Soc. Photogrammetry, 1975), Glossary of Geology (Am. Geological Institute, 1972), and Remote Sensing Techniques for Environmental Analysis (Estes and Senger, 1974).

absorbed light: Light rays that are neither reflected nor transmitted when directed toward opaque or transparent materials.

absorption: (1) The process by which radiant energy is absorbed and converted into other forms of energy. Absorption takes place only after the radiant flux enters a medium and thus acts only on the entering flux and not on the incident flux, some of which may be reflected at the surface of the medium. A substance which absorbs energy may also be a medium of refraction, diffraction, or scattering; these processes, however, involve no energy retention or transformation, and are to be clearly differentiated from absorption. (2) In general, the taking up or assimilation of one substance by another. See adsorption.

absorption band: A range of wavelengths (or frequencies) in the electromagnetic spectrum within which radiant energy is absorbed by a substance. See absorption spectrum.

absorption line: A minute range of wavelengths (or frequencies) in the electromagnetic spectrum within which radiant energy is absorbed by the medium through which it is passing. Each line is associated with a particular mode of electronic excitation induced in the absorbing atoms by the incident radiation. See absorption spectrum, Fraunhofer lines, absorption band.

absorption spectrum: The array of absorption lines and absorption bands which results from the passage of radiant energy from a continuous source through a selectively absorbing medium cooler than the source. See electromagnetic spectrum. The absorption spectrum is a characteristic of the absorbing medium, just as an emission spectrum is a characteristic of a radiator. An absorption spectrum formed by a monatomic gas exhibits discrete dark lines, whereas that formed by a polyatomic gas exhibits ordered arrays (bands) of dark lines, which appear to overlap. This type of absorption is often referred to as line absorption. The spectrum formed by a selectively absorbing liquid or solid is typically continuous in nature (continuous absorption).

active microwave: Ordinarily referred to as radar, which see.

active systems: (1) A system having its own source of EMR as for ex-
     ample a radar or an ultraviolet blacklight.   (2) A system that
     measures EMR that is reflected from a surface or object, and not
     produced (emitted) by the surface or object.   Compare passive
     systems.

adit: A horizontal or nearly horizontal passage driven from the surface
     for the working or unwatering of a mine.   If driven through the
     hill or mountain to the surface on the opposite side it would be a
     tunnel.

additive color process: A method for creating essentially all colors
     through the addition of light of the 3 additive color primaries
     (blue, green, and red) in various proportions through the use of 3
     separate projectors.   In this type of process each primary filter
     absorbs the other 2 primary colors and transmits only about one-
     third of the luminous energy of the source.   It also precludes the
     possibility of mixing colors with a single light source because the
     addition of a second primary color results in total absorption of
     the only light transmitted by the first color.

adsorption: adherence of gas molecules or of ions or molecules in
     solutions to the surfaces of solids with which they are in contact.
     Adsorbed water in soil is held so strongly that it is resistant to
     the pull of gravity and to capillary action.

aerial photograph, vertical: An aerial photograph made with the optical
     axis of the camera approximately perpendicular to the Earth's
     surface and with the film as nearly horizontal as is practicable.

aerial photographs, overlapping: Two or more aerial photographs to
     which a portion of the total area projected thereon is common.
     Such photographs are used for stereoscopic studies and for making
     mosaics.   Overlap may be end or forward (along the flight path) or
     side (taken during two or more parallel flights); both end and side
     overlap are customary when more than one line or strip is flown.

albdeo: (1) The ratio of the amount of EMR reflected by a body to the
     amount incident upon it, often expressed as a percentage, as, the
     albedo of the Earth is 34 percent.   (2) The reflectivity of a body
     as compared to that of a perfectly diffusing surface at the same
     distance from the Sun, and normal to the incident radiation (see
     band, albedo, reflectance).   Albedo is sometimes used to mean the
     flux of the reflected radiation as, the Earth's albedo is 0.64
     calorie per square centimeter.   This usage should be discouraged.
     Albedo may refer to the entire solar spectrum or merely to the
     visible portion.

alluvium: A general term for unconsolidated detrital material deposited during recent geologic time by a stream as a sorted or semi-sorted sediment.

angle of sun: The angle of the sun above the horizon. Not only the quantity (lunes) of light being reflected to the aerial camera but also the spectral quality, are influenced by sun-angle. Also called sun elevation, sun elevation angle.

angstrom (A or Å): Unit of measurement, 10^{-10} m.

annotated photograph: A photograph on which planimetric, hypsographic, geologic, cultural, hydrographic, or vegetation information has been added to identify, classify, outline, clarify, or describe features that would not otherwise be apparent in examination of an unmarked photograph.

antenna, synthetic aperature (radar): The effective antenna produced by storing and comparing the doppler signals received while the aircraft travels along its flight path. This synthetic antenna (or array) is many times longer than the physical antenna, thus sharpening the effective beam width and improving azimuth resolution.

anticline: A fold, the core of which contains the stratigraphically older rocks: it is convex upward. Ant: syncline.

azimuth: The direction of a line given as an angle measured clockwise from a reference direction, usually north. (2, radar): Direction at right angles to the antenna beam. In side-looking radar, the direction parallel to ground track.

band: See spectral band

band-pass filter: (2) A wave filter that has a single transmission band extending from a lower cutoff frequency greater than zero to a finite upper cutoff frequency.

bandwidth: (1) In an antenna, the range of frequencies within which its performance, in respect to some characteristic, conforms to a specified standard. (2) In a wave, the least frequency interval outside of which the power spectrum of a time-varying quantity is everywhere less than some specified fraction of its value at a reference frequency. (3) The number of cycles per second between the limits of a frequency band. Sense 2 permits the spectrum to be less than the specified fraction within the interval. Unless otherwise stated, the reference frequency is that at which the spectrum has its maximum value.

basin range: (1) A relatively long and narrow mountain range that owes its present elevation and structural form mainly faulting and tilting of strata and that is isolated by alluvium-filled basins or

valleys. (2) A tilted fault block--Etymol: from the Great Basin, a region in SW U.S. characterized by fault-block mountains.

bearing: Direction of a line measured as an acute angle from a reference meridian. Compare with azimuth.

blackbody, black body: An ideal emitter which radiates energy at the maximum possible rate per unit area at each wave-length for any given temperature. A blackbody also absorbs all the radiant evergy incident upon it. No actual substance behaves as a true blackbody although platinum black and other soots rather closely approximate this ideal. In accordance with Kirchhoff's law, a blackbody not only absorbs all wavelengths, but emits at all wavelengths and does so with maximum possible intensity for any given temperature.

black-body radiation: The electromagnetic radiation emitted by an ideal black body; it is the theoretical maximum amount of radiant energy of all wavelengths which can be emitted by a body at a given temperature. The spectral distribution of black-body radiation is described by Planck's law and related radiation laws. If a very tiny opening is made into an otherwise completely enclosed space (hohlraum), the radiation passing out through this hole when the walls of the enclosure have come to thermal equilibrium at some temperature will closely approximate ideal black-body radiation for that temperature.

brute force: A sidelooking radar system that transmits and receives from a long physical antenna to narrow the beamwidth and increase azimuth resolution; the received returned EMR is used directly to produce an image. Compare synthetic aperature.

camera, metric: A specially constructed and calibrated camera used to obtain geometrically accurate photographs for use in photogrammetric instruments.

camera, multiband: A camera that exposes different areas of one film, or more than one film, through one lens and a beam splitter, or two or more lenses equipped with different filters, to provide two or more photographs in different spectral bands.

case hardening: The process by which the surface of a porous rock (esp. tuff and certain sandstones) is coated with a cement or desert varnish formed by evaporation of mineral-bearing solutions. Adj: case-hardened. Also spelled: casehardening.

colluvium: (1) A general term applied to any loose, heterogeneous, and incoherent mass of soil material or rock fragments deposited chiefly by mass-wasting, usually at the base of a steep slope or cliff; e.g. talus, cliff debris, and avalanche material. (2) Alluvium deposited by unconcentrated surface run-off or sheet erosion, usually at the base of a slope.

color balance: The proper intensities of colors in a color print, positive transparency, or negative, that give a correct reproduction of the gray scale (as faithful as can be achieved by photographic representation of the true colors of a scene).

color composite (multiband photography): A color picture produced by assigning a color to a particular spectral band. In LANDSAT, ordinarily blue is assigned to band 1 or 4 (∿500 to 600 nm), green to band 2 or 5 (∿600 to 700 nm), and red to band 3 (∿700 nm to 1 μm) or 7 (∿800 nm to 1.1 μm), to form a picture closely approximating a color-infrared photograph.

contact: A plane or irregular surface between two different types or ages or rocks.

contact print: A print made from a negative or a diapositive in direct contact with sensitized material.

coverage, stereoscopic: Aerial photographs taken with sufficient overlap to permit complete stereoscopic examination.

cut-off filter: A filter, shaped to remove unwanted radiation, either above (low-pass) or below (high-pass) a desired band of radiation.

densitometer: An instrument for the measurement of optical density (density of the silver deposit) (photographic transmission, photographic reflection, visual transmission, etc.) of a material, generally of a photographic image. There are many varieties, but all are alike in providing means for reducing the intensity of a standard light constantly until it matches an identical beam of light which has passed through the material being measured. See also microdensitometer.

depression angle: (1, general) any angle measured from the horizontal to an object below the observer. (2, radar) The angle formed by the horizontal plane and the line of the radar beam to a ground feature.

desert varnish: A thin, dark, hard, shiny or glazed iridescent (red, brown, black) film, coating, stain, or polish composed of iron oxide accompanied by traces of manganese oxide and silica, formed in desert regions after long exposure upon the surfaces of pebbles, boulders, and other rock fragments, as well as upon the cracked walls of ledges and other rock out-crops; it is believed to be caused by exudation of mineralized solutions from within and deposition by evaporation on the surface. A similar appearance produced by wind abrasion is properly known as desert polish. Syn: desert patina; desert lacquer; desert crust; desert rind.

diapositive: A positive image on a transparent medium such as glass or film; a transparency. The term originally was used primarily for a transparent positive on a glass plate used in a plotting instrument, a projector, or a comparatory, but now is frequently used for any positive transparency.

dike: A tabular igneous intrusion that cuts across the planar structures of the surrounding rock.

dip: The angle at which a stratum or any planar feature is inclined from the horizontal.

disconformity: An unconformity in which the bedding planes above and below the break are essentially parallel, indicating a significant interruption in the orderly sequence of sedimentary rocks, generally by a considerable interval of erosion (or sometimes of non-depostion), and usually marked by a visible and irregular or uneven erosion surface of appreciable relief; e.g. an unconformity in which the older rocks remained essentially horizontal during erosion or during simple vertical rising and sinking of the crust (without tilting or faulting). The tendency is to apply the term to breaks represented elsewhere by rock units of formation rank.

displacement: Any shift in the position of an image on a photograph which does not alter the perspective characteristics of the photograph (i.e. shift due to tilt of the photograph, scale change in the photograph, and relief of the objects photographed).

dissected: Cut by erosion into hills and valleys or into flat upland areas separated by valleys.

diurnal (thermal) wave: The daily temperature rise of the surface soils, under the heating of the sun, progresses downward as a heavily dampened wave which dies out about 30 cm below the surface. Below this point relatively constant daily temperatures may be experienced.

electromagnetic radiation (EMR): Energy propagated through space or through material media in the form of an advancing interaction between electric and magnetic fields. The term radiation, alone, is used commonly for this type of energy, although it actually has a broader meaning. Also called electromagnetic energy. See electromagnetic spectrum.

electromagnetic spectrum: The ordered array of known electromagnetic radiations extending from the shortest cosmic rays, through gamma rays, X-rays, ultraviolet radiation, visible radiation, infrared radiation, and including microwave and all other wavelengths of radio energy.

emission: (1) With respect to EMR, the process by which a body emits EMR usually as a consequence of its temperature only. Compare reflection, transmission. See emissitivity.

emission spectrum: The array of wavelengths and relative intensities of EMR emitted by a given radiator.

emissivity: A ratio relating the amount of energy given off by an object to the amount given off by a "black body" at the same temperature, and normally expressed as a real positive number between 0 and 1.

erosion: (1) The general process or the group of processes whereby the earthy and rocky materials of the Earth's crust are loosened, dissolved, or worn away, and simultaneously removed from one place to another by natural agencies that include weathering, solution, corrasion, and transportation, but usually exclude mass-wasting; specif. the mechanical destruction of the land and the removal of material (such as soil) by running water (including rainfall), waves and currents, moving ice or wind. The term is sometimes restricted by excluding transportation (in which case "denudation" is the more general term) or weathering (thus making erosion a dynamic or active process only). (2) An instance or product, or the combined effects, of erosion.

exposure: (1) The total quantity of light received per unit area on a sensitized plate or film; may be expressed as the product of the light intensity and the exposure time, in units of (for example) meter-candle-seconds or watts per square meter. (2) The act of exposing a light-sensitive material to a light source. (3 geol.) A continuous area in which a rock formation or geological structure is visible, either naturally or artificially, and is unobscured by soil, vegetation, water or the works of man.

fault: A fracture surface or zone in rock along which a measureable displacement has taken place.

filter: (1, noun) Any material which, by absorption or reflection, selectively modifies the radiation transmitted through an optical system. Such a filter may operate by polarization, scattering, etc., and may also be electronic. Also called wave filter. The filter usually is interposed between the film and the scene being photographed, but it may form part of the film itself. (2, verb) To remove a certain component or components of EMR, usually be means of a filter, although other devices may be used.

flatiron: One of a series of short, triangular-shaped hogbacks terminating a spur or ridge on the flank of a mountain, having a narrow apex at the top and a broad base below, resembling (when viewed from the side) a huge flatiron standing on its heel; it

usually consists of a plate of steeply inclined resistant rock adhering to the dip slope.

flight altitude: The vertical distance above a given datum, usually mean sea level, of an aircraft in flight or during a specified portion of a flight. In aerial photography, when the datum is mean ground level of the area being photographed, this distance is called flight height or sometimes obsolute altitude. (see also, above mean terrain, AMT)

flight strip: A succession of overlapping aerial photographs taken along a single course.

focal length, calibrated: An adjusted value of the equivalent focal length, computed to equalize the positive and negative values of distortion over the entire field used in the aerial camera. Also stated as the distance along the lens axis from the interior per-spective center to the image plane; the interior center of the perspective being selected so as to equalize the positive and negative values of lens distortion over the field. The calibrated focal length is used when determining the setting of diapositives in plotting instruments and in photogrammetric computations based on linear measurements on the negative, such as those made with a precision comparator.

fold: (struc. geol). A curve or bend of a planar structure such as rock strata, bedding planes, foliation, or cleavage. A fold is usually a product of deformation, although its definition is descriptive and not genetic and may include primary structures.

foliation: (struc. geol). A general term for a planar arrangement of textural or structural features in any type of rock, e.g., cleavage in slate or schistosity in a metamorphic rock. It is most commonly applied to metamorphic rock.

footwall: The underlying side of a fault. Cf: hanging wall.

fracture: A surface along which loss of cohesion has taken place. That is in geology, a general term for any break in a rock. A fracture along which no displacement has occurred is a joint, while one along which the rock has been displaced is a fault.

Fraunhofer line(s): Dark line(s) in the absorption spectrum of solar radiation due to absorption by gases in the outer portions of the Sun and in the Earth's atmosphere. Fraunhofer lines are designated by letters, as the K-line, or by wavelength, as the 4046-anstrom line of iron.

gneiss: A foliated rock formed by regional metamorphism in which bands or lenticles of granular minerals alternate with bands and lenticles

in which minerals having flaky or elongate prismatic habits pre-
dominate. Generally less than 50% of the minerals show preferred
parallel orientation. Although a gneiss is commonly feldspar- and
quartz-rich, the mineral composition is not an essential factor in
its definition (American usage). Varieties are distinguished by
texture (e.g. augen gneiss), characteristic minerals (e.g. horn-
blende gneiss), or general composition and/or origins (e.g. granite
gneiss).

gray body: A radiating surface whose radiation has essentially the same
spectral energy distribution as that of a blackbody at the same
temperature, but whose emissive power is less. Its absorptivity is
nonselective. Also spelled grey body.

gray scale: A monochrome strip of shades ranging from white to black
with intermediate shades of gray. The scale is placed in a setup
for a color photograph and serves as a means of balancing the
separation negatives and positive dye images.

Greenwich mean time (abbr GMT): Local mean time at the Greenwich meridi-
an; the arc of the celestial equator, or the angle at the celestial
pole, between the lower branch of the Greenwich celestial meridian
and the hour circle of the mean sun, measured westward from the
lower branch of the Greenwich celestial meridian through 24 hours;
Greenwich hour angle of the mean sun, expressed in time units, plus
12 hours. Also called universal time, Z-time. Mean time reckoned
from the upper branch of the Greenwich meridian is called Greenwich
astronomical time.

ground truth (jargon): Term coined for data/information obtained on
surface/subsurface features to aid in interpretation of remotely
sensed data. A vague, misleading term suggesting that the truth
may be found on the ground. Ground data and ground information are
preferred terms.

ground water: (a) That part of the subsurface water that is the zone of
saturation, including underground streams. See also phreatic
water. Syn: plerotic water. (b) Loosely, all subsurface water
(excluding internal water) as distinct from surface water--Also
spelled, groundwater, ground-water.

hanging wall: The overlying side of a fault. Dv: footwall.

Hertz (abbr. Hz): The unit of frequency, cycles per second.

hydrothermal alteration: Alteration of rocks or minerals by the reac-
tion of hydrothermal water with preexisting solid phases.

igneous: Said of a rock or mineral that solidified from molten or
partly molten material, i.e., from a magma; also, applied to pro-
cesses leading to, related to, or resulting from the formation of

227

such rocks. "Igneous" rocks consitute one of the three main classes into which all rocks are divided (i.e. igneous, metamorphic, sedimentary). Etymol: Latin ignis, "fire".

illumination: The intensity of light striking a unit surface is known as the specific illumination of luminous flux. It varies directly with the intensity of the light source and inversely as the square of the distance between the illuminated surface and the source. It is measured in a unit called the lux. The total illumination is obtained by multiplying the specific illuminiation by the area of the surface when the light strikes. The unit of total illumination is the lumen.

image: (1) The counterpart of an object produced by the reflection of refraction of light when focused by a lens or mirror.

image: (2) The recorded representation of an object produced by optical, electro optical, optical mechanical, or electronic means. It is generally used when the EMR emitted or reflected from a scene is not directly recorded on film.

image enhancement: The manipulation of image density to more easily see certain features of the image.

imagery: The products of image-forming instruments (analogous to photography).

infrared (abbr. IR): Pertaining to or designating the portion of the EM spectrum with wavelengths just beyond the red end of the visible spectrum, such as radiation emitted by a hot body (see infrared radiation).

infrared line scanner: See scanning radiometer.

infrared photographic: (1) Pertaining to or designating the portion of the EM spectrum with wavelengths just beyond the red end of the visible spectrum, such as radiation emitted by a hot body (over 500° C); generally defined as from 0.7 to about 1.0 mm, or the useful limits of film sensitivities.

infrared radiation: EMR in the wavelength interval from about .75 mm to 1 mm. Also called long wave radiation. At its lower limit, infrared radiation spectrum is bounded by visible radiation, and on its upper limit by microwave radiation.

intrusive body: (ign) the igneous rock mass formed by the emplacement of magma in pre-existing rock.

joint: A surface or actual or potential fracture or posting in a rock, without displacement; the surface is usually plane and often occurs with parallel joints for form part of a joint set.

K-band: A frequency band used in radar extending approximately from 10.9 gigahertz to 36 gigahertz.

large-scale: (1) Aerial photographs with a representative fraction of 1:500 to 1:10,000. (2) Maps with a representative fraction (scale) greater than 1:100,000.

lineament: (photo). Any line, on an aerial photograph, that is structurally controlled, including any alignment of separate photographic images such as stream beds, trees, or bushes that are so controlled. The term is widely applied to lines representing beds, lithologic horizons, mineral bandings, veins, faults, joints, unconformities, and rock boundaries (Allum, 1966, p.31).

lineament: (tect). Straight or gently curved, lengthy features of the Earth's surface, frequently expressed topographically as depressions or lines of depressions; these are prominent on relief models, high-altitude air photographs, and radar imagery. Their meaning has been much debated; some certainly express valid structural features, such as faults, aligned volcanoes, and zones of intense jointing with little displacement, but the meaning of others is obscure, and their origins may be diverse, or purely accidental. Syn: linear.

linear: Arranged in a line or lines, as a linear dike swarm. It is a one-dimensional arrangement, in contrast to the two-dimensional planar arrangement.

lithology: (1) The description of rocks, esp. sedimentary clastics and esp. in hand specimen and in outcrop, on the basis of such characteristics as color, structures, mineralogic composition, and grain size. As originally used, "lithology" was essentially synonymous with petrography as currently defined. (2) The physical character of a rock ---- Adj; lithologic.

medium scale: (1) Aerial photographs with a representative fraction of 1:12,000 to 1:30,000. (2) Maps with a representative fraction (scale) of 1:100,000 to 1:1,000,000.

metamorphic: Pertaining to the process of metamorphism or to its results. n. A metamorphic rock, usually used in the plural, e.g. "the metamorphics" of an area.

metasediments: (1) A sediment or sedimentary rock which shows evidence of having been subjected to metamorphism. (2) A metamorphic rock of sedimentary origin.

Microdensitometer: A special form of densitometer for reading densities in very small areas; used for studying astronomical images, spectroscopic records, and for measuring image edge gradients and graininess in films.

229

multiband system: A system for simultaneously observing the same (small) target with several filtered bands, through which data can be recorded. Usually applied to cameras, may be used for scanning radiometers which utilize dispersant optics to split wavelength bands apart for viewing be several filtered detectors. See spectra zonal.

multi-lens camera: (1) A camera having two or more lenses pointing at the same taret, which when used with different film/filter combinations, produces multiband photographs. (2) A camera having two or more lenses pointed at an angle to one another, and taking two or more overlapping pictures, simultaneously.

multispectral: Generally used for remote sensing in two or more spectral bands, such as visible and IR.

multispectral (line) scanner: A remote sensing device which operates on the same principle as the infrared scanner except that it is capable of recording data in the ultraviolet and visible portions of the spectrum as well as the infrared. See scanning radiometer.

nanosecond (abbr. nsec): A prefix meaning multiplied by 10^{-9} second. Formerly called millimicrosecond.

near infrared: The preferred term for the shorter wavelengths in the infrared region extending from about 0.7 micrometers (visible red), to around 2 or 3 micrometers (varying with the author). The longer wavelength end grades into the middle infrared. The term really emphasizes the radiation reflected from plant materials, which peaks around 0.85 micrometers. It is also called solar infrared, as it is only available for use during the daylight hours.

negative: (1) A photographic image on film, plate, or paper, in which the tones are reversed. (2) A film, plate, or paper containing such a reversed image.

nonconformity: (1) An unconformity developed between sedimentary rocks and older rocks (plutonic igneous or massive metamorphic rocks) that had been exposed to erosion before the overlying sediments covered them. The restriction of the term to this usage was proposed by Dunbar & Rodgers (1957, p. 119). Although the term is "well known in the classroom", it is "not commonly used in practice" (Dennis, 1967, p. 160). Syn. heterolithic unconformity. (2) A term that formerly was widely, but now less commonly, used as a syn. of angular unconformity, or as a generic term that includes angular unconformity--term proposed by Pirsson (1915, p. 291-293).

normal fault: A fault in which the hanging wall appears to have moved downward relative to the footwall. The angle of the fault is usually 45-90°. There is dip separation but there may or may not be dip slip. Cf: thrust fault. Syn: gravity fault: normal slip fault; slump fault.

panchromatic: Used for films that are sensitive to broad band (e.g.,
    entire visible part of spectrum) EMR, and for broad band photo-
    graphs.

passive system: A sensing system that detects or measures radiation
    emitted by the target. Compare active system.

photomap: A single photo, composite, or mosaic showing coordinates and
    marginal information: normally reproduced in quantity.

polarization: (1) The direction of the electric vector in an EM wave
    (light or radio). A wave is said to be unpolarized if the direction
    of the electric vector is randomly disturbed (has random orienta-
    tion), so that the direction at any instant cannot be predicted.
    Natural radiation from gases is usually unpolarized, but radiation
    from manmade sources is always polarized in radio wavelengths and
    often polarized even in optical wavelengths. Because reflection is
    different for different polarizations, reflected waves are always
    polarized to some extent even though they may be originally emitted
    in unpolarized form. Waves may be plane-polarized, or linearly
    polarized, in which case the electric vector is in the same direc-
    tion at all points in the wave. They may also be circularly or
    elliptically polarized, in which case the direction of the electric
    vector at some point changes with time (circular) or both direction
    and amplitude change in a relative manner (elliptical). (2) With
    respect to particles or crystals in an electric field, the displace-
    ment of charge centers from their normal positions caused by the
    force of the electric field.

polarizing filter: A filter which passes light waves vibrating in one
    polarization direction only. Used over camera lenses to cut down
    or remove, rays of any or all other polarization direction(s) when
    they may constitute objectionable reflections from glass, water, or
    other highly reflecting surfaces.

positive: (1) A photographic image having approximately the same ren-
    dition of light and shade as the original subject. (2) A film,
    plate, or paper containing such an image.

prime meridian: An arbitrary meridian selected as a reference line
    having a longitude of zero degrees and used as the origin from
    which other longitudes are reckoned east and west to 180 degrees;
    specif. the Greenwich meridian. Local or national prime meridians
    are occasionally used. Syn: aero meridian; initial meridian; first
    meridian.

pyroclastics: Pertaining to clastic rock material formed by volcanic
    explosion or aerial expulsion from a volcanic vent; also, pertain-
    ing to rock texture of explosive origin. It is not synonymous with
    the adjective "volcanic".

quartzite: (met). A metamorphic rock consisting mainly of quartz and
    formed by recrystallization of sandstone or chert by either re-
    gional or thermal metamorphism; meta-quartzite.

quartzite: (sed). A very hard but unmetamorphosed sandstone consisting
    chiefly of quartz grains that have been so completely and solidly
    cemented (diagenetically) with secondary silica that the rock
    breaks across or through the individual grains rather than around
    them; an orthoquartzite. The cement grows in optical and crystal-
    lographic continuity around each quartz grain, thereby tightly
    interlocking the grains as the original pore spaces are completely
    filled with secondary enlargements developed on the grains.
    Skolnick (1965) believes that most sedimentary quartzites are
    compacted sandstones developed by pressure solution of quartz
    grains.

radar: Acronym for radio detection and ranging. A method, system, or
    technique, including equipment components, for using beamed, re-
    flected, and timed EMR to detect, locate, and (or) track objects,
    to measure altitude and to acquire a terrain image. In remote
    sensing of the Earth's or a planetary surface, it is used for
    measuring, and often, mapping the scattering properties of the
    surface.

radar, brute force: A radar imaging system employing a long physical
    antenna to achieve a narrow beam-width for improved resolution.

radar, synthetic aperature (SAR): A radar in which a synthetically long
    apparent or effective aperture is constructed by integrating mul-
    tiple returns from the same ground cell, taking advantage of the
    Doppler effect to produce a phase history film or tape that may be
    optically or digitally processed to reproduce an image.

radiation: The emission and propagation of energy through space or
    through a material medium in the form of waves; e.g., the emission
    and propagation of EM waves, or of sound and elastic waves. The
    process of emitting radiant energy.

radiometer: An instrument for quantitively measuring the intensity of
    EMR in some band of wavelengths in any part of the EM spectrum.
    Usually used with a modifier, such as IR radiometer or microwave
    radiometer. Most radiometers measure the difference between the
    source radiation incident on the detector and a radiant energy
    (blackbody) reference. Comparison between the two is often
    achieved by mechanically interposing a reflective chopper, so
    that both sources can be viewed consecutively by the same detector,
    or by electrically switching, as in a microwave radiometer.

reflectance: A measure of the ability of a body to reflect light or
     sound. The reflectance of a surface depends on the type of surface,
     the wavelength of the illumination, and the illumination and view-
     ing angles.

remote sensing: In the broadest sense, the measurement of acquisition
     of information of some property of an object or phenomenon, by a
     recording device that is not in physical or intimate contact with
     the object of phenomenon under study; e.g., the utilization at a
     distance (as from aircraft, spacecraft, or ship) of any device and
     its attendant display for gathering information pertinent to the
     environment, such as measurements of force fields, electromagnetic
     radiation, or acoustic energy. The technique employs such devices
     as the camera, lasers, and radio frequency receivers, radar systems,
     sonar, seismographs, gravimeters, magnetometers, and scintillation
     counters. (2) The practice of data collection in the wavelengths
     from ultraviolet to radio regions. This restricted sense is the
     practical outgrowth from airborne photography. Sense 1 is pre-
     ferred and thus includes regions of the EM spectrum as well as
     techniques traditionally considered as belonging to conventional
     geophysics.

resolution: The ability of an entire remote sensor system, including
     lens, antennae, display, exposure, processing, and other factors,
     to render a sharply defined image. It may be expressed as line
     pairs per millimeter or meters, or in many other manners. In
     radar, resolution usually apples to the effective radar, resolution
     usually applies to the effective beamwidth and range measurement
     width, often defined as the half-power points. For infrared line
     scanner scanners the resolution may be expressed as the instanteous
     field-of-view, which see. Resolution also may be expressed in
     terms of temperature or other physical property being measured.

reststraheln or (residual) rays: An almost metallic reflection occurs
     in transparent materials where either the refractive index (n) is
     high, or when the absorption coefficient (K) is large. These
     narrow bands of reflectance are called the residual rays. Such
     wavelength regions show higher reflectance (and lower emittance)
     than elsewhere and provide chemical and structural information
     which may be remotely sensed.

reverse fault: Generally considered a fault with a dip between 45° and
     vertical in which the hanging wall has moved upward in relation to
     the footwall. In a broad sense thrust faults are also reverse
     faults.

scale: (1) The full range of tones of which a photographic paper is
     capable of reproducing is called the scale of the paper, it is also
     termed dynamic range, which see. (2) The ratio of a distance on a
     photograph or map to its corresponding distance on the ground. The

scale of a photograph varies from point to point because of dis- placements caused by tilt and relief, but is usually taken as f/H where f is the principal distance (focal length) of the camera and H is the height of the camera above mean ground elevation. Scale may be expressed as a ratio, 1:24,000; a representative fraction, 1/24,000; or an equivalence, 1 in. = 2,000 ft. See also represen- tative fraction.

scanners: (1) Any device that scans, and by this means produced an image. See scanning radiometer. (2) A radar set incorporating a rotatable antenna, or radiator element, motor drives, mounting, etc. for directing a searching radar beam through space and im- parting target information to an indicator.

scanning radiometer: A radiometer, which by the use of a rotating or oscillating plane mirror, can scan a path normal to the movement of the radiometer. The plane mirror may move in various patterns - arcs, circles, lines. The mirror directs the incoming radiation to a detector, which converts it into a electrical signal. This signal is amplified to stimulate a device such as a tape recorder, or glow tube or CRT that can be photographed to produce a picture. When the system is moved forward at velocity V and at altitude H, a suitable V/H ratio may be established, so that consecutive scans are just touching. This is often called an IR-imager, but is only so restricted because of the optical materials used, all-reflective optics being as useful in the UV and visible regions. They may all be single-or multiple-band.

scarp: (1) A line of cliffs produced by faulting or by erosion. The term is an abbreviated form of escarpment, and the two terms com- monly have the same meaning, although "scarp" is more often applied to cliffs formed by faulting. (2) A relatively steep and straight, cliff-like face or slope of considerable linear extent, breaking the general continuity of the land by separating level or gently sloping surfaces lying at different levels, as along the margin of a plateau, mesa, terrace, or bench. A scarp may be of any height. The term should not be used for a slope of highly irregular outline. (3) beach scarp. (4) A steep surface on the undisturbed ground around the periphery of a landslide, caused by movement of slide material away from the undisturbed ground; also, a similar but smaller feature on the disturbed material, produced by differential movements within the sliding mass.

schist: A strongly foliated crystalline rock formed by dynamic meta- morphism which can be readily split into thin flakes or slabs due to the well developed parallelism of more than 50% of the minerals present, particularly those of lamellar or elongate prismatic habit, e.g. mica, hornblende. The mineral composition is not an essential factor in its definition (American usage) unless specifi- cally included in the rock name, e.g. quartz-muscovite schist.

234

Varieties may also be based on general composition, e.g. calc-silicate schist, amphibolite schist, or on texture, e.g. spotted schist.

sediment: (1) Solid fragmental material, or a mass of such material, either inorganic or organic, that originates from weathering of rocks and is transported by, suspended in, or deposited by, air, water, or ice, or that is accumulated by other natural agents, such as chemical precipitation from solution or secretion by organisms, and that forms in layers on the Earth's surface at ordinary temperatures in a loose, unconsolidated form; e.g., sand, gravel, silt, mud, till, loess, alluvium. (2) Strictly, solid material that has settled down from a state of suspension in a liquid --- in the singular, the term is usually applied to material held in suspension in water or recently deposited from suspension, in the plural, the term is applied to all kinds of deposits, and refers to essentially unconsolidated materials; the plural usage as applied to consolidated sedimentary rocks should be avoided (USGS, 1958, p.86) Cf: deposit.

sedimentary: adj. (1) Pertaining to or containing sediment; e.g., a "sedimentary deposit" or a "sedimentary complex." (2) Formed by the deposition of sediment (e.g., a "sedimentary clay"), or pertaining to the process of sedimentation (e.g., "sedimentary volcanism"). --- n. A sedimentary rock or deposit.

sensor: Any device which gathers energy EMR or other and presents it in a form suitable for obtaining information about the environment. Passive sensors, such as thermal infrared and microwave, utilize EMR produced by the surface or object being sensed. Active sensors, such as radar, supply their own energy source. Aerial cameras use natural or artifically produced EMR external to the object or surface being sensed.

serpentine: A group of common rock-forming minerals having the formula: $(MG,Fe)_3Si_2O_5(OH)_4$. Serpentines have a greasy or silky luster, a slightly soapy feel, and a tough, conchoidal fracture; they are usually compact but may be granular or fibrous, and are commonly green, greenish yellow, or greenish gray (sometimes brown, black, or white) and often veined or spotted with red, green, and white. Serpentines are always secondary minerals, derived by alteration of magnesium-rich silicate minerals (esp. olivines), and are found in both igneous and metamorphic rocks.

sidelooking radar: An all weather, day/night remote sensor which is particularly effective in imaging large areas of terrain. It is an active sensor, as it generates its own energy which is transmitted and received to produce a photo-like picture of the ground. Also referred to as sidelooking airborne radar.

signature: Any characteristic or series of characteristics by which a material may be recognized. Used in the sense of spectral signature, as in photographic (color reflectance).

signature analysis techniques: Techniques which use the variation in the spectral reflectance or emittance of objects as a method of identifying the objects.

sinkhole: A geomorphic feature produced where rocks such as salt, gypsum, or limestone have been locally dissolved away. The earth may sink and form a cup-shaped basin to which this name is given. Syn: sink; lime sink; limestone sink; leach hole.

spectral band: An interval in the electromagnetic spectrum defined by two wavelengths, frequencies, or wave numbers.

spectral signature: Quantitative measurement of the properties of an object at one or several wavelength intervals.

spectrometer: A device to measure the spectral distribution of EMR. This may be achieved by a dispersive prism, grating, circular interference filter with a detector placed behind a slit. If one detector is used, the dispersive element is moved as to sequentially pass all dispersed wavelengths across the slit. In an inteferometer-spectometer, on the other hand, all wavelengths are examined all the time, the scanning effect being achieved by rapidly oscillating two, partly reflective, (usually parallel) plates so that interference fringes are produced. A Fourier transform is required to reconstruct the spectrum. Also called spectroradiometer.

spectrum: (1) In physics, any series of energies arranged according to wavelength (or frequency). (2) The series of images produced when a beam of radiant energy is subject to dispersion. A rainbow-colored band of light is formed when white light is passed through a prism or a diffraction grating. This band of colors results from the fact that the different wavelengths of light are bent in varying degrees by the dispersing medium and is evidence of the fact that white light is composed of colored light of various wavelengths.

standard meridian: (1) The meridian used for determining standard time. (2) A meridian of a map projection, along which the scale is as stated.

stereogram: A stereo pair of photos or drawings correctly orientated and permanently mounted for stereoscopic examination.

stereo pair: A pair of photos which overlap an area and are suitable for stereoscopic examination.

stereoscope: A binocular optical instrument for assessing the observer to view two properly oriented photographs or diagrams to obtain the mental impression of a three-dimensional model.

stereoscopic image: That mental impression of a three-dimensional object which results from stereoscopic vision (stereviewing).

stereo triplet: A series of three photos, the end members of which overlap sufficiently on the central one to provide complete stereoscopic coverage for the latter.

stereoscopic vision (stereo vision): Binocular vision which enables the observer to view an object simultaneously from two different perspectives (as two photographs taken from different camera stations) to obtain the mental impression of a three-dimensional model.

strike: The direction or bearing of a horizontal line in the plane of an inclined stratum, joint, fault or other structural plane.

structure: The general disposition, attitude, arrangement, or relative positions of the rock masses of a region or area; the sum total of the structural features of an area, consequent upon such deformational processes as faulting, folding, and igneous intrusion.

subtractive color process: A method of creating essentially all colors through the subtraction of light of the 3 subtractive color primaries (cyan, magenta and yellow) in various proportions through use of a single white light source.

syncline: A fold, the core of which contains the stratigraphically younger rocks; it is concave upward. Ant. anticline.

talus: (1) talus slope. (2) Rock fragments of any size or shape (usually coarse and angular) derived from and lying at the base of a cliff or very steep, rocky slope. Also, the outward sloping and accumulated heap or mass of such loose broken rock, considered as a unit, and formed chiefly by gravitational falling, rolling or sliding.

target: (1) The distinctive marking or instrumentation of a ground point to aid in its identification on a photograph. In photogrammetry, target designates a material marking so arranged and placed on the ground as to form a distinctive pattern over a geodetic or other control-point marker on a property corner on line, or at the position of an identifying point above an underground facility or feature. (2) In radar, an object returning a radar echo to the receiver.

tectonic: Said of or pertaining to the forces involved in, or the resulting structures or features of, tectonics. Syn; geotectonic.

thermal anomaly: A pattern of thermal energy distribution which appears anomalous relative to adjoining areas. If linear, these patterns can be termed thermal linears, in the same context as structural linears.

thermal band: A general term for middle-infrared wavelengths which are transmitted through the atmosphere window at 8-13 micrometers. Occasionally also used for the windows around 3-6 micrometers.

thermal inertia: Sometimes referred to as the thermal contact coefficient, it is a measure of the rate of heat transfer and is the product of thermal conductivity and thermal capacity. The reciprocal is often used instead, and is termed the "thermal parameter." Sometimes called conductive capacity.

thermal infrared: The preferred term for the middle wavelength ranges of the IR region, extending roughly from 3 micrometers at the end of the near infrared, to about 15 to 20 micrometers where the far infrared commences. In practice the limits represent the envelope of energy emitted by the earth behaving as a greybody with a surface temperature around 290°K (27°C). Seen from any appreciable distance, the radiance envelope has several brighter bands corresponding to windows in the atmospheric absorption bands. The thermal band most used in remote sensing extends from 8-13 micrometers.

thrust fault: A fault with a dip of 45° or less in which the hanging wall appears to have moved upward relative to the footwall. Horizontal compression rather than vertical displacement is its characteristic features. Cf; normal fault. Syn. reverse fault; reverse slip fault; thrust slip fault; thrust. Partial syn: overthrust; contraction fault; overlap fault.

tuff: A compacted phyroclastic deposit of volcanic ash and dust that may or may not contain up to 50% sediments such as sand or clay. The term is not to be confused with tufa. Adj; tuffaceous.

unconformity: (1) A substantial break or gap in the geologic record where a rock unit is overlain by another that is not next in stratigraphic succession, such as an interruption in the continuity of a depositional sequence of sedimentary rocks or a break between eroded igneous rocks and younger sedimentary strata. It results ·from a change that caused deposition to cease for a considerable span of time, and it normally implies uplift and erosion with loss of the previously formed record. An unconformity is of longer duration than a diastem. (2) The structural relationship between rock strata in contact, characterized by a lack of continuity in deposition, and corresponding to a period of nondeposition, weathering, or esp. erosion (either subaerial or subaqueous) prior to the deposition of the younger beds, and often (but not always)

marked by absence of parallelism between the strata; strictly, the
relationship where the younger overlying stratum does not "conform"
to the dip and strike of the older underlying rocks, as shown
specif. by an angular unconformity.

unconsolidated material: (1) A sediment that is loosely arranged or
unstratified, or whose particles are not cemented together, occur-
ring either at the surface or at depth. (2) Soil material that is
in a loosely aggregated form.

visible radiation: EMR of the wavelength interval to which the human
eye is sensitive, the spectral interval from approximately 0.4 to
0.7 μm (4000 to 7000 A).

volcanic rocks: A generally finely crystalline or glassy igneous rock
resulting from volcanic action at or near the Earth's surface,
either ejected explosively or extruded as lava. The term includes
near-surface intrusions that form a part of the volcanic structure.

wavelength (symbol λ): Wavelength = velocity/frequency. In general,
the mean distance between maximums (or minimums) of a roughly
periodic pattern. Specifically, the least distance between par-
ticles moving in the same phase of oscillation in a wave distur-
bance. Optical and IR wavelengths are measured in nanometers
(10^{-9}m), micrometers (10^{-6}m) and Angstroms (10^{-10}m).

weathering: The destructive process or group of processes constituting
that part of erosion whereby earth and rocky materials on exposure
to atmospheric agents at or near the Earth's surface are changed in
character (color, texture, composition, firmness, or form), with
little or no transport of the loosened or altered material; specif.
the physical disintegration and chemical deposition of rock that
produce an in-situ mantle of waste and prepare sediments for trans-
portation. Most weathering occurs at the surface, but it may take
place at considerable depths, as in well-jointed rocks that permit
easy penetration of atmospheric oxygen and circulating surface
waters. Some authors restrict weathering to the destructive pro-
cesses of surface waters occurring below 100°C and 1 kb; others
broaden the term to include biologic changes and the corrosive
action of wind, water, and ice.

window: A band of the electromagnetic spectrum which offers maximum
transmission and minimal attenuation through a particular medium
with the use of a specific sensor.

APPENDIX C

BASIC IMAGERY INTERPRETATION

1.0 INTRODUCTION

The application of remote sensor data to geological analysis, i.e., photointerpretation, has been conducted commercially for 50 years. It was, however, only after World War II, when a large number of geologists trained by the military services in photo-intelligence were released from service that the use of photogeology became widespread. The trafficability and engineering aspects of photointerpretation were largely ignored as the applications were primarily for petroleum and mineral exploration.

The use of remote sensor data is similar to many other survey techniques in that the attainment of optimum results requires training and continued practice of the skills. A competent geologist is not necessarily a competent image analyst and interpreter. Too often image interpretations are made by an individual(s) not adequately qualified[1]/ to extract full information from the imagery. The quality of the analysis for the particular project suffers as does the project manager's inclination to use that particular approach on another project. The proficient use of imagery from sensors other than conventional aerial cameras requires further skills which most geologists do not have the opportunity to adequately develop. Although there are reams of literature discussing various aspects of imagery interpretation both photographic and non-photographic, the very mass of data discourages use. Some of the better references for interpretation guidance are the manuals published by the American Society of Photogrammetry, particularly the two-volume compilation on remote sensing just published (Am. Soc. Photogrammetry, 1975). The following brief discussions, however, are an attempt to present salient points which will aid the geologist and engineer in the interpretation of remote sensor data.

---

[1]/

This factor is difficult to assess as the individual himself is not necessarily qualified to judge his competence. After three months of rather concentrated imagery analysis, the individual will no doubt feel that he is well-qualified. Experience of companies specializing in photogeological services has shown that on an average a year of continued daily application of photointerpretation skills is required to attain full proficiency in photoanalysis. This is assuming a geologist of B.S. level with course work in structure and stratigraphy.

Black-and-white aerial photography is the most widely used product from remote sensors, and, without doubt, the most highly developed. Consequently, this discussion will devote considerable space to the use of this medium. Much of the data presented can be applied to the analysis of other imagery as well.

Color and color-infrared photography have been improved substantially over the years but still lack the resolution of black-and-white panchromatic film. They add another dimension to the analysis and should be used when possible in conjunction with or in place of black-and-white photography.

In tunnel siting studies the stereoscopic interpretation of medium-to-large-scale aerial photography is usually a part of the initial data-gathering source for preliminary lithologic and structural interpretation. Although existing photography is normally used in this phase, it is not necessarily the best choice. The conditions that existed at the time of image acquisition can drastically influence the interpretability and information content of the image. Normally, in temperate zones the best time for image acquisition for geological analysis is in late fall or early spring when vegetational differences are the most contrasting. In areas where vegetational cover is extensive, as in the eastern half of the United States, photography should be acquired when leaf cover is minimal.

Patterns visible from aerial photographs usually provide adequate data for lithologic reconnaissance, particularly in areas where bedrock is exposed. However, experienced photointerpreters may be able to identify lithologic units even where bedrock may be obscured by soil or vegetative cover. By noting the topography, rock and soil color, vegetative zoning, primary and secondary structure, and solution topography on the aerial photography, an accurate identification of lithology is usually possible. Stratigraphic irregularities, and therefore faulting, are normally more evident on aerial photography than in the field. The photography will certainly identify areas that need additional checking in the field.

The presence of certain potentially hazardous lithologies in a test area should be carefully investigated. For example, limestone in a temperate-to-humid climate may contain cavernous, structurally weak zones, which could initiate collapse of a tunnel. Collapse in limestone strata is more probable where the rock contains groundwater in fractures which chemically weathers the limestone. Structural failure may occur in sequences of permeable-impermeable lithologies where groundwater seepage may lubricate the zone and initiate slippage. Certain sedimentary sequences are incompetent, and should be avoided where possible, and experienced photogeologists also consider the variation in rock competency as it may be influenced by climatic regions.

Photogeology is a powerful tool for structural geology. The attitudes of rock (strike and approximate dip) are normally apparent on aerial photographs. Fault and fracture zones are equally apparent, largely because of the effects of long-time differential weathering and erosion, or by stratigraphic disruptions which are indicative of faulting.

The initial identification of linears on small-scale (1:80,000-1:120,000) aerial photographs is important in the site selection phase, especially if the lineations represent fracture or fault zones which could contribute to lithologic weakness and water leakage within the tunnel. These zones should be further investigated and where significant, eliminated as potential tunnel locations. (Larger scale, i.e. <1:20,000) photography can be utilized by photogeologists to obtain more detailed geologic information in the more desirable locations. With this approach field work is reduced, as well as the total expense of the project.

2.0 PHOTOGEOLOGICAL INTERPRETATION KEYS

The systematic application of five important "keys," developed by
Professor Donald J. Belcher of Cornell University, will lead to the
identification of a landform. These "keys" are topography, drainage,
erosion, vegetation, and image tone. Using overlapping photographs and
a stereoscope, every landform is identified by its own specific varia-
tion of the five keys.

Instrumental to the analysis of a landform is its topographic
expression which is easily determined from the photographs using ster-
eoscopic vision. A topography noted to rise sharply and steeply nor-
mally represents a terrain which is shallow to bedrock, whereas a very
flat topography may represent an extremely deep mantle of residual soil,
with bedrock existing at depth. In the stereoscopic analysis of aerial
photographs, topography is the most prominent and obvious feature, and
is the first key to be applied.

The second key, drainage, is one of the more important characters
of a landform, and the drainage interpretation quickly eliminates im-
probable landform. The drainage pattern consists of the headwaters,
tributaries, and the major stream and the pattern must have originated
on the landform. Surface drainage reflects the character of the land-
form, the most important of which is its permeability. In comparing two
landforms, the one with the greater number of drainage channels per unit
area is often the less permeable. A controlled drainage pattern ex-
hibiting tributaries that are straight or angular may indicate a shal-
low-to-bedrock landform which contains joints or fractures. In such
areas excavation could be difficult and expensive. However, in hydro-
geological investigations, the presence of these angular tributary
channels, in an otherwise impermeable water-tight landform, may indicate
fractured or faulted areas containing groundwater.

It is important to note on the photographs any change in surface
drainage patterns, as this may indicate a complete change in landform.
The major types of drainage patterns are dendritic, pinnate, rectangu-
lar, trellis, parallel, radial, and internal.

A dendritic drainage system exhibits a "tree-like" drainage pattern
(Figure 49A), consisting of an integrated tributary system. Two impor-
tant categories of landforms containing a dendritic pattern are imperme-
able, unconsolidated deposits and horizontally bedded sediments con-
sisting of easily weathered bedrock.

A rectangular drainage system is actually a dendritic pattern which
is strongly controlled by resistant bedrock (Figure 49B). In this case,
the tributary channels are sharply angular or straight which is indi-
cative of shallow-to-bedrock areas.

243

244

A. DENDRITIC
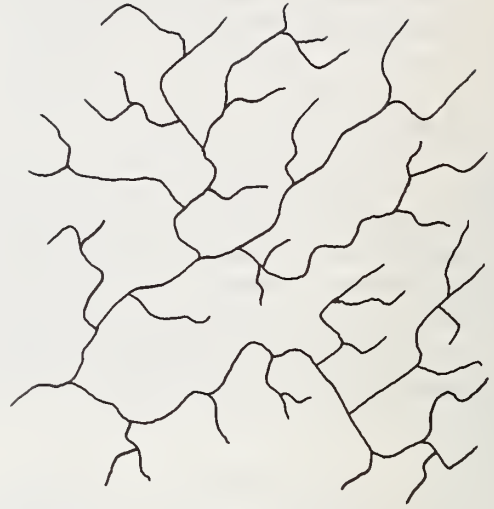
B. RECTANGULAR
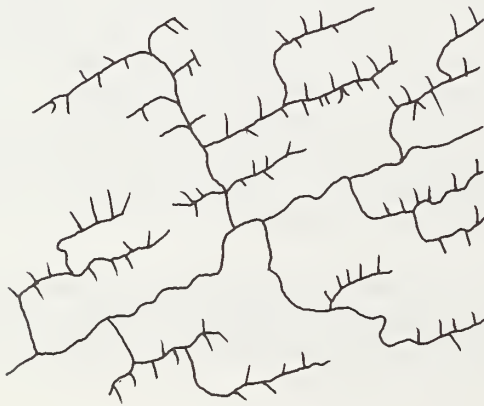
C. TRELLIS
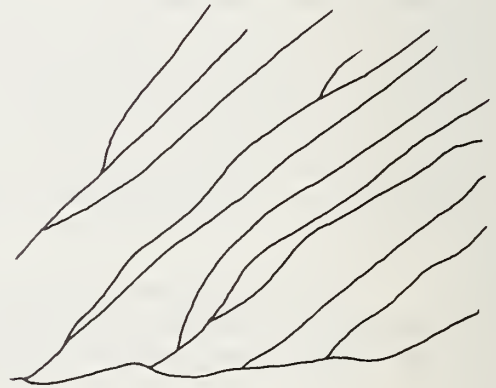
D. PARALLEL

Figure 49A - A-D. Some of the basic drainage patterns which provide information as to the lithology and structure of an area.

A trellis drainage system (Figure 49C) is generally indicative of tilted sedimentary rocks of diverse lithologies. The drainage pattern is a manifestation of non-uniformity within the landform, representing non-uniform weathering among these lithologies.

A parallel drainage system is best seen on photomosaics or on small-scale photographs where drainage flow is toward the direction of regional slope (Figure 49D).

A radial drainage system (Figure 49E) also is best observed on wide-area photographic coverage. It develops in areas with regional highs or lows where the channels originate either from the high or terminate at the low. Intrusive bodies can be delineated where the drainage pattern changes abruptly to a radial system.

Sedimentary strata that have been warped into domal or anticlinal and synclinal folds develop an angular drainage pattern (Figure 49F) between the more resistant strata and reflect the character of the structure. This drainage pattern is normally accompanied by a radial pattern in the center of the structure.

A pinnate "feather-like" drainage pattern is also a modification of the pure dendritic form (Figure 49G). This pattern is an almost sure indication of silt-size, unconsolidated deposits, such as loess, mica schist derived soil, or volcanic ash.

An internal drainage pattern (Figure 49H) is indicative of highly permeable landforms where the development of surface drainage is all but impossible and groundwater flow becomes the norm. The probability of seepage problems during excavation is high in these landforms.

The third key, erosion, is the most important direct clue used in the aerial photographic identification of soil texture. Erosion, in the form of gully erosion, occurs in landforms where water initially collects as surface runoff and creates definite scars of soil removal. Gullies occur only in the soil mantle, terminating where bedrock is encountered; therefore, gullies are only a clue to bedrock identification where the weathered soil profile is a reflection of the primary parent rock type. The characteristics of a gully are unique to specific cohesive or non-cohesive soil textures. Gully analysis is the most difficult of the five keys to master, but it can be a powerful tool in any landform interpretation.

Vegetation, the fourth of the "keys" to be discussed, can be of interpretative value in a general sense, but if the interpreter has a strong background in the plant sciences, it can be an even more useful tool. There can be no set rules for vegetation analysis as applied to landforms as it is a complex system with incredible diversity and variation per climatic regime.

245
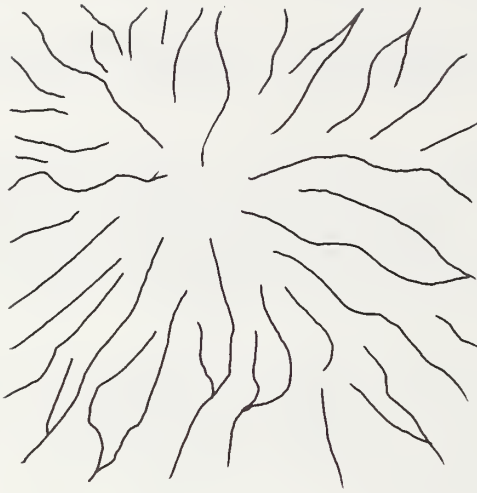
E. RADIAL
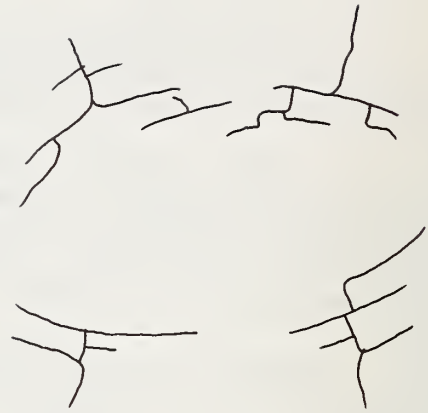
F. ANNULAR
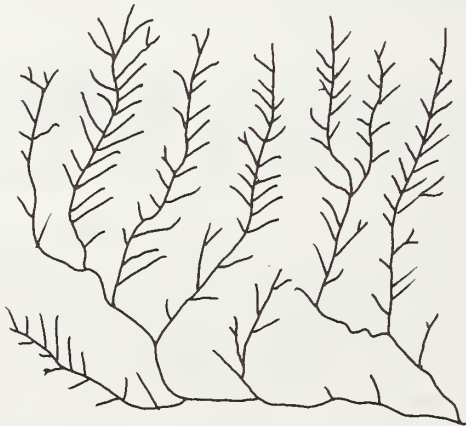
G. PINNATE
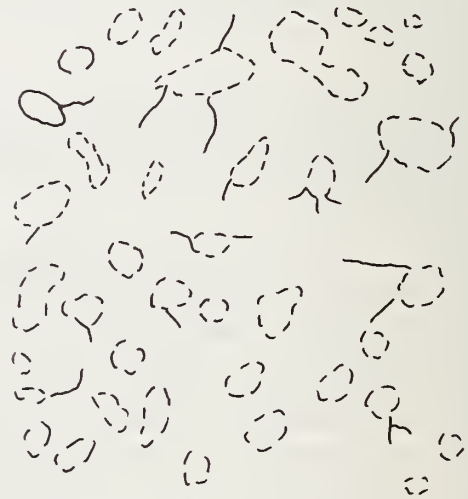
H. INTERNAL

Figure 49B - E-H. Some of the basic drainage patterns which provide information as to the lithology and structure of an area.

In most temperate regions, a greater concentration or larger physical dimension of the vegetation reflects increased moisture availability of the soils in that region, and if this occurs in a pronounced linear zone, it could reflect the existence of a water carrying fault zone.

In areas of flat-lying sedimentary rocks, vegetation often is specific to a certain marker bed; in temperate regions, it is common to note on the photographs a distinctive "contour-like" map of denser bands of vegetation following shale rather than sandstone outcrops. Here, the shale slopes are usually less steep and the derived soil cover more fertile and moist than that of the sandstone slope. (This trend may be reversed in more arid climates where the sandstone beds may contain more water, and thus support more vegetation).

Tone, which refers to the lightness or darkness of the photo image, is the last key to be discussed because it is the least reliable and accurate. However, tone can be an invaluable criterion when combined with the four previous keys and used by an interpreter experienced in soils, geology, and the analysis of aerial photographs.

On black-and-white photographs, a dark photographic tone is generally associated with a terrain of a high soil moisture content or soils with a high clay and organic fraction, which, in turn, supports a dense vegetative cover. Moreover, the presence of a high moisture content reduces the reflectivity of a soil and produces a dark photographic tone, even when not marked by a vegetative cover. However, in areas of excessive moisture such as a swamp, the photographic tone may be very light (close to white) due to a cover of light green swamp grass. In general, a light photographic tone is associated with permeable, coarse textured soils.

Varied tones in a cultivated field, visible on black-and-white aerial photographs as light streaks or blotchy areas in bare soil or by patches of less vigorous cropland, may be indicative of shallow bedrock areas. Dark toned streaks in cultivated fields, noted continuously during the growing season, may indicate joints in the underlying bedrock. Here, a patchy crop may be evident because of too wet conditions created by the moist, weathered, rock zone in the joint.

247

3.0 LANDFORM ANALYSIS

This chapter is a general summary of the methodology used by aerial photointerpreters for the analysis of some of the more common sedimentary, igneous, and metamorphic landforms.

3.1 Sedimentary Landforms

3.1.1 Clay Shale

Clay shale consists of thinly bedded indurated clays, which are highly impermeable and easily eroded. In humid climates, the landform is a gently rounded landscape with a vertical relief of up to approximtely 400 meters. In more arid or semi-arid areas, the topography is more rough and the hills exhibit nearly vertical sideslopes. Due to the inherent weakness of the landform, a dendritic drainage pattern is normal.

The derived soils contain a significant argillic fraction, creating a fair regime for agriculture. Contour plowing is not necessarily practiced on the slopes as the soil is not highly erodible; however, clay gullies usually are active somewhere on the landscape. (Clay shales may be confused with unconsolidated upper coastal plains, but the coastal plains because of their erodability, are usually contour plowed and this is evident on the aerial photographs.)

Landslides are a common phenomenon, especially if the clay shale is overlain with a pervious cover allowing water to accumulate at the pervious-impervious contact.

3.1.2 Sandy Shale

Sandy shale consists of thinly bedded sandstones (or sediments containing a significant sand fraction) inter-bedded with thin clay shale seams. Topographically, the landform often reaches 2500 meters; a massive, slightly rounded topography results because of the weathering and eroding off of the sandstone followed by the rounding off of the clay shale seams. The landform is fairly impermeable because of the plugging effect of the clay seams, and sur-face run-off creates a dendritic drainage pattern.

If the layering within the sandy shale landform con-sists of fairly thin beds, smoothly rounded slopes result; however, where more massive beds of sandstones-clay shales occur, steep sided sandstone outcrops maintain contact with the more gently sloping clay shale outcrops. This phen-omenon is caused by differential weathering between the

248

lithologies. This ragged, rough side slope may be marked
with landslides at contacts of the more permeable sandstones
and the underlying shales. Because of the differential
weathering characteristics of these members, derived soil
specific to the parent lithology results, often with a
specific vegetative cover. On the photographs, a distinct
"contour-like" map of the differing tones of these various
derived soils and surface vegetation can be traced as marker
beds.

3.1.3   Sandstone

The pure sandstone landform is massive, permeable,
and resistant to erosion. In humid climates the topography
is rolling to bold hills, but in the more arid areas the
erosion of joints creates steep, vertical cliffs. The
permeability does not permit surface runoff, and drainage
occurs only in the well-developed system of joints, creating
a regional rectangular drainage pattern.

The derived soil is usually shallow, as the slopes
are too steep for extensive soil profile development and
they are droughty and rather infertile; therefore, in most
regions the vegetation is usually left in the virgin state.
In the tropics, a deep soil cover can easily exist because
of the excessive chemical weathering common to these cli-
matic regimes. Where not mantled by low reflecting vege-
tation, the photo tone is light.

3.1.4   Limestone

In humid regions, limestone is valley-forming and
topographically low, but in the more arid regions it is
among the most resistant of the highlands. Limestone is
extremely susceptible to chemical weathering, and because of
the virtual lack of this process in dry regions, it exists
as massive and durable highs. The limestone - lowland
boundary is sudden and sharp because limestone possesses an
internal drainage system which is incapable of depositing
alluvial fans at the boundary.

In humid regions, the collapse of many sinkholes
along joints in the rock that concentrate groundwater flow,
creates linear, steep sided, flat bottomed valleys, usually
devoid of tributaries.

The drainage pattern is internal, consisting of sink-
holes perhaps with "lost" rivers. These rivers may dis-
appear into a sinkhole and then reappear at a distant locale.
If a drainage pattern is noted on the photos adjacent to an

internally drained limestone area, another landform, perhaps a shale, has been encountered.

The trend of soils developed from limestone is to have a significant silt content. The soil gullies in these limestone derived soils are light to white toned, and they have collapsing cup-like gully heads. Where sinkholes are bordered by white radial lines, it is inferred that they are actively collapsing, the light lines being unvegetated soil scars. Often, white toned "blotches" are noted where water seeps out from outcrops and precipitates calcium carbonate.

If landslides are detected on the photography, another more impermeable landform is present under the limestone, as landslides are not characteristic of pure thick limestone.

3.1.5 Tilted Sedimentary Rocks

A few statements concerning tilted sedimentary rocks are warranted. Unless the landform is a tilted pure clay shale, a trellis drainage pattern will be present. Where clay shale is a member, it often forms the valleys, as it is so easily eroded, and its local drainage pattern is dendritic within the total trellis system. In humid regions limestones also form valleys, leaving the sandstones as the adjacent highlands. Tilted limestone often has oblong sinkholes, reflecting the sloping groundwater table. Also, a definite linear boundary occurs between an intrusion and tilted sedimentary rocks.

3.2 Igneous Landforms

3.2.1 Granite

Granite, an intrusive of felsic composition, produces three distinct topographies. In the tropics, massive dome shaped hills of varying elevations created by an exfoliation process are common. In precambrian shields, the rock maintains a fairly low topographic expression normally characterized by thousands of lakes. In higher altitudes or in climatic regions where physical weathering is of more significance than chemical weathering, "A-shaped," massive mountains are common. In all three cases, stress relief fractures abound and are easily identified on the aerial photographs. These fractures seem not to have a definite orientation, unlike those of sedimentary landforms.

The boundary between granite and bodies of water is irregular, reflecting the difficulty of smoothing-off the granite shores. With careful stereoscopic interpretation,

it is common to be able to identify large granitic boulders which have fallen into the water, or which mantle the surface of the intrusion.

Alluvial fans issuing from this landform are often granular, steep sided, and of significant size. Springs issuing from their edges may contain dense patches of vegetation as evidenced by darker photographic tones.

The drainage pattern is regionally dendritic, however, local "pincer-like" drainage is locally superimposed, indicating that the drainage must curve locally around resistant granitic masses.

The soils derived from granite vary depending upon the climatic regime and upon the chemical composition of the granite. In general, granitic derived soils in the tropics become sandy clays, those in the artic are granular, and those in temperate climates fall somewhere in between, depending on parent rock composition. Only a careful stereoscopic analysis of the gully development will determine the soil type.

The tone of granite is generally light, except where fractured or faulted. Here, the deeper weathered soil zones contain more moisture and a linear, darker photographic tone results. The intersection of these fractures or faults are potential aquifers sought for in groundwater exploration, but they may be zones of seepage in tunnel excavation.

3.2.2 Basalts and Fast Cooled Lavas

Basalt flows maintain an irregular, almost pitted surface due to collapse of the rock during the cooling process and also to subsequent collapse following internal stream erosion. These depressions may become filled with windblown debris, creating a pock-marked, "lizard-skin" appearance on the aerial photography. Recent lava flows terminate in a lobate form, unless encountering a water body, and their surface is "wrinkled" due to cooling irregularities within the lava body.

Basalt is extremely permeable due to the formation, during cooling, of columnar joints. Precipitation percolates into these joints and a lack of surface drainage results. Because the extrusives usually flowed down existing valleys before cooling, many flows now mantle pre-existing buried watercourses. The internal drainage of the permeable basalt or lava may concentrate into these watercourses, forming great aquifers for groundwater.

Regionally, a parallel drainage pattern is present. A local surface drainage pattern results from impermeability caused by inter-layers of basalts or lavas and their derived cohesive soils. Landslides are common in basalts overlying more impermeable stratum, for water seepage lubricates the zone of contact, causing the slides. Potential landslide areas can often be delineated by noting darker toned zones of water accumulation on the surface of a scarp.

Basalt talus, present at the bottom of scarps, is a noteworthy photointerpretation clue. The bounding scarps maintain a jagged, saw-toothed appearance due to the collapse of the columnar jointed columns. Also, horizontal stratification lines are usually obvious on cliff faces.

3.2.3 Tuff (volcanic ash deposit)

A steep topography, a fine-textured, dendritic drainage pattern, pronounced silt gullies, and excessive erosion characterize the landform produced on volcanic ash deposits. In general, the hills are knife-edged, and over broad areas the elevation of the hilltops do not conform to any given elevation, but rapidly decline toward the lowland boundary. Because of the erosiveness of the tuff, the lowland boundary has numerous indentations. The steep highlands have equal sideslopes, indicating deep and uniform materials.

3.2.4 Interbedded Pyroclastics and Flows

Interbedded pyroclastics and flows have a gentle and subdued boundary with the lowlands. When a flow surface has not been highly dissected, the original flow pattern is preserved, but with moderate dissection, it generally forms sloping ridges with roughly parallel branches. The surface drainage is moderately developed and generally integrated into a dendritic pattern, with roughly parallel, often sickle-like, branches.

Most extrusives, regardless of composition, can be identified by their ragged and rough outcrops. Unlike sedimentary rocks, where marker beds can usually be traced, volcanics tend to crop out in an irregular pattern, reflecting the probable irregular pre-flow topography which it mantles.

3.2.5 Dikes

Dikes, when their compositional material is more resistant to erosion than the surrounding rock mass, form topographic highs. Groundwater may be dammed at depth when encountering these impermeable landforms.

3.3 Metamorphic Landforms

3.3.1 Gneiss

Mollard (1957) describes gneiss topography as follows:

1) At the contact with water bodies, gneiss maintains a highly irregular shoreline.

2) In shield areas, gneiss is foliated, showing a characteristic wavy banding. There are truncated folds composed of metamorphosed sedimentary rocks (metasediments) and local "scraps" of contorted metasediments that occur on the largely granitic shield.

3) In temperate areas, the gneiss forms anomalous large ridges which are locally sinuous and sub-parallel in plan view.

4) In sub-tropical areas, gneiss occurs as softly rounded, smooth, low hills with non-accordant ridge summits. No banding or foliation is apparent.

The drainage pattern is rectangular dendritic, for the drainageways intersect at nearly right angles and the tributaries have abrupt bends, forced by fracturing and foliation of the bedrock. Regionally, the dendritic drainage pattern may be somewhat parallel because of a ridge and valley topography.

The derived soils are extremely erosive, and contour plowing is practiced on the slopes.

3.3.2 Schist

Schist in hand samples is thinly laminated. Aerially, schist terrain is also banded, on a much larger scale, and the difference in resistance to weathering within these bands creates a somewhat parallel topography. A more rough topography exists in arid than in more humid climates and the parallelism of the uplands in arid regions is pronounced. However, in humid climates a deeply weathered zone may mantle and subdue the topography. Here, the schist is well dissected, producing hills with rounded crests and steep sideslopes. In all climates, the drainage pattern is rectangular.

The soils vary from a sandy silt to a sandy clay, depending upon climate and parent rock mineralogy. The gullies are closely spaced, long, and parallel in humid regions (Mollard, 1957).

3.3.3 Slate

Topography produced on slate is rugged in both humid and arid areas, the size of the hills being fairly uniform and small. The drainage pattern is fine textured, rectangular dendritic, and the gullies are steep and parallel, entering the tributaries at nearly right angles. The residual soil is relatively infertile and vegetation usually remains in the virgin state.

3.3.4 Serpentine

Serpentine masses form long sinuous ridges having smooth surfaces and convex sides. Such ridges connect elongated cone-shaped hills which become more and more rounded and independent from the main mass as dissection progresses. When bounded by water, the shoreline is smoothly curving with numerous indentations. Only regionally is a dendritic drainage pattern developed. The gullies are short and steep, the soil normally weathering to a clay, but varying from a silty clay to bare rock.

A significant photointerpretation clue is that soils developed from serpentine are highly infertile, and no matter the climatic regime, they support a lesser concentration of vegetation than adjacent areas. This is often the first clue to the presence of a serpentine body.

APPENDIX D

LOW SUN ANGLE PHOTOGRAPHY (LSAP) MISSION PLANNING

1.0 DISCUSSION

Low sun angle photography can be acquired with either conventional panchromatic aerial film or with black-and-white infrared film and a red filter. The image contrast for LSAP should be greater than for normal black-and-white aerial photography. Thus, if panchromatic film is used, it should be processed in a high contrast developer and printed on high contrast paper. Some experimentation may be needed to attain the desired results.

Timing of the overflight for a specific solar elevation is critical and this should be emphasized to the pilot and photographer. In order to document the overflight parameters the camera should be equipped with a data chamber that includes an operating clock that can be read to the nearest minute. The data chamber should also include the altitude and correct date. The appropriate "standard time" to be used should be clearly specified.

The photographic crew will need a schedule of flight times for several dates in the event that weather or other factors preclude overflights on a specific day.

The selection of solar elevation and azimuth for optimum enhancement of geology is dependent upon the relief in an area and the slope of topographic features. LSAP is most effective in areas of low (5-10'; 1.5-3 m) to moderately high local relief (2000'-4,000'; 610-1220 m). To cast the shadow, the angular elevation of the sun above the horizon must be less than the ground slope angle. The percent shadow needed for the best enhancement of topographic features is subjectively judged to be between 25% and 50% of the image area. Topographic maps of the target area should be closely examined to determine the best solar elevation and azimuth for shadow enhancement of terrain features. The azimuth of the sun depends upon the season, and at different times of the year, shadows will fall in a range of directions. Care must be taken to plan LSAP missions so that shadows will not obscure important topographic features. Figure 50 is a hypothetical topographic situation which illustrates the importance of selecting the proper azimuth for shadow enhancement of geologic features at low solar elevation at certain times of the year.

Suppose the geologic features in the valley (Figure 50) need to be investigated using the shadow enhancing technique. If a solar elevation of 15°, azimuth 70° is used the ridge will be shadow enhanced but the sink hole and any other geologic features in the valley will be obscured by shadow. If an angle of 25°, azimuth 70° is used the ridge will still be enhanced but the sink hole still will not be
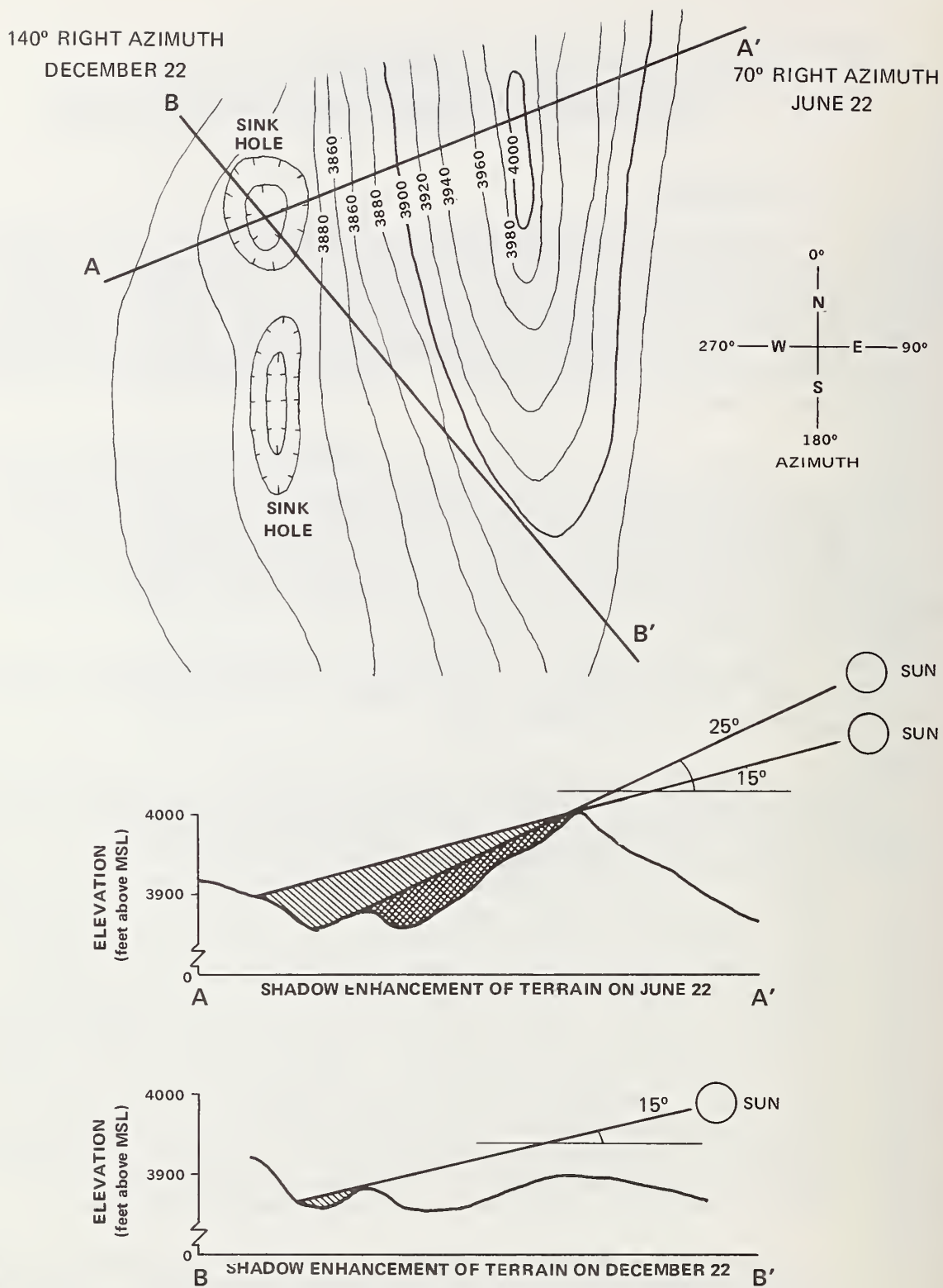
Figure 50 - An illustration of the importance of selecting the proper azimuth to enhance geologic features (for complete discussion see text).

256

detected. If, however, a solar elevation of 15° is used with an azimuth of greater than 128° then shadow enhancement of the sink hole will occur.

The angular elevation of the sun changes at a maximum rate of 1° every four minutes (15° per hour). The overflight time of LSAP missions, therefore, must be precise in order to obtain the desired shadow enhancement of topographic features. One can determine when to make LSAP overflights by:

1. Mathematical calculation of the desired solar elevation and azimuth.

2. Graphical solution using time and azimuth charts in the Smithsonian Institution Meteorological Tables.

3. Actual on-site observations of the shadows.

2.0 MATHEMATICAL CALCULATION OF SOLAR ELEVATION AND AZIMUTH

The solar elevation and azimuth can be calculated using the following formulas:

$$SINa = SIN\phi \ SIN\sigma + COS\phi \ COS\sigma \ COSh \qquad (1)$$

The formula for the calculation of solar azimuth is:

$$SIN\alpha = \frac{- COS\sigma \ SINh}{COSa} \qquad (2)$$

a = elevation of the sun (angular elevation above the horizon)

ϕ = latitude of the observer

σ = declination of the sun

h = hour angle of the sun (angular distance from the meridian of the observer)

$$COSh = \frac{SINa - SIN\phi \ SIN\sigma}{COS\phi \ COS\sigma} \qquad (3)$$

Formula 3 can be used to calculate the precise time to make an overflight to obtain a desired solar elevation.

257

The declination of the sun can be obtained from Table 12. The latitude of the observer should be expressed in degrees and fraction of degrees. The hour angle is the time of day expressed as an angle formed by the intersection of a line drawn from the sun to the center of the earth and a line drawn from the solar zenith to the center of the earth. The hour angle is graphically represented in Figure 51.
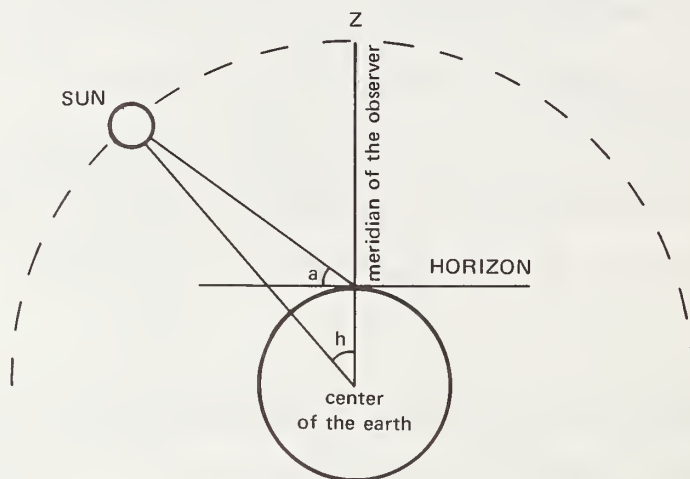
Figure 51. Graphic illustration of hour angle.

Z = Solar zenith (12 noon true solar time) at
    point of observation.

a = elevation of the sun (angular elevation above the horizon).

h = hour angle of the sun.

To calculate the hour angle it is necessary to convert the time to hours and fractions of hours. Morning times are subtracted from 12 noon (12 represents the solar zenith at the meridian of the observer). The result, in hours and fractions, is then multiplied by 15° to obtain the hour angle. For times after 12 o'clock noon, simple multiplication by 15° will yield the hour angle.

Table 12. Ephemeris of the Sun[1] (printed with permission of the Smithsonian Institution)

All data are for 0^h Greenwich Civil Time in the year 1950. Variations of these data from year to year are negligible for most meteorological purposes, the largest variation occurs through the 4-year leap-year cycle. The year 1950 was selected to represent a mean condition in this cycle.

The *declination* of the sun is its angular distance north (+) or south (−) of the celestial equator.

The *longitude* of the sun is the angular distance of the meridian of sun from the vernal equinox (mean equinox of 1950.0) measured eastward along the ecliptic.

The *equation of time* (apparent − mean) is the correction to be applied to mean solar time in order to obtain apparent (true) solar time.

The *radius vector* of the earth is the distance from the center of the earth to the center of the sun expressed in terms of the length of the semimajor axis of the earth's orbit.

[1] U. S. Naval Observatory, The American ephemeris and nautical almanac for the year 1950, Washington, 1948.

EPHEMERIS OF THE SUN

| Date	Declination ° '	Longitude ° '	Equation of time m. s.	Radius vector	Date	Declination ° '	Longitude ° '	Equation of time m. s.	Radius vector
Jan. 1	−23 4	280 1	− 3 14	0.98324	Feb. 1	−17 19	311 34	−13 34	0.98533
5	22 42	284 5	5 6	.98324	5	16 10	315 37	14 2	.98593
9	22 13	288 10	6 50	.98333	9	14 55	319 40	14 17	.98662
13	21 37	292 14	8 27	.98352	13	13 37	323 43	14 20	.98738
17	20 54	296 19	9 54	.98378	17	12 15	327 46	14 10	.98819
21	20 5	300 23	11 10	.98410	21	10 50	331 48	13 50	.98903
25	19 9	304 27	12 14	.98448	25	9 23	335 49	13 19	.98991
29	18 8	308 31	13 5	.98493					
Mar. 1	− 7 53	339 51	−12 38	0.99084	Apr. 1	+ 4 14	10 42	− 4 12	0.99928
5	6 21	343 51	11 48	.99182	5	5 46	14 39	3 1	1.00043
9	4 48	347 51	10 51	.99287	9	7 17	18 35	1 52	1.00160
13	3 14	351 51	9 49	.99396	13	8 46	22 30	− 0 47	1.00276
17	1 39	355 50	8 42	.99508	17	10 12	26 25	+ 0 13	1.00390
21	− 0 5	359 49	7 32	.99619	21	11 35	30 20	1 6	1.00500
25	+ 1 30	3 47	6 20	.99731	25	12 56	34 14	1 53	1.00606
29	3 4	7 44	5 7	.99843	29	14 13	38 7	2 33	1.00708
May 1	+14 50	40 4	+ 2 50	1.00759	June 1	+21 57	69 56	+ 2 27	1.01405
5	16 2	43 56	3 17	1.00859	5	22 28	73 46	1 49	1.01465
9	17 9	47 48	3 35	1.00957	9	22 52	77 36	1 6	1.01518
13	18 11	51 40	3 44	1.01051	13	23 10	81 25	+ 0 18	1.01564
17	19 9	55 32	3 44	1.01138	17	23 22	85 15	− 0 33	1.01602
21	20 2	59 23	3 34	1.01218	21	23 27	89 4	1 25	1.01630
25	20 49	63 14	3 16	1.01291	25	23 25	92 53	2 17	1.01649
29	21 30	67 4	2 51	1.01358	29	23 17	96 41	3 7	1.01662
July 1	+23 10	98 36	− 3 31	1.01667	Aug. 1	+18 14	128 11	− 6 17	1.01494
5	22 52	102 24	4 16	1.01671	5	17 12	132 0	5 59	1.01442
9	22 28	106 13	4 56	1.01669	9	16 6	135 50	5 33	1.01384
13	21 57	110 2	5 30	1.01659	13	14 55	139 41	4 57	1.01318
17	21 21	113 51	5 57	1.01639	17	13 41	143 31	4 12	1.01244
21	20 38	117 40	6 15	1.01610	21	12 23	147 22	3 19	1.01163
25	19 50	121 29	6 24	1.01573	25	11 2	151 14	2 18	1.01076
29	18 57	125 19	6 23	1.01530	29	9 39	155 5	1 10	1.00986
Sept. 1	+ 8 35	157 59	− 0 15	1.00917	Oct. 1	− 2 53	187 14	+10 1	1.00114
5	7 7	161 52	+ 1 2	1.00822	5	4 26	191 11	11 17	1.00001
9	5 37	165 45	2 22	1.00723	9	5 58	195 7	12 27	0.99888
13	4 6	169 38	3 45	1.00619	13	7 29	199 5	13 30	.99774
17	2 34	173 32	5 10	1.00510	17	8 58	203 3	14 25	.99659
21	+ 1 1	177 26	6 35	1.00397	21	10 25	207 1	15 10	.99544
25	− 0 32	181 21	8 0	1.00283	25	11 50	211 0	15 46	.99433
29	2 6	185 16	9 22	1.00170	29	13 12	214 59	16 10	.99326
Nov. 1	−14 11	217 59	+16 21	0.99249	Dec. 1	−21 41	248 13	+11 16	0.98604
5	15 27	222 0	16 23	.99150	5	22 16	252 16	9 43	.98546
9	16 38	226 1	16 12	.99054	9	22 45	256 20	8 1	.98494
13	17 45	230 2	15 47	.98960	13	23 6	260 24	6 12	.98446
17	18 48	234 4	15 10	.98869	17	23 20	264 28	4 17	.98405
21	19 45	238 6	14 18	.98784	21	23 26	268 32	2 19	.98372
25	20 36	242 8	13 15	.98706	25	23 25	272 37	+ 0 20	.98348
29	21 21	246 11	11 59	.98636	29	23 17	276 41	− 1 39	.98334

3.0 GRAPHIC SOLUTION

Solar elevation and azimuth can be determined graphically by the use of a series of charts published by the Smithsonian Institution ("Smithsonian Meteorological Tables," Publication Number 4014, pp. 495-505). Figure 52 is an example of a chart for 40° latitude. The following instructions for the use of these charts are reprinted here with permission.
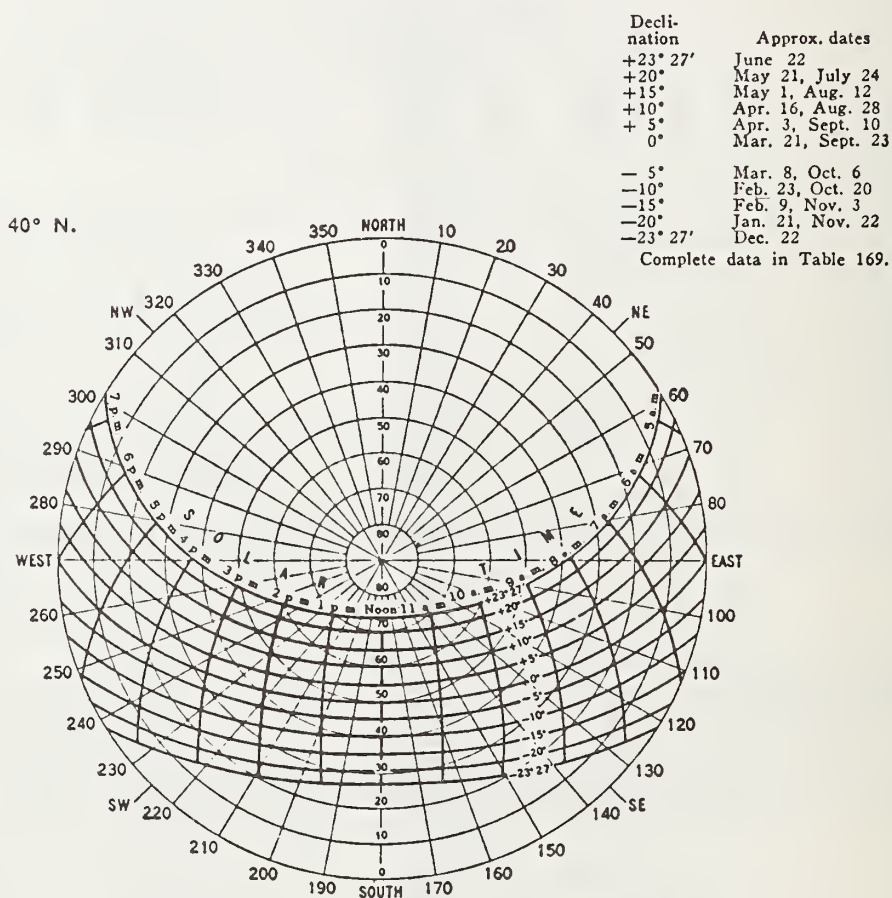
SMITHSONIAN METEOROLOGICAL TABLES

Figure 52 - This chart permits the graphic determination of solar azimuth and altitude for any time or day of the year for 40° latitude north or south. The chart is one of a series constructed for different latitudes which were published by the Smithsonian Institution in their "Smithsonian Meteorological Tables" Publ. No. 4014; reproduced here with permission.

260

This series of charts, one for each five degrees of latitude (except 5°, 15°, 75°, and 85°), gives the altitude and azimuth of the sun as a function of the true solar time and the declination of the sun as a function of the true solar time. Linear interpolation for intermediate latitudes will give results within the accuracy to which the charts can be read.

On these charts a point corresponding to the projected position of the sun is determined from the heavy lines corresponding to declination and solar time.

To find the solar altitude and azimuth:

1. Select the chart or charts appropriate to the latitude.
2. Find the solar declination δ corresponding to the date in question from the Ephemeris (Table 1).
3. Determine the true solar time as follows:
   a. To the local standard time (zone time) add 4 minutes for each degree of longitude the station is east of the standard meridian, or subtract 4 minutes for each degree west of the standard meridian to get the local mean solar time.
   b. To the local mean solar time add algebraically the equation of time obtained from the Ephemeris; the sum is the required true solar time.
4. Read the required altitude and azimuth at the point determined by the declination and the true solar time. Interpolate linearly between two charts for intermediate latitudes.

Altitude and azimuth in southern latitudes.—To compute solar altitude and azimuth for southern latitudes, change the sign of the solar declination and proceed as above. The resulting azimuths will indicate angular distance from south (measured eastward) rather than from north.

4.0 VISUAL OBSERVATION

Approximations of suitable shadow lengths for structural enhance-
ment of an area can be made by on-site observations. Observations
made in the morning and evening a day or two prior to the planned
photographic mission will provide insight as to the time the shadows
are of appropriate length to give maximum enhancement of the topo-
graphy. To determine the correct times for following days when shadows
will be the same length, consult the weather section of the local
paper or the Weather Bureau for the daily change in time of sunrise
and sunset. This factor can be added or subtracted from the observed
time as appropriate when preparing instructions for the flight crew.

This method lacks precision and it is recommended that supple-
mental photography be acquired approximately 20 minutes before and
after the selected time to assure usable photography. For small,
specific areas such as a tunnel site, this multiple overflight ap-
proach is of merit regardless of the method of determining overflight
times. The additional costs will be small.

APPENDIX E

FIELD REFLECTANCE STUDIES AT
CARLIN CANYON, NEVADA

1.0 SPECTRORADIOMETRIC FIELD INVESTIGATIONS

On August 5, 1975 during a field trip to the Carlin Canyon site, spectroradiometric measurements were made of the reflectance properties of the Diamond Peak conglomerate and the Strathearn limestone. The measurements were made at two sites with an ISCO, model SR, instrument which permits continuous wavelength scanning between 380 and 1,350nm. The sensing bandwidth of the system is 25nm in the 380-750nm range and 50nm in the 750-1,350nm range. A fiber optic extension head with a diffusing disk was used for the field measurements. Typical rock exposures were selected for measurement with the sensing head positioned approximately 12 inches from the rock surface. The weather was excellent and the sky clear of clouds, so solar readings were taken as a suite of measurements immediately before or after the reflectance measurements of the outcrop. A period of approximately 4-5 minutes separated these readings.

Figure 53 are the relative reflectance curves prepared from these measurements. They show that there is, with few exceptions, less than 3% difference in relative reflectance of the two rock materials on a weathered surface.
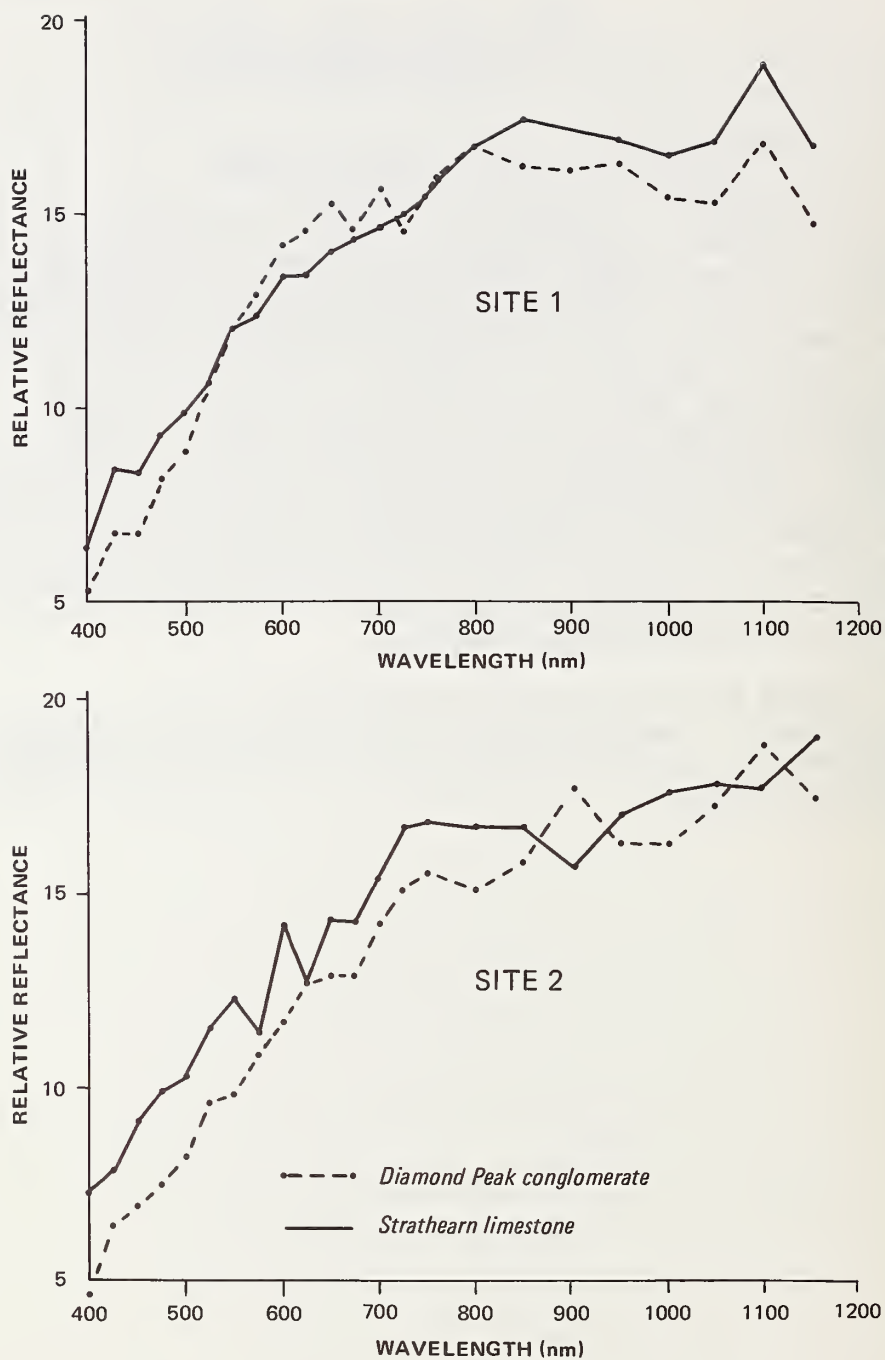
Figure 53 - Relative reflectance measurements made with an ISCD spectroradiometer. The results show only minor differences in the relative reflectance of the Diamond Peak conglomerate and the Strathearn limestone.

2.0 FIELD RADIOMETRY

On October 23, 1975, Dr. R.J.P. Lyon of Stanford University joined the Earth Satellite Corporation field crew at Carlin Canyon to make measurements with two Exotech Model 800 radiometers.

The Exotech unit is a four-band radiometer filtered optically to match the LANDSAT satellite system. It is a solid state, battery powered unit and easily portable. Two of these instruments are normally used at once - one pointing upwards for global irradiance measurements, and one pointing at the target. Lenses of 1° and 15° fields-of-view (FOV) are available with 2π diffusers for irradiance measurements.

The field measurements were conducted after the analysis of flight data from the 11-channel multispectral scanner (MSS) indicated relatively poor separability channel-by-channel. Some improvement had been noted when the MSS channels were combined to approximate LANDSAT channels, and it was desirable to verify this fact in the field. Field measurements were planned for October 18, 1975, exactly one year after the remote sensing overflight, but logistic problems made this impossible. It was possible to mobilize five days later on October 23, which unfortunately was a somewhat snowy and cloudy day.

2.1 Exotech Radiometer Field Data (E-Channels)

2.1.1 Sky Illuminance Effects

The measurement technique includes the continual monitoring of the incoming irradiance of the sky. This serves to check for anomalies, either in the global illumination (sun plus sky) or in the equipment. A predictable pattern of sky readings should emerge from the data set.

The Carlin sky data showed two populations; one was relatively constant when the sky was clear of any clouds, and the other quite variable when clouds were actively forming and dissipating near the sun. The restriction of measurements to that time when the sun was actually clear of clouds was not entirely successful. The proximity to the sun of existing clouds, or more probable, variations in the atmospheric water-ice-snow content and pre-cloud water vapor formation, severely attentuated the incoming radiation. This was doubly complicating, as a part of the measurement technique is to take long, 1° FOV sitings on steep sloping outcrops sufficiently far away for the narrow beam to integrate statistically a large outcrop area (e.g. at 1,000 feet (305m) distance the 1° FOV covers 17 (5m) feet of outcrop).

Often the illumination at the outcrop was not the same as the illumination at the instrument station. As a consequence, the corrections to the standards were not always the same as the corrections needed for a target.

2.1.2 Field Data Selection

Because of these problems only about 50% of the data were selected for further analysis based upon (a) global irradiance values which matched predicted patterns; (b) duplicate readings; (c) replicated readings (at a slightly later time) which were similar; and (d) vertically-viewed data (using the 15° field-of-view, about three square feet in size) when factor "a" was acceptable.

2.1.3 Field Data Reduction

The Exotech data (E-set) were processed at the Stanford University Remote Sensing Laboratory by the computer ratioing program (ERTSRATS). This program calculates, for the sky:

a) E-channel irradiance (2π) in units of watts/cm^2/μm band-pass.

b) Normalized channel irradiance (normalized to 1μm band-pass to take care of the greater band-pass width of channel E-7 (LANDSAT 7) which is 2.5 times the width of channels E4, E5, and E6 with units of watts/cm^2/μm band-pass.

c) CIE color coordinates of sky color temperature (this is a measure of illumination quality and is used for monitoring). Channels E4, E5, and E7 are used so as to include solar infrared radiation, therefore, correctly, the factor "c" is a "pseudo" CIE value, but comparable to the use of color infrared film.

For the target, we calculated similarly:

d) E-channel radiance (brightness) in units of watts/cm^2/μm in band-pass for the four channels.

e) Normalized R-channel radiance in units of watts/cm^2/μm.

f) CIE coordinates as in Item C above.

266

For the target-sky pair we can now calculate several forms of reflectance.

g) Bi-directional reflectance if the same FOV lenses are used on each unit (A or B) and one unit (B) is looking down at a horizontal white reflectance standard ($BaSO_4$) commercially known as FIBERFRAX (see Watson, R.D., 1971). Irradiance (2π) is not measured.

h) Directional reflectance if the "standard" unit B is equipped with 2π diffusers and is viewing the sky at the zenith.

In both cases, the A and B units must be read at closely concurrent times, and particularly so under the poor and variable lighting conditions that prevailed at the Carlin Canyon site (see Section 2.4 for instrumentation and technique description on how this is accomplished).

Suitable factors can be calculated from mixing both types of geometry in the data set collection. Unit A with 1° or 15°FOV lenses views FIBERFRAX standards vertically below the lenses, while the B unit with 2π diffuser views the incoming global irradiance.

Theoretically, this factor should be $1/\pi$ or 0.318. In practice, we calculate empirically values from within the data set matrix for that day, thereby effecting several other small normalizations which are advantageous.

In addition, we calculate several sets of ratios including reflectance ratios, and express them usually in the sequence used by R. Vincent (Vincent & Thompson, 1973) as ratios Ch 7/6, Ch 7/5, Ch 7/4, Ch 6/5, and Ch 5/4[2]; thereby being able to effect a comparison with a growing body of information from several sets of workers as to how the LANDSAT spectral signatures and ratios for various terrains are correlating with ground measurements.

2.2 Exotech Results

Two tables of detailed groupings of rock outcrop areas (Tables 13 and 14) and a summary table (Table 15) have been prepared from the 50 spectra selected and are considered to be free from atmospheric problems.

[2] These numbers refer to LANDSAT multispectral scanner data channels which spectrally have bandwidths as follows: Ch 4 = .5-.6μm, Ch 5 = .6-.7μm, Ch 6 = .7-.8μm, and Ch 7 = .8-1.1μm.

Table 13 FIELD MEASURED RADIOMETRIC DATA, CARLIN CANYON, NEVADA WITHIN GROUP MEANS (COEFFICIENT-OF-VARIBILITY IN PARENTHESES) ONLY FULL SUNLIGHT DATA USED

	R4	R5	R6	R7	RX	RY	N
Conglomerate							
N. Hill	195 (.30)	401 (.26)	405 (.25)	494 (.27)	404 (.02)	290 (.06)	4
Spur	200 (.19)	358 (.13)	378 (.11)	474 (.19)	386 (.07)	284 (.09)	7
4E & 4W							
N.E. of River	214 (.61)	391 (.58)	393 (.54)	449 (.53)	402 (.01)	262 (.02)	5
Red Patches							
Near summit	150 (.08)	312 (.07)	344 (.07)	448 (.06)	392 (.02)	317 (.03)	5
Conglomerate Average	190 (.15)	366 (.11)	380 (.07)	466 (.05)	396 (.02)	288 (.08)	
Yellow area W. of N. Hill	623	812	972	908	401	234	2
Limestone							
N. Hill (A)	262	331	394	499	377	291	5
N. Hill (B)	347	652	637	673	416	242	2
Spur	231 (.20)	419 (.16)	414 (.20)	528 (.19)	390 (.04)	277 (.07)	5
N.E. of River	194 (.43)	372 (.40)	372 (.42)	436 (.40)	411 (.01)	263 (.15)	5
Limestone Average	259 (.25)	444 (.32)	454 (.27)	534 (.19)	399 (.05)	268 (.08)	
Sandbar in River	364	621	616	679	396	244	1
Sagebrush A	150 (.33)	217 (.51)	400 (.22)	418 (.36)	332 (.17)	342 (.08)	5
Sagebrush B	334 (.10)	604 (.05)	639 (.08)	691 (.01)	406 (.-)	261 (.06)	3
Sagebrush Avg.	242	410	519	555	369	302	50

Table 14 Field Measured Radiometric Data Ratios - Carlin, Nevada. Within Group Means (Coefficient of Variability in Parentheses.) Only Full Sunlight Data Used.

	R76	R75	R74	R65	R64	R54	N
Conglomerate							
N. Hill	121 (.06)	122 (.07)	254 (.12)	100 (.08)	210 (.11)	207 (.07)	4
Spur	125 (.10)	131 (.11)	241 (.20)	105 (.13)	193 (.21)	183 (.18)	7
4E & 4W N.E. of River	116 (.09)	116 (.07)	216 (.13)	98 (.05)	185 (.07)	185 (.06)	5
Red Patches Near summit	130 (.04)	143 (.03)	299 (.07)	110 (.06)	230 (.09)	208 (.06)	5
Conglomerate Average	123 (.05)	128 (.09)	252 (.14)	103 (.05)	205 (.10)	196 (.07)	4
Yellow Area W. of N. Hill	94 (.07)	110 (.09)	160 (.29)*	117 (.16)	167 (.22)*	147 (.38)*	2
Limestone							
N. Hill Set-A	129 (.13)	152 (.14)	187 (.17)	118 (.04)	146 (.17)	123 (.15)	5
N. Hill Set-B	105 (.01)	103 (.01)	193 (.01)	97 (.01)	183 (.02)	187 (.01)	2
Spur	129 (.17)	125 (.05)	231 (.18)	99 (.13)	180 (.11)	183 (.14)	5
N.E. of River	112 (.12)	112 (.19)	200 (.30)*	100 (.10)	176 (.20)	177 (.19)	7
Limestone Average	119 (.10)	123 (.17)	203 (.10)	104 (.09)	171 (.10)	168 (.18)	4
Sandbar in River	110	109	186	99	169	170	1
Sagebrush Type-A	125 (.10)	204 (.25)	276 (.13)	166 (.32)	220 (.09)	142 (.28)	4
Sagebrush Type-B	109 (.09)	115 (.05)	208 (.11)	106 (.07)	192 (.04)	181 (.07)	3
Between Group Means	120 (.07)	130 (.19)	237 (.15)	107 (.16)	196 (.10)	186 (.09)	50

* Higher values

Table 15 SUMMARY TABULATION OF REFLECTANCE GROUP AVERAGE VALUES OF MEANS
CARLIN, NEVADA

	R4	R5	R6	R7	RX	RY	R76	R75	R74	R65	R64	R54	N
Conglomerate	190 (.15)	366 (.11)	380 (.07)	466 (.05)	396 (.02)	288 (.08)	123 (.05)	128 (.09)	252 (.14)	103 (.05)	205 (.10)	196 (.07)	21
Limestone	259 (.25)	444 (.32)	454 (.27)	534 (.19)	399 (.05)	268 (.08)	119 (.10)	123 (.17)	203 (.10)	104 (.09)	171 (.10)	168 (.18)	29
Sandbar	364	621	616	678	396	244	110	109	186	99	169	170	1
Yellow Area	623	812	972	908	401	234	94	110	160	117	167	147	2
Rock Avg.	359 (.53)	561 (.35)	605 (.44)	647 (.30)	398 (.01)	259 (.09)	112 (.11)	118 (.08)	200 (.18)	105 (.07)	178 (.10)	170 (.12)	43
Sagebrush	242	410	519	555	369	302	117	159	242	136	206	162	7
Average (Between Group Means)	336 (.51)	531 (.35)	588 (.39)	624 (.28)	392 (.03)	267 (.11)	120 (.07)	130 (.19)	237 (.15)	107 (.16)	196 (.10)	186 (.09)	50

270

These tables list band-pass reflectance values for each group (R4, R5, R6, R7) and the ratios of those reflectances arranged in the Vincent sequence as R76, R75, R74, R65, R64, R54[3/]. Each value is the mean of that group of N measurements multiplied by 100, to give an integer value. The value in parentheses is the coefficient-of-variability (COV) for that mean or the percent variability as found by dividing the standard deviation for that group by its mean (COV = $\sigma/\bar{x}$).

2.2.1 Summary

From Table 15 the following observation can be made. The R54 ratio has the highest group mean of 196 for the targets most red within the conglomerate facies; the "yellow area" near Point a; Figure 32 on the hill north of the river has the lowest value and is least red with R54 = 147. Vegetation (sagebrush) is intermediate with an R54 value of 162, similar to the sandbar with R54 of 170. An image of R54, therefore, should be a moderate discriminator showing about 33% contrast[4/], with the conglomerate highest or white and the yellow area lowest or dark gray.

The R54 ratio as detailed in Table 15 indicates the four localities of conglomerate have a group mean value of R54 = 196, but the individual localities show considerable variation; North Hill, R54 = 207, and the red patches near Carlin Peak summit above the tunnel, R54 = 208. These sites have extra contrast of 14% as compared to the spur, R54 = 183, and on the northeast portion of the river bend R54 = 185, all sites which have similar facies. Thus, they should (and do) show as brighter patches or higher image contrast areas on the R54 imagery, even relative to the other outcrops to the same conglomerate facies.

Ratio R74 has a much better group mean spread with conglomerate (252), contrasting with the sandbar (186) and the yellow area (160); this gives 58% contrast as defined above.

An image of R74, therefore, should show conglomerate as light toned, sand intermediate and the yellow area darker gray.

3/

This shorthand notation used was originated by R. Vincent (1970) for designating ratios by channel number. For example, R64 indicates a ratio of Channel 6/ Channel 4.

4/

Contrast = max/minimum.

Sixty-four characteristics similar to R74, but with a group mean for conglomerate of 205, the yellow area, 167 and the sandbar, 169. This should reverse the image contrast making the sequence: conglomerate lightest in tone and the yellow area and sandbar medium gray.

The vegetation (sagebrush) may be discriminated using R75 or R65 with the sagebrush brightest with group mean values of 159 and 136 for the two ratios, with conglomerate showing 128 and 103 equally with limestone, the sandbar showing 109 and 99, and the yellow area showing 110 and 117.

The coefficient-of-variability (COV) of group means in the parenthetic statement in the lowest line of the table may be used as a crude measure of the relative discrimin- ability of each variable - the larger the COV the greater the spread of the means (provided the populations have comparable standard deviations). Thus, R75 with a COV equal to 0.19 would be the best to maximize the data spread. A tabulation R75 contrast is as follows: conglomerate 17%; limestone 13%; sandbar 0%; indicating a 17% spread in the three rock types.

Both R75 and R65 are vegetation sensitive; thus, R74 with group mean COV equal to 0.15 is the best for rock discrimination. The R74 lithology contrasts are conglomerate 35%, limestone 9%, and the sandbar 0%; a spread of 35% contrast between the sandbar and the conglomerate.

2.3 Bar Graph

A bar graph (Figure 54) has been prepared to show visually the spread of group ratio means R54 and R75 (plotted as the abscissa). The horizontal extent of the symbol indicates a 1σ spread. Where n is equal to or less than three, values which are plotted directly as σ have no real meaning.

The ordinate is artificial and represents an attempt to portray the size (n) of each group to give some meaning to the standard deviation spread. Inspection of the graph indicates that an R75 is a good discriminant for limestone, whereas an R54 is a better discriminant for conglomerate.

The field measurement data and the flight imagery strips, while both showing low contrasts, do substantiate each other rather well. This is so regardless of the fact that the field data are all for small outcrop areas up to 20 feet or so in diameter and the imagery analyst is viewing much larger areas of terrain.
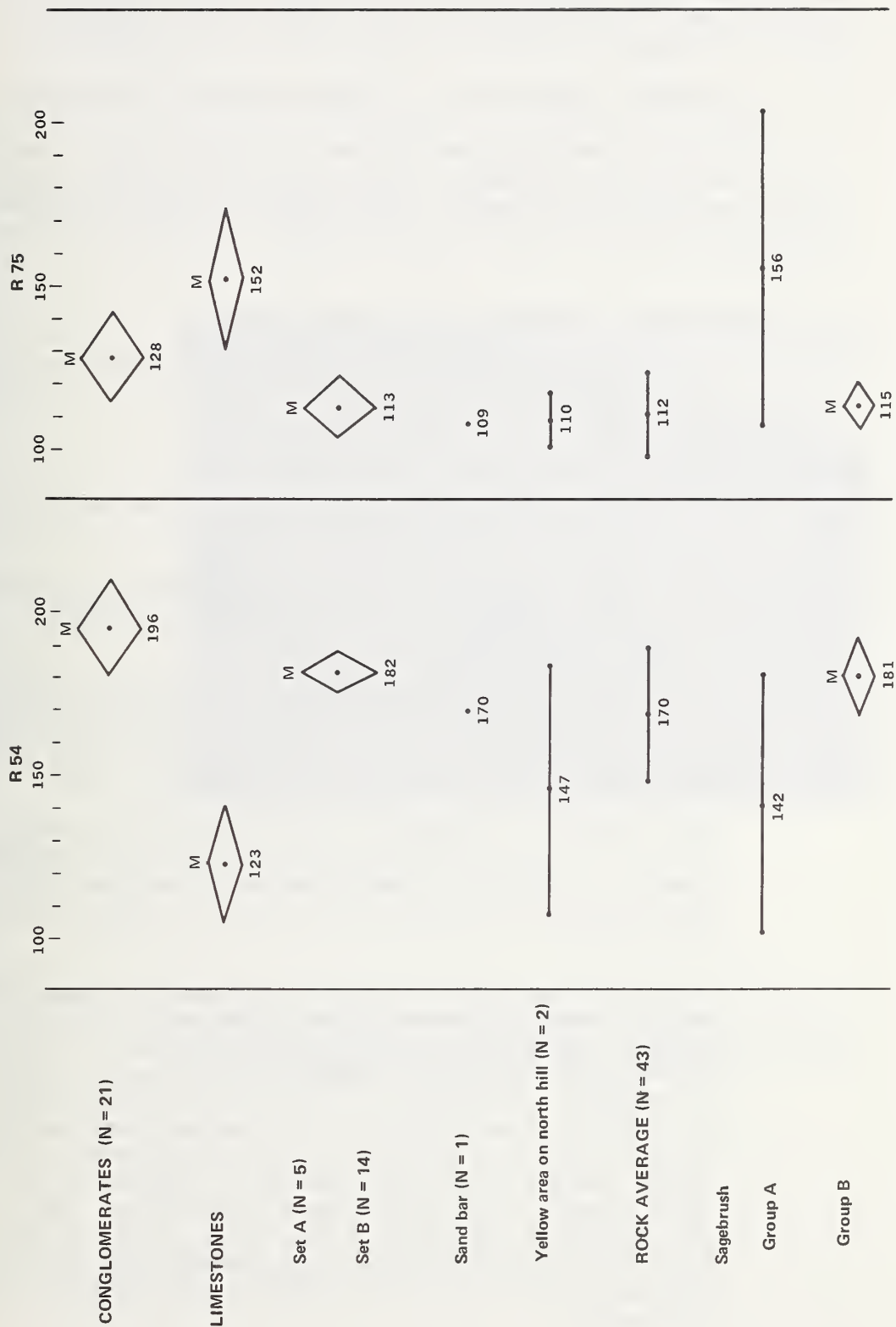
Figure 54. Bar graph of spread of group ratio means of R 54 and R 75 ratios on the abscissa. The horizontal extent of the symbol indicates the 1 σ spread. The ordinate is artificial and represents an attempt to portray the size of "N" of each group to give some meaning to the standard deviation spread.

Ground measurements of the kind detailed above should enable one to predict the image contrast on later flight imagery and aid in selection of multispectral scanner bands to be composited for better enhancement in the final three-band color presentations.

2.4 Supplemental Information on Exotech Reflectance Measurements

The field instrumentation used was two Exotech four-channel radiometers which are filtered to match the four LANDSAT satellite filters and a Fluke multimeter (Type 8,000) for digital readout of the eight channels (four upward-viewing, four downward-target viewing).

The principal advantage of the units are:

* Very portable, weighing about four pounds for each unit.

* Battery powered (rechargeable).

* Solid rugged design, using solid state amplifiers and silicon detectors.

The total system, including a standard reflectance panel can be easily carried by two men over average terrain. A typical measurement profile involves the following:

1. Mount the Exotech radiometer with the diffusing disks on the upward-viewing unit to measure the 2π irradiance of the infalling sunlight. The 15° field-of-view (FOV) lenses are usually used for these close-up views.

2. Mount downward-viewing unit in proximity to the other unit to view the reflectance standard (we used FIBERFRAX sheets, a refractory fiber sheet which has good photo-metric properties and a 90+% reflectance between 400nm and $2.5\mu m$).

3. Attach the swith box and Fluke multimeter to record the digital output (the switch box allows one to switch rapidly from Channel 4-up to Channel 4-down; to 5-up to 5-down, etc. All eight channels can be read in about 30 seconds). Figure 55 is a typical calibration setup. Each of the up and down pairs of readings required for reflectance ratios are made within ten seconds of each other, greatly alleviating the drift effects due to rapid changes in the atmospheric transmission - at least those on the order of one minute or so, commonly found affecting reflectance measurements made with the ISCO spectroradiometer which take at least five minutes to compile.

274

Figure 55. This photograph shows the dual radiometer calibration configuration used in in the field measurement program. The radiometer on the right is pointed vertically to measure sky irradiance. The instrument on the left is pointed downward to measure reflected energy from a FIBERFRAX panel on the ground.

4.   Measurements are recorded while viewing FIBERFRAX to
      determine the local inter-calibration between 2π
      irradiance and 15° FOV reflected irradiance. A straight
      line relationship, with the correlation R = 0.95, is
      usually observed in these types of standard measure-
      ments. (On this particular day, intermittent snow and
      rapidly changing cloud patterns caused a marked departure
      from the ideal.)

5.   Where outcrops could be observed directly the FIBERFRAX
      panel was removed and the double unit (Exotech radio-
      meters) placed on the outcrop.

6.   Most of the data was taken with the double unit assembled
      so that each radiometer was on a tripod. The 2π
      upward-viewing unit was placed vertically, diffusing
      disks upward. The target unit now changed to a 1° FOV
      was used like a TV camera to view selected targets
      at
      varying distances using the calibrated co-linear 1:1
      telescope as a viewing device. For data recording
      purposes, a 35mm color photo was taken of almost every
      target directly through this telescope.

7.   Software programs were used to reduce the voltage
      output data from each of the eight channels to irradiance
      and radiance values, the ratio of which is <u>hemispherical
      reflectance</u>. This factor is usually lower than those
      of the geometry more normally reported, i.e. bi-direc-
      tional reflectance, which is obtained by using both
      units downward-viewing with the same field-of-view. A
      simple factor, however, relates to numbers.

8.   All reflectance measurements were taken using the
      geometry shown in Figure 56 and calculated to the
      geometry shown in Figure 57 using this factor.

9.   Because of the rapidly changing lighting conditions
      which prevailed during the data collection period, only
      those data acquired during bright sunlit conditions
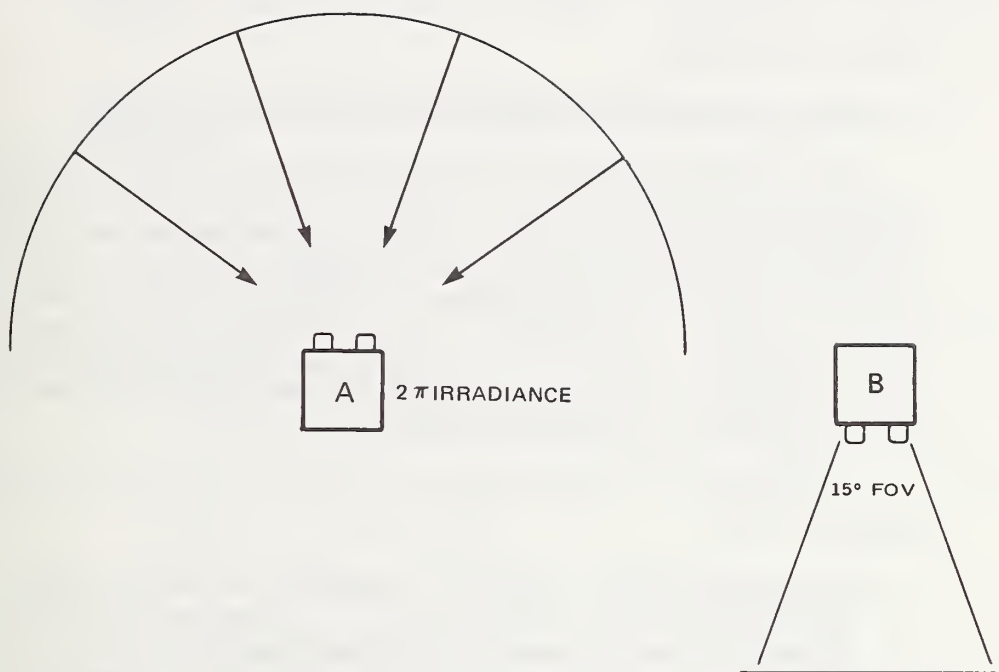   were used for data analysis.

Figure 56 - Radiometer orientation for B/A, hemispherical reflectance measurements.
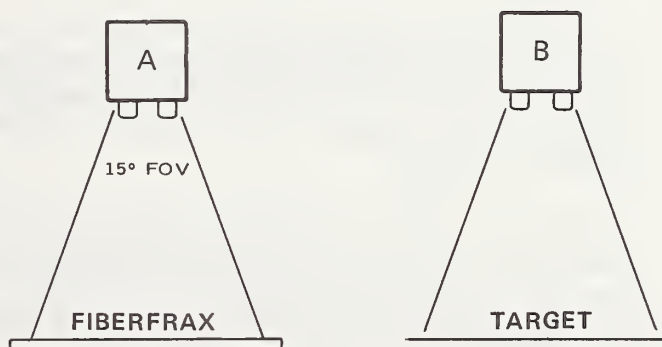

Figure 57 - Radiometer orientation for B/A, bi-directional reflectance measurements.

APPENDIX F

MULTISPECTRAL AND THERMAL INFRARED DATA ACQUISITION AND PROCESSING

1.0 DATA ACQUISITION

1.1 Description of DS-1230/1250 Multispectral Scanner

The thermal infrared and multispectral airborne data acquisition phase of this program utilized the Daedalus DS-1230/1250 multispectral scanner system. This scanner system was designed to provide the capability to quickly change from a dual-channel quantitative thermal infrared scanner to a full eleven-channel multispectral scanner. Therefore, it was possible to provide dual-channel thermal infrared data during the hours of darkness and eleven channels of multispectral data during daylight hours on both the eastern and western test sites.

The complete system consists of the following major components:

Scan Head & Gyro. The dual-channel scan head contains two detector mounts, focusing optics, a dichroic mirror to divide the energy beam to the two detector systems, rotating assembly consisting of the scanning mirror, sync generator slugs and drive motor, and the reference source(s).

The roll correction system includes an on-head mounted military specification vertical gyro assembly.

Detectors. In this investigation, two 8-14 μm tri-metal (Hg, Cd, Te) detectors were used for the thermal studies. A ten-channel spectrometer head and one thermal detector was used for other phases of data acquisition.

The ten-channel spectrometer head contains the detector array, solid-state planar diffuse silicon photodiodes which cover the .38-1.10 μm region, pre-amplifier electronics, and imaging optics which focus the collected energy into the detector array.

Data Recording. In-flight data recording is accomplished by employing a wideband Group II FM magnetic tape recorder. The tape recorder carries 9200 feet of 1" 14-track and at 30 ips permits one hour of full multispectral recording.

Other Components. Other major electronic components which are required to complete the system are: Spectrometer

278

Control Console, Scanner Control Console, and Power Distrib-
utor and Reference Source Controller.

The reference source controller maintains pre-set tempera-
tures to the calibration sources (blackbody temperature ref-
erences) located on the scan head. Temperature readout is in
C° and indicates 0.1 degree.

The basic operating parameters of the system are as
follows:

Operating Wavelength	.38-14.0 μm
Aperture	five-inches
Focal Length	six-inches
Optical Aperture (effective)	f/2
Scan Rate	80 scans per second
Total Field of View	87°20'
Gated Field of View	77°20'
Instantaneous Field of View	Infrared: 2.5 or 1.7 mrad
	Visible: 2.5 mrad
Temperature Resolution	Infrared: 0.2°C
V/H	.2
Roll Correction	Total: ±10°; Unvig-netted: +5°
Reference Sources	Infrared: two con-trollable thermal blackbodies
	Visible: one fixed voltage broadband visible/IR light source
Reference Range	Infrared: -10°C to +40°C with respect to scan head heat sink
	Visible: .35 - 1.2 μm
Temperature Sensor Indicator Range	Infrared: -10°C to +50°C

1.2 Spectral Configurations Used

In order to provide optimum multispectral data for geologic
analysis of the tunnel sites, the DS-1250 scanner was configured
for different spectral recording during the day and night flights.
The daytime flights utilized one infrared detector and the ten-
channel spectrometer with the standard dichroic filter. This
configuration provides the following spectral response for each of
the eleven channels:

Channel	Spectral Region	Channel	Spectral Region
1	.38 - .42 μm	7	.65 - .69 μm
2	.42 - .45 μm	8	.70 - .79 μm
3	.45 - .50 μm	9	.80 - .89 μm
4	.50 - .55 μm	10	.92 - 1.10 μm
5	.55 - .60 μm	11	8.0 -12.5 μm
6	.60 - .65 μm		

Figure 58 is a cross-section of the scan head showing the configuration of detectors and filters for the daytime flights.

For the night flights it was desired to divide the normal 8-14 μm thermal infrared window into two regions, 8-10 μm and 10-12 μm, in order to investigate the possibility of discriminating rock types on the basis of emissivity differences in these two bands. Therefore, a special dichroic filter was manufactured to accomplish this division and detectors and optical filters were chosen to provide the best possible match in terms of efficiency. The resulting efficiency values for the two bands were as follows:

8-10 μm Region

        Average detector response   = 90%
        Average filter transmission   = 90%
        Average dichroic reflectance = 99%; or
        .90 x .90 x .99 = 80% efficient.

10-12 μm Region

        Average detector response   = 90%
        Average dichroic transmission = 90%; or
        .90 x .90 = 81% efficient.

Considering the 50% points of each band, the actual spectral coverage was as follows:

    8.2 - 10.2 μm for the nominal 8-10 μm region.
    10.3 - 12.5 μm for the nominal 10-12 μm region.

Figure 59 is a cross-section of the scan head showing the configuration of detectors and filters for the night flight.

Figure 60 is a graphic representation of the relative spectral response of each of the detector/filter combinations.

1.3 Scanner Operation

The in-flight operation of the DS-1230/1250 multispectral scanner system is performed from the master control console. This console contains controls for all electrical power to the
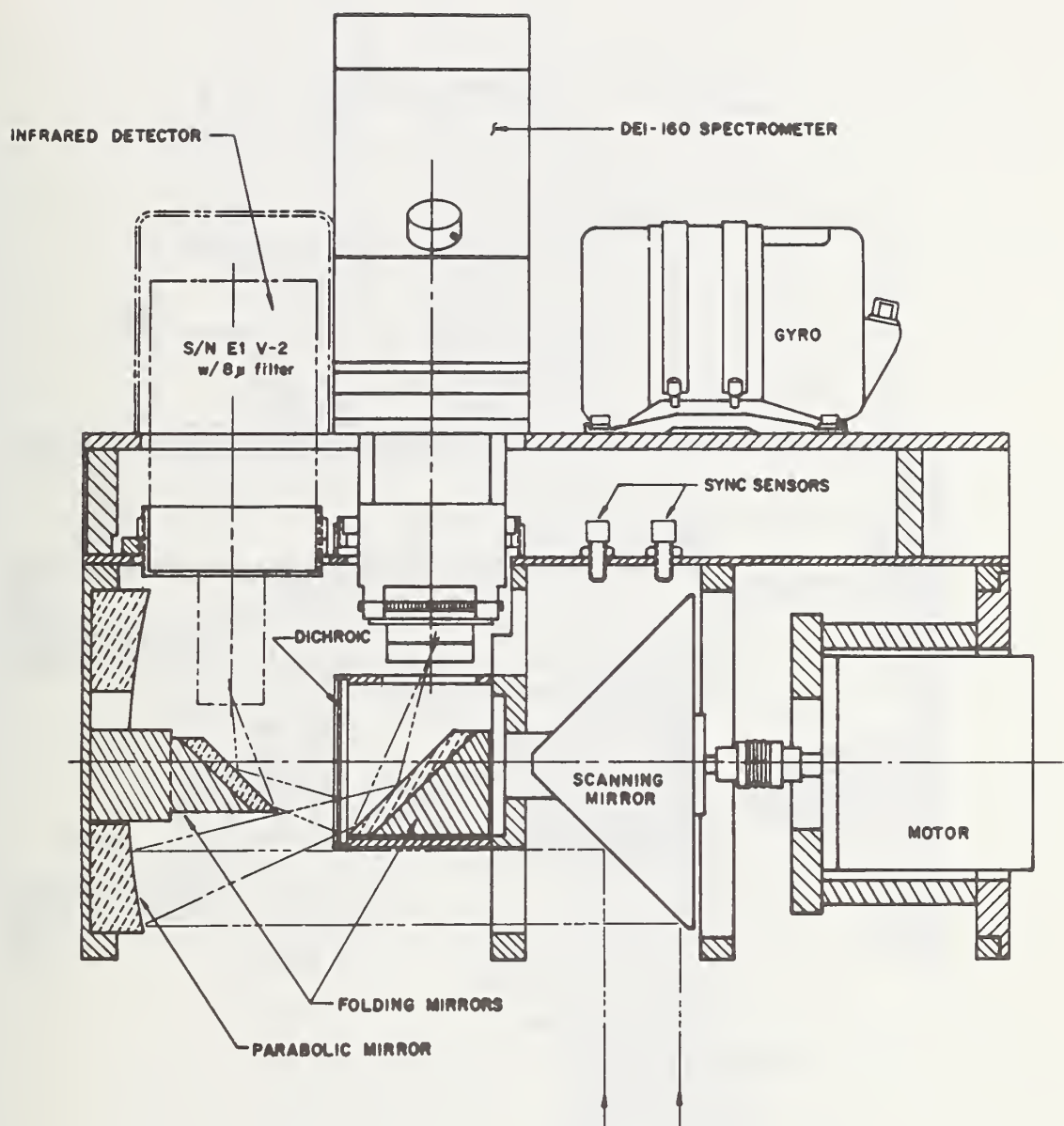
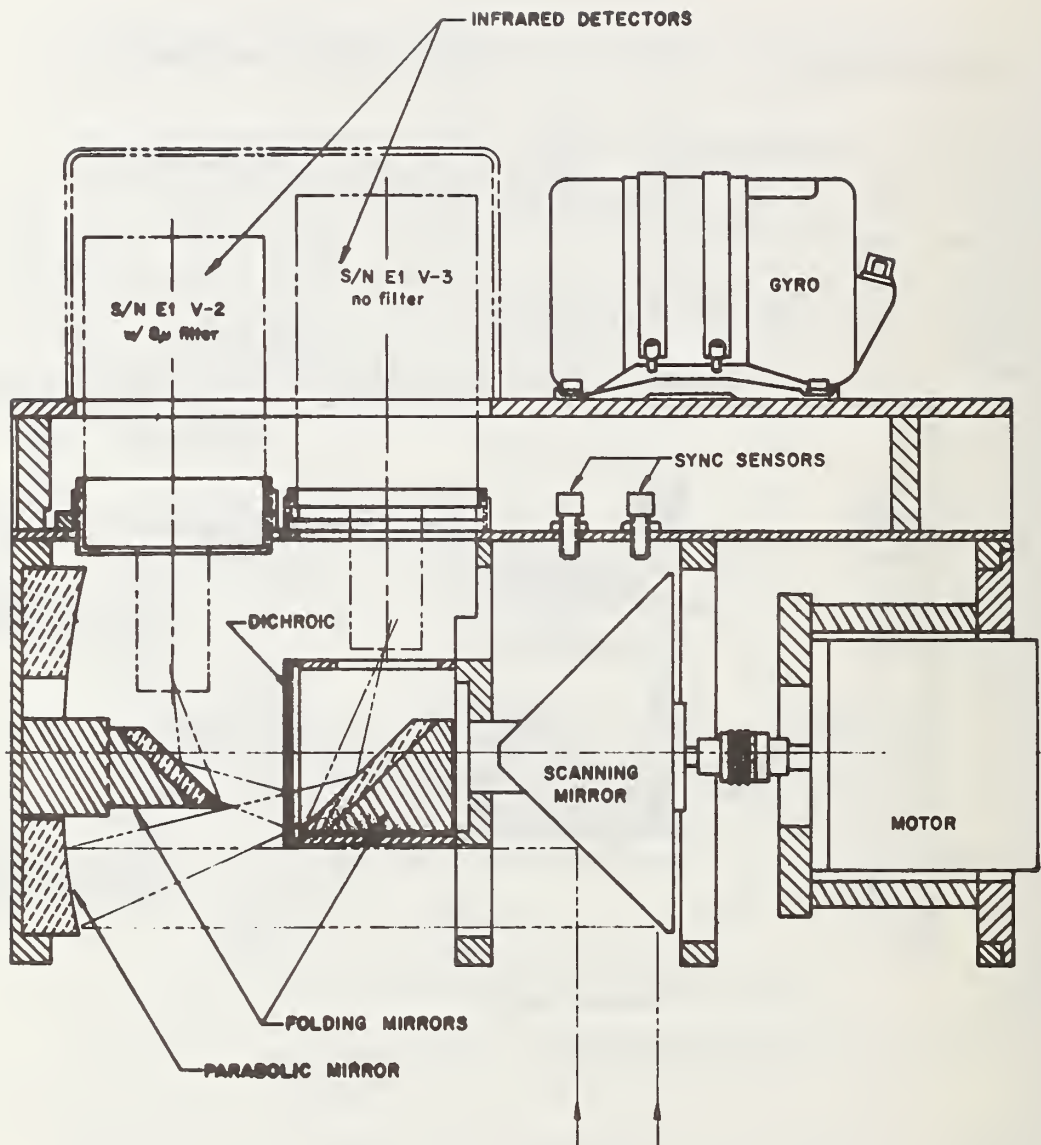Figure 58 - Scanner Configuration - DOT Tunnel Study - Day Flights.

281

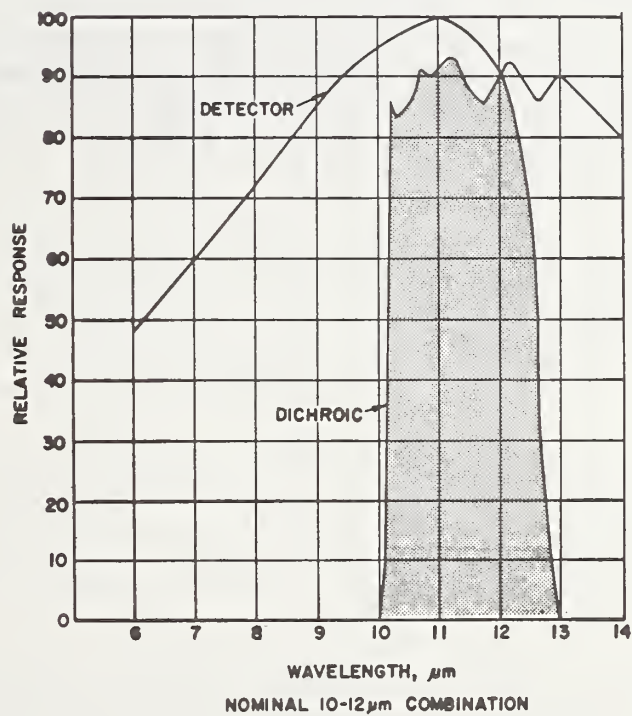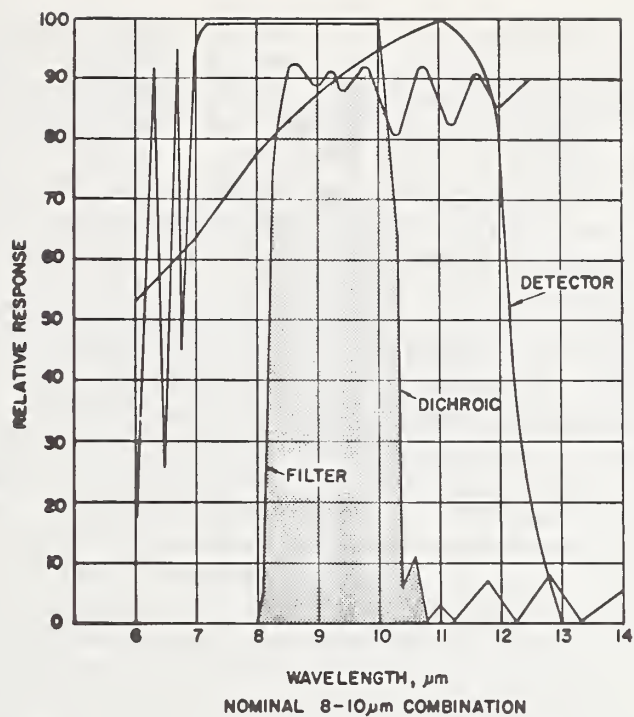Figure 59 - Scanner Configuration - DOT Tunnel Study - Night Flights.

Figure 60 - Relative Spectral Response of Detector/Filter Combinations.

major system components and for remote control of the magnetic tape recorder. The operator's console contains a dual-channel oscilloscope for monitoring the video signals from the detectors. In the dual channel configuration, the operator continuously monitors the output of both detectors. In the eleven-channel multispectral configuration the operator has the option of either static monitoring of any two channels or automatically sequencing through all eleven channels with each channel displayed for approximately ten seconds at a time. In all cases, the operator monitors the signals from the reproduce heads of the tape recorder so that the signals he sees have already been recorded on magnetic tape. In this manner, the operator can be sure that he has a good tape recording of the signals from the detectors.

The initial setup of each channel of the scanner is also facilitated by the use of the in-flight monitor scope. The operator can see not only the detector output from each scan across the terrain, but also the reference sources are temperature controlled blackbody radiators for the infrared detectors and a calibrated broad spectrum lamp for the spectrometer detector. The operator uses the reference sources to establish the optimum amplifier gain and DC level for each of the detector outputs in order to faithfully record the entire dynamic range of signal on magnetic tape.

All of the amplifier settings are recorded on a flight log by the operator for each flight line. In addition to these settings, the flight log contains flight line identification, time, altitude, speed, and heading information; all of which is used during playback to reconstruct the scene viewed by the scanner.

2.0 DATA PROCESSING

2.1 Description and Operation of DS-1850 Multispectral Ground Station

All of the magnetic tape playback of the data from the Tunnel Study multispectral scanner flights was performed on the DS-1850 ground station illustrated in Figure 61. This playback system is specifically designed to handle data recorded by the DS-1250 multispectral scanner and incorporates a number of features to automate the data handling.

A flow diagram showing the components and processing steps involved in the DS-1850 data processor is illustrated in Figure 62. The basis of this processing approach, is that the interpretability of multispectral data can frequently be improved by examining ratios of the signals from various channels rather than the raw signals themselves.

The first step in the pre-processor is the formation of signals A and B from combinations of any or all of the available spectral channels. This is accomplished by first phase adjusting each channel to correct any registration errors across channels[1] which may have been introduced by the tape recorder and then calibration of the signal amplitude through the use of the internal calibration reference signals to bring all signals to the same power reference base. Any combination of spectral channels can then be created by activation of a four-position switch for each channel on the pre-processor front panel.

Once signals A and B have been formed, a function switch allows them to be transformed into a resultant output signal representing either the product AB, the difference A-B, the ratio A/B, or the difference ratio (A-B)/B. Since any combination of spectral signals can be used to form the signals A and B, the flexibility of the system in terms of spectral comparisons which can be made is almost unlimited.

When the desired spectral function is obtained, the output signal may either be supplied directly to the DEI-616 printer for film recording or to the post-processor, DEI-612, for calibration and digitization prior to printing. In the case of ratio, difference, or product signals, the post-processor would allow the

---

[1] The analysis conducted during this study necessitated the running of the taped data many hundreds of times. Stretching of the tape occurred creating some registration problems. On future research projects of this type a duplicate tape should be made for the routine experimentation.
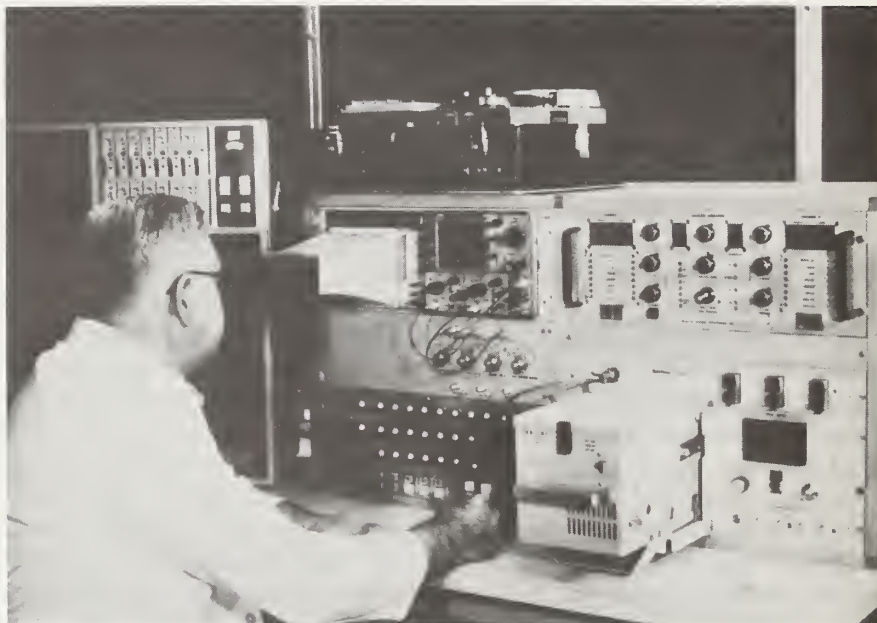
285

Figure 61 - The DS-1850 ground station provides a wide range of functions for processing of the analog recorded multispectral data. The unit protruding on the right is the film magazine used for making film copy of the imagery.
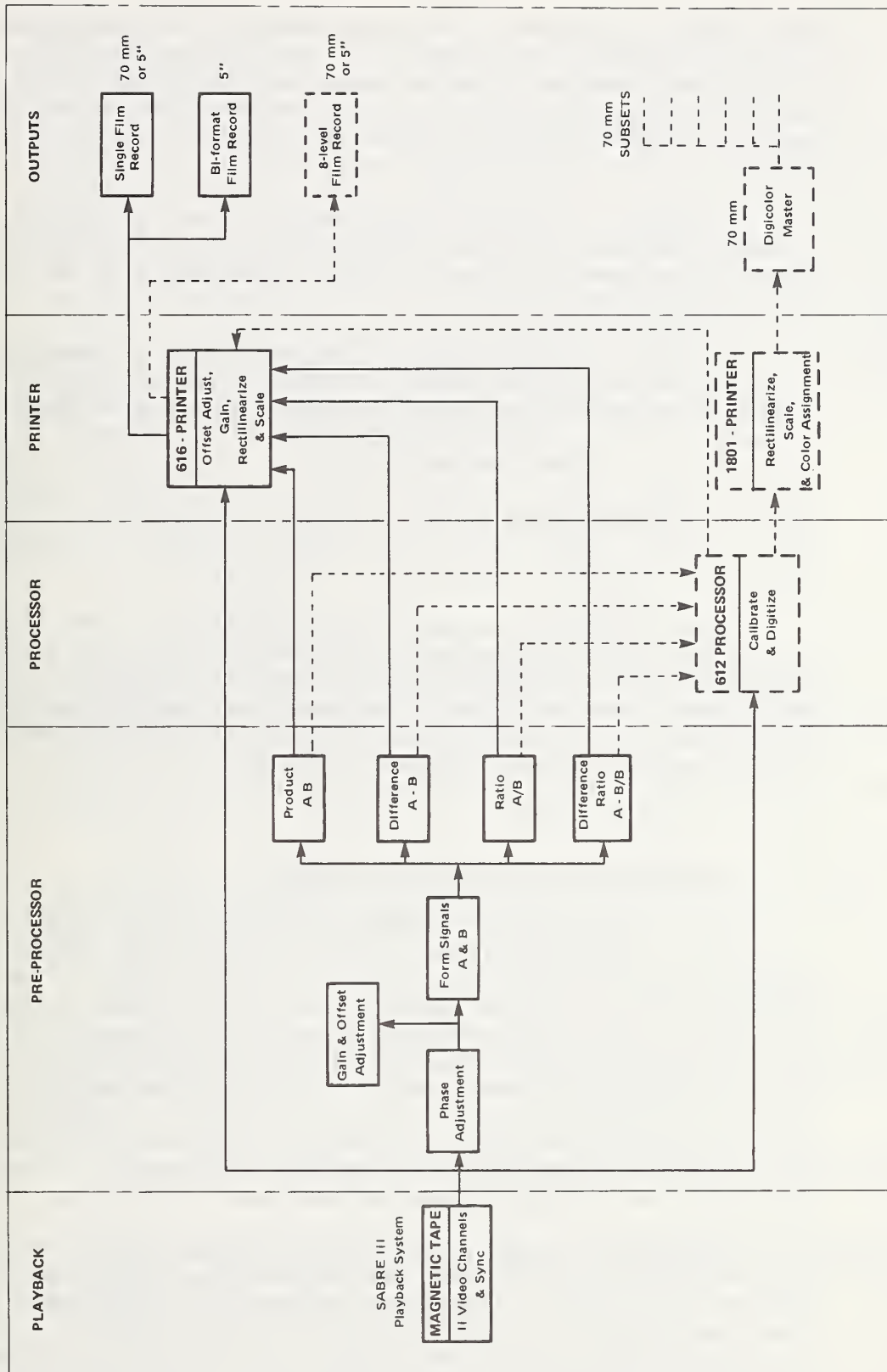
Figure 62 - Flow diagram of the components and processing steps in the DS-1850 data processor.

287

total range of derived values to be divided into eight discrete ranges for printing on either black-and-white or color film. With careful spectral function selection, this would permit the automatic display of desired terrain features in a pre-selected density on black-and-white film or as a specified color on color film.

The range of possible outputs varies from a single spectral channel printed on 70 mm or five-inch film to a complete set of color separations on 70 mm color film, depending upon the desires of the console operator.

The DEI-616 printer records the signal data by means of a fiber optics-cathode ray tube. Permanent records are obtained on either direct print paper or photographic film. The printer has a removable film cassette which provides either 70 mm or five-inch film on an interchangeable basis. The fiber optics face plate transmits the light beam from the inner phosphor coating of the CRT to the polished outer surface with negligible diffusion. This permits a sharp image to be exposed on paper or film which moves continuously in close contact with the face of the CRT.

Selectable single or dual channel operation of the printer is provided for by an analog multiplexer and split screen re-cording. This feature permits two channels of multiband data to be recorded side-by-side on five-inch film. An important addi-tional feature is rectilinearized (tangential) scale correction of the sweep to minimize image distortion.

2.2 Multispectral Processing Algorithms

One of the processor's primary functions is to establish repeatable, calibrated video signal levels from the ground scene relative to known voltage references. If the video is from a quantitative line scanner which contains two calibrated thermal reference sources, the output voltages from the thermal sources provide the calibration standardization and all video levels can be assigned absolute temperatures. If the scanner does not contain calibrated thermal sources, the video is compared to preset calibratation voltages within the processor to yield repeat-able relative video thermal assignments which are not directly related to an absolute temperature scale.

In addition to providing calibrated video, the signal pro-cessor also includes several methods for enhancing the presen-tation of the ground scene video information. These enhancements, when used properly, can help speed data interpretation, emphasize important details within the imagery especially for untrained observers, and improve understandability of data presentation in

reports. The signal processor is primarily a digital device which generates several calibrated levels within the full references voltage range in the 8 Level mode of processing. Each calibrated level prints as a uniform gray level on film (eight levels were chosen as a practical maximum number of gray scales which can be distinguished when widely separated on film). An ISOLEVEL mode prints out a single one of the calibrated levels as black on a white background; for example, one which might represent all areas between 32°C and 33°C. A CONTOUR mode prints dark for 20 micro-seconds after transition between any adjacent levels, resulting in contour lines of constant temperatures. The isolevel or contour line can be superimposed upon reduced-amplitude normal video in the ANALOG mode of operation to provide a spatial reference background. The available modes are summarized below with correspondence between DIGITAL and ANALOG modes indicated:

SIGNAL PROCESSOR MODES

Digital Modes	Analog Modes
8 Level	Analog
Isolevel	Anal/Iso
Contour	Anal/Ctr

Usefulness of the 8-LEVEL, ISOLEVEL, and CONTOUR modes depends upon the character of the input video signal since too many transitions between levels may destroy the continuity of the enhanced presentation. Thus, it is very important that the operator recognize the types of video and the processor modes and settings which are likely to yield the most useful results.

The DEI-612 signal processor is also designed to combine two video signals through an analog processor that performs such functions as AB, A/B, (A-B/B), A-B, and B-A.

Many combinations of processor mode and analog function algorithms were used on the DOT Tunnel data from both test sites. In general, it was found that the 8-level and isolevel modes were most useful with single channel thermal infrared data, while most of the multispectral ratio data were displayed in analog image form.

The contour mode proved to be especially useful in analyzing patterns of linears on the test sites.

The following tables are a listing of the various types of processing performed on the multispectral and thermal data during the analysis and interpretation.

Table 16 MULTISPECTRAL AND THERMAL INFRARED DATA PROCESSING PERFORMED: CARLIN CANYON TUNNEL SITE

ID IMAGE	FLIGHT NO.	FLIGHT LINE	DAY/NIGHT	SPECTRAL BANDWIDTH (μm)	ALGORITHM	COMMENTS
1	1	A	NIGHT	8-10		
2	1	A	NIGHT	10-12		
3	1	D	NIGHT	8-10		
4	1	D	NIGHT	10-12		
5	1	A	NIGHT	8-10	8-LEVEL	0-18°C
6	1	A	NIGHT	8-10	CONTOUR	0-18°C
7	1	D	NIGHT	8-10	8-LEVEL	0-18°C
8	1	D	NIGHT	10-12	8-LEVEL	0-18°C
9	1	D	NIGHT	$\dfrac{(10-12)-(8-10)}{8-10}$	DIFFERENCE RATIO	
10	1	D	NIGHT	$\dfrac{8-10}{10-12}$		
11	1	D	NIGHT	$\dfrac{(8-10)-(10-12)}{10-12}$	DIFFERENCE RATIO	
12	1	D	NIGHT	8-10	CONTOUR	0-18°C
13	1	D	NIGHT	$\dfrac{8-10}{10-12}$	ANALOG RATIO	
14	1	E	NIGHT	10-12		
15	1	E	NIGHT	10-12		
16	1	E	NIGHT	8-10		
17	1	E	NIGHT	8-10	8-LEVEL	0-18°C
18	1	E	NIGHT	10-12	8-LEVEL	0-18°C
19	1	E	NIGHT	$\dfrac{8-10}{10-12}$	ANALOG	
20	2	A	DAY	8-10		
21	2	A	DAY	10-12		

Table 16   MULTISPECTRAL AND THERMAL INFRARED DATA PROCESSING PERFORMED: CARLIN CANYON TUNNEL SITE—Contd.

ID IMAGE	FLIGHT NO.	FLIGHT LINE	DAY/NIGHT	SPECTRAL BANDWIDTH (μm)	ALGORITHM	COMMENTS
22	2	A	DAY	8–10	8–LEVEL	10–46°C
23	2	A	DAY	8–10	CONTOUR	10–46°C
24	2	D	DAY	8–10		
25	2	D	DAY	10–12		
26	2	D	DAY	8–10	8–LEVEL	10–28°C
27	2	D	DAY	8–10	8–LEVEL	10–46°C
28	2	D	DAY	8–10	8–LEVEL	22–40°C
29	2	D	DAY	8–10	8–LEVEL	28–46°C
30	2	D	DAY	10–12	8–LEVEL	10–46°C
31	2	D	DAY	$\dfrac{(10-12)-(8-10)}{8-10}$	DIFFERENCE RATIO	
32	2	D	DAY	$\dfrac{(8-10)-(10-12)}{10-12}$		
33	2	D	DAY	8–10	CONTOUR	10–46°C
34	2	D	DAY	8–10	CONTOUR	22–40°C
35	2	D	DAY	$\dfrac{8-10}{10-12}$	ANALOG	
36	2	E	DAY	8–10		
37	2	E	DAY	8–10		
38	4	A	DAY	.38 – .42		
39	4	A	DAY	.42 – .45		
40	4	A	DAY	.45 – .50		
41	4	A	DAY	.50 – .55		
42	4	A	DAY	.55 – .60		
43	4	A	DAY	.60 – .65		
44	4	A	DAY	.65 – .69		

Table 16 MULTISPECTRAL AND THERMAL INFRARED DATA PROCESSING PERFORMED: CARLIN CANYON TUNNEL SITE--Contd.

ID IMAGE	FLIGHT NO.	FLIGHT LINE	DAY/NIGHT	SPECTRAL BANDWIDTH (µm)	ALGORITHM	COMMENTS
45	4	A	DAY	.70 - .79		
46	4	A	DAY	.80 - .89		
47	4	A	DAY	.92 -1.10		
48	4	A	DAY	8-12		
49	4	D	DAY	.38 - .42		
50	4	D	DAY	.42 - .45		
51	4	D	DAY	.45 - .50		
52	4	D	DAY	.50 - .55		
53	4	D	DAY	.55 - .60		
54	4	D	DAY	.60 - .65		
55	4	D	DAY	.65 - .69		
56	4	D	DAY	.70 - .79		
57	4	D	DAY	.80 - .89		
58	4	D	DAY	.92 -1.10		
59	4	D	DAY	8-12		
60	4	D	DAY	Subsets 1, 2, 3 .60 - .69	8-LEVEL	
61	4	D	DAY	Subsets 4, 5, 6 .60 - .69	8-LEVEL	
62	4	D	DAY	8-12 - (.10-.79)	ANALOG	
63	4	D	DAY	8-12 - .55-.60	ANALOG	
64	4	E	DAY	.38 - .42		
65	4	E	DAY	.42 - .45		
66	4	E	DAY	.45 - .50		
67	4	E	DAY	.50 - .55		
68	4	E	DAY	.55 - .60		

Table 16 MULTISPECTRAL AND THERMAL INFRARED DATA PROCESSING PERFORMED: CARLIN CANYON TUNNEL SITE–Contd.

ID IMAGE	FLIGHT NO.	FLIGHT LINE	DAY/NIGHT	SPECTRAL BANDWIDTH (μm)	ALGORITHM	COMMENTS
69	4	E	DAY	.60 – .65		
70	4	E	DAY	.65 – .69		
71	4	E	DAY	.70 – .79		
72	4	E	DAY	.80 – .89		
73	4	E	DAY	.92 –1.10		
74	4	E	DAY	8–12		
75	5	D	PREDAWN	8–10		
76	5	D	PREDAWN	10–12		
77	1	D	NIGHT	$\dfrac{8-10^2}{10-12}$ 8–10² – 10–12	RATIO	
78	1	D	NIGHT	8–10	SUBSET 5 8-LEVEL	12–15°C
79	1	D	NIGHT	8–10	SUBSET 4&5 B-LEVEL	9–15°C
80	1	D	NIGHT	8–10	MASTER ISO LEVEL 5	
81	1	D	NIGHT	8–10	ANALOG ISO LEVEL	12–15°C
82	2	D	DAY	8–10	SUBSET 4,5,6 CONTOUR	28–46°C
83	2	D	DAY	8–10	SUBSET 3-4 CONTOUR	22–34°C
84	2	D	DAY	8–10	MASTER ANALOG CONTOUR	10–46°C
85	2	D	DAY	8–10	ANALOG CONTOUR SUBSET 4,5,6	28–46°C
86	4	D	DAY	$\dfrac{.60 - .69}{.80 - .89}$	RATIO	
87	4	D	DAY	$\dfrac{.60 - .69}{.70 - .79}$	RATIO	

Table 16   MULTISPECTRAL AND THERMAL INFRARED DATA PROCESSING PERFORMED: CARLIN CANYON TUNNEL SITE—Contd.

ID IMAGE	FLIGHT NO.	FLIGHT LINE	DAY/NIGHT	SPECTRAL BANDWIDTH (µm)	ALGORITHM	COMMENTS
88	4	D	DAY	.60 – .69 / .50 – .60	RATIO	
89	4	D	DAY	.60 – .69 / .45 – .55	RATIO	
90	4	D	DAY	.50 – .55 / .80 – .89	RATIO	
91	4	D	DAY	.55 – .60 / .80 – .89	RATIO	
92	4	D	DAY	.42 – .45 / .55 – .65	RATIO	
93	5	A	PREDAWN	8-10	ANALOG	
94	5	A	PREDAWN	8-10	MASTER 8-LEVEL	
95	5	A	PREDAWN	8-10	MASTER ANALOG/CONTOUR	
96	5	A	PREDAWN	8-10	ANALOG	
97	5	A	PREDAWN	8-10	MASTER 8-LEVEL	
98	5	A	PREDAWN	8-10	MASTER ANALOG CONTOUR	
99	5	D	PREDAWN	8-10 / 10-12	RATIO	
100	4	D	DAY	.60 – .65 / .45 – .50	RATIO	
101	5	E	PREDAWN	10-12 / 8-10	RATIO	
102	5	D	PREDAWN	10-12 / 8-10	RATIO	
103	5	C	PREDAWN	10-12 / 8-10	RATIO	
104	5	B	PREDAWN	10-12 / 8-10	RATIO	

Table 16 MULTISPECTRAL AND THERMAL INFRARED DATA PROCESSING PERFORMED: CARLIN CANYON TUNNEL SITE—Contd.

ID IMAGE	FLIGHT NO.	FLIGHT LINE	DAY/NIGHT	SPECTRAL BANDWIDTH(μm)	ALGORITHM	COMMENTS
105	1	B	NIGHT	$\frac{10-12}{8-10}$	RATIO	
106	1	C	NIGHT	$\frac{10-12}{8-10}$	RATIO	
107	1	D	NIGHT	$\frac{10-12}{8-10}$	RATIO	
108	1	E	NIGHT	$\frac{10-12}{8-10}$	RATIO	
109	4	D	DAY	.42 – .50	ANALOG	
110	4	D	DAY	.45 – .55	ANALOG	
111	4	D	DAY	.50 – .60	ANALOG	
112	4	D	DAY	.60 – .69	ANALOG	
113	4	D	DAY	.65 – .79	ANALOG	
114	4	D	DAY	.70 – .89	ANALOG	
115	4	D	DAY	$\frac{.42 - .45}{.70 - .89}$	RATIO	
116	4	D	DAY	$\frac{.45 - .55}{.65 - .79}$	RATIO	
117	4	D	DAY	$\frac{.50 - .60}{.70 - .89}$	RATIO	
118	4	D	DAY	$\frac{.50 - .60}{.42 - .50}$	RATIO	
119	4	D	DAY	$\frac{.60 - .69}{.70 - .79}$	RATIO	
120	4	D	DAY	$\frac{.60 - .69}{.45 - .55}$	RATIO	

Table 16   MULTISPECTRAL AND THERMAL INFRARED DATA PROCESSING PERFORMED: CARLIN CANYON TUNNEL
SITE—Contd.

ID IMAGE	FLIGHT NO.	FLIGHT LINE	DAY/NIGHT	SPECTRAL BANDWIDTH (μm)	ALGORITHM	COMMENTS
121	4	D	DAY	.60 – .69 / .50 – .60	RATIO	
122	4	D	DAY	.60 – .69 / .80 – .89	RATIO	
123	4	D	DAY	.70 – .79	ANALOG	
124	4	D	DAY	.80 – .89	ANALOG	

Table 17 MULTISPECTRAL AND THERMAL INFRARED DATA PROCESSING PERFORMED: EAST RIVER MOUNTAIN TUNNEL SITE

ID IMAGE	FLIGHT NO.	FLIGHT LINE	DAY/NIGHT	SPECTRAL BANDWIDTH (μm)	ALGORITHM	COMMENTS
1	1	1	DAY	.38 – .42		
2	1	1	DAY	.42 – .45		
3	1	1	DAY	.45 – .50		
4	1	1	DAY	.50 – .55		
5	1	1	DAY	.55 – .60		
6	1	1	DAY	.60 – .65		
7	1	1	DAY	.65 – .69		
8	1	1	DAY	.70 – .79		
9	1	1	DAY	.80 – .89		
10	1	1	DAY	.92 –1.10		
11	1	2	DAY	.38 – .42		
12	1	2	DAY	.42 – .45		
13	1	2	DAY	.45 – .50		
14	1	2	DAY	.50 – .55		
15	1	2	DAY	.55 – .60		
16	1	2	DAY	.60 – .65		
17	1	2	DAY	.65 – .69		
18	1	2	DAY	.70 – .75		
19	1	2	DAY	.80 – .89		
20	1	2	DAY	.92 –1.10		
21	1	3	DAY	.38 – .42		
22	1	3	DAY	.42 – .45		
23	1	3	DAY	.45 – .50		
24	1	3	DAY	.50 – .55		
25	1	3	DAY	.55 – .60		
26	1	3	DAY	.60 – .65		

Table 17   MULTISPECTRAL AND THERMAL INFRARED DATA PROCESSING PERFORMED: EAST RIVER MOUNTAIN TUNNEL
SITE—Contd.

ID IMAGE	FLIGHT NO.	FLIGHT LINE	DAY/NIGHT	SPECTRAL BANDWIDTH (μm)	ALGORITHM	COMMENTS
27	1	3	DAY	.65 – .69		
28	1	3	DAY	.70 – .79		
29	1	3	DAY	.80 – .89		
30	1	3	DAY	.92 –1.10		
31	2	1	DAY	8–10		
32	2	1	DAY	10–12		
33	2	1	DAY	10–12	8–LEVEL	10–30°C
34	2	1	DAY	10–12	CONTOUR	10–30°C
35	2	2	DAY	8–10		
36	2	2	DAY	10–12		
37	2	3	DAY	8–10		
38	2	3	DAY	10–12		
39	2	2	DAY	8–10	CONTOUR	10–30°C
40	2	2	DAY	8–10	CONTOUR	
41	2	2	DAY	8–10	8–LEVEL	10–19°C
42	2	2	DAY	8–10	ANALOG ISOLEVEL	10–18°C
43	2	2	DAY	8–10	8–LEVEL	10–30°C
44	2	3	DAY	8–10	8–LEVEL	10–30°C
45	2	3	DAY	8–10	CONTOUR	10–30°C
46	2	3	DAY	8–10 / 10–12	RATIO	ANALOG
47	3	1	NIGHT	8–10		
48	3	1	NIGHT	10–12		
49	3	1	NIGHT	8–10 / 10–12	RATIO	ANALOG
50	3	1	NIGHT	10–12	8–LEVEL	(–1°)–19°C
51	3	1	NIGHT	10–12	CONTOUR	(–1°)–19°C

298

Table 17 MULTISPECTRAL AND THERMAL INFRARED DATA PROCESSING PERFORMED: EAST RIVER MOUNTAIN TUNNEL SITE—Contd.

ID IMAGE	FLIGHT NO.	FLIGHT LINE	DAY/NIGHT	SPECTRAL BANDWIDTH (μm)	ALGORITHM	COMMENTS
52	3	2	NIGHT	8-10		
53	3	2	NIGHT	10-12		
54	3	2	NIGHT	10-12	8-LEVEL	(-1°)-19°C
55	3	2	NIGHT	10-12	CONTOUR	(-1°)-19°C
56	3	3	NIGHT	8-10		
57	3	3	NIGHT	10-12		
58	3	3	NIGHT	8-10 / 10-12	RATIO/8-LEVEL	
59	3	3	NIGHT	10-12	CONTOUR	(-1°)-19°C
60	3	3	NIGHT	8-10 x 10-12	PRODUCT/8-LEVEL	
61	3	3	NIGHT	10-12	8-LEVEL	(-1°)-19°C
71	1	3	DAY	.60 - .69 / .60 - .65	RATIO	
72	1	3	DAY	.60 - .69 / .55 - .60	RATIO	
73	1	3	DAY	.60 - .69 / .50 - .55	RATIO	
74	1	3	DAY	.60 - .69 / .45 - .50	RATIO	
75	1	3	DAY	.60 - .69 / .45 - .55	RATIO	
76	1	3	DAY	.60 - .69 / .50 - .60	RATIO	
77	1	3	DAY	.60 - .69 / .70 - .79	RATIO	
78	1	3	DAY	.60 - .69 / .80 - .89	RATIO	

Table 17 MULTISPECTRAL AND THERMAL INFRARED DATA PROCESSING PERFORMED: EAST RIVER MOUNTAIN TUNNEL SITE—Contd.

ID IMAGE	FLIGHT NO.	FLIGHT LINE	DAY/NIGHT	SPECTRAL BANDWIDTH (μm)	ALGORITHM	COMMENTS
79	3	2	NIGHT	10–12	ANALOG ISOLEVEL 5	12–15°C
80	3	2	NIGHT	10–12	ANALOG ISOLEVEL 4	9–12°C
81	3	3	NIGHT	10–12	ANALOG ISOLEVEL 5	12–15°C
82	3	3	NIGHT	10–12	ANALOG ISOLEVEL 4	9–12°C
83	3	3	NIGHT	10–12	SUBSET 4–5 ISOLEVEL 5	11°C
84	3	3	NIGHT	10–12	SUBSET 4–5 ISOLEVEL 6	12°C
85	3	3	NIGHT	10–12	SUB 5–6 ISOLEVEL 1	12°C
86	3	3	NIGHT	10–12	SUB 5–6 ISOLEVEL 2	13°C
87	3	3	NIGHT	10–12	SUB 4–5 ISOLEVEL 1	9°C
88	3	3	NIGHT	10–12	SUB 4–5 ISOLEVEL 2	9°C
89	3	3	NIGHT	10–12	SUB 4–5 ISOLEVEL 3	10°C
90	3	3	NIGHT	10–12	MASTER ISOLEVEL 3	6–9°C
91	3	3	NIGHT	10–12	SUB 3–4 ISOLEVEL 6	8°C
92	3	3	NIGHT	10–12	SUB 3–4 ISOLEVEL 5	8°C
93	3	3	NIGHT	10–12	SUB 4–5 ISOLEVEL 4	10°C

Table 18 MULTISPECTRAL AND THERMAL INFRARED DATA PROCESSING PERFORMED: BIG WALKER MOUNTAIN TUNNEL SITE

ID IMAGE	FLIGHT NO.	FLIGHT LINE	DAY/NIGHT	SPECTRAL BANDWIDTH (μm)	ALGORITHM	COMMENTS
62	2	1	DAY	8-10		
63	2	1	DAY	10-12		
64	2	1	DAY	10-12	CONTOUR	10-30°C
65	2	1	DAY	10-12	8-LEVEL	10-30°C
66	3	1	NIGHT	8-10		
67	3	1	NIGHT	10-12		
68	3	1	NIGHT	10-12	8-LEVEL	1-21°C
69	3	1	NIGHT	10-12	CONTOUR	1-21°C
70	3	1	NIGHT	10-12 / 8-10	RATIO	ANALOG
94	2	1	DAY	10-12 / 8-10	8-LEVEL RATIO	
95	2	1	DAY	10-12 / 8-10	ANALOG RATIO	
96	2	1	DAY	8-10 x 10-12	8-LEVEL PRODUCT	
97	2	1	DAY	8-10 x 10-12	ANALOG PRODUCT	
98	2	1	DAY	10-12	1-7 MASTER ISO 1	10-13°C
99	2	1	DAY	10-12	1-7 MASTER ISO 2	10-16°C
100	3	1	NIGHT	10-12	1-8 MASTER ISO 2	4-8°C
101	3	1	NIGHT	10-12	1-8 MASTER ISO 3	8-11°C

APPENDIX G

AIRBORNE ELECTROMAGNETIC SYSTEM (DIGHEM)

1.0 INTRODUCTION

The name, DIGHEM is an acronym derived from "digital-helicopter-electromagnetic". Basically, DIGHEM is an audio-frequency (918 Hz), double-dipole electromagnetic system consisting of a transmitter-receiving system mounted in a 30 foot (9m) fiberglass tube commonly called a "bird." The transmitter coil is located at one end of the bird and mounted vertically with its axis parallel to the flight direction. The three receiver coils are mounted at the opposite end of the bird, at right angles to each other as shown in Figure 63. A signal broadcast by the transmitter may be affected by differences in conductivity of the near-surface material of the earth and eddy currents generated. The receiver coils measure the three mutually perpendicular space components of the anomalous field.

A DIGHEM survey (Figure 64) of 50 line-miles was flown between October 9 and October 22, 1975 over the East River Mountain and Walker Mountain tunnel sites in Virginia and West Virginia.
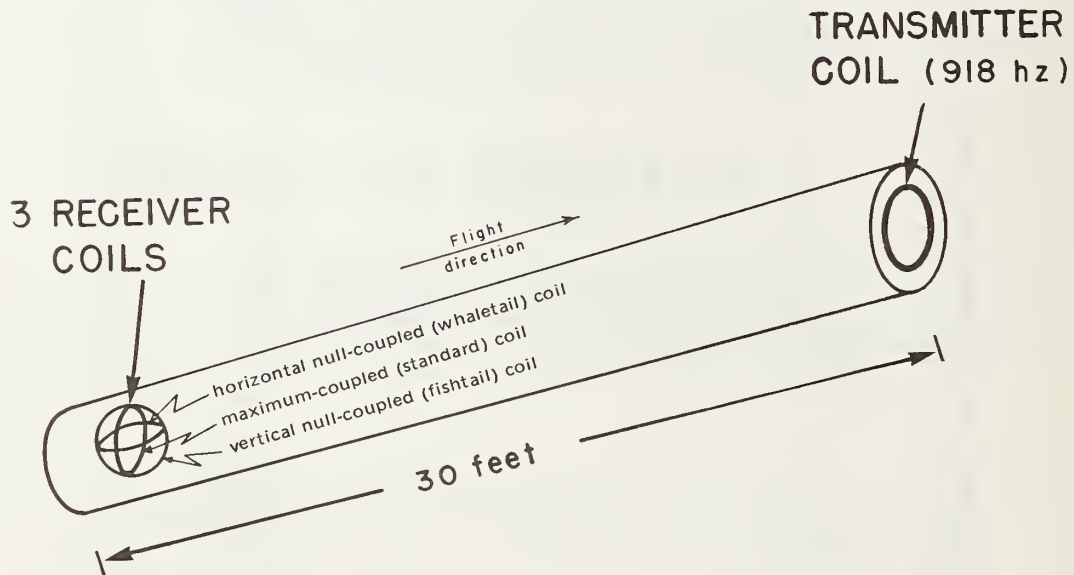
Figure 63 - Transmitter and receiving coil orientation as mounted in the 30-foot (9m) multicoil bird.

Figure 64 - Dighem system flying an electromagnetic survey

303

2.0 SURVEY DESCRIPTION

The survey was conducted with an Alouette II jet helicopter, C-GNQX, which flew with an average airspeed of 60 mph and EM bird height of 130 feet. Ancillary equipment consisted of a Barringer Research Limited AM-104 magnetometer with its bird at an average height of 180 feet, a Bonzer radaraltimeter, Geocam sequence camera, 60 hz monitor, MFE eight-channel hot pen analog recorder, and a Geometrics G-704 digital data acquisition system with a Facit 4070 punch paper tape recorder. The analog equipment recorded six channels of EM data at approximately 900 hz (or, alternatively, five channels of EM and one of sferics), magnetics and radaraltitude. The digital equipment recorded the magnetic field to an accuracy of one gamma.

The flight record is a roll of chart paper which moves through the recorded console at a speed of 1.5 mm/sec. This provides a ground scale on the flight record in feet/mm which is approximately equal to the helicopter flight speed in mph. Thus, for example, the ground scale of the flight record is approximately 70 feet/mm when the helicopter flies at 70 mph.

The flight record consists of eight channels of information as follows, from top to bottom:

Channel		Time Constant	Scale units/mm	Noise [1]
1	whaletail null coil quadrature	4 sec	2 ppm	2 ppm
2	fishtail null coil quadrature	4 sec	2 ppm	2 ppm
3	maximum-coupled coil inphase	1 sec	5 ppm	5 ppm
4	maximum-coupled coil inphase	4 sec	2 ppm	2 ppm
5 [2]	maximum-coupled coil quadrature	1 sec	5 ppm	5 ppm
6	maximum-coupled coil quadrature	4 sec	2 ppm	2 ppm
7	radaraltitude	1 sec	10 feet	
8	magnetometer: 1 gamma/step	1 sec	2.5 gamma	

In addition, three fiducial markers are used between the channels, as follows:

---

[1] The quoted noise levels are generally valid for wind speeds up to 20 mph. Higher winds may cause the system to be grounded because excessive bird swinging produces control difficulties in piloting the helicopter. The swinging results from the 50 square feet of area which is presented by the bird to broadside gusts.

[2] A "sferic" detector replaced this channel on some flights for purposes of monitoring the inflight ambient noise, e.g. from distant thunder storms.

Fiducial	Occurrence
60-Hz marker	occurs only over power lines
camera fiducials	occurs regularly at 3 mm intervals on every line
navigator fiducials	occurs discontinuously on every line

The 60-Hz fiducial identifies anomalies generated by power lines, allowing them to be deleted from the EM map.

The navigator fiducial marks represent points on the ground which were recognized by the aircraft navigator. These are the initial base points for flight path recovery. The flight line begins with a single navigator fiducial. This is followed by a series of unevenly-spaced fiducials moving right-wards along the record, which is in the direction of the flight. The end of the line is flagged by a string of three navigator fiducial marks.

The camera fiducial marks indicate each point where a photograph was taken. These photographs are used to provide accurate photo-path recovery locations for the navigator fiducials, which are then plotted on the geophysical maps to provide the track of the aircraft.

The navigator fiducial locations on both the flight records and flight path maps are examined by a computer for unusal helicopter speed changes. Such changes often denote an error in flight path recovery. The resulting flight path locations therefore reflect a more stringent checking than is provided by standard flight path recovery techniques.

3.0 DATA PRESENTATION

3.1 The Three Conductor Models

DIGHEM anomalies may be interpreted according to three con-
ductor models, as follows:

Vertical dike (half plane)

> The vertical dike is the most suitable representation of
> steeply-dipping bedrock conductors. For base metal
> exploration, EM anomalies are plotted on a map and are
> interpreted according to this model. The three re-
> ceiver coils of DIGHEM allow correction for the response
> when the flight line crosses a conductor at an oblique
> angle.

Horizontal sheet (whole plane)

> The horizontal sheet is suitable for flatly-dipping
> thin layers of conductive clay or lake silt. For the
> normal base metal survey programs, the conductance and
> depth values are given in the anomaly list appended to
> the rear of the survey report, but do not appear on the
> EM map. These values are to be viewed with caution
> unless it is known that a horizontal sheet is a fair
> representation of the conductors. It is a highly
> specialized model with a limited application.

Conductive earth (half space)

> The conductive earth model is suitable for flay-dipping,
> thick bedrock conductors, saline water-saturated sedi-
> mentary formations, thick conductive overburden and
> geothermal zones. The resistivity and depth values may
> be contoured for applications involving resistivity
> mapping. The following section describes the con-
> ductive earth model in detail because it was used for
> the tunnel site survey.

3.2 Resistivity Mapping with DIGHEM

DIGHEM has encountered areas of widespread conductivity
while surveying for base metals. Under such conditions, anom-
alies can be generated by changes of only 20 feet in survey
altitude, as well as by changes in conductivity. Figure 65
shows a DIGHEM flight record where inphase and quadrature channels
are continuously active; local peaks reflect either increases in
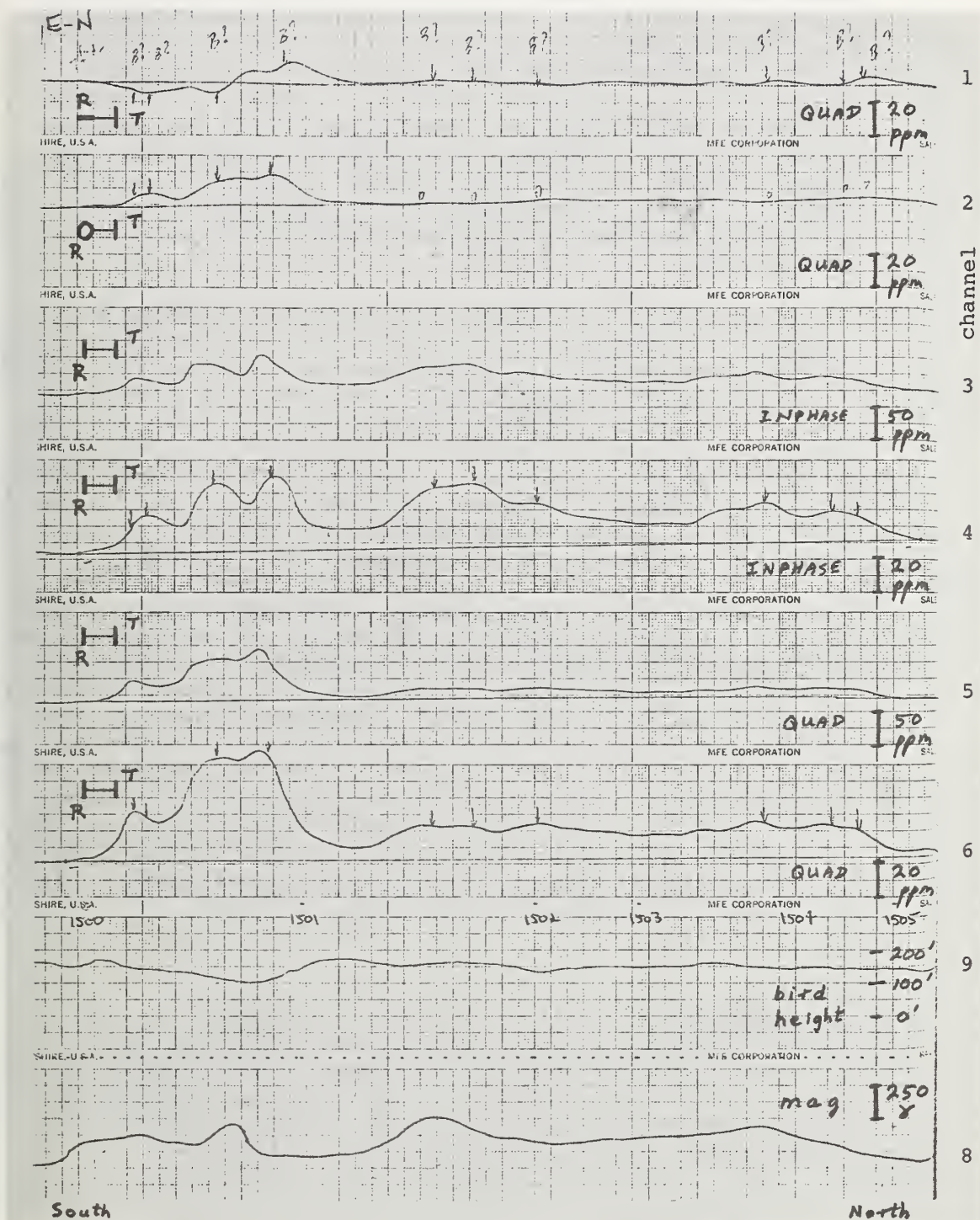
Figure 65 - Dighem flight record. Local peaks reflect either increases in conductivity or decreases in altitude.

307

conductivity or decreases in altitude. For such survey areas, apparent resistivity maps should be produced from the airborne data. The advantage of the contoured map is that anomalies caused by altitude changes are eliminated, and the contours reflect only the conductive anomalies. In areas of considerably widespread conductivity, the conventional EM map may be practically useless. Contoured resistivity maps improve the interpreter's ability to distinguish between conductive trends in the bedrock and those patterns typical of conductive overburden. The computer software uses a conductive earth algorithm derived from Frischknecht.

The inputs to the DIGHEM algorithm are the inphase and quadrature ppm of the maximum-coupled coil. The outputs from the algorithm are resistivity in ohm-meters and distance from the EM bird. The radar altitude is subtracted from this distance to provide a depth below surface to the conductive earth. Because depth is a parameter derived from the analysis, the formulation is not a half-space algorithm in the strictest sense. In actual fact, it represents a two-layer case where the resistivity of the upper layer is assumed to be infinite, and the resistivity of the lower layer is that of the conductive earth (Figure 66).

Figure 67 presents the results of a DIGHEM survey for base metals. Resistivity contours in ohm-meters are superimposed on the EM anomaly photomosaic. The EM anomaly patterns are misleading because they suggest the existence of specific conductor axes which are indicative of steeply-dipping conductors. In reality, broad patterns such as those of Figure 65 imply that the induced current flow paths were primarily horizontal rather than steeply-dipping. Resistivity contours provide a truer representation of the conductive environment, and indicate that the ENE-striking 30 ohm-meter band in the east-half of Figure 67 is caused by bedrock conduction. This band strikes perpendicular to the drainage in an area of moderately high relief.

3.3 Magnetics

The digitally recorded magnetometer data from the airborne survey has a usable resolution of approximately five gammas. The digital tape is processed by computer to yield a standard total field magnetic map contoured at 25 gamma intervals.
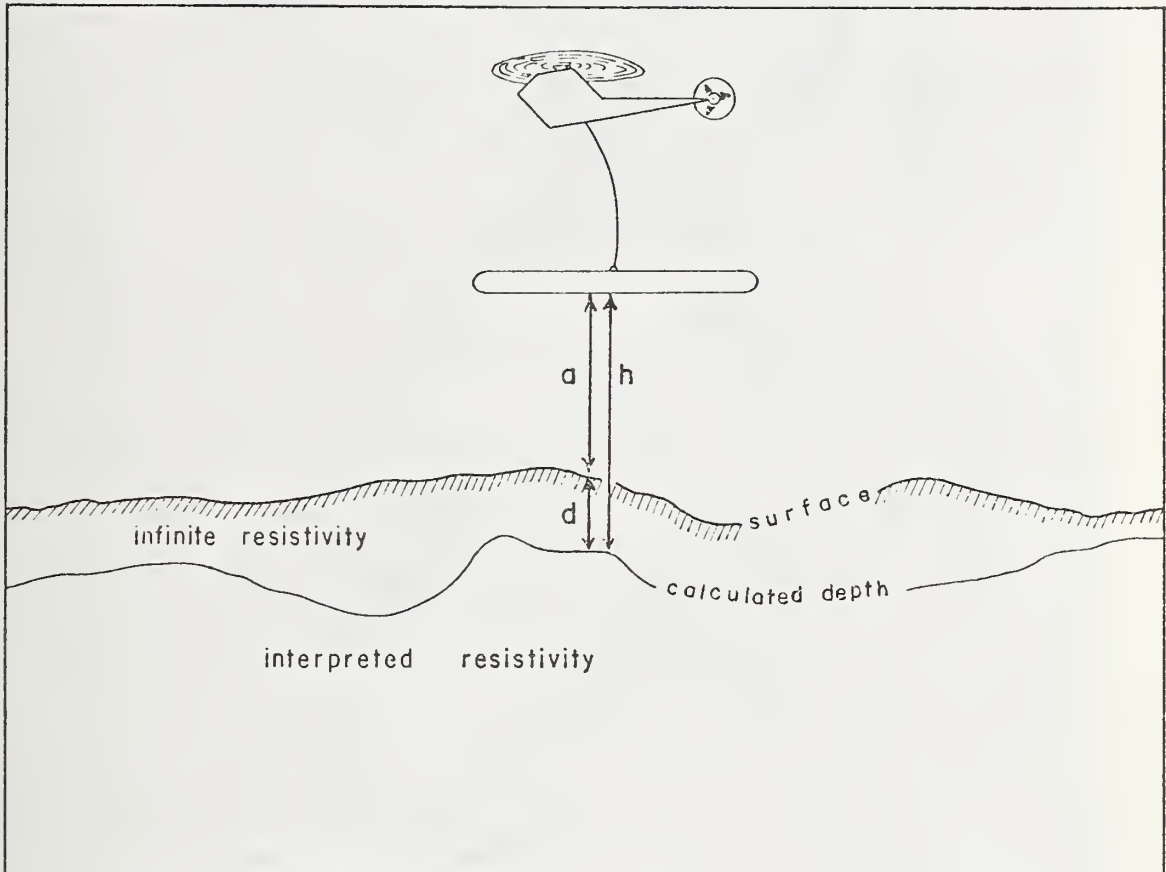
Figure 66 - The conductive earth model is actually a two-layer case where the upper layer has an infinite resistivity. The calculated depth d is the difference between the interpreted height h and the radar altitude a.
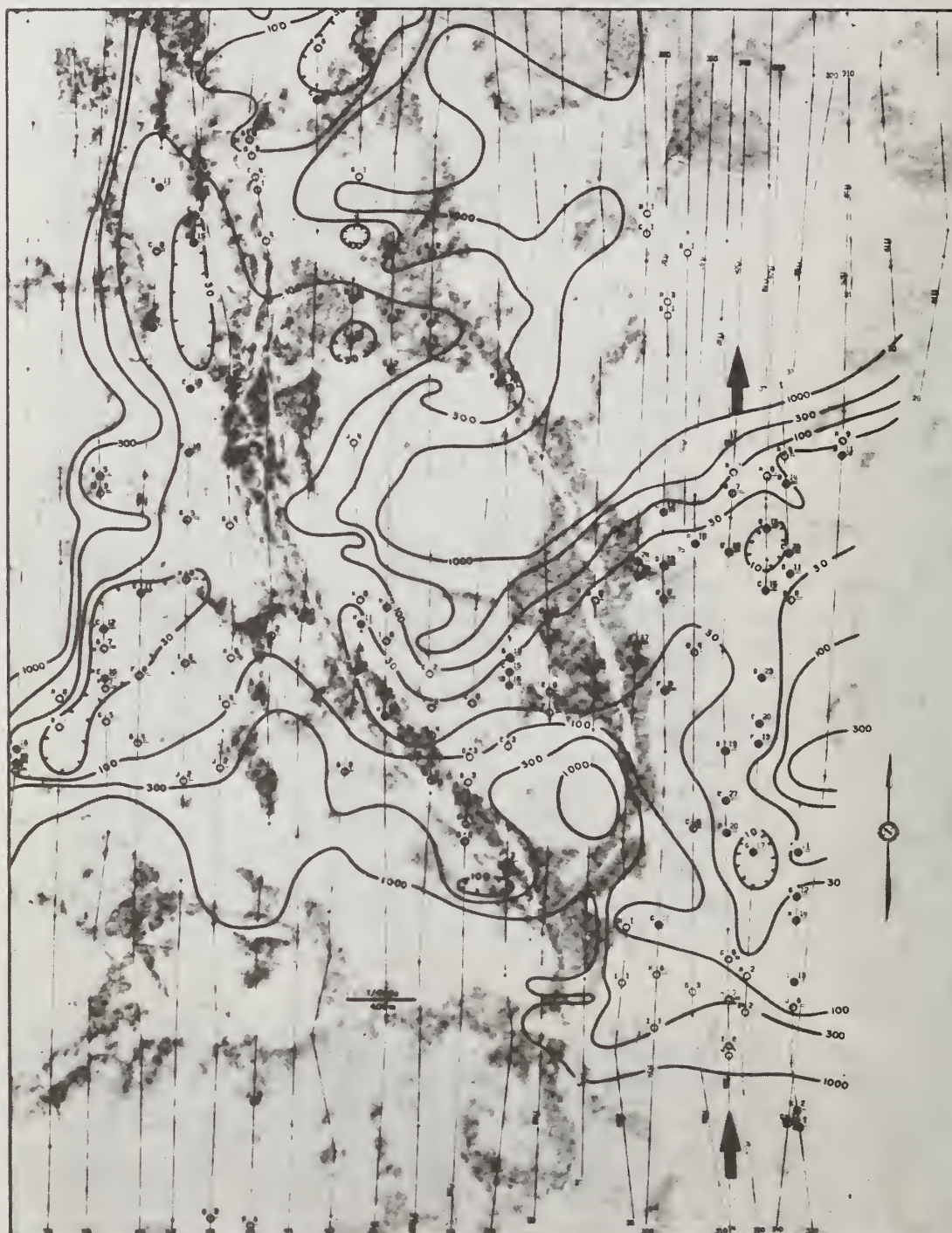
Figure 67 - Apparent resistivity map with contours in ohm-meters. The survey was flown with a Dighem electromagnetic system operating at 900Hz. The arrows identify the flight line of Figure 65.

APPENDIX H

COMMERCIALLY AVAILABLE RADAR AND AIRBORNE
ELECTROMAGNETIC SURVEY SERVICES

1.0 RADAR

Should it be desirable or necessary to obtain new radar imagery
of a specific area, three organizations in the United States provide
commercial services for radar imagery acquisition. These are:

> ERIM
> P.O. Box 618
> Ann Arbor, Michigan 48107
> Tel: 313-994-1200

ERIM system has a dual frequency (X and L bands) synthetic apera-
ture radar in a DC-3 aircraft. The system has a capability of trans-
mitting in either horizontal or vertical polarization and receiving in
both vertical and horizontal polarization for a total of four channels
of data.

> Aero Services Division
> Western Geophysical Company of America
> 4219 Van Kirk Street
> Philadelphia, Pennsylvania 19135
> Tel: 215-533-3900

Aero Services has an exclusive arrangement with Goodyear Aero-
space Corporation to use their synthetic aperature, X-band radar
system for commercial purposes. This system, mounted in a Caravelle
twin-jet aircraft, can map a swath of terrain 20 nautical miles (36 km)
wide with a uniform resolution of about 40 feet (16 m) throughout the
imagery.

> Motorola Aerial Remote Sensing, Inc.
> 4039E. Raymond St.
> Phoenix, Arizona 85040
> Tel: 602-244-5751

Motorola's AN/APS-94D, brute-force, radar system is flown commer-
cially in a Grumman Gulfstream aircraft. The depression angle on this
system is readily changeable which is of advantage for areas of differ-
ent relief characteristics.

Goodyear Aerospace is the repository for Air Force radar imagery from certain programs. Within this repository there are approximately six million square miles of radar imagery covering the United States. Most of this radar imagery is available to non-military organizations. The radar imagery that is available is at four different resolutions and scales. (Resolution-10-, 20-, 40-, 50-foot, and scales from 1:100,000 to 1:600,000). The military has recently declassified 10-foot resolution radar imagery at a scale of 1:100,000 of the United States.

Goodyear Aerospace has information pertaining to this radar imagery catalogued for retrieval by a number of categories including geographic coordinates. When a request is received for a certain area, the geographic coordinates and a radius is entered into a computer. The computer will print out information for all coverage over this coordinate, such as flight number, pass number, start and end coordinates, and coded information, for resolution and scale. The computer printout is then mailed to the requester with an explanation on how to use it. The requester will have to plot the coordinates from the printout and determine which pass or passes of radar imagery cover his/her area of interest. The requester will then send a letter to the address above requesting the pass/passes that cover their area. A statement explaining what the imagery will be used for should accompany the request.
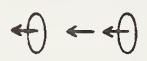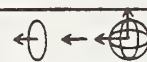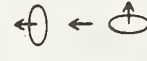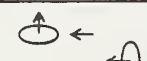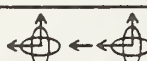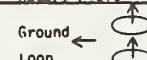
There is a charge for reproduction of $40.00 per pass; for this fee a contact transparency and a paper print are reproduced and shipped to the requester, usually within a week. This reproduction - depending on resolution and scale of the radar imagery - will cover between 100 and 2500 square miles. The size of the reproduction will be approximately 5" x 15". Additional prints and enlargements are available upon request. Price will be provided when requested.

A 10" x 13" reproduction of a wall map showing coverage of the United States also may be obtained upon request.

2.0 ELECTROMAGNETIC SURVEYS

There are a number of companies that provide airborne electro-
magnetic surveys. The capabilities of the different systems used vary
and should be thoroughly evaluated for the job requirement before
contracting. Table 19 (after Hood, 1974) lists a series of service
companies with such equipment and provides some guidance as to systems
characteristic and sensitivity.

Table I9 Chart of Electromagnetic System Operating Parameters

EM SYSTEM Tx Rx Flight Dirn	MANUFACTURER/ CONTRACTOR - Survey Platform	NORMAL SURVEY HEIGHT IN METRES Tx	Rx	COIL SEPARATION	FREQ. (Hz)	MEASURE I/P-In Phase O/P-Out of Phase	NOISE LEVEL in parts per million	RESPONSE FROM OVERBURDEN (in Canada)
Vertical Coaxial Rigid Coupled	Barringer - Helicopter	30 m	30 m	9.1 or 4.9m	900	I/P and O/P	2 ppm	Small
	Kenting - Canso	45 m	45 m	25 m	390	I/P and O/P	15 ppm	Small
	Northway LHEM 200 LHEM 250	30 m 30 m	30 m 30 m	9.1 m 9.1 m	4000 1000	I/P and O/P I/P and O/P	5 ppm 5 ppm	Moderate Small
	Sander - helicopter	40 m	40 m	7 m	500	I/P and O/P	±1 ppm I/P ±.5 ppm O/P	Small
	Scintrex Helicopter HEM 701	30 m	30 m	9.1 m	1600	I/P and O/P	3 ppm	Small
Multicoil Room Rigid Coupled	Barringer - Helicopter Aerodat Dighem	30 m	30 m	9.1 m	914	I/P and O/P	2-4 ppm	Whale Tail - large Fish Tail & Coaxial- Small
Min. Coupled Towed Bird	Northway LHEM 210	137 m	70 m	130 m	400 & 2300	O/P	840 ppm	Large
	McPhar F-400	130 m	40 m	120m; 60m behind & 90m below	340 and 1070 Hz -time shared	O/P	500 ppm	Medium
	McPhar F-500	130 m	40 m	120m; 60m behind & 90m below	340, 1070 & 3450	O/P	500 ppm	Medium
Time Domain Towed Bird	Barringer INPUT Geoterrex-Canso Questor-Canso & Skyvan	120 m	50 m	75m behind and 75m below	286 pulsed ½ sine waves per sec.	Transient at 6 intervals		Large on Channel 1 decreasing to zero on other channels
Wing Mounted Max. Coupled	Geoterrex Otter Kenting Otter	45 m	45 m	19 m	320	I/P and O/P	20 ppm	Small
	SOQUEM Cessna 305	40 m	40 m	11 m	694	I/P and O/P	30 ppm	Small
	Scintrex- Tridem	60 m	60 m	17.7 m	500 2000 8000	I/P and O/P 3 freq. simultaneously	20-40 ppm " "	Small Moderate Large
Rotary Field	ABEM (Sweden) - two plane	80 m	80 m	300 m	880	Relative I/P and O/P	1%	Fairly Large
Ground Loop	Scintrex- Turair II	Ground Loop	60 m	Several kilometres	200 & 400	Field Strength Ratio and Phase Gradient	0.1%	Variable
Very Low Frequency (VLF)	Barringer Radiophase and E-Phase	30 - 300 m	30 - 300 m	∞	15 KHz to 25 KHz	I/P and O/P		Large
	Geonics EM-18	60 - 90 m	60 - 90 m	∞	15 KHz to 25 KHz	I/P and O/P	0.5%	Large
	McPhar KEM	30 - 300 m	30 - 300 m	∞	15 KHz to 25 KHz	Dip Angle and Amplitude	0.5 V at sensor coils	Large
AFMAG	McPhar AF-4	30 - 300 m	30 - 300 m	∞	140 & 500 Hz	Tilt Angle essentially I/P	1° - 2°	Small

314

APPENDIX I

ACQUISITION OF EXISTING REMOTE SENSOR DATA FROM FEDERAL AGENCIES

Several federal government agencies acquire remote sensor data
which have been made available to the public for a nominal cost.
These data consist primarily of aerial photography and satellite
imagery, but limited amounts of radar thermal and multispectral scanner
imagery are also available. Many potential users who could benefit
from the services are not aware of the availability of the different
types of imagery and the procedures for acquiring these data. Con-
sequently, considerable detail is presented about the data and ser-
vices provided. Much of the following section has been extracted ver-
batim from an EROS publication.

1.0 EROS DATA CENTER

Although several outlets exist for government acquired remote
sensor data, the largest is the EROS (Earth Resources Observation
System) Program of the U.S. Department of Interior. This program,
administered by the Geological Survey, maintains a major storage and
retrieval facility in Sioux Falls, South Dakota.

They operate a computerized data storage and retrieval system
which is based on a geographic system of latitude and longitude,
supplemented by information about image quality, cloud cover, and type
of data. A customer's inquiry about availability of remotely sensed
data may be about a geographic point location or a rectangular area
specified by latitude and longitude corner coordinates. Depending on
customer requirements, a computer geographic search will print out a
listing of available imagery and photography from which the requester
can make a final selection. Receipt of a pre-paid order initiates
processing. To place an order, to inquire about the availability of
data, or to establish a standing order, contact:

   User Services Unit
   EROS Data Center
   Sioux Falls, South Dakota 57198
   Phone: 605-594-6511, extension 151
   FTS: 605-594-6151

1.1 EROS Data Reference Files

EROS Data Reference Files have been established throughout
the United States to maintain microfilm copies of the data avail-
able from the Data Center and to provide guides to assist the

visitor in reviewing and ordering data. This allows the visitor to view microfilm copies of the data before placing an order. Applications assistance by scientists is not provided at EROS Data Reference Files. The table below lists the address, telephone number, and hours of operation of each of the 11 Data Reference Files.

EROS Data Reference File
Public Inquiries Office
U.S. Geological Survey
108 Skyline Building
508 Second Avenue
Anchorage, Alaska 99501
Phone: 907-277-0577
Hours: 9:00-5:30

EROS Data Reference File
Public Inquiries Office
U.S. Geological Survey
Room 7638, Federal Building
300 North Los Angeles Street
Los Angeles, California 90012
Phone: 213-688-2850
Hours: 9:30-4:00

EROS Data Reference File
State Topographic Office
Lafayette Building, Koger Office
  Center
Tallahassee, Florida 32304
Phone: 904-488-2168
Hours: 8:15-5:15

EROS Data Reference File
University of Hawaii
Department of Geography
Room 313C; Physical Science
  Building
Honolulu, Hawaii 96825
Phone: 808-944-8463
Hours: 8:00-4:00

EROS Data Reference File
U.S. Geological Survey
5th Floor
80 Broad Street
Boston, Massachusetts 02110
Phone: 617-223-7202
Hours: 9:00-5:00

EROS Data Reference File
Public Inquiries Office
U.S. Geological Survey
Room 678, U.S. Court House
  Building
West 920 Riverside Avenue
Spokane, Washington 99201
Phone: 509-456-2524
Hours: 9:00-4:30

EROS Data Reference File
Topographic Office
U.S. Geological Survey
900 Pine Street
Rolla, Missouri 65401
Phone: 314-364-3680
Hours: 8:00-5:00

EROS Data Reference File
Water Resources Division
U.S. Geological Survey
975 West Third Avenue
Columbus, Ohio 43212
Phone: 614-469-5553
Hours: 8:00-4:30

EROS Data Reference File
Water Resources Divison
U.S. Geological Survey
Room 343, Post Office and
  Court House Building
Albany, New York 12201
Phone: 518-474-3107 or 6042
Hours: 8:00-4:30

EROS Data Reference File
Bureau of Land Management
729 NE. Oregon Street
Portland, Oregon 97208
Phone: 503-234-3361, ext.4000
Hours: 8:00-4:00

EROS Data Reference File
Maps and Surveys Branch
Tennessee Valley Authority
20 Honey Building
311 Broad Street
Chattanooga, Tennessee 37401
Phone: 615-755-2133
Hours: 8:00-4:00

1.2 EROS Applications Assistance Facilities

The EROS Data Center also operates several Applications Assistance Facilities which maintain microfilm copies of data archived at the Center and provide computer terminal inquiry and order capability to the central computer complex at the EROS Data Center. Scientific personnel are available for assistance in applying the data to a variety of resource and environmental problems and for assistance in ordering data from the Data Center.

The Applications Assistance Facilities should be contacted by phone or mail in advance, so that suitable arrangements can be made for a visit.

EROS Applications Assistance
  Facility
U.S. Geological Survey
Room 202, Building 3
345 Middlefield Road
Menlo Park, California 94025
Phone: 415-323-2727
Hours: 8:00-4:15

EROS Applications Assistance
  Facility
EROS Data Center
U.S. Geological Survey
Sioux Falls, South Dakota 57198
Phone: 605-594-6511
Hours: 8:00-4:30

EROS Applications Assistance
  Facility
U.S. Geological Survey
Room 8-210, Building 1100
National Space Technology
  Laboratories
Bay St. Louis, Mississippi 39520
Phone: 610-688-3472
Hours: 8:00-4:30

EROS Applications Assistance
  Facility
University of Alaska
Geophysical Institute
College, Alaska 99701
  (Fairbanks)
Phone: 907-479-7558
Hours: 8:00-5:00

317

EROS Applications Assistance
   Facility
HQ Inter-American Geodetic
   Survey
Headquarters Building
Drawer 934
Fort Clayton, Canal Zone
Phone: 83-3897
Hours: 7:00-3:45

EROS Applications Assistance
   Facility
U.S. Geological Survey
Room 2404B, Building 25
Federal Center
Denver, Colorado 80225
Phone: 303-234-4879
Hours: 8:00-4:30

EROS Applications Assistance
   Facility
U.S. Geological Survey
Room 5017, Federal Building
230 North First Avenue
Phoenix, Arizona 85025
Phone: 602-261-3188
Hours: 8:00-5:00

EROS Applications Assistance
   Facility
U.S. Geological Survey
1925 Newton Square East
Reston, Virginia 22090
Phone: 703-860-7868
Hours: 8:00-4:15

1.3 LANDSAT (Earth Resources Technology Satellite) Data

The first Earth Resources Technology Satellite, ERTS-1 (now
re-named LANDSAT-1), was launched July 23, 1972. LANDSAT-2 was
launched on January 22, 1975. LANDSAT flies in a circular orbit
570 miles (920 km) above the Earth's surface and circles the
Earth every 103 minutes, or roughly 14 times per day. Each
daytime orbital pass is from north to south. From such a vantage
point, each LANDSAT can cover the entire globe, except for the
poles, with repetitive coverage every 18 days. A unique feature
of the satellite, because of the orbit, is that it views the
Earth at the same local time, roughly 9:30 a.m. at the Equator,
on each pass. The sensors on board the spacecraft transmit
images to NASA receiving stations in Alaska, California, and
Maryland either directly or from data stored on tape recorders.
The data are converted from electronic signals to photographic
images and computer compatible tapes at NASA's Goddard Space
Flight Center (GSFA) in Greenbelt, Maryland. Master reproducible
copies are flown to the EROS Data Center in Sioux Falls, South
Dakota, where images are placed in the public domain, and where
requests for reproductions are filled for the scientific com-
munity, industry, and the public at large. Because of the experi-
mental nature of the satellite and the limited capabilities of
NASA ground processing equipment at Greenbelt, approximately 30
days are required from the time the signals are first received on
the ground to the time that the data are available to the public
at the EROS Data Center.

LANDSAT presently carries three data acquisition systems:
(1) a multispectral scanner (four spectral bands), (2) a return
beam vidicon (RBV) or television system, and (3) a data collec-
tion system (DCS) to relay environmental data from ground-based
data collection platforms (DCP's). The multispectral scanner, or
MSS, is the primary sensor system and acquires images of 111
miles (185 km) per side in four spectral bands in the visible and
near-infrared portions of the electromagnetic spectrum. These
four bands are:

> Band 4, the green band, 0.5 to 0.6 micrometers, emphasizes
> movement of sediment laden water and delineates areas of
> shallow water, such as shoals, reefs, etc.;

> Band 5, the red band, 0.6 to 0.7 micrometers, emphasizes
> cultural features;

> Band 6, the near-infrared band, 0.7 to 0.8 micrometers,
> emphasizes vegetation, the boundary between land and water,
> and landforms; and

> Band 7, the second near-infrared band, 0.8 to 1.1 micro-
> meters, provides the best penetration of atmospheric haze
> and also emphasizes vegetation, the boundary between land
> and water, and landforms.

An analysis of the four individual black-and-white images or
the false-color infrared composite images often permits scien-
tists to identify and inventory different environmental phenomena,
such as distribution and general type of vegetation, regional
geologic structure, and areal extent of surface water. The
repetitive (9 or 18 days) and seasonal coverage provided by
LANDSAT imagery is an important new tool for the interpretation
of dynamic phenomena. It should be noted that because of the
Earth's rotation and the fact that the image is created by an
optical-mechanical scanner, ERTS MSS images are parallelograms,
not squares. The sides are parallel to the orbital track of the
satellite on the Earth's surface. RBV images have a square
format because the image is acquired instantaneously.

The arbitrary forward overlap between consecutive LANDSAT
images is approximately ten percent. The sidelap between ad-
jacent orbits ranges from fourteen percent at the Equator to
eighty-five percent at the 80° parallels of latitude.

Latitude and longitude tick marks are depicted at 30-minute
intervals outside the image edge. These geographic reference
marks are annotated in degrees, minutes, and compass direction.
A 15-step gray-scale tablet is exposed on every frame of LANDSAT
imagery as it is produced. This scale is used to monitor and

control printing and processing functions and to provide a reference for analysis related to a particular image. The annotation block directly over the gray scale contains data that give the unique image identification, the geographic location, and the time (with respect to Greenwich mean time) an image was acquired.

If you wish to order a single black-and-white image, it is best to order band 5. This band usually gives the best general-purpose view of the Earth's surface. By ordering a complete set of black-and-white images from all four bands, however, you can see how the same area differs in appearance when filtered to green, red, and near-infrared wavelengths. MSS false-color composites are available as standard products. An MSS false-color composite image is generally created by exposing three of the four black-and-white bands through different color filters onto color film. On these false-color images, healthy vegetation appears bright red rather than green; clear water appears black; sediment-laden water is powder blue in color; and urban centers often appear blue or blue-gray. MSS false-color composite images which have not already been prepared can be ordered from the Data Center but carry a one-time initial preparation charge of $50, not including the cost of any products ordered from the resulting composite.

A set of LANDSAT images has been prepared for the conterminous United States. The 470 scenes required to cover the United States are available in a single black-and-white (band 5), all four bands of black-and-white, or high-quality color composites. The scenes selected were chosen on the basis of quality, optimum time of year (generally spring or summer), and minimum cloud cover.

LANDSAT data in digital form are available as Computer Compatible Tapes (CCT). The tapes are standard one-inch-wide (12.7-mm) magnetic tapes and may be requested in either seven- or nine-track format at 800 or 1,600 bpi. Four CCT's are required for the digital data corresponding to one LANDSAT image. The data for the four bands are interleaved among the four tapes thereby necessitating all tapes to complete a set. The cost of one set (one LANDSAT image) is $200.

1.4 Skylab Data

The NASA Skylab Program consisted of one unmanned and three manned missions. The unmanned space vehicle was placed in orbit in February 1973. The manned missions were Skylab 2, launched on May 22, 1973, and recovered on June 22, 1973; Skylab 3, in orbit

320

from July 28 to September 25, 1973; and Skylab 4, launched on November 16, 1973, and recovered on February 8, 1974.

The spacecraft traveled in an orbit 270 miles (430 km) above the Earth and acquired photography, imagery, and other data of selected areas between latitudes 50°N. and 50°S. The data covered a number of scattered test sites selected to support Earth resources experiments. The photography, however, does not provide complete, cloud-free, and systematic coverage of the Earth's surface between 50°N. and S. latitudes.

The Skylab Earth Resources Experiment Package (EREP) consisted of six remote-sensing systems and was designed as a space-borne facility to be used by the scientific community. Only two of the systems are of interest for tunnel site investigations;

S190-A - Multispectral Photographic Camera. A six camera array was designed to provide high-quality photography of a wide variety of phenomena on the Earth's surface. Each camera used 70 mm film and was a six-inch (152-mm) focal length lens. The films used were filtered black-and-white, color, and false-color infrared. The area covered by each image of this system is 90 by 90 miles (144 by 144 km).

S190-B - Earth Terrain Camera. A single, high resolution Earth terrain camera was selected to provide high-resolution photography for scientific study. It used five-inch (127-mm) film and an eighteen-inch (457-mm) focal length lens. Various black-and-white, color, and false-color infrared films were used in the camera. The area covered by each frame of this system was 60 by 60 miles (96 by 96 km).

1.5 NASA Aerial Photography

NASA aerial photography is the product of aerial surveys carried out by the NASA Earth Resources Aircraft Program. The program is directed primarily at testing a variety of remote-sensing instruments and techniques in aerial flights generally over certain pre-selected test sites within the continental United States, but also includes sites in a few foreign areas.

Aerial photography is available in a wide variety of formats from flights at altitudes of a few thousand feet (1,000 m) up to U-2 and RB-57F flights at altitudes above 60,000 feet (18,000 m). The high-altitude photography is generally available on a nine- by nine-inch (23- by 23-cm) film format at approximate scales of 1:120,000 and 1:60,000. In general, each high-altitude frame of nine-inch (23-cm) film format photography at 1:120,000 scale shows an area approximately 15 miles (24 km) on a side.

Aerial photography is available in black-and-white, color, or false-color infrared. Since these data are acquired at relatively low altitudes, ground features such as roads, farms, and cities are easily identifiable. Cloud cover is present in some photographs, and NASA aerial photographic coverage is not available for all areas of interest. Some electronic data from the more sophisticated research sensors on the aircraft may also be obtained through the Data Center. These data, however, are of limited areas and long delivery times must be expected.

1.6 Aerial Mapping Photography

Aerial photography during the past 25 years was acquired by the U.S. Geological Survey and other Federal Government agencies for mapping of the United States. The photography is black-and-white and has less than five percent cloud cover.

Depending on the planned use of the photographs, the aerial-survey altitude ranged from 2,000 feet (600 m) to 40,000 feet (12,000 m). The basic film format is nine by nine inches (23 by 23 cm) and shows areas from three to nine miles (4.8 to 14.4 km) on a side depending on the scale of the photograph.

Because of the large number of aerial photographs necessary to show an area on the ground, the photographs have been indexed by mounting a series of consecutive and adjacent overlapping photographs to create a mosaic of photographs of a specified area. These aerial photographic mosaics are referred to as "photo indexes" and allow for rapid identification of photographic coverage of a specific area. Presently, some 43,000 photo indexes are available at the Data Center. To order aerial photography from the Data Center, it is necessary that you initially order a photo index of your area of interest to determine the specific aerial photography needed.

Should you have difficulty in placing an inquiry or order, need assistance in selection of data, or have questions regarding your order or additional services, you may write or call:

> Customer Relations Unit
> EROS Data Center
> Sioux Falls, South Dakota 57198
> Phone: 605-594-6511, extension 151
> FTS: 605-594-6151

Allow a minimum of two to three weeks for delivery of all orders. A longer time may be required for the production of computer compatible tapes or the completion of very large or complex orders.

1.7 The Geographic Search and Inquiry System

Requests for information about imagery of a specific area will initiate a computerized geographic search. The search can be initiated by mail, visit, or phone, to either the EROS Data Center or one of the EROS Applications Assistance Facilities. You may request a geographic search using any of the three following options:

1. Point search - all images or photographs with any portion falling with 50 miles (80 km) of the point will be included.

2. Area rectangle - any area of interest defined by four corner coordinates of latitudes and longitudes. All images or photographs with any coverage of the area will be listed. The area must not exceed 200 one-degree squares (for example, 10° latitude by 20° longitude).

3. You may enclose a map with a point or area indicated.

When requesting a geographic search from the Data Center, be sure to provide all relevant information. This should include acceptable dates and seasons, type of imagery preferred, color, false-color infrared, or black-and-white, cloud cover, and quality. Cloud cover is given only in percentage, hence no assurance can be given as to where clouds will appear on the resulting photographs or images. A description of your intended application and the use of the data will assist the researcher at the Data Center who initiates the search, thereby resulting in a more concise response to your inquiry.

GEOGRAPHIC AREAS MUST BE CLEARLY IDENTIFIED AND SHOULD BE LIMITED IN SIZE AS MUCH AS POSSIBLE TO AVOID A POTENTIALLY LONG COMPUTER LISTING AND THE NEED TO REVIEW LARGE NUMBERS OF CHOICES. LATITUDE AND LONGITUDE COORDINATE SPECIFICATION IS PREFERRED, SINCE THIS IS THE METHOD REQUIRED FOR THE COMPUTER GEOGRAPHIC SEARCH.

Specification in degrees and minutes normally provides sufficient locations accuracy. (Each degree of latitude or longitude is divided into 60 minutes, and each minute into 60 seconds. One minute of latitude is roughly one mile.)

The computerized geographic search is made free of charge. Allow at least two weeks for the search to be completed and for the computer listing to be sent to you for image or photograph selection.

1.8 Placing An Order

Orders for reproductions of data from the EROS Data Center can be placed by personal visit, telephone, or mail to the Data Center. Orders can also be placed at any of the EROS Applications Assistance Facilities.

All orders must be accompanied by check, money order, purchase order, or authorized account identification; processing cannot be initiated until valid and accurate payment is received. Your check or money order should be made payable to the U.S. Geological Survey.

2.0 OTHER GOVERNMENT AGENCIES

2.1 U.S. Department of Agriculture

The Department of Agriculture maintains a distribution facility in Salt Lake City, Utah for the reproduction of LANDSAT and Skylab imagery, Soil Conservation Service aerial photography, and some NASA aerial photography. They will provide free Photographic Coverage Status Maps for each state. These maps show the scale, date and areal coverage for different photographic missions. For more specific information, photo indexes can be purchased for $5 each.

The address is:

> Aerial Photography Field Office
> USDA
> 2505 Parley's Way
> Salt Lake City, Utah 84109
> Phone: 801-524-5856

2.2 National Oceanic and Atmospheric Administration

Weather satellite data, plus LANDSAT and SKYLAB imagery, are available through the Environmental Data Service Section of the National Oceanic and Atmospheric Administration (NOAA). For tunnel siting studies the weather satellite imagery will probably be of no value. Computer searches can be made for a printout of coverage of specific areas of interest, and orders for LANDSAT and Skylab imagery are currently filled in seven to ten days.

2.3 NOAA Browse File Locations

NOAA maintains browse files at various locations in the country which can be visited to examine the 16 mm film catalogs of imagery.

University of Alaska
Arctic Environmental Information
  and Data Center
142 East Third Avenue
Anchorage, Alaska 99501
Telephone: 907-279-4523

Inter-American Tropical Tuna
  Commission
Scripps Institute of
  Oceanography
Post Office Box 109
LaJolla, California 92037
Telephone: 714-453-2820

National Geophysical and Solar
  Terrestrial Data Center
Solid Earth Data Service
  Branch
Boulder, Colorado 80302
Telephone: 303-499-1000,
  ext. 6915

National Oceanographic Data
  Center
Environmental Data Service
2001 Wisconsin Avenue
Washington, D.C. 20235
Telephone: 202-634-7510

Atlantic Oceanographic and Meteorological
  Laboratories
15 Rickenbacker Causeway, Virginia Key
Miami, Florida 33149
Telephone: 305-361-3361

National Weather Service, Pacific Region
Bethel-Pauaha Building, WFP 3
1149 Bethel Street
Honolulu, Hawaii 96811
Telephone: 808-841-5028

National Ocean Survey - C3415
Building #1, Room 526
6001 Executive Boulevard
Rockville, Maryland 20852
Telephone: 301-443-8601

Atmospheric Sciences Library - D821
Gramax Building, Room 816
8060 13th Street
Silver Spring, Maryland 20910
Telephone: 301-427-7800

National Environmental Satellite Service
Environmental Sciences Group
Suitland, Maryland 20233
Telephone: 301-763-5981

Northeast Fisheries Center
Post Office Box 6
Woods Hole, Massachusetts 02543
Telephone: 617-548-5123

Lake Survey Center - CLx13
630 Federal Building & U.S.
  Courthouse
Detroit, Michigan 48226
Telephone: 313-226-6126

National Weather Service,
  Central Region
601 East 12th Street
Kansas City, Missouri 64106
Telephone: 816-374-5672

National Weather Service,
  Eastern Region
585 Stewart Avenue
Garden City, New York 11530
Telephone: 516-248-2105

National Climatic Center
Federal Building
Asheville, North Carolina
  28801
Telephone: 704-258-2850,
  ext. 620

National Severe Storms Lab
1313 Halley Circle
Norman, Oklahoma 73069
Telephone: 405-329-0388

Remote Sensing Center
Texas A & M University
College Station, Texas 77843
Telephone: 713-845-5422

National Weather Service,
  Southern Region
819 Taylor Street
Fort Worth, Texas 76102
Telephone: 817-334-2671

National Weather Service,
  Western Region
125 South State Street
Salt Lake City, Utah 84111
Telephone: 801-524-5131

Atlantic Marine Center - CAMO2
439 West York Street
Norfolk, Virginia 23510
Telephone: 804-441-6201

Northwest Marine Fisheries
  Center
2725 Montlake Boulevard East
Seattle, Washington 98112
Telephone: 206-442-4760

University of Wisconsin
Office of Sea Grant
610 North Walnut Street
Madison, Wisconsin 53705
Telephone: 608-263-4836

2.4 National Ocean Survey

The National Ocean Survey (NOS) has substantial quantities of aerial photography of areas immediately adjacent to the coastline of the United States. The scale of aerial photographic reproduction is secondary to the National Ocean Survey's responsibility for charting. Normally, outside orders will be filled in less than 30 days but official charting requirements will be given priority. The requester should describe the specific area of interest by geographic coordinates, a detailed description or a sketch. (See discussion below on PHOTO INDEX SHEETS.)

Payment by check, money order, or draft, payable to National Ocean Survey, Commerce Department, shall accompany orders. No discount is offered for quantity purchases.

Prints are not stocked. They are custom processed for each order and cannot be returned for credit or refund. This includes mis-ordered prints.

Shipment by parcel post is pre-paid. Shipment by express, airmail, or involving special handling must be paid for by the purchaser.

Authorization to purchase photographs of classified areas must be obtained by the purchaser from appropriate military authorities. This office will inform the requester when such clearance is required and how to submit the application.

National Ocean Survey aerial photography is of a single lens type, some panchromatic, some color and a smaller portion of black-and-white infrared and false-color infrared.

Single lens aerial photographs are usually exposed at scales from 1:10,000 to 1:40,000.

The National Ocean Survey's aerial photography is special purpose photography. Usually it consists of a single strip or a few parallel strips of photographs. It is impracticable to index this photography by the single mosaic method commonly used by other government agencies.

The photographs are usually indexed on 1:250,000 scale base maps that cover an area of 1° of latitude by 1° of longitude with each individual exposure indicated by a dot. Occasionally, larger scale bases are used for indexes. Separate series of photo indexes are maintained for the different categories of photography as follows:

Panchromatic, black-and-white infrared, natural color, and false-color infrared.

Diazo prints of indexes are available at $.50 each upon request. For further information or to place an order, contact:

Coastal Mapping Division C3415
National Ocean Survey, NOAA
6001 Executive Blvd.
Rockville, Md. 20852
Phone: 301-443-8601
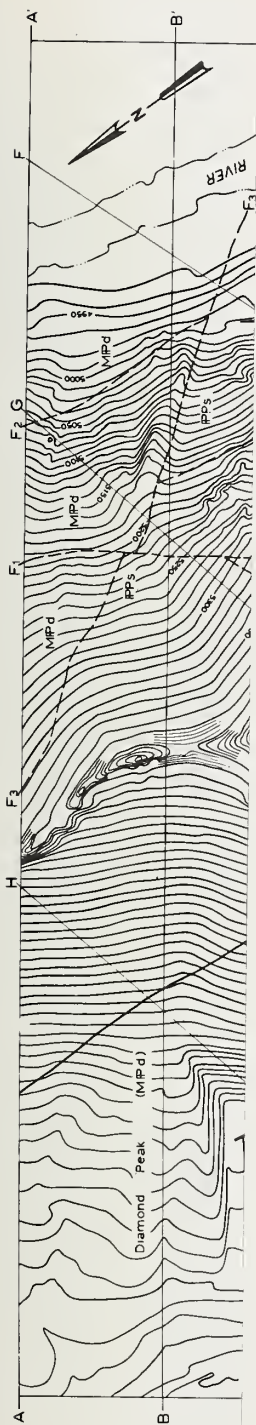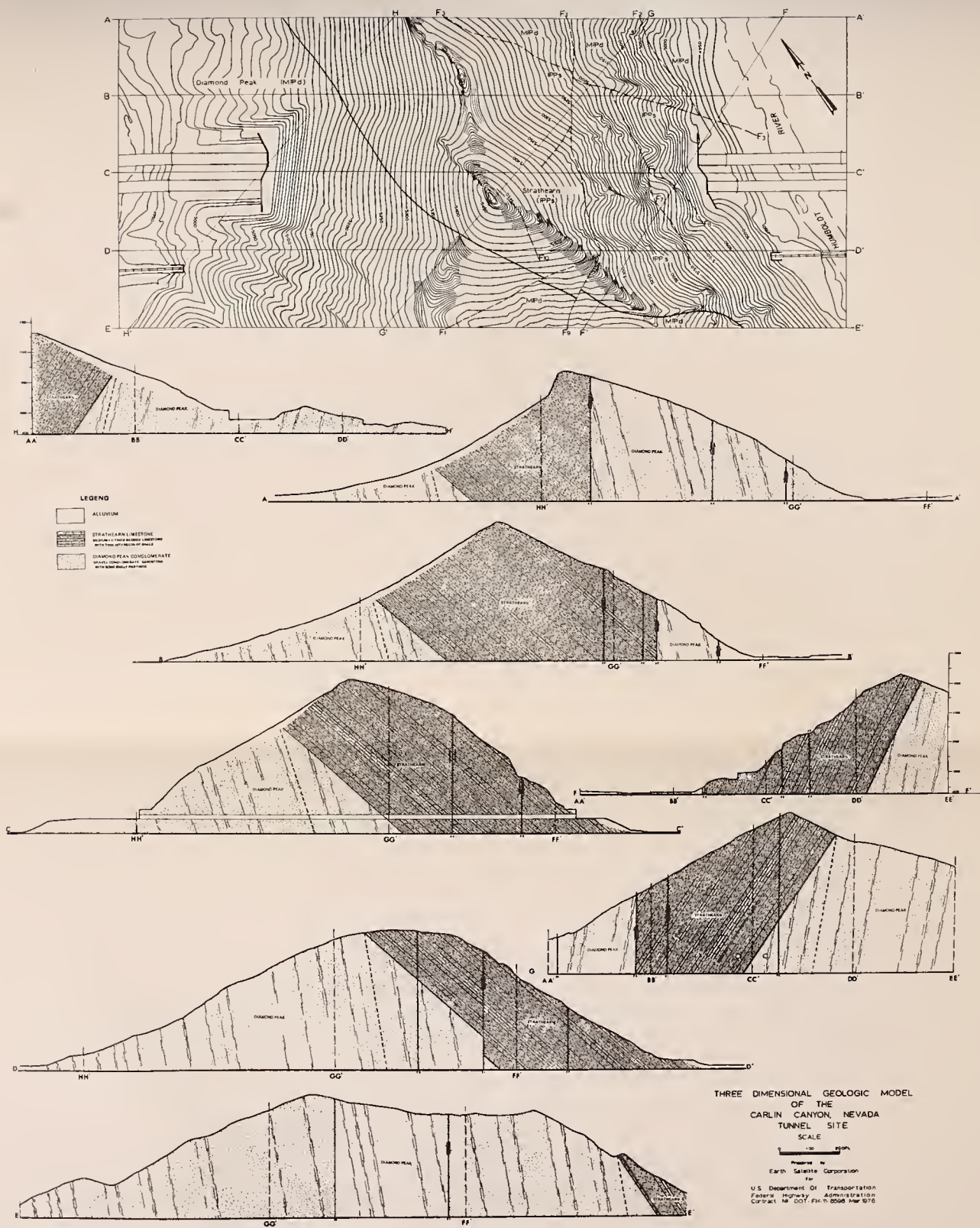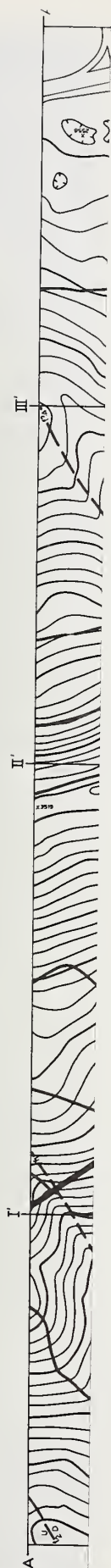
329-330

LEGEND

ALLUVIUM

STRATHEARN LIMESTONE
MEDIUM + THICK BEDDED LIMESTONE
WITH THIN LAYERS OF MEDIUM GRAINED

DIAMOND PEAK CONGLOMERATE
GRAVEL CONGLOMERATE CEMENTING
WITH SOME SHALY PARTINGS

THREE DIMENSIONAL GEOLOGIC MODEL
OF THE
CARLIN CANYON, NEVADA
TUNNEL SITE
SCALE

Prepared by
Earth Satellite Corporation
For
U.S. Department Of Transportation
Federal Highway Administration
Contract № DOT-FH-11-8598 Mar 1976
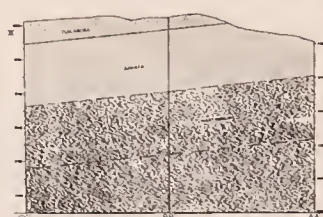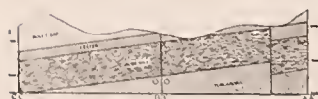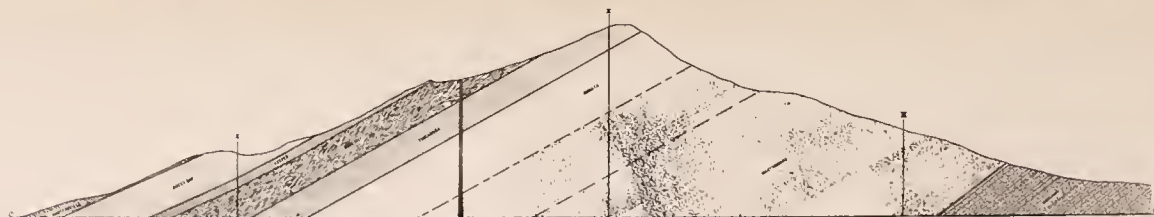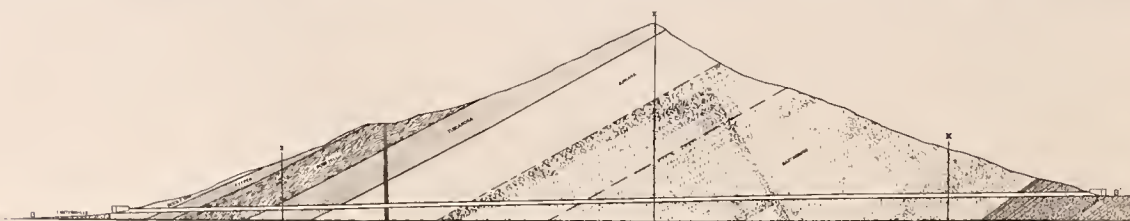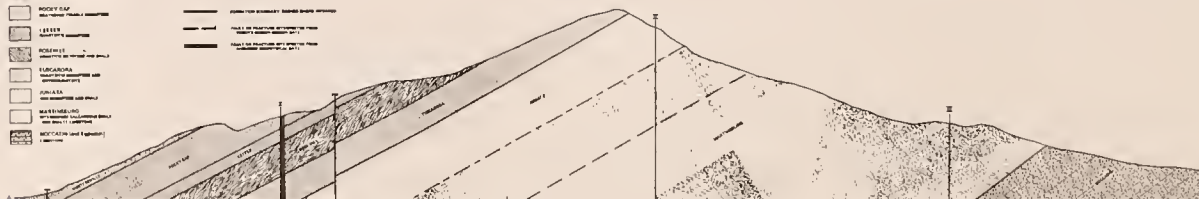
THREE DIMENSIONAL GEOLOGIC MODEL
OF THE
EAST RIVER MOUNTAIN
VIRGINIA-WEST VIRGINIA
TUNNEL SITE

333-334
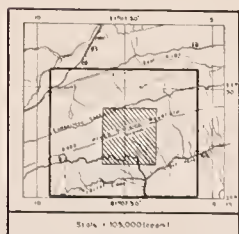
AEROMAGNETIC SURVEY
EAST RIVER MOUNTAIN SITE

(CONDUCTED BY DIGHEM LIMITED)
MARCH 1976

Prepared for
Office of Research
FEDERAL HIGHWAY ADMINISTRATION
U S DEPARTMENT OF TRANSPORTATION

Prepared by
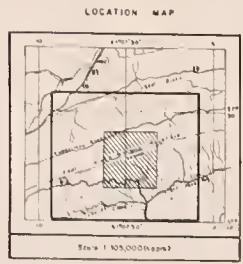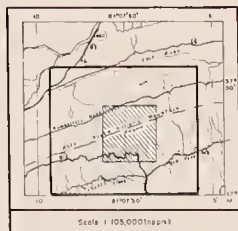EARTH SATELLITE CORPORATION
Contract No DOT FH 11 8598

Scale

PLATE III

LOCATION MAP

Scale = 100,000 (approx)

ISOMAGNETIC LINES
(enhanced field)

5000 gammas
1000 gammas
200 gammas
100 gammas

magnetic depression

flight line

frequency response of
magnetic operator
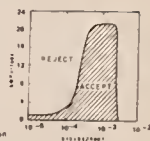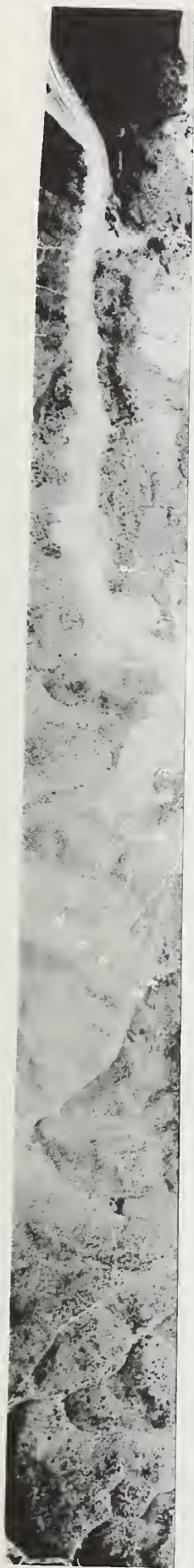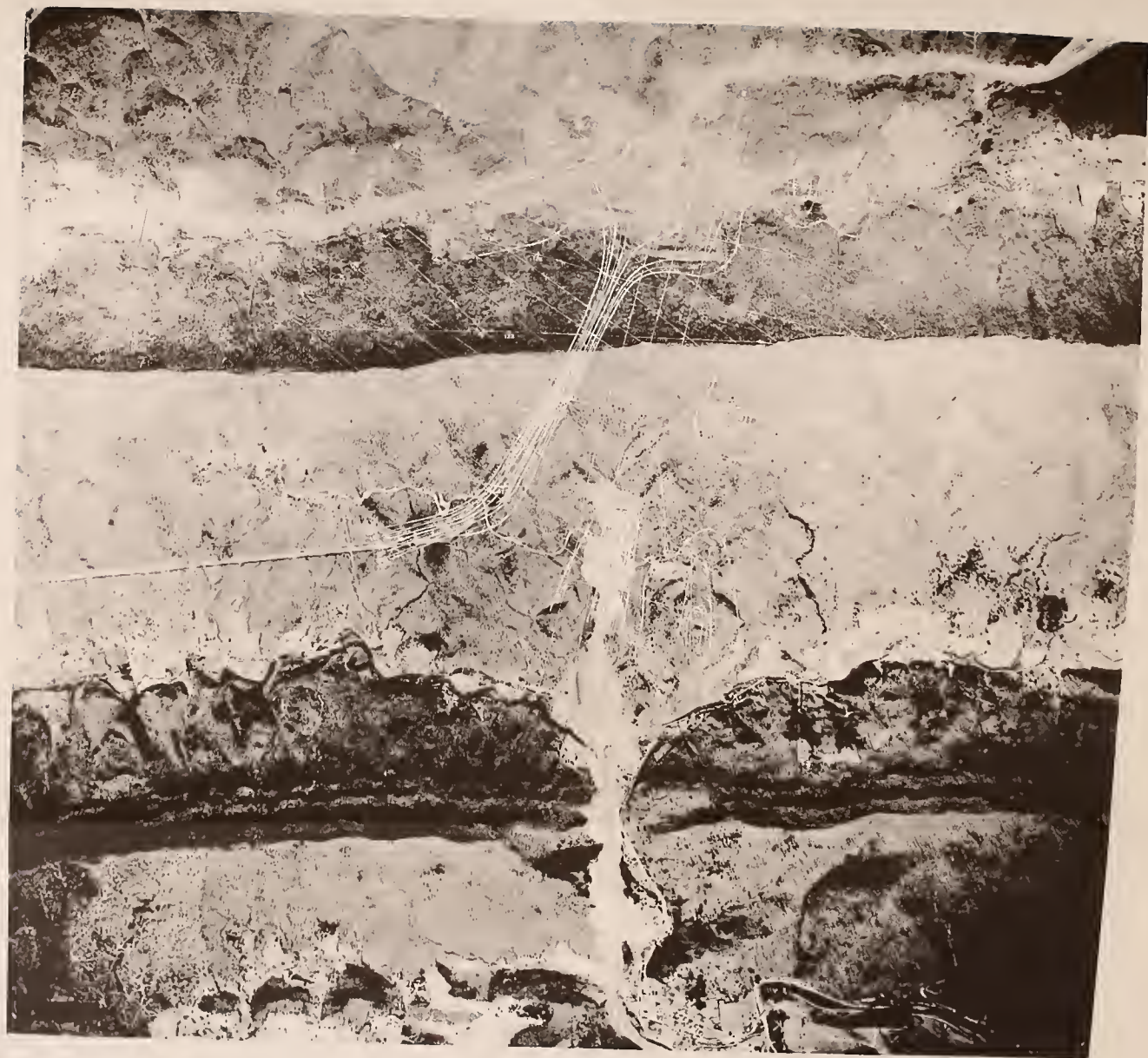
AIRBORNE RESISTIVITY SURVEY
EAST RIVER MOUNTAIN SITE

(CONDUCTED BY DIGHEM LIMITED)
MARCH 1976

Prepared for
Office of Research
FEDERAL HIGHWAY ADMINISTRATION
U S DEPARTMENT OF TRANSPORTATION

Prepared by
EARTH SATELLITE CORPORATION
Contract No. DOT FH 11-8598

LOCATION MAP

PLATE IV

335-336

337-338

FHWA

R & D